Development of a Breath Analyzer for Detecting BTEX in the Oil and Gas Industry: Design, Implementation, and Validation

Thesis submitted in

partial fulfillment for the

Award of Degree

Doctor of Philosophy

by

ALISHA DAS

RAJIV GANDHI INSTITUTE OF PETROLEUM TECHNOLOGY,
BENGALURU, 562 165

20EB0002 **2025**

CERTIFICATE

It is certified that the work contained in the thesis titled "***DEVELOPMENT OF A BREATH ANALYZER FOR DETECTING BTEX IN OIL AND GAS INDUSTRY: DESIGN, IMPLEMENTATION AND VALIDATION***" by ***Ms. ALISHA DAS***, has been carried out under my/our supervision and that this work has not been submitted elsewhere for a degree.

It is further certified that the student has fulfilled all the requirements for the Comprehensive, Candidacy, and SOTA programs.

Signature:

Supervisor

Dr. Roopa Manjunatha

Assistant Professor

RGIPT, Bengaluru

DECLARATION BY THE CANDIDATE

I, "***ALISHA DAS***" certify that the work embodied in this thesis is my own bona fide work and carried out by me under the supervision of ***"Dr. ROOPA MANJUNATHA"*** from August 2020 to June 2025 at Rajiv Gandhi Institute of Petroleum Technology, Bengaluru. The matter embodied in this thesis has not been submitted for the award of any other degree. I declare that I have faithfully acknowledged and given credit to the research workers wherever their works have been cited in my work in this thesis. I further declare that I have not wilfully copied any other's work, paragraphs, text, data, results, etc., reported in journals, books, magazines, reports, dissertations, theses, etc., or available at websites, and have not included them in this thesis and have not cited them as my work.

Date:

Alisha Das

Place:

CERTIFICATE BY THE SUPERVISOR (S)

We certify that the above statement made by the student is accurate to the best of our knowledge.

Supervisor

Dr. Roopa Manjunatha

Assistant Professor

RGIPT, Bengaluru

Signature & Seal of Head of Department

CERTIFICATE

I certify that the work contained in the thesis titled "**DEVELOPMENT OF A BREATH ANALYZER FOR DETECTING BTEX IN OIL AND GAS INDUSTRY: DESIGN, IMPLEMENTATION AND VALIDATION"** by Ms. **ALISHA DAS** has been carried out under my supervision. It is also certified that she fulfilled the mandatory requirement of TWO quality publications arising out of her thesis work.

It is further certified that the two publications (copies enclosed) of the aforesaid Ms. Alisha Das have been published in the journal indexed by

(a) SCI

(b) SCI Extended

(c) SCOPUS

Signature

( )

Dr. Roopa Manjunatha

Supervisor

Signature

( )

Dr. Sivasankari Sundaram

DPGC Convener

COPYRIGHT TRANSFER CERTIFICATE

Title of the Thesis: Development of a Breath Analyzer for Detecting BTEX in the Oil and Gas Industry: Design, Implementation, and Validation.

Name of the Student: Alisha Das

Copyright Transfer

The undersigned hereby assigns to the Rajiv Gandhi Institute of Petroleum Technology, Bengaluru, all rights under copyright that may exist in and for the above thesis submitted for the award of the "Doctor of Philosophy".

Date:

Place:

Alisha Das

RAJIV GANDHI INSTITUTE OF PETROLEUM TECHNOLOGY

(BENGALURU)

***

FOR SUBMISSION OF PH.D. THESIS

PERSONAL DETAILS

Name of the Student: Alisha Das **Roll no.:**20EB0002

Term of Registration:16-Aug-2020

Category of Registration: Full-Time Regular

Fulfilled required Minimum Residence period:

4 semester /**5** semester /**6** semester (Pl. Tick)

Supervisor: Dr. Roopa Manjunatha

Department: *RGIPT, Bengaluru*

Title of the Thesis: Development of a Breath Analyzer for Detecting BTEX in Oil and Gas Industry: Design, Implementation, and Validation.

Dedicated

to

My loving

Parents and Husband

ACKNOWLEDGEMENT

I want to express my sincere gratitude to my supervisor, ***Dr. Roopa Manjunatha****, for her invaluable guidance, constant encouragement, insightful discussions, and unwavering support throughout my Ph.D. program. Her profound knowledge and meticulous feedback were instrumental in the successful completion of this research. I am immensely thankful to the RGIPT, Bengaluru, for providing an excellent research environment, state-of-the-art facilities, and financial assistance that made this work possible. I extend my sincere thanks to* ***Dr. Rajib Bandyopadhyay*** *(Dept of Instrumentation and Electronics Engg, Jadavpur University),* ***Dr. Priya Ranjan Muduli*** *(Department of Electronics Engineering, Indian Institute of Technology (BHU) Varanasi) and* ***Dr. K Naveen Kumar*** *(Nitte Meenakshi Institute of Technology, Bengaluru) for their collaborative contributions and insightful discussions that significantly enriched this research.*

I want to express my sincere gratitude to ***Dr. Rohit Bansal****, In-Charge, RGIPT, Bengaluru, and* ***Dr. Sivasankari Sundaram****, DPGC, RGIPT, whose unconditional support was instrumental in navigating the challenging times. Furthermore, I would like to extend my heartfelt thanks to all faculty members, staff, and fellow research scholars at the Energy Institute for their support and camaraderie. Finally, I would like to thank my family and friends for their continuous love, encouragement, and understanding throughout this demanding period. Their belief in me kept me motivated.*

…. Alisha Das

TABLE OF CONTENTS

ACKNOWLEDGEMENT ..... **viii**
LIST OF FIGURES ..... **xii**
LIST OF TABLES ..... **xv**
ABBREVIATIONS/NOTATIONS ..... **xvii**
PREFACE ..... **xix**
Chapter 1: Introduction **1**
1.1 Importance of BTEX Monitoring and Its Health Implications 1
1.1.1 Prevalence of BTEX in the ONG Industry 1
1.1.2 Toxicity of BTEX Compounds 7
1.1.3 Occupational Health Risks 7
1.2 BTEX Detection Methods 9
1.2.1 Analytical Techniques 9
1.2.2 Resistive sensor 12
1.2.3 Quartz Crystal Microbalance sensor 13
1.3 Breath Analysis in BTEX Monitoring. 16
1.4 Research Gap 18
1.5 Research Objective 19
1.6 Dissertation Outline 21
Chapter 2: BTEX Exposure and Occupational Health Monitoring: A Comprehensive Review **23**
2.1 Abstract 23
2.2 Introduction 24
2.3 Methodology 28
2.3.1 Selection Criteria 28
2.3.2 Literature Search Strategy 30
2.3.3 Quality Assessment 33
2.3.4 Exposure Guidelines 33
2.3.5 Health Risk Assessment 36
2.3.6 Detection and Analysis Methods 38
2.4 Results and Discussions 40
2.4.1 Sources of emission 40
2.4.2 Health effects of BTEX 53
2.4.3 BTEX detection techniques 63

2.5 Study Limitation 68
2.6 Conclusion 69
Chapter 3: Design and Fabrication of QCM Sensor for BTEX Detection 71
3.1 Abstract 71
3.2 Introduction 73
3.2.1 Quartz Crystal Microbalance sensor 75
3.2.2 Polyvinyl Acetate (PVAc) 77
3.2.3 Tungsten Oxide (WO_3) 79
3.3 Methodology 81
3.3.1 PVAc deposition 81
3.3.2 WO_3 Deposition 83
3.4 Experimental Setup and Analyte Generation 85
3.4.1 Electronic Circuit Design 85
3.4.2 Experimental Setup 86
3.4.3 Volatile Test Analyte Preparation 89
3.5 Results and Discussion 91
3.5.1 PVAc Sensing Layer characterization and response 91
3.5.2 WO_3 Sensing Layer characterization and response 98
3.5.3 Study of Effect of Humidity 115
3.5.4 Stability Analysis 117
3.5.5 Parametric Analysis of Fabricated Sensor 119
3.6 Conclusion 122
Chapter 4: Development of Breath Analyzer for Real-Time BTEX Detection 123
4.1 Abstract 123
4.2 Introduction 124
4.3 Methodology 128
4.3.1 Breath Analyzer Design 129
4.3.2 GC-MS Calibration 136
4.4 Results and Discussion 139
4.4.1 Parametric Analysis of the Developed Breath Analyzer 139
4.4.2 Correlation Analysis 144
4.4.3 Machine learning models for BTEX Classification 146
4.5 Conclusion 151
Chapter 5: Real-Time Testing and Validation of the Breath Analyzer 152

5.1 Abstract 152
5.2 Introduction 153
5.3 Methodology 158
5.3.1 Study Design 158
5.3.2 Sampling and Analysis 159
5.3.3 Statistical Analysis 161
5.4 Results and Discussion 162
5.4.1 Sensor Implementation and Validation 162
5.4.2 Data Analysis 169
5.4.3 Study Limitation 175
5.5 Conclusion 178
Chapter 6: Conclusions and Future Scope 180
6.1 Summary of Key Findings 180
6.1.1 Sensor Design and Performance 180
6.1.2 Portable Breath Analyzer Development 181
6.1.3 Validation Against GC-MS 182
6.1.4 Real-World Exposure Assessment 182
6.1.5 Machine Learning-Based BTEX Classification 185
6.2 Contribution of the Research to Occupational Health 185
6.3 Advantages and Limitations of the Study 186
6.4 Future Scope 189
6.4.1 Future Improvements in Sensor Design and System Integration 189
6.4.2 Potential Applications in Other Industries 190
6.4.3 Recommendations for Future Research 191
List of Publications 193
References 194
APPENDIX-A 216

LIST OF FIGURES

Figure 1.1 Pictorial representation of VOCs' presence in Oil and Gas Industries reported by research articles from 2012 to 2020. 3

Figure 1.2 GC-MS Technique for BTEX Detection. 9

Figure 1.3 Schematic of a Photoionization Detector. 10

Figure 1.4 Schematic of a Flame Ionization Detector 11

Figure 1.5 Structure of MOS gas sensor and electrochemical gas sensor. 12

Figure 1.6 Illustration of Quartz Crystal Microbalance sensor operation to detect nano-gram concentration of gas molecules on its surface... 13

Figure 1.7 Breath Analysis for VOC Detection. 17

Figure 2.1 PRISMA flowchart for screening research articles 32

Figure 2.2 (a) & (b) Source profile of BTEX concentration (ppm) during upstream, midstream, and downstream operations in ONG industries.. 49

Figure 2.3 Comparison of Limit of Detection (LOD) for different E-Nose sensors used for BTEX detection 67

Figure 3.1: Illustration of a 10MHz quartz crystal microbalance sensor 76

Figure 3.2 Functionalization of QCM sensor with Polyvinyl Acetate 82

Figure 3.3 Illustration of WO_3 Sputtering on QCM sensor surface. 83

Figure 3.4 Oscillator Circuit Design for 10MHz Crystal 85

Figure 3.5 Digital storage oscilloscope output of the uncoated QCM sensor signal from the oscillator circuit 85

Figure 3.6 (a) Gas Sensing Setup for Detection of BTEX vapors (b) Schematic Illustration of experimental BTEX Sensing Setup 87

Figure 3.7 (a) SEM images and (b) X-ray diffraction intensity profile of PVAc spin-coated on glass substrate at a spin speed of 1500rpm. 93

Figure 3.8 Concentration vs. frequency plot of QCM sensor functionalized with Polyvinyl acetate (QP1500) with different concentrations (2-10 ppm) at (27±1) °C, 16% RH, and standard atmospheric pressure……...96

Figure 3.9 PVAc varied thickness coated sensor response to three repeatable exposures of 10 ppm of Benzene. 97

Figure 3.10 (a) The step height of the WO_3 sputtered QCM sensor for a nine-minute deposition time. (b) Variation of thin film thickness with deposition time, (c) Frequency deviation of the sensor for BTEX at different sputtering deposition times.....100-101

Figure 3.11 XRD pattern of WO_3 deposited on Quartz crystal substrate …….103

Figure 3.12 FESEM Images of (a) Uncoated QCM electrode, (b) QCM electrode with WO_3 sputtered for 60 seconds, and (c) QCM electrode with WO_3 sputtered for 540 seconds. 104

Figure 3.13 Pore size distribution of QCM electrode with (a) WO_3 sputtered for 60 seconds, (b) WO_3 sputtered for 540 seconds.....105

Figure 3.14 (a) 2D surface Profiles, (b) 3D surface Profiles of Uncoated QCM Sensor, (c) 2D surface Profiles, (d) 3D surface Profiles of WO_3-coated (540 seconds) QCM Sensor. 106

Figure 3.15 Dynamic Adsorption Behavior of BTEX Compounds on WO_3-Coated QCM Sensor.....109

Figure 3.16 TGA thermogram of uncoated and WO_3-Coated QCM sensors..110

Figure 3.17 Sensitivity plot of WO_3 sputtered sensor after exposure to BTEX with different concentrations (2-10 ppm) at (27±1) °C, 16% RH, and standard atmospheric pressure. 112

Figure 3.18 Response-Recovery Characteristics of the WO_3-Coated Sensor (540 seconds) for (a) Benzene, (b) Toluene, (c) Ethylbenzene, (d) Xylene at (27±1)°C, 16% RH, and standard atmospheric pressure...112-113

Figure 3.19 WO_3 Coated QCM Sensor (540 seconds sputtered) and PVAc Coated QCM sensor (1500rpm spin coated) frequency deviation at different humidity values……116

Figure 3.20 Stability Assessment of (a) WO_3 Coated QCM Sensor (540 seconds sputtered) (b) PVAc Coated QCM sensor (1500rpm spin coated) exposed to BTEX Vapours. 117-118

Figure 4.1 Block diagram representation of the Breath analyzer. 129

Figure 4.2 (a) Schematic diagram of an electronic circuit for a 10 MHz QCM sensor array (b) Graphical user interface for the acquisition of QCM sensor array data (QCM sensor coated with PVAc (S0), uncoated QCM sensor (S1), and QCM sensor coated with WO_3 (S2)). 133

Figure 4.3 Experimental setup sample formation for GC-MS Analysis. 137

Figure 4.4 (a) Image of the portable BTEX detection system using a QCM-based electronic nose, (b) Response curve of PVAc and WO_3 coated QCM sensor when exposed to the normal breath sample (1 & 2) and breath sample of petrol station worker (3 & 4) (c) GC-MS chromatogram confirming BTEX compound. 142-143

Figure 4.5 Correlation Analysis of QCM sensor frequency deviation versus GC-MS peak area of (a) Benzene, (b) Toluene, (c) Ethylbenzene, (d) Xylene 145-146

Figure 4.6 Flowchart illustrating the execution flow of PCA and clustering analysis. 148

Figure 4.7 Clustering Results of QCM sensor-based e-nose system (a) k-Means (b) BIRCH. 150

Figure 5.1 Satellite image showing the location of petrol stations where breath sampling was performed. 158

Figure 5.2 Illustration of methodology for breath sampling using QCM-based breath analyzer and GC-MS. 159

Figure 5.3 Bland Altman Analysis graph of PVAc coated QCM sensor for (a) Benzene, (b) Toluene, (c) Ethylbenzene, and (d) Xylene. 163-164

Figure 5.4 Bland Altman Analysis graph of WO_3 coated QCM sensor for (a) Benzene, (b) Toluene, (c) Ethylbenzene, and (d) Xylene. 164-165

Figure 5.5 GC-MS peak area vs concentration plot of sample no 7 169

LIST OF TABLES

Table 1.1 VOCs emitted during different ONG operations. 2

Table 1.2 Key Structural, Physical, and Chemical Properties of BTEX Compounds……..……..6

Table 1.3 Health Risks Studies of VOCs in Oil and Gas Operations Reported in Research Articles 8

Table 2.1 Exposure Limits and Risk Assessment Parameters for BTEX 35

Table 2.2 Summary of emission studies performed during oil and natural gas operations in the US, Europe, and Africa.....43-44

Table 2.3 Summary of emission studies performed during oil and natural gas operations in Asia.....45-47

Table 2.4 Summary of Health Risk Assessment Studies to estimate LCR and HQ in different oil and natural gas operations 56-57

Table 2.5 Summary of observational studies on health effects of BTEX to workers of the ONG industry 61-62

Table 2.6 List of methodology for detection of BTEX in ambient air…..64-65

Table 3.1 Specifications of Quartz Crystal Microbalance sensor 77

Table 3.2 The parameters maintained for sputtering on a WO_3 thin layer onto the QCM sensor.....84

Table 3.3 Thickness of PVAc at varied spin coating speed. 92

Table 3.4 Comparison of Adsorption Energies (ΔEad in μeV) for BTEX Molecules on WO_3 Substrate in (3×3×1) WO_3 supercell and (5×5×1) WO_3 supercell Configurations. 103

Table 3.5 Adsorption Parameters and Molecular Properties of BTEX Compounds on WO_3-Coated QCM Sensor. 109

Table 3.6 Performance Comparison of PVAc and WO_3 Coatings for QCM Sensors in Detecting BTEX Compounds. 119

Table 3.7 Comparative analysis of optimized WO_3 sputtered QCM sensor against reported works on metal oxide sensors 120

Table 3.8 Comparative analysis of optimized PVAc spin-coated QCM sensor against reported works on polymer-coated QCM sensors. 121

Table 4.1 GC-MS Calibration data for Benzene, Toluene, Ethyl-Benzene, and Xylene 138

Table 4.2 Summary of Portable devices developed for real-time detection of BTEX. 141

Table 4.3 Performance Metrics of Various Clustering Algorithms applied to the QCM sensor array dataset. 149

Table 5.1 Comparison of Breath VOC Sampling and Analysis Methods Used in BTEX Exposure Studies……..……..157

Table 5.2 Concentrations of BTEX Compounds in Breath Samples of Petrol Station Workers…… …170

Table 5.3 Health Risk Assessment result of 20 samples of petrol station workers…….....173

Table 5.4 Concentrations in Breath Samples of Petrol Station Workers (n=20) and Statistical Significance Against Reference Values…….…..174

Table 6.1 Comparison of the PVAc-coated QCM sensor results with the GC-MS results for breath samples. 183

Table 6.2 Comparison of the PVAc-coated QCM sensor results with the GC-MS results for breath samples. 184

ABBREVIATIONS/NOTATIONS

mg/kg.day	milligram per kg per day
BTEX	Benzene, Toluene, Xylene, Ethylbenzene
CDi	Chronic Daily Intake
Ci	Average Daily Concentration
CL	Ceiling Limit
CO	Carbon monoxide
E-Nose	Electronic Nose
g/ml	gram per millilitre
H_2S	Hydrogen Sulphide
H_3O+	Hydronium ion
HR_i	Hazard Ratio
kPa	Kilo Pascal
LCR_i	Lifetime Cancer Risk
LOD	Limit of Detection
$m^3\ h^{-1}$	meter cube per hour
mg m^{-3}	milligram per meter cube
ml/min	millilitre per minute
MOS	Metal Oxide Semiconductor
NIOSH	National Institute of Occupational Safety and Health
OISD	Oil Industry Safety Directorate
ONG	Oil and Natural Gas
OSHA	Occupational Safety and Health Administration
PEL	Permissible Exposure Limit
ppb	parts per billion
ppmv	parts per million by volume
RC	Reference Concentration

REL	Recommended Exposure Limit
Sf	Slope Factor
STEL	Short-term Exposure Limit
TLV	Threshold Limit Value
TWA	Time Weighted Average
VOCs	Volatile Organic Compounds
PVAc	Polyvinyl Acetate
WO_3	Tungsten Oxide
sccm	Standard cubic centimetre per minute
PTFE	Polytetrafluoroethylene

PREFACE

The global energy sector fundamentally relies on the Oil and Natural gas (ONG) industry. This industry, despite its critical role in powering various international activities, is associated with significant environmental and occupational health hazards. A primary concern is the emission of Volatile Organic Compounds (VOCs), particularly Benzene, Toluene, Ethylbenzene, and Xylene (BTEX). These compounds are well-established air toxics that pose considerable risks to human health, including carcinogenic and other long-term systemic effects, and require rigorous monitoring and control. The core motivation for this thesis is to develop a portable system to monitor BTEX exposure among ONG workers and mitigate occupational health risks.

Chapter 1 of this thesis provides background, defines the problem statement, and outlines the research goal for developing a portable system for occupational safety. Traditional BTEX detection methods, such as Gas Chromatography-Mass Spectrometry (GC-MS), are highly accurate but are known to be bulky, expensive, and time-consuming. These limitations prevent real-time, on-site data collection, leading to monitoring gaps and delays in exposure assessments for workers. This research was motivated by the necessity to develop a portable, sensitive, and real-time solution for monitoring BTEX.

Chapter 2 systematically reviews BTEX emission profiles from upstream, midstream, and downstream ONG operations. It details their documented health impacts. It also evaluates existing detection techniques, including electronic nose (E-Nose) technology, which offers a practical approach to chemical sensing via arrays of chemical sensors and has emerged as a promising technology for real-time detection of BTEX. Quartz Crystal Microbalance (QCM) sensors were selected as

the primary sensing platform due to their high sensitivity to minute mass changes on a crystal surface. This principle renders QCM sensors highly suitable for detecting trace levels of BTEX.

However, uncoated QCM sensors lack the specific chemical selectivity required to differentiate between various VOCs, including closely related BTEX compounds. To address this, Chapter 3 meticulously details the optimization of active sensing layers by judiciously selecting and applying two distinct materials: Polyvinyl Acetate (PVAc) and Tungsten Oxide (WO_3). PVAc, an organic polymer, was chosen for its absorption characteristics and affinity for nonpolar volatile organic compounds. Its optimization involved precise control of spin-coating parameters to achieve desired film thicknesses and morphologies. Concurrently, WO_3, an inorganic metal oxide semiconductor, was investigated for its established gas-sensing properties at trace levels. The chapter provides a comprehensive analysis of the individual sensitivities, repeatability, and reproducibility of both PVAc-coated and WO_3-coated QCM sensors. This comparative performance evaluation assesses the strengths and weaknesses of the individual BTEX components, laying the foundation for the multi-sensor array design of the final breath analyzer. Following the successful development and characterization of the optimized QCM sensors, the next imperative was to integrate these components into a functional and portable analytical system. Chapter 3 also provides an outline of the experimental setup for testing the fabricated QCM sensor against BTEX. The experimental setup has a custom-fabricated sensing chamber, ensuring controlled exposure to gas samples. A crucial element for precise experimentation and accurate sample delivery was the design of a controlled gas inlet and outlet system to generate and deliver BTEX vapors at specific concentrations.

Chapter 4 details the design of a portable breath analyzer. This phase involved integrating diverse hardware and software modules to create an efficient unit engineered explicitly for real-time breath analysis in industrial environments. The system's architecture was designed with a focus on portability, robust data acquisition, and intelligent processing capabilities. The hardware design incorporates an array of optimized, fabricated QCM sensors. The development of any novel analytical instrument, particularly one intended for critical applications in occupational health, requires stringent validation to ensure accuracy, reliability, and precision. This crucial validation process constitutes the core of Chapter 4 and also details the calibration of the developed breath analyzer against GC-MS. GC-MS is universally recognized as the "gold standard" in analytical chemistry for the identification and quantification of volatile organic compounds, offering unparalleled accuracy and sensitivity. Chapter 4 elaborates on the meticulous experimental setup employed for this calibration. This included the precise preparation of BTEX gas standards of known concentration, a critical step to ensure the integrity of the calibration data. The central aspect of the calibration procedure involved simultaneously exposing both the developed breath analyzer system and the GC-MS to the prepared gas standards. This concurrent measurement methodology enabled a direct, real-time comparison of the breath analyzer’s frequency responses with the highly accurate concentration readings from the GC-MS. Beyond the physical hardware, Chapter 4 also covers the intricate software development, including the firmware for accurate sensor data readout and algorithms for signal processing and feature extraction, which are fundamental for converting raw sensor data into meaningful chemical signatures.

With the breath analyzer rigorously calibrated and its foundational accuracy confirmed in controlled laboratory settings, the next critical phase involved its evaluation in real-world environments. This comprehensive validation process is the central theme of Chapter 5. This chapter describes the practical deployment and performance assessment of the developed system, specifically focusing on its capability to detect and quantify BTEX compounds in real-time human breath samples. This chapter presents a statistical analysis of BTEX concentration variability. This statistical approach is employed to precisely assess the agreement between the QCM sensor measurements and the established GC-MS reference method for each BTEX compound.

The culmination of this doctoral research is presented in Chapter 6, which serves as a comprehensive synthesis of the entire investigation. This concluding chapter provides a concise summary of the key findings derived from the various stages of the research, from initial problem identification and sensor development to system integration and rigorous real-time validation. It quantifies the significant contributions this research makes to the critical field of occupational health and safety within the oil and natural gas industry. Beyond summarizing the achievements, this chapter offers a forward-looking perspective, outlining a range of potential improvements in sensor design and system integration. Chapter 6 concludes with specific recommendations for future research, identifying areas for continued investigation, technological refinement, and broader impact, thereby charting a roadmap for continued innovation in occupational exposure assessment.

Chapter 1: Introduction

1.1 Importance of BTEX Monitoring and Its Health Implications

The importance of Oil and Natural Gas (ONG) products is evident in every aspect of life. Workers at ONG extraction sites perform physically demanding work, often involving travel to remote locations, drilling, and well servicing, as well as exposure to hydrocarbon gases and vapors, an oxygen-deficient atmosphere, and the risk of fires and explosions. Inhalation of hazardous gases and vapors poses a significant occupational health risk to workers in the ONG industry[1]. Many workers are killed in the ONG operations in India, mainly due to gas leakage events as reported by OISD (Oil Industry Safety Directorate) under the Ministry of Petroleum and Natural Gas in India[2]. In addition to gas leakage, workers in these industries are exposed to hazardous pollutants, especially Volatile Organic Compounds VOCs [3], [4]. Different VOCs that are emitted during ONG operations are tabulated in **Table 1.1.** Analysis of the research work reported on the presence of significant concentrations of VOCs in the ONG industries, as summarized in **Figure 1.1**.

1.1.1 Prevalence of BTEX in the ONG Industry

Benzene, Toluene, Ethylbenzene, and Xylene (BTEX), which are carcinogenic, mutagenic, and teratogenic VOCs, are also released during ONG operations [5]. There are different sources of exposure to BTEX in ONG operations. Drilling of wells and construction of associated facilities are associated with the release of

trapped hydrocarbons, including BTEX, during drilling activities[6]. BTEX is reported to be present around the well pads [14].

Table 1.1 VOCs emitted during different ONG operations.

Alkanes	Alkenes
Ethane	Ethylene
Propane	Propylene
i-Butane	Trans-2-butene
n-Butane	1-Butene
Cyclopentane	Cis-2-Butene
i-Pentane	1-Pentene
n-Pentane	Trans-2-Pentene
2,2-Dimethylbutane	Isoprene
2,3-Dimethylbutane	Cis-2-Pentene
2-Methylpentane	1-Hexene
3-Methylpentane	Acetylene
n-Hexane	Aromatics
2,4-Dimethylpentane	Benzene
Methylcyclopentane	Toluene
2-Methylhexane	Ethylbenzene
Cyclohexane	m- and p-Xylene
2,3-Dimethylpentane	o- Xylene
3-Methylhexane	Styrene
2,2,4-Trimethylpentane	Iso-propylbenzene
n-Heptane	n-propylbenzene
Methylcyclohexane	m-Ethyltoluene
2,3,4-Trimethylpentane	p-Ethyltoluene
2-Methylheptane	1,3,5-Trimethylbenzene
n-Octane	o-Ethyltoluene
n-Nonane	1,2,4-Trimethylbenzene
n-Decane	1,2,3-Trimethylbenzene
n-Undecane	m-Diethylbenzene
n-Dodecane	p-Diethylbenzene

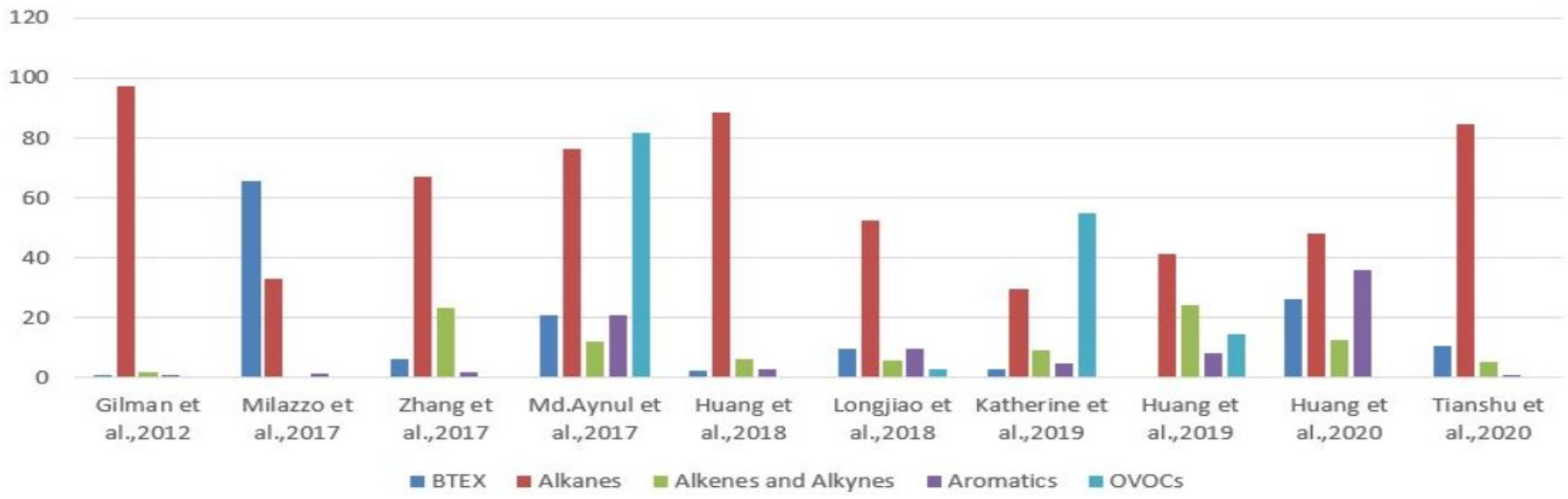

Figure 1.1 Pictorial representation of VOCs' presence in ONG Industries reported by research articles from 2012 to 2020.

Wellhead compressors, pneumatic devices, separators, and dehydrators release BTEX during ONG production and processing [6]. The processed fluid is stored in storage tanks where, with the help of the thief hatch, manual gauging and sampling are performed, and workers are exposed to BTEX [1], [7]. BTEX are released during charging/discharging, transportation, and crude oil washing operations of tankers. Crude desalting process, distillation, fluid catalytic cracking, catalytic reforming, alkylation, thermal cracking, catalytic hydrocracking, coking, isomerization, ether manufacture (MTBE), catalytic hydrotreating, and Chemical treating processes, such as sweetening and the Merox process, are some other techniques in which BTEX is emitted with wastewater[7]. The National Institute of Occupational Safety and Health (NIOSH) and the Occupational Safety and Health Administration (OSHA) identified several circumstances that can increase the risk of hydrocarbon exposure. In the United States, OSHA adopts and enforces health and safety standards, defining the Permissible Exposure Limit (PEL) as the maximum allowable exposure time for an employee to any chemical substance or physical agent, at 8 hours. Benzene is classified as a Group A pollutant and has a PEL of approximately one ppm, with a half-life (the time it takes for one-half of the chemical to be degraded) of about 10 days. The. The exposure limit for Toluene, xylene, and Ethylbenzene is about 100-200 ppm. The half-life of toluene and xylene can extend up to a few hours, but the half-life of ethylbenzene extends up to 2 days. **Table 1.2** gives structural information about BTEX.

Different control strategies have been employed for VOC abatement in ONG operations, including recovery, suppression, and destruction methods. A significant concentration of VOCs is reported even after adopting these methodologies [1], [6], [8].

Table 1.2: Key Structural, Physical, and Chemical Properties of BTEX Compounds.

Property Type	**Property**	**Benzene (C_6H_6)**	**Toluene (C_7H_8)**	**Ethylbenzene (C_8H_{10})**	**Xylenes (C_8H_{10}) (Ortho, Meta, Para isomers)**
Structural	Molecular Formula	C_6H_6	C_7H_8	C_8H_{10}	C_8H_{10} (for all isomers)
	Molecular Weight (g/mol)	78.11	92.14	106.17	106.17 (for all isomers)
Physical	Odor	Aromatic, characteristic, sweet	Sweet, pungent, benzene-like	Aromatic	Aromatic, characteristic
	Boiling Point (°C)	80.1	110.6	136.2	o-xylene: 144.4, m-xylene: 139.1, p-xylene: 138.4
	Melting Point (°C)	5.5	-95	-95	o-xylene: -25.2, m-xylene: -47.9, p-xylene: 13.3
	Density (g/mL)	~0.879 (at 20°C)	~0.867 (at 20°C)	~0.867 (at 20°C)	~0.86-0.88 (at 20°C, varies slightly by isomer)
	Vapor Pressure (mmHg)	~75 (at 20°C)	~22 (at 20°C)	~7 (at 20°C)	~6-16 (at 20°C, varies by isomer)
Chemical	Flammability	Highly flammable	Highly flammable	Flammable	Flammable
	Reactivity	Undergoes electrophilic aromatic substitution and hydrogenation.	Similar to benzene, but the methyl group activates the ring.	Similar to benzene, but the ethyl group activates the ring.	Similar to benzene, with two activating methyl groups.

1.1.2 Toxicity of BTEX Compounds

BTEX compounds exhibit varying degrees of toxicity. Benzene is a Group 1 carcinogen (IARC), causing cancer in humans and leading to haematological disorders like anaemia and leukaemia[9]. Toluene causes acute symptoms (dizziness, headaches) and potential long-term neurological effects[10], [11]. Ethylbenzene and xylene also pose health risks, including respiratory irritation and damage to the liver and kidneys[12].

1.1.3 Occupational Health Risks

Workers in the ONG industry face direct inhalation risks[13], leading to chronic health problems. Communities near ONG facilities experience indirect exposure through airborne emissions [14], [15]. Elevated benzene levels near gasoline stations highlight the significant cancer risk. Inhalation of BTEX in the occupational environment results in several health effects. Some health risk studies are reported in **Table 1.3** [11], [19], [20-25]. A more detailed discussion on the health effects of BTEX is presented in Chapter 2. Health effects of BTEX exposure include the risk of diseases such as lung, stomach, colon, and liver neoplasms, as well as symptoms like headache, dizziness, nausea, and insomnia. [11]. Exposure to BTEX is associated with an increased risk of cardiovascular disease, dyslipidemia, and leukocytosis, which negatively impact lipid profiles and white blood cell counts[21].

Table 1.3: Health Risks Studies of VOCs in Oil and Gas Operations Reported in Research Articles.

Place of investigation	Air pollutant	Criteria of Health Risk Assessment
Petrochemical industry in Iran[17]	Benzene, Toluene, Xylene	Estimation of the mean cancer risks of workers exposed to benzene, and non-cancer risks for BTX.
Canadian oil sands[14]	Benzene, Toluene, Ethylbenzene, Xylene, n-hexane, Acetone, Methanol, Acetaldehyde	Estimation of carcinogenic and non-carcinogenic risk estimates of identified VOC sources
Oil and gas exploration in Colorado (USA) [15]	56 VOCs, Benzene, and Ethylbenzene	Estimation of acute and chronic non-cancer hazard quotient and lifetime cancer risk of Benzene and ethylbenzene
Unconventional oil and natural gas operations[19]	Polyaromatic compounds and BTEX	Neurodevelopment and neurological health effects of VOCs

1.2 BTEX Detection Methods

1.2.1 Analytical Techniques

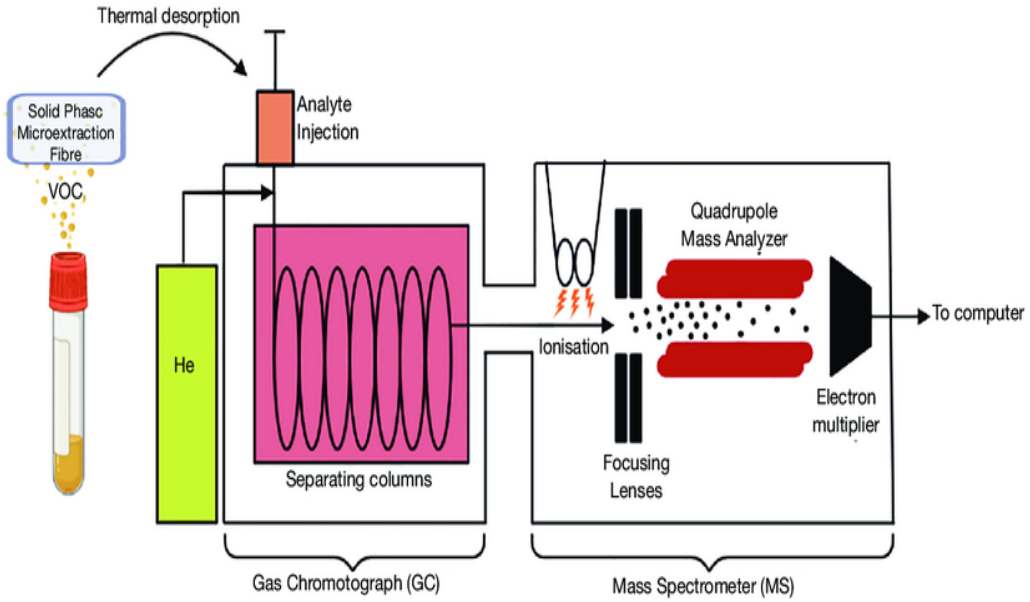

Figure 1.2 GC-MS Technique for BTEX Detection [22].

Gas Chromatography-Mass Spectrometry (GC-MS) is widely regarded as the gold standard for detecting BTEX compounds due to its high sensitivity and specificity, as it effectively separates volatile compounds through gas chromatography and identifies them via mass spectrometry. GC-MS is a two-step analytical technique that combines the principles of gas chromatography (GC) and mass spectrometry (MS). GC separates the components of a mixture based on their interaction with a stationary phase inside a chromatographic column. Compounds are eluted from the column at different times (retention times), creating a chromatogram that represents their relative abundance and retention characteristics. MS ionizes chemical

compounds to generate charged molecules (ions), which are then separated in a mass analyzer based on their mass-to-charge ratio (m/z). Solid-phase microextraction (SPME) is performed using an SPME syringe, which is inserted into the GC-MS column for further analysis, as shown in **Figure 1.2** [22]. However, GC-MS is time-consuming, often requiring several minutes to hours for analysis, and it depends on controlled laboratory conditions and skilled personnel, which limits its suitability for field use[11], [23]. It also involves high operational and equipment costs.

Photoionization Detection (PID), which utilizes ultraviolet light to ionize gas molecules for detecting VOCs (**Figure 1.3**[24]), including BTEX, offers faster detection but suffers from limitations such as susceptibility to interference from other compounds, poor selectivity between BTEX isomers, and calibration sensitivity influenced by environmental conditions, including humidity and temperature [24].

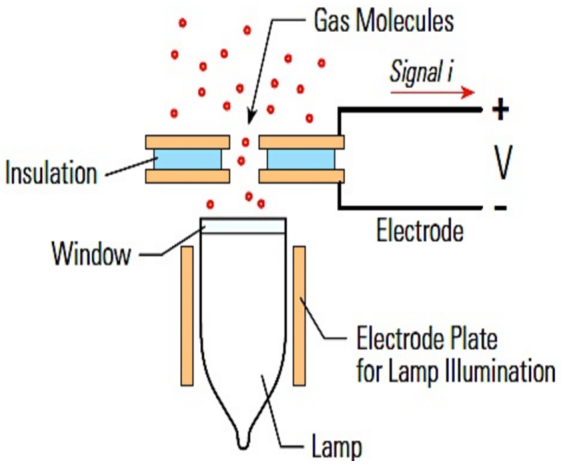

Figure 1.3 Schematic representation of a Photoionization Detector [25].

Flame Ionization Detection (FID) detects hydrocarbons by measuring ions formed during combustion in a hydrogen-air flame (**Figure 1.4[26]**). However, it lacks selectivity for individual BTEX compounds, poses safety risks due to its use of an open flame, and requires a complex, non-portable setup [26].

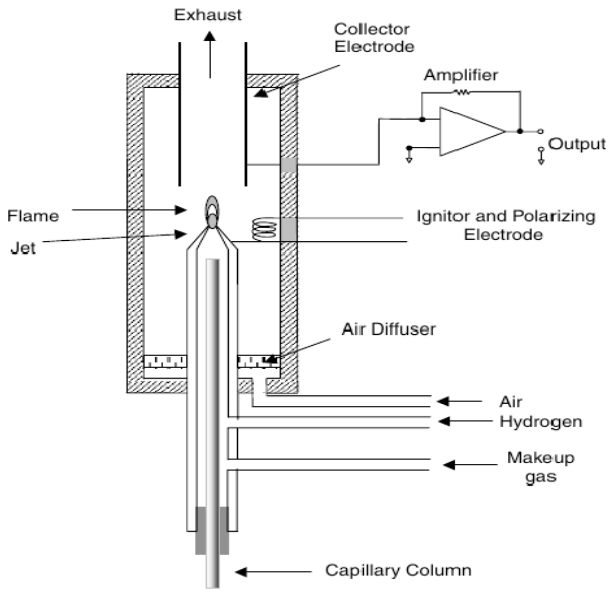

Figure 1.4 Schematic representation of a Flame Ionization Detector [27].

Thermal Desorption Gas Chromatography-Mass Spectrometry (TD-GC-MS), which enhances trace-level detection by combining thermal desorption with GC-MS, also shares similar drawbacks, including reliance on specialized, non-portable equipment, a lack of real-time monitoring capability, and high operational costs that can hinder widespread adoption [28].

Real-time sensor-based methods for detecting BTEX have attracted significant attention for their potential to monitor and assess exposure levels in diverse environments,

particularly in the oil and gas industry. These methods utilize various sensor technologies that offer rapid response times, portability, and the ability to operate in dynamic field conditions.

1.2.2 Resistive sensor

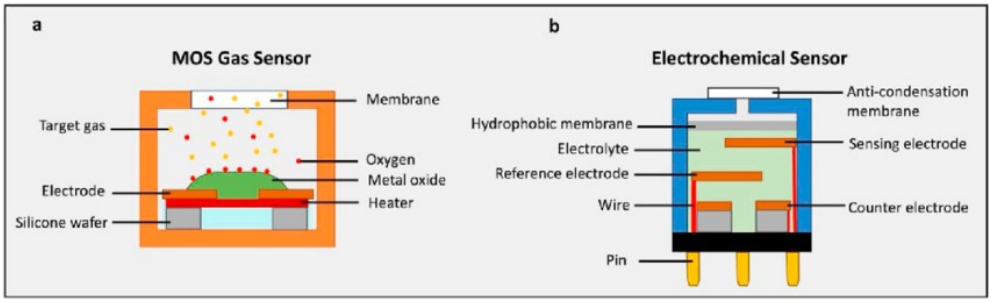

Figure 1.5 Structure of the MOS gas sensor and the electrochemical gas sensor[29].

Metal Oxide Semiconductor (MOS) and Electrochemical sensors are two common types of gas sensors that can function as resistive sensors for detecting BTEX compounds (**Figure 1.5[29]**). MOS sensors use a metal oxide layer (such as SnO_2 or WO_3) whose resistance changes in response to redox reactions with BTEX gases; at high operating temperatures (150–400 °C), oxygen adsorbs onto the surface and traps electrons, increasing resistance, while BTEX exposure reduces this resistance by donating electrons back through oxidation reactions. In contrast, electrochemical sensors operate at room temperature and detect gases via oxidation or reduction reactions at electrodes immersed in an electrolyte, generating a current proportional to the gas concentration. Although primarily amperometric, they can also exhibit changes in charge-transfer resistance, behaving like resistive sensors under certain conditions. While MOS sensors are low-cost and straightforward, with moderate

selectivity, they require high temperatures and are influenced by humidity. In contrast, electrochemical sensors offer higher selectivity and lower power consumption, but can have shorter lifespans and require regular calibration. Both sensor types can be optimized for BTEX detection using selective catalysts, electrode materials, and advanced signal processing techniques.

1.2.3 Quartz Crystal Microbalance sensor

Quartz Crystal Microbalance (QCM) sensors exhibit high sensitivity for detecting BTEX, as they respond to minute mass changes on the crystal surface when exposed to these volatile organic compounds. Operating at room temperature and requiring minimal power, QCM sensors are portable and suitable for real-time monitoring in various environments[35-37]. It also requires minimal sample preparation and provides rapid analysis, making it ideal for on-site applications. Additionally, integrating selective coatings enhances their ability to differentiate between BTEX compounds, ensuring accurate detection even in complex mixtures. Overall, QCM sensors offer a reliable, efficient, and cost-effective solution for monitoring BTEX levels, particularly in industrial settings where exposure risks are significant.

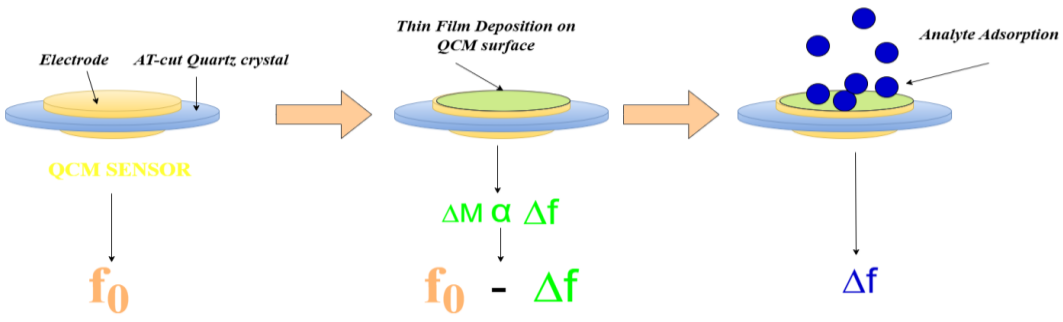

Figure 1.6: Illustration of QCM sensor operation to detect nano-gram concentration of gas molecules on its surface.

QCM sensors are piezoelectric materials that oscillate at a resonance frequency when an AC voltage is applied through metal electrodes. QCM is an acoustic sensor that operates in bulk thickness shear mode and can be used to analyze target molecules in both gaseous and liquid phases. AT-cut quartz crystals are used to fabricate QCM sensors operating at 10 MHz with a zero-temperature coefficient at room temperature. The crystal resonance frequency changes upon the deposition of the calculated mass amount on the electrode surface, as shown in **Figure 1.6**. This change in frequency can be calibrated to determine the properties of molecules deposited on the QCM surface by measuring a change in mass. The relationship between changes in frequency and changes in mass is expressed through the Sauerbrey **Equation (1.1)**.

$$\Delta f_g = -\frac{2f_0^2 \Delta M}{\rho_q \mu_q A} \quad (1.1)$$

where $\boldsymbol{\Delta f_g}$ is the change of resonance frequency after depositi $\boldsymbol{f_0}$ is the fundamental resonance frequency of oscillation, $\boldsymbol{\rho_q}$, $\boldsymbol{\mu_q}$ is density and shear modulus of quartz crystal, $\boldsymbol{\Delta M}$ represents change in mass and A represents active area for deposition of mass on electrode. QCM sensors are used for VOC detection because they can detect nanogram-level mass changes.

The choice of the quartz crystal's crystallographic cut is paramount to the performance of a QCM sensor. While quartz exhibits piezoelectricity, only specific cuts provide the required frequency stability for high-precision mass measurements. Among these, the AT-cut crystal, characterized by its orientation at 35° 15' to the Z-axis, is the industry standard for thickness shear mode resonators used in

QCMs[33]. The critical advantage of the AT-cut is its exceptional thermal stability. It exhibits a third-order dependence of resonant frequency on temperature, resulting in a zero-temperature coefficient of frequency (ZTCF) near room temperature. This significantly minimizes frequency drift caused by ambient thermal fluctuations, a non-negotiable requirement for sensitive measurements. In contrast, cuts like the BT-cut (rotated 49°), while simpler to manufacture, have a lower ZTCF and a more pronounced parabolic frequency-temperature curve, leading to much lower frequency stability.

This thermal stability directly translates to superior performance in terms of the following parameters:

Resonant Frequency Stability: The AT-cut maintains a highly predictable and stable baseline frequency, which is essential for accurate frequency-to-mass conversion.

Long-term stability is affected by aging, a slow, irreversible frequency drift caused by physical changes at the crystal surface, such as stress relaxation in the mounting material or electrode material deposition. To counteract aging and residual thermal drift, QCM systems often employ sophisticated temperature control and a two-crystal configuration (one reference crystal and one sensing crystal) to enable real-time compensation of non-mass-related frequency shifts, further improving measurement stability.

Crystal thickness and Sensitivity: As sensitivity is proportional to the square of the nominal frequency (f_0), and f_0 is inversely proportional to crystal thickness, AT-cut crystals are necessarily thinner (approximately 0.16 mm for a 10MHz crystal) to achieve high operating frequencies, thus maximizing sensitivity while retaining

sufficient mechanical stability for the application. Its stable operation and high Q-factor (quality factor) enable the detection of minute frequency shifts, thereby directly maximizing the sensor's mass sensitivity. Because sensitivity is inversely proportional to the crystal's nominal frequency, AT-cut crystals are typically chosen in the 5-10 MHz range to balance high sensitivity with robust mechanical handling. *Environmental Conditions:* For optimal operation of the QCM sensor, the room temperature (20˚C to 30˚C) should be maintained at standard atmospheric pressure. In a breath analysis application where high humidity (~90% at 34˚C) is inherent to the sample, active humidity measurement and compensation, or water removal, are essential steps.

1.3 Breath Analysis in BTEX Monitoring.

Human breath, comprising a complex mixture of gases and over 500 volatile components, serves as a direct conduit to an individual's metabolic state[34]. The fundamental principle lies in the three-stage breathing process, in which endogenous molecules produced by metabolic processes readily transfer from the blood into alveolar air and subsequently into exhaled breath [35]. The variations in the concentration of these molecules can indicate changes in metabolism or the presence of various diseases. This exact physiological mechanism enables the absorption of exogenous compounds, such as BTEX, into the bloodstream and subsequent excretion, providing a direct reflection of an individual's exposure to these compounds. Past research unequivocally demonstrates the efficacy of breath analysis in detecting disease-related biomarkers. For example, elevated VOCs like benzene are observed in lung cancer patients[36], [37], nitric oxide is exhaled in a

fractional amount by asthma patients[38], [39], acetone is abundant in diabetics [40], [41], increased level of pentane and carbon disulphide in schizophrenia patients[42], [43], [44] and ammonia is high in renal disease patients[36]. These findings underscore the capacity of breath to reveal crucial information about an individual's physiological and exposure status. Furthermore, breath analysis offers significant practical advantages: it is a non-invasive method that provides real-time results. Exhaled breath is sampled using a sensor; the sensor output is then processed and analyzed to interpret the compounds in the breath sample (**Figure 1.7**).

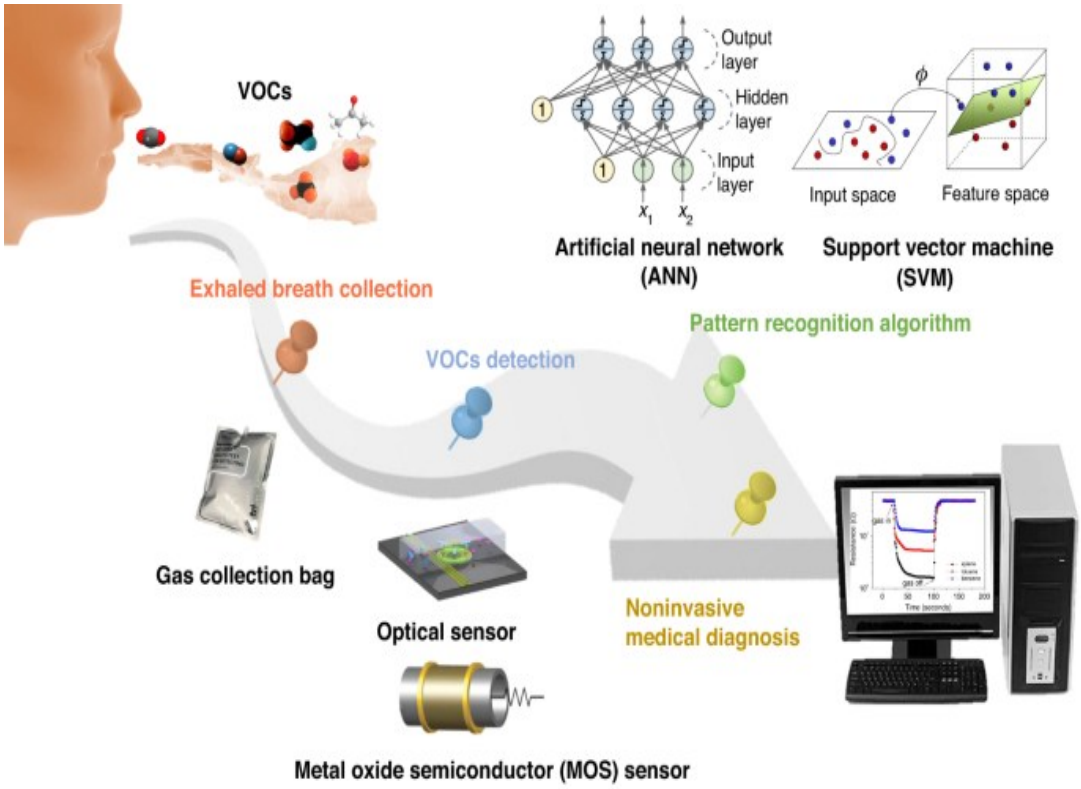

Figure 1.7 Breath Analysis for VOC Detection [45].

These benefits make breath analysis an ideal and efficient methodology for assessing occupational BTEX exposure. The Traditional methods of BTEX

detection, such as GC-MS, while highly sensitive and accurate, are often limited to laboratory settings due to their bulkiness, high costs, and time-consuming processes. This creates significant gaps in real-time monitoring, which is crucial for timely interventions to protect worker health [38-40]. By analyzing exhaled breath, the developed breath analyzer can provide a direct measure of internal exposure to BTEX compounds, thereby enhancing the accuracy of exposure assessments compared to those based on ambient air monitoring.

1.4 Research Gap

The thesis addresses several critical research gaps in the field of BTEX detection, particularly through the development of a breath analyser:

- *Limited Research in the Indian Context:* Although a growing body of literature exists on BTEX emissions and their health impacts globally, there is a notable scarcity of research specifically focused on the Indian oil and gas industry. This thesis aims to fill this gap by providing localized data on BTEX emissions and exposure levels, particularly in high-risk environments such as petrol stations and oil refineries.
- *Focus on Breath Analysis:* Most existing studies on BTEX detection have relied on traditional methods such as Gas Chromatography-Mass Spectrometry (GC-MS) or other laboratory-based techniques, which are often not feasible for real-time monitoring in occupational settings. This research introduces a novel approach: a portable breath analyzer that detects BTEX compounds in exhaled breath, providing a non-invasive, immediate assessment of exposure levels.

- *Field Validation with Petrol Station Workers:* By focusing on breath samples from petrol station workers—an occupational group known to be at high risk for BTEX exposure—the research provides valuable insights into the effectiveness of the developed breath analyzer. This aspect is particularly significant as there is limited research on the health impacts of BTEX exposure among petrol station workers in India.
- *Real-Time Monitoring Capabilities:* The development of a breath analyzer capable of real-time monitoring addresses a critical gap in existing detection methods. Traditional techniques often lack the immediacy required for timely interventions in occupational health settings. The breath analyser developed in this thesis can detect BTEX mixtures at levels below four ppm in less than 3 minutes, thus enabling prompt responses to elevated exposure levels.
- *Integration of Robust low-cost sensor:* There is a pressing need for cost-effective and energy-efficient monitoring solutions in the oil and gas industry, particularly in developing countries like India. The breath analyzer developed in this thesis aims to meet these requirements by providing a low-cost, low-power, and reliable device that can be easily deployed in various occupational settings, thus enhancing the feasibility of regular monitoring.

1.5 Research Objective

This research aims to address the identified gap by developing and validating a portable breath analyzer for real-time detection of BTEX. The specific objectives include:

- *Designing and fabricating highly sensitive QCM sensors:* This involves optimizing the deposition methodologies for Polyvinyl Acetate (PVAc) and Tungsten Oxide (WO_3) thin films on QCM sensors.
- Characterizing their sensing properties, including sensitivity, repeatability, reproducibility, and selectivity to BTEX compounds.
- *Developing a portable breath analyzer system:* This objective encompasses the design and integration of a compact device comprising a Teflon sensing chamber, a data acquisition unit, and a purging unit, ensuring low power consumption and ease of operation under ambient conditions.
- *Calibrating and validating the developed system:* This involves conducting rigorous correlation analysis between the QCM sensor responses and GC-MS measurements to ensure the accuracy and reliability of the sensor for quantitative BTEX detection across various concentrations.
- *Implementing machine learning models for BTEX classification:* This objective focuses on utilizing advanced analytical techniques, such as PCA and clustering algorithms (K-Means, BIRCH), to effectively classify and distinguish individual BTEX compounds based on the sensor array's responses.
- *Performing real-time testing and validation with human breath samples:* This crucial objective involves conducting a pilot study using exhaled breath samples from individuals, such as petrol station workers, to evaluate the system's performance in a real-world scenario and assess occupational exposure to BTEX.

1.6 Dissertation Outline

The proposed dissertation will be structured into several interconnected chapters, each building upon the previous one to systematically address the research objectives and culminate in a comprehensive understanding and practical solution for BTEX monitoring in the breath of oil and natural gas (ONG) workers.

Chapter 1: Introduction

This chapter sets the context for the research, emphasizing the importance of BTEX monitoring in occupational environments such as petrol stations and refineries. The chapter identifies a research gap in portable real-time detection systems. The objectives include designing a selective sensor system, developing a breath analyzer, and validating it through a real-world application. The chapter concludes with a structured outline of the thesis flow.

Chapter 2: BTEX Exposure and Occupational Health Monitoring – A Comprehensive Review

This review chapter explores the toxicological properties of BTEX compounds, their sources in oil and gas operations, and exposure routes in ONG operations. It evaluates current monitoring technologies and highlights their limitations in field applications. The chapter discusses the BTEX emission profile, emerging technologies such as electronic noses (E-noses), and their advantages for VOC detection. It concludes with an overview of research perspectives.

Chapter 3: Sensor Design and Fabrication for BTEX Detection

This chapter presents the design and development of a QCM sensor for detecting BTEX. Two selective sensing materials—polyvinyl acetate (PVAc) and tungsten oxide (WO_3)—are deposited on QCM crystals using spin coating and sputtering.

Material characterization techniques, such as SEM, TGA, and response analysis, are used to assess morphology, chemical interactions, and sensor performance. The sensors are evaluated for sensitivity, selectivity, and repeatability.

Chapter 4: Development of a Breath Analyzer for BTEX Detection

This chapter details the hardware and software implementation of the breath analyzer system. The device is designed to be compact, portable, and battery-operated. A Graphical User Interface (GUI) was also developed for real-time monitoring and logging. The system is calibrated against standard BTEX mixtures using GC-MS to ensure analytical reliability. Data from sensor responses is processed using machine learning algorithms.

Chapter 5: Real-Time Testing and Validation of the Breath Analyzer

A pilot study was conducted among petrol station workers, in which breath samples were collected and analyzed in real time using the developed breath analyzer. This chapter compares the breath analyzer response to BTEX concentrations with the GC-MS results. The breath analyzer exhibited reliable differentiation between sample groups. Challenges such as breath-sample variability, environmental interference, and field-deployment logistics are also discussed.

Chapter 6: Conclusions and Future Scope

This final chapter summarizes the key findings, including the successful development and validation of a low-cost, real-time breath analyzer for detecting BTEX. The research makes a significant contribution to the field of occupational health monitoring, particularly for industries with VOC exposure risks. The chapter highlights potential future improvements, including the use of AI-based data interpretation and integration with wearable health systems.

Chapter 2: BTEX Exposure and Occupational Health Monitoring: A Comprehensive Review

2.1 Abstract

The ONG industry emits VOC such as BTEX, which pose health risks to workers. This study analyzed peer-reviewed research articles to provide BTEX emission profiles from the three primary ONG operations and their associated health risks. PRISMA (Preferred Reporting Items for Systematic Reviews) was used to choose relevant articles for this review paper. The analysis revealed that in ONG operations, upstream operations involving gas flaring (benzene: 0.115±0.1 ppmv; toluene: 0.029±0.001 ppmv; ethylbenzene: 0.002±0.001 ppmv; xylene: 0.123±0.001 ppmv) contributed to lower BTEX emissions. Meanwhile, midstream operations involving tanker loading (benzene: 5.391±28.670 ppmv; toluene: 10.376±48.929 ppmv; ethylbenzene: 1.583±6.563 ppmv; xylene: 2.067±9.211 ppmv) contributed to significant BTEX emissions. On the other hand, downstream operations involving refinery operation zone (benzene:3.5 ± 1.69 ppmv, toluene: 4 ± 0.87 ppmv, ethylbenzene: 1.2 ± 0.24 ppmv, xylene:6.6±1.34 ppmv) and refueling station (benzene:1.164±0.408 ppmv, toluene 2.394±1.086 ppmv, ethylbenzene:1.301±0.779 ppmv, xylene: 1.736±0.898 ppmv) exhibited higher BTEX emissions. A Lifetime Cancer Risk (*LCRi*) for benzene was greater than 10^{-6} near gasoline pump stations (1400×10^{-6}) and loading operations (160×10^{-6}).

Ethylbenzene also had a significant LCR_i value of 1×10^{-6} during loading operations. Other ONG activities, such as gas flaring, inspection operations, and gasoline station pumps, have Hazard Ratios > 1. The study highlights BTEX emissions in all three ONG sectors, with significant contributions from midstream tanker loading and downstream refinery and refueling stations. E-nose techniques are promising for BTEX detection due to their real-time measurement capabilities and ease of use. Some Asian countries have reported benzene concentrations exceeding permissible limits during tanker loading and refueling operations. Overall, BTEX emissions are a cause for concern and should be addressed in ONG operations.

2.2 Introduction

The oil and natural gas (ONG) industry primarily involves the processing and handling of hydrocarbons, exposing workers to significant occupational hazards [5-7]. Given the inherent risks, monitoring occupational health is paramount to safeguard workers' productivity and well-being. However, mere monitoring alone is insufficient; it must serve as a foundation for proactive prevention of hazardous exposures. During exploration, transportation, storage, and processing of crude oil and natural gas, numerous light and heavy hydrocarbons, including dangerous Volatile Organic Compounds (VOCs) such as benzene, toluene, ethylbenzene, and xylene (BTEX), are released into the atmosphere [8-11]. While BTEX compounds are significant contributors, aliphatic compounds, though less hazardous, are more abundant in the overall spectrum of VOCs released from ONG activities. In the ONG industry, inhaling BTEX compounds during various

operations poses significant health risks to exposed workers. Benzene, a recognized human carcinogen, can induce adverse health effects ranging from dizziness and headaches to a rapid heart rate. Chronic exposure increases the risk of anemia and leukemia [12-16]. Toluene, another BTEX component, presents acute symptoms such as light-headedness, euphoria, and confusion, with chronic exposure potentially leading to unconsciousness and even death [10]. Inhalation of ethylbenzene can cause immediate irritation of the eyes, nose, and throat, while long-term exposure may harm the liver, kidneys, and central nervous system [18-20]. Xylene isomers contribute to respiratory irritation, and chronic exposure may have adverse effects on the nervous and respiratory systems [21-24]. These health risks extend to workers engaged in various ONG operations, including drilling, production, transportation, refining, and distribution. Furthermore, nearby communities may face risks if ONG facilities are located in residential areas, as BTEX emissions can travel through the air, potentially exposing residents, particularly those living downwind of these operations, to chronic exposure [66]. The toxicity profiles of BTEX underscore the importance of considering exposure concentrations when assessing their effects, underscoring the need for comprehensive reviews of their hazardous properties.

This chapter aims to provide a comprehensive analysis of inhalation risks associated with ONG emission sources, with a specific focus on workers involved in various aspects of ONG operations. The ONG industry is broadly categorized into three primary operations: upstream, midstream, and downstream. In upstream operations, BTEX emissions occur during activities such as identifying and evaluating potential oil and gas reservoirs, drilling wells, and transporting

hydrocarbons to processing facilities [26-28].

Notably, fracking fluids used in extraction represent significant sources of BTEX, releasing these compounds during the high-pressure injection process in hydraulic fracturing [29-30]. Gas flaring, a common industry practice, releases BTEX during the open-air burning of petroleum or solution gas [31-33]. Crude oil itself is a natural source of BTEX, and low concentrations of these compounds are present in groundwater near oil and gas deposits [75].

BTEX emissions are also prevalent during midstream operations, which involve the transportation and storage of crude oil and natural gas. Volatile BTEX compounds escape into the atmosphere during tank filling processes, and storage tanks are significant sources of BTEX, as these compounds are released during the storage of petroleum and natural gas [35-38].

Downstream operations in the ONG industry involve refining, processing, storage, and distribution of petroleum products and petrochemicals. Refining crude oil into various products in downstream operations releases BTEX [39-40]. The separation of hydrocarbons through fractional distillation, conversion processes like cracking and reforming, and purification methods to remove impurities all contribute to the release of BTEX compounds. Additionally, blending with additives to improve product performance can further increase BTEX emissions. Equipment leaks from flanges, valves, seals, lines, and connections are also sources of fugitive BTEX emissions [53], [82]. Refueling stations are also a significant source of BTEX emission [83].

Different control strategies, primary and secondary vapor recovery technologies, suppression, and destruction techniques, have been adopted for VOC abatement in ONG operations [53]. Techniques used in the recovery process to collect, store, and reuse VOCs include membrane separation, condensation, adsorption, and absorption. Suppression techniques use gelling material foams (polyurethane-type foam, thin-film surface-active material, aqueous foam, clay nanoparticle-embedded aqueous foam) to provide a barrier against VOCs. Destruction techniques utilize thermal incineration, photocatalytic oxidation, plasma techniques, electron beam technology, biofiltration, and flares to convert VOCs into simple, safe compounds, such as carbon dioxide and water. However, many studies on BTEX emission and associated health risks have been reported even after adopting these methodologies. The chapter outlines the impact of BTEX on operations, segregated into upstream, midstream, and downstream segments. We have analyzed studies published after 2010 to provide an updated summary of peer-reviewed literature on BTEX emissions and their health impacts among workers involved in ONG operations. A comprehensive review of these studies can provide a more current understanding of the occupational health risks posed by BTEX compounds in various streams of ONG operations. Identifying and mitigating BTEX emissions across the ONG industry's operational phases is essential to ensuring sustainable, responsible practices in this sector.

2.3 Methodology

2.3.1 Selection Criteria

This systematic review aims to answer research questions defined using PECO criteria [84]. This criterion includes and excludes articles for analysis in this study.

2.3.1.1 Inclusion Criteria

Study Population (P): Workers employed in the oil and gas industry, including those engaged in upstream, midstream, or downstream operations. 1) Studies were conducted on both male and female workers. 2) Studies conducted on workers of all age groups.

Exposure (E): The occupational exposure of workers to BTEX compounds in the oil and gas industry. Studies that measure BTEX exposure levels using different monitoring techniques.

Comparison (C): The comparison is implicitly addressed by examining the relationship between BTEX exposure and health outcomes within the same population of oil and gas workers.

Outcome (O): The potential health effects or risks associated with BTEX exposure in oil and gas industry workers.

Study Design: Only observational studies, including cross-sectional, cohort, and case-control designs, will be considered. The studies must be published in peer-reviewed journals or reputable scientific sources.

2.3.1.2 Exclusion Criteria

Irrelevant Population: Studies focusing on populations other than oil and gas industry workers (e.g., general population, laboratory animals) were excluded.

Irrelevant Exposure: Studies that do not investigate the occupational exposure of workers to BTEX compounds in the oil and gas industry were excluded. Studies that did not provide clear information on BTEX exposure or that used other exposure sources were excluded.

Non-English Studies: Studies published in languages other than English were excluded due to limitations in translation resources.

Studies with Insufficient Data: Studies with insufficient data (sample sizes < 5, or incomplete or inadequate reporting of data and methods) to assess the relationship between BTEX exposure and health outcomes were excluded.

Animal Studies: Studies conducted solely on laboratory animals were excluded, as the focus is on human oil and gas workers.

This study discusses available techniques and emerging methodologies for detecting BTEX in ONG operations.

2.3.2 Literature Search Strategy

This review paper presents a systematic search to gather comprehensive information on BTEX emissions, health risks, and detection techniques related to BTEX exposure in ONG operations. The PRISMA diagram, as illustrated in **Figure 2.1** [85], represents the systematic search and screening process to select relevant articles for this review**.** A systematic search was conducted from 2010 to 2023 in the following databases and resources: Scopus, ISI Web of Knowledge, PubMed, Embase, Cochrane Library, and Google Scholar. The Publish and Perish software was utilized to extract articles from these databases. Hazardous VOC guidelines and emission limits were studied in reports from international and national agencies, including OSHA, NIOSH, and OISD. Three keyword sets were used for article extraction. For articles related to BTEX emission in ONG operations, the keywords included BTEX, "benzene toluene ethylbenzene xylene," "emission," "inventory," "flaring," "hydraulic fracturing" "pollution," "production," "gasoline station," "fuel station," "petrochemical," and variations of terms related to petrol, petroleum, oil, natural gas, and refinery. For health effects associated with BTEX emission, the keywords involved "oil," "petrol*," "natural gas," "health," "disease," "cancer," "hazard quotient," "lifetime cancer risk," "risk assessment" "carcinogenic" "biomarkers" "respiratory" "inhalation" "exposure" "fuel station" "gas station" "refinery" "petrochemical" and concentrations of specific BTEX compounds. For identification of articles related to VOC/BTEX detection techniques, keywords included "sensor," "monitoring," "sampling," "analysis" "gas chromatography" "mass spectroscopy" "detection," "sensitivity," "concentration,"

and variations of terms related to BTEX, Benzene, Toluene, ethylbenzene, xylene, oil, petrol, and natural gas.

The systematic review, conducted following PRISMA guidelines, identified 1233 articles across various databases (**Figure 2.1**). After removing duplicates, 1202 articles were screened based on titles, resulting in the exclusion of 830 non-BTEX-related articles. Abstracts of the remaining 372 articles were reviewed, leading to the exclusion of 214 articles related to occupational exposure to BTEX and BTEX sensing mechanisms. A full-text review of 158 articles was conducted, of which 86 were excluded for various reasons, including an irrelevant population or exposure, non-English studies, and insufficient data, as detailed in "Selection criteria". The final selection included 72 articles, categorized into BTEX emission studies (28), BTEX health effects studies (21), and exposure detection studies (29). In the BTEX emission and health effects studies, eight studies were common, including both emission analyses and health risk assessments conducted among fuel station workers. A total of 72 articles were considered for review. **Figure 2.1** gives a detailed flowchart of the study selection process.

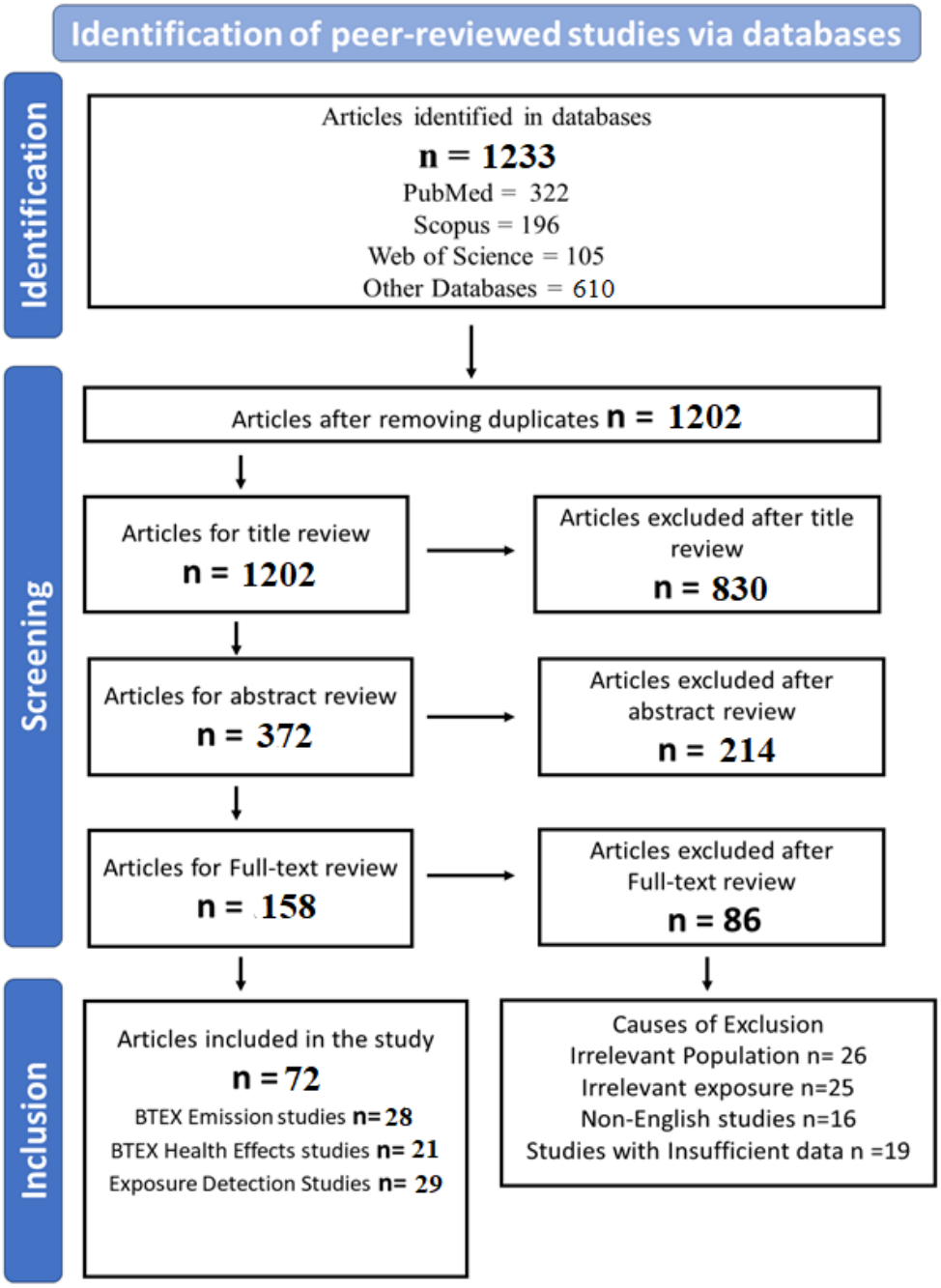

Figure 2.1 PRISMA flowchart for screening research articles

2.3.3 Quality Assessment

A risk-bias analysis was conducted on 35 studies on BTEX emissions and their health effects on ONG workers [86]. It focused on critical parameters, including blinding of outcome assessment (detection bias), incomplete outcome data (attrition bias), selective reporting (reporting bias), and other potential biases. These different biases encompassed selection bias (analysis is not representative of the broader population from which it is drawn), Measurement bias (possible limitations or inaccuracies in the analytical methods), Confounding bias (influence of unmeasured or uncontrolled factors), and publication bias (likelihood of reporting significant or positive results over non-significant or negative findings). The risk bias graph (A.1) indicated high risk for detection bias and other biases, primarily due to the prevalence of observational studies on BTEX emissions in the ONG industry. Therefore, the quality assessment of the included studies may downgrade the quality of evidence by 1 level, given severe limitations reported by the authors.

2.3.4 Exposure Guidelines

Several international agencies have established formal exposure limits for BTEX (**Table 2.1**). For example, OSHA [87] adopts and enforces the standard permissible exposure limit (PEL) for employees, defined as the maximum exposure to any chemical substance or physical agent that an employee may experience during an 8-hour workday.

Similarly, the threshold limit value (TLV), defined as the maximum 8-hour time-weighted average exposure limit to a hazardous material that a healthy worker can be exposed to without experiencing any occupational safety and health effects, was established by the American Conference of Governmental and Industrial Hygienists [88]. In addition, the National Institute of Occupational Safety and Health [89] recommended Exposure Limits (RELs) to OSHA as new acceptable exposure levels. These exposure limits include three subcategories: Time-Weighted Average (TWA), Ceiling Limit (CL), and Short-Term Exposure Limit (STEL). TWA is measured by sampling the worker's breathing zone for the entire workday and dividing the exposure value by 8 to account for an 8-hour test. The CL is the highest permissible level of a hazardous pollutant that should never be exceeded throughout the working day. The Short-Term Exposure Limit (STEL) is the maximum allowable concentration of a dangerous substance to which workers can be exposed for a short period (15 minutes) during the workday. STELs complement the time-weighted average (TWA) exposure limit by providing additional protection against short-term spikes in concentration. The chemical's half-life is also an essential parameter for determining its persistence in the Environment. The half-life of a pollutant is defined as the time it takes for one-half of the chemical to degrade. The half-life of benzene is 3-10 days [90].

Table 2.1 Exposure Limits and Risk Assessment Parameters for BTEX

Compound	Chronic non-cancer inhalation level RC_i (mg/m^3)	Carcinogenicity				Half Life (days)	Exposure Limits for BTEX			
		[e]EPA	[i]IARC	Inhalation Unit Risk $(\mu g/m^3)^{-1}$	Inhalation Cancer Slope Factor $(mg/kg/day)^{-1}$		[g]PEL (ppm)	[h]TLV (ppm)	[c]RELs	
									TWA (ppm)	STEL (ppm)
Benzene	0.03	GROUP A	1	0.0000078	[d]0.0027	3-10	1	0.5	0.1	1
Toluene	5	GROUP D	3	—	—	0.5-2.7	200	20	100	150
Ethylbenzene	1	GROUP D	2B	—	[d]0.0087	03-10	100	20	100	125
Xylene	0.1	GROUP D	3	—	—	5.6 hours	100	20	100	150

[a]US EPA Integrated Risk Information System (IRIS) [c]National Institute for Occupational Safety and Health (NIOSH) [d]Risk Assessment Information System(RAIS) [e]EPA Cancer Classification [g]Occupational Safety and Health Administration [h]American Conference of Governmental Industrial Hygienists [i]International Agency for Research on Cancer (IARC).

2.3.5 Health Risk Assessment

The BTEX health risk is evaluated in terms of hazard ratio (to quantify non-cancer risk) and lifetime cancer risk (to quantify cancer risk) from direct or indirect exposure. Slope Factor refers to a measure of the cancer-causing potential of a substance or exposure, usually expressed as the increase in the risk of developing cancer per milligram per kilogram of body weight per day, as per Risk Assessment Guidance for Superfund RAGS PART A and PART F [91]. The United States Environmental Protection Agency has developed slope factors for many chemicals, including benzene and ethylbenzene. The slope factor for benzene is 0.0027 per milligram per kilogram of body weight per day and 0.0087 per milligram per kilogram per day for ethylbenzene [92], which means that for every milligram of benzene per kilogram of body weight that a person is exposed to every day over a lifetime, the estimated increase in the risk of developing cancer is 0.027%. The carcinogenic Potency is estimated using the inhalation unit risk (IUR) [91]. The IUR $(\mu g/m3)^{-1}$ represents the incremental lifetime cancer risk estimated to result from continuous inhalation exposure to a unit concentration of a particular chemical in the air. Benzene is classified as a Group 1 carcinogen by the International Agency for Research on Cancer (IARC), meaning it is a known human carcinogen. Ethylbenzene is classified as a Group 2B carcinogen by the IARC, which means it is possibly carcinogenic to humans. The Hazard Ratio (HR_i) is evaluated using **Equation (2.1)** [93],

$$HR_i = \frac{C_i}{RC_i} \tag{2.1}$$

C_i is the average daily Concentration, and RC_i is the Reference Concentration of a particular VOC. If the value of HR_i is significantly less than 1, it is unlikely to cause health effects from airborne hazardous toxic substances [51], [53-54]. However, long-term exposure may produce non-carcinogenic harmful health effects with HR_i values greater than one [55-57]. The Hazard Index (HI) is calculated as the summation of *HRi*. A HI value of less than one is considered acceptable [51], [53-54]. **Equation (2.2)** can be used to determine the chronic daily intake (CD_i) value in mg kg^{-1} day^{-1} [93].

$$CDi = \frac{C \times I \times E \times f \times Ly}{B \times Lt \times N} \quad (2.2)$$

$$LCRi = CDixSf \quad (2.3)$$

Here, C= mean concentration (mg m^{-3}), I= inhalation rate (m3 h^{-1}), E= exposure duration (h $week^{-1}$), f = exposure frequency (week $year^{-1}$), Ly= number of years of exposure (year), B= Body weight (kg), Lt = mean lifetime (years), N=No of days in the year. Lifetime cancer risk (LCR_i) can also be calculated by multiplying the value of CD_i by the slope factor (Sf) for benzene and ethylbenzene, as shown in **Equation (2.3)**. An LCR_i value greater than 10^{-6} is considered a definite risk, and a value less than or equal to 10^{-6} is considered acceptable [92]. The risk is also classified as definite (LCRi> 10^{-4}), probable ($10^{\wedge-4}$ to 10^{-5}), or possible (10^{-5} to 10^{-6}) [58-59].

2.3.6 Detection and Analysis Methods

NIOSH Method 1501 is one of the standardized analytical techniques for BTEX analysis in occupational Environments[99], [101]. This method collects air samples using sorbent tubes containing coconut-shell charcoal as the solid adsorbent. After sample collection, the sorbent tubes are desorbed with a suitable solvent to extract the BTEX compounds. The extracted samples are then analyzed by Gas Chromatography (GC), in which the analytes are separated based on their physical-chemical properties. The separated compounds are detected using a flame ionization detector (FID) or mass spectrometer (MS). Calibration with standard reference gas mixtures ensures the accurate quantification of BTEX compounds.

In addition to the GC-MS method, other analytical techniques are widely used for the detection and quantification of BTEX compounds, viz., photoionization detection (PID)[102], flame ionization detection (FID)[103], thermal desorption gas chromatography-mass spectrometry (TD-GC-MS), proton-transfer-reaction mass spectrometry (PTR-MS)[23]. GC-MS involves separating analytes based on their physical-chemical properties, followed by mass spectrometric detection, providing both identification and quantification. FID and TD-GC-MS are two different analytical techniques used in GC to detect and analyze BTEX. TD-GC-MS combines thermal desorption, gas chromatography, and mass spectrometry to detect trace levels of compounds. FID measures the concentration of hydrocarbons and other organic compounds by detecting ions produced during combustion in a hydrogen-oxygen flame.

PID methodology uses ultraviolet (UV) light to ionize and detect BTEX compounds. PTR-MS is a direct mass spectrometric technique for detecting BTEX in ambient air. It involves the reaction of analyte molecules with H_3O+ ions in a drift tube, producing protonated analyte ions, which are then detected by the mass spectrometer.

Additionally, significant advancements in BTEX detection have led to the emergence of novel analytical techniques. Some of these new methodologies include metal oxide sensors (MOX sensors)[104], field effect transistors (FET)[105], conducting polymer sensors[106], surface acoustic wave (SAW) sensors[107], quartz crystal microbalance sensors (QCM)[108], optical sensors (Infrared sensor, surface plasma resonance (SPR) sensor, colorimetric sensors and spectroscopic methods) [69-72] and Portable GC[113], a miniaturized version of traditional GC that separates and quantifies BTEX. An Electronic-Nose (E-Nose) uses different sensors, as mentioned above, to detect trace levels of BTEX and is an emerging alternative for real-time detection of compounds [114].

MOS, FET, and conducting polymer sensors are specific chemo-resistive (CR) gas sensors that operate on the principle of changes in electrical resistance due to gas interactions [115]. SAW sensors and QCM sensors are considered gravimetric sensors, which operate on the principle that when mass is added or removed from the sensing element, it leads to a change in the resonant frequency of the sensor [116]. Optical sensors for BTEX detection exploit interactions between light and specific materials or molecules to detect and quantify BTEX compounds [117].

2.4 Results and Discussions

2.4.1 Sources of emission

Based on 22 articles screened for emission analysis, this review presents a comprehensive overview of these studies conducted in different regions, to measure the concentrations of BTEX in the upstream, midstream, and downstream operations **(Table 2.2)** and **(Table 2.3)**.

In the US, Europe, and the African region, some emission studies were conducted in the near areas of upstream operations, focusing on natural gas development and drilling activities, using the US EPA guidance to estimate BTEX emissions for regions near the wells. McKenzie et al. (2012) conducted a study in a natural gas development area (directional drilling and hydraulic fracturing) in Colorado, focusing on BTEX concentrations near natural gas wells [118]. The study suggests that closer proximity to natural gas wells poses greater health risks from air emissions associated with natural gas development. Though Benzene levels were reported to be < 0.001 ppmv near natural gas wells, the findings can be extrapolated to assess occupational exposure risk. Gilman et al. (2013) and Colborn et al. (2014) conducted a study near natural gas wells in Colorado in 2011 [120], [121], in which BTEX concentrations were significantly below PELs. Colborn et al. (2014) highlight potential air quality concerns in areas where natural gas drilling occurs, and Gilman et al. (2013) provide valuable insights into overall VOC emissions from ONG operations, including BTEX compounds. In Canada,

Bari et al. (2018) focused on emissions near the oil sands region, analyzing ambien30 30-minute levels and employing receptor models to identify emission sources [122]. Oil sands fugitives, liquid/unburned fuel, and petroleum processing were identified as oil sands-related emissions. Maximum Benzene concentrations were < 0.001 ppmv, and toluene, ethyl benzene, and Xylene concentration values were within permissible limits. An emission study conducted in Spain by Ramírez et al.2012 near an industrial complex (with an oil refinery) also reported a lower concentration of BTEX[122]. Moolla et al.(2015), monitored BTEX concentrations at a diesel refueling bay in Johannesburg, South Africa, using gas chromatography coupled with a photoionization detector[124] The results indicate the concentration of benzene (0.313±0.015 ppmv) were of concern at the refueling site On the other hand, many studies reported BTEX emissions during ONG operations in Asian countries. Mirrezaei & Orkomi (2020) performed a health risk assessment of BTEX emissions from gas flaring in Iran's South Pars gas complex [126]. Benzene's maximum 1-hour median concentration exceeds its NIOSH RELs, whereas its annual average concentration is lower.

Studies conducted in China by Chen et al. (2020), Tong et al. (2020), and Zheng et al. (2018) provided insight into VOC exposure in oil and gas regions and refineries.[57], [90-91]. The study by Zheng et al. (2018), aimed to assess the levels, compositions, and sources of VOCs in an oil and gas station in northwest China over a year-long period. The study showed main sources of VOCs (BTEX) were natural gas (62.6%), fuel evaporation (21.5%), combustion sources (10.9%), oil refining processes (3.8%), and asphalt (1.3%). BTEX concentration within OSHA limit values. Chen et al. (2020) reported emissions near the oil and natural

gas exploration region in China's Yellow River Delta. The toluene concentration was higher when sampling was performed in winter than in summer. Tong et al. (2020) investigated refinery operations at five sites: an aromatic hydrocarbon extraction device (AEHD), disproportionation and transalkylation devices (DATD), an isomerization reaction device (IRD), an adsorption separation device (ASD), and a xylene fractionation device (XFD). The study reported a higher benzene concentration near AEHD (0.673±0.213 ppmv). Jalilian et al. 2022b) conducted air sampling in an Iranian oil refining company and applied risk assessment methods to evaluate the health risks for workers [129]. The results showed that employees were exposed to BTEX pollutants during their work, and benzene (0.3176±0.001 ppmv) had the highest risk ranking compared to toluene, ethylbenzene, and xylene.

Table 2.2 Summary of emission studies performed during oil and natural gas operations in the US, Europe, and Africa

Reference	Country	Year of Study	Description (Distance from ONG site)	Location /Operation	Sample collection duration (Analysis Methodology)	Sample collection frequency	Time of day	Season	Benzene (ppmv)	Toluene (ppmv)	Ethylbenzene (ppmv)	m,p-Xylene (ppmv)	o-Xylene (ppmv)
Upstream operations													
McKenzieLM (2012)	United States (Colorado)	2008-2010	Natural Gas Development area (>800m)	Natural gas wells (directional drilling, hydraulic fracturing)	24 hour (GC-FID)	6 days for 1065 days	All day	All seasons	<0.001	0.001±0.006	<0.001	<0.001	<0.001
			Well Completion (40m to 150m)		24-27 hours (GC-FID)				0.002±0.014	0.007±0.067	<0.001	0.007±0.194	0.001±0.04
Gilman (2013)	United States (Colorado)	2011	Air Quality Monitoring near oil and natural gas wells (300m)	Oil and natural gas wells (production)	5 minute (GC-MS)	30min for 19 days	All day	Winter	<0.001	<0.001	<0.001	<0.001	<0.001
Colborn (2014)	United States (Colorado)	2010-2011	Near Natural gas wells (1.1 Km)	Natural gas wells (drilling and hydraulic fracturing)	24-hour/4 hour (GC-MS)	Every 7 days for 487 days	12 noon - 12 noon /10:00 AM-2:00 PM	All seasons	<0.001	0.001±0.0009	—	<0.001	—
Bari (2018)	Canada (Alberta)	2010-2015	Regional Air Quality (Fort McKay <20km)	Oil Sands (production)	24 hours (GC-MS)	1-in -12 days (2010-2011) Every 6 days (2012-2015)	All day	All seasons	<0.001	0.003±0.009	<0.001	0.001±0.002	<0.001
			Regional Air Quality (Fort McMurray >30km)						<0.001	0.003±0.011	<0.001	0.001±0.002	<0.001

Midstream and downstream operations													
Ramirez (2012)	Catalonia (Spain)	Oct-2008 - Jan-2009/ Oct - 2009 - June-2010	Industrial Complex [site 1]	Industrial Complex (Oil refinery)	24 hours/2 hours	394 days/24 days	All day	Winter /Autumn /spring	0.001±0.003	0.002±0.004	0.001±0.005	0.001±0.001	<0.001
			Industrial Complex [site 2]		(GC-MS)				0.001±0.001	0.004±0.015	0.001±0.008	0.001±0.001	<0.001
			Industrial Complex [site 3]						<0.001	0.001±0.0002	<0.001	<0.001	<0.001
Moolla (2015)	Johannesburg (South Africa)	June - August 2013	Diesel Refuelling Bay	Refuelling bay (Distribution)	24 hours	91 days	All day	Winter	0.313±0.015	0.188±0.11	0.637±0.162	0.85±0.286	
					(GC-PID)								
*The values are presented in (mean±Standard deviation) or (median±Standard deviation) unless stated.													

Table 2.3: Summary of emission studies performed during oil and natural gas operations in Asia

Reference	Country	Year of Study	Description (Distance from ONG site)	Location /Operation	Sample collection Duration (Analysis Methodology)	Sample collection duration	Time of day	Season	Benzene (ppmv)	Toluene (ppmv)	EthylBenzene (ppmv)	m,p-Xylene (ppmv)	o-Xylene (ppmv)
Upstream operations, Midstream and Downstream operations													
Mirrezaei (2020)	Asalouyeh gas refinery (Iran)	2013-2014	Gas Flaring (100 Km)	Gas Refinery Complex (Production & Refining)	24 hour (GC-FID)	7 days	All day	All seasons	*[1h]0.115±0.1* *[an]0.001±0.0001*	*[1h]0.029±0.001* *[an]0.007±0.0001*	*[1h]0.002±0.001* *[an]0.013±0.001*	*[1h]0.123± 0.001* *[an]0.002±0.0001*	
Chen (2020)	Yellow Delta River (China)	2017	Oil Field (10Km)	Oil and Natural Gas Exploration	30 seconds	Every 2-3 hours for 90 days	07:00 to 19:00 local time (LT)/06:00 to 21:00 LT	Winter-Spring	0.001±0.0005	0.014±0.05	0.006±0.001	0.001±0.004	<0.001
		2017			(GC-FID/GC-MS)			Summer	<0.001	<0.001	<0.001	<0.001	<0.001
Heibati (2017)	Northern (Iran)	2016	Tank Loading operation	Oil Distribution Company (Tank loading and gauging)	8 hours	30 days	8-hour working shift	Winter	5.391±28.670	10.376±48.929	1.583±6.563	2.067±9.211	
			Tank Gauging Operation		(GC-FID)				0.83±4.76	1.28±6.472	0.192±0.651	0.274±0.616	
Heibati (2017)	Northern (Iran)	2016	Tank Loading operation	Oil Distribution Company	8 hours	30 days	7:00 AM-3:00 PM	Winter	5.390±8.602	10.876±15.331	1.583±2.837	2.067±3.037	

			Tank Gauging operation	(Tank loading and gauging)	(GC-FID)				`0.830±1.827	1.209±2.430	0.193±0.227	0.274±0.202	
Zheng (2018)	North West (China)	2014-2015	Oil Refining Operations	Oil and Gas Station (Production & Refining)	2 hour (GC-FID)	365 days	All day	All seasons	0.001±0.001	0.001±0.001	<0.001	<0.001	<0.001
Chaiklieng (2019)	Khon Kaen (Thailand)	2018	Fueling Operations	Gasoline station (Distribution)	8 hours (GC-FID)	250 days	8 hour working shift	Winter	0.031±0.022	—	—	—	
			Cashier						<0.001±0.002				
Harati (2020)	Iran	2016	Petrochemical Operation	Petrochemical Industry (Distribution)	8 hours (GC-FID)	3 hours	3 hour in working shift	Winter	2.12±0.95	9.84±2.53	—	11.87±4.44	
Harbi (2020)	Hawalli (Kuwait)	2013	Pump	8 Gasoline Stations (Distribution)	12 hour (GC-MS)	Two consecutive days	8:00AM to 8:00PM	Summer	0.723±0.0001	0.545±0.0001	0.373±0.0001	0.71±0.0011	
			Gasoline Station workers						0.135±0.0012	1.812±0.0011	1.606±0.0001	3.3±0.0001	
Tong (2020)	Hawalli (Kuwait)	2014	AHED	Refinery Complex (Distribution)	24 hour (GC)	6 days	9:00 AM-12:00 PM	Summer	0.673±0.213	0.024±0.04	0.415±0.092	0.039±0.011	
			DATD						0.975±0.3	0.063±0.02	0.023±0.007	0.026±0.007	
			IRD						0.03±0.009	0.02±0.021	0.018±0.008	0.034±0.01	
			ASD						0.027±0.007	0.014±0.002	0.02±0.004	0.016±0.004	
			XFD						0.12±0.021	0.69±0.08	0.031±0.003	0.438±0.318	
Molaei (2020)	Garmsar (Iran)	2018	Packing operation	Secondary Oil re-refining Plant (Distribution)	2-3 hour (GC-FID)	Every 6 hour	8:00 AM-2:00 PM	Spring-Winter	0.035±0.006	0.027±0.003	0.006±0.001	0.018±0.002	
			Filteration operation						0.045±0.006	0.033±0.005	0.008±0.001	0.02±0.006	
Chaiklieng (2021)	Khon Kaen (Thailand)	2018	Dispensing operations	Gasoline station (Distribution)	4 hours (GC-FID)	24 hour	Each working shift	Summer	0.033±0.460	0.142±1.577	0.114±0.106	0.041±0.480	
Jalilian (2022)	Abadan (Iran)	2020	Refinery operation	Oil refining company	8 hours (GC-FID)	Every 4 hour	Morning	All seasons	0.3176±0.001	0.4011±0.001	0.6645±0.001	0.1034±0.001	
Yousefi (2022)	Mashhad (Iran)	2018	Dispensing operations	Gasoline station (Distribution)	1 hour 15 minutes (GC-FID)	24 hour	Morning, noon, night	Autumn	0.872±0.457	0.928±0.369	0.482±0.187	0.262±0.096	
Khoshakhlagh (2023)	Khuzestan (Iran)	2021	Refinery operation	Oil refinery Complex (Distribution)	8 hours GC-FID	Beginning, Middle and End of workshift for summer and Winter	Beginning, Middle and End of workshift	Summer	0.963±1.663	3.739±5.929	2.103±3.974	1.838±2.746	
								Winter	0.480±0.640	1.699±2.703	1.377±2.598	1.504±3.030	

Alimohommadi (2023)	Karaj (Iran)	2021	Dispensing operations	Fuel station (Distribution)	90 minutes	Beginning, Middle and End of workshift for summer and Winter	Beginning, Middle and End of workshift	Summer	1.164±0.408	2.394±1.086	1.301±0.779	1.736±0.898	
					GC-FID			Winter	1.248±0.492	2.496±1.107	1.407±0.710	1.798±0.898	
Kumari (2023)	Delhi (India)	2021-2022	Dispensing operations	Petrol Pump (Distribution)	1 hour	Every alternate week for 211 days	Afternoon	Winter	0.112±0.054	0.219±0.159	0.085±0.02	0.104±0.076	0.095±0.066
					(GC-FID)								

[1h]one hour average concentration [an]annual average concentration AHED=aromatic hydrocarbon extraction device DATD=disproportionation and transalkylation devices IR= isomerization reaction device ASD = adsorption separation device XFD=xylene fractionation device *The values are presented in (mean±Standard deviation) or *(median±Standard deviation)* unless stated.

Chaiklieng et al. (2019 &2021) published studies for Benzene exposure at gasoline stations in Thailand in winter and in summer highlighting potential risks to gasoline station workers [130]-[131], Molaei et al.(2020), conducted a study from personal samples of workers in secondary oil re-refining unit in Iran and reported concentration for benzene (0.035±0.006 to 0.045±0.006) near the worker breathing zone [97]. Heibati et al. (2017) studied tanker loading and gauging operations at an oil distribution company in Iran and reported a significantly higher benzene concentration (5.391±28.670) [132]. The study was conducted during the winter season. Al-Harbi et al. (2020) noted that the benzene concentration at gasoline stations (0.723±0.0001) exceeded both the NIOSH REL of 0.1 ppmv and the AGCIH TLV of 0.5 ppmv [135]. The study by Kumari et al. (2023) investigated the concentrations of BTEX compounds at a fuel station in India after implementing a vapor recovery system (VRS) [82]. The results indicated that toluene had the highest average concentration (0.219±0.159), followed by benzene (0.112±0.051), xylene (0.103±0.075), and ethylbenzene (0.019±0.004). Yousefi et al. (2022) conducted a similar study to investigate the air emissions of benzene, toluene, ethylbenzene, and xylene (BTEX) at 13 gas stations in Mashhad, Iran.[133] The study found that the mean benzene concentration (0.872±0.457) exceeded the NIOSH REL and the AGCIH TLV. Harati et al. (2020) sampled workers' breathing zones in the petrochemical industry in Iran and found that the average benzene concentration (2.12±0.95 ppmv) exceeded the TLV [134].

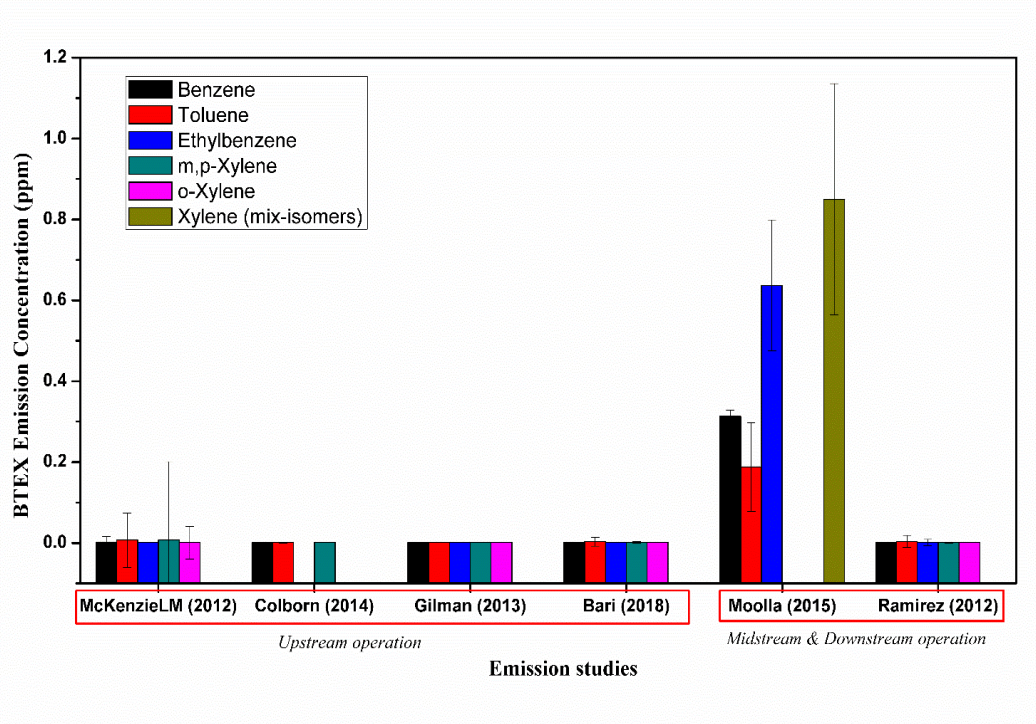

(a)

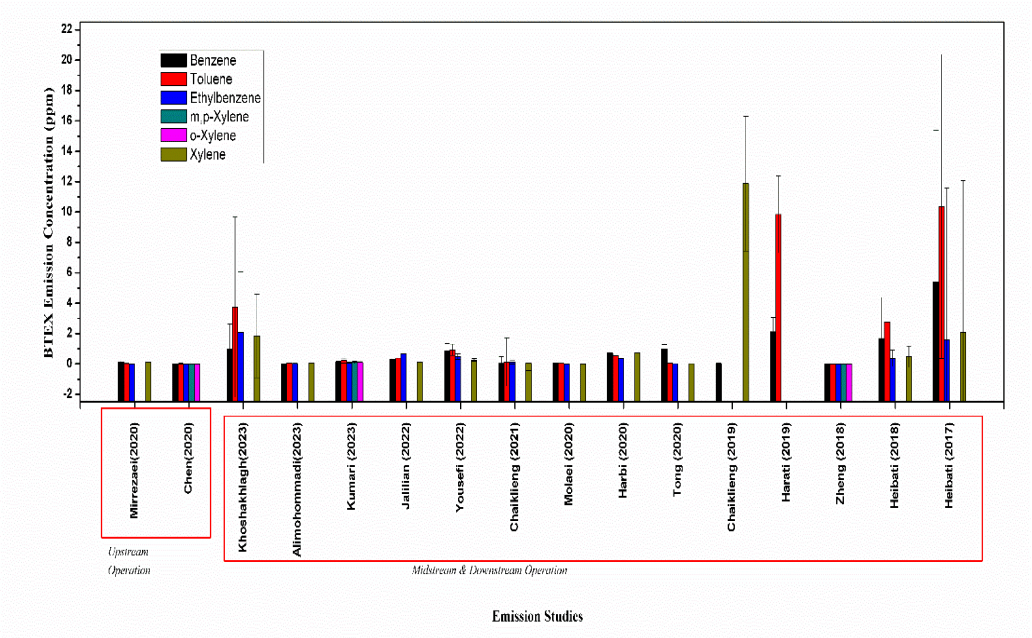

(b)

Figure 2.2 (a) & (b) Source profile of BTEX concentration (ppm) during upstream, midstream, and downstream operations in ONG industries.

Alimohammadi et al. (2023) assessed occupational exposure to BTEX compounds among workers at gasoline fuel distribution stations in Karaj [135]. The study identified a high concentration of benzene in the breathing zone of gasoline station workers both in summer and winter. Similarly, Khoshakhlagh et al. (2023) collected air samples from workers' breathing zones in an oil refinery and reported a high benzene concentration (0.963±1.663 ppmv) [136].

In this review, articles were segregated based on upstream, midstream, and downstream operations (**Figure 2.2(a) & (b)**), and the concentration of BTEX was reported in ppmv. As indicated in Figure 2.3, emissions from upstream operations involving the gas flaring (benzene: 0.115±0.1 ppmv, toluene: 0.029±0.001ppmv, ethylbenzene: 0.002±0.001ppmv, xylene: 0.123± 0.001ppmv); Midstream operation involving tanker loading (benzene: 5.391±28.670 ppmv, toluene: 10.376±48.929 ppmv, ethylbenzene: 1.583±6.563 ppmv, xylene: 2.067±9.211 ppmv), downstream refinery operation zone (benzene: 3.5 ± 1.69 ppmv, toluene: 4 ± 0.87 ppmv, ethylbenzene: 1.2 ± 0.24 ppmv, xylene: 6.6 ± 1.34 ppmv) and refueling station (benzene: 1.164±0.408 ppmv, toluene 2.394±1.086 ppmv, ethylbenzene: 1.301±0.779 ppmv, xylene: 1.736±0.898 ppmv) contributes to the significant BTEX emission. Most of the BTEX emissions in downstream operations are from workers' breathing zones. Upstream operations reported lower BTEX emissions concentrations than midstream and downstream operations. Possible reasons for lower reported BTEX emissions during upstream operations could be improved emission controls, such as closed-loop drilling systems and vapor recovery units, local weather conditions, topography, atmospheric dispersion, and the distance of monitoring locations from the well sites, which is

farther away, resulting in lower measured concentrations at monitoring sites. The concentrations of benzene, a known carcinogen, are relatively low, and any exposure should be minimized as much as possible. While toluene and xylenes are not classified as carcinogens, they can influence metabolism because they share a metabolic pathway with benzene [137]. This can potentially increase the amount of time that known carcinogens like benzene and ethylbenzene stay in the body, which may indirectly increase the risk of cancer. Overall, the presence of significant concentrations of toluene, xylenes, and ethylbenzene, along with low levels of benzene, suggests a potential health risk associated with these emissions, particularly their potential to influence the metabolism of known carcinogens in the BTEX mixture.

Various studies highlight the environmental risks associated with waste treatment methods such as evaporation ponds, sludge pits, and burn pits, which contribute to BTEX emissions. Ziaei Seginsara and Khazini's (2021) study on refinery wastewater treatment ponds observed substantial BTEX emissions, particularly benzene, toluene, and xylene, which pose health risks to refinery staff and local communities[138]. Nyieku et al. (2024) discuss the presence of dissolved organics in produced water, including BTEX, which, if inadequately treated, can result in occupational hazards to workers and affect aquatic life[139]. Nasiri et al. (2017) emphasize that while compact treatment systems like hydrocyclones are suitable for oil-water separation, they do not effectively manage dissolved organics, a limitation when dealing with evaporation ponds that expose BTEX to the environment[140]. Nath et al. (2023) suggest that gravity-based separators (e.g., API separators) often fail to remove smaller hydrocarbon particles, underscoring

the need for advanced treatment at sites using evaporation ponds [141]. Al-Mebayedh et al. (2022) focus on oilfield sludge pits, where volatile hydrocarbons rapidly evaporate, especially under sunlight, necessitating containment strategies to reduce atmospheric release[142]. Penuelas and Lo (2024) examine the various pathologies linked to burn pit emissions, highlighting the urgent need for further research to understand the chronic effects of these toxic exposures on respiratory and neurological health[143]. This concern is reinforced by Woskie et al. (2023), which reveals that a substantial majority of over 475,000 veterans deployed in Iraq and Afghanistan were exposed to burn pits, reflecting the extensive use of these disposal methods and the associated risks[144]. Despite this widespread exposure, there has been limited research specifically addressing the harmful emissions of BTEX from these waste treatment methods.

This study also examines the geographic distribution of BTEX impacts in ONG and finds that BTEX concentrations were generally below permissible limits in the United States and Europe. In contrast, in Asian countries, tanker loading and dispensing operations reported significantly higher BTEX concentrations exceeding allowable limits. The results are bimodal, with some studies reporting BTEX concentrations within permissible limits and others exceeding exposure limits, indicating a complex, heterogeneous picture of emissions in the oil and gas industry. The variability in emission levels can be attributed to several factors, including differences in geographical locations, specific operational practices, the implementation of safety measures, and the use of different technologies.

2.4.2 Health effects of BTEX

The 21 reviewed studies encompassed health risk assessments of BTEX in a wide range of locations, including oil refineries, petrol stations, gas flaring sites, petrochemical industries, and natural gas development projects. The risk assessments were conducted using different methodologies, including US EPA guidelines, probabilistic risk assessments, and specific analytical methods such as gas chromatography. Peer-reviewed research articles focusing on health risk analysis associated with BTEX exposure are tabulated in **Table 2.4**.

Few studies have focused mainly on health risk assessment by analyzing air samples from workers' breathing zones [93], [95], [109-110], [111-112]. These studies consistently reported elevated LCR_i and HQ values, indicating increased health risks from exposure to hazardous air pollutants among workers. Studies on petrol station workers in Thailand [146] and gasoline station workers [145], [148] have reported elevated LCR_i and HQ values for BTEX compounds, particularly benzene and ethylbenzene, indicating a potential risk of cancer and non-cancer health effects due to exposure. Tunsaringkarn et al. (2012) conducted a cross-sectional study to assess the risk of BTEX exposure at gasoline stations in Thailand and implemented an intervention involving mask use and handwashing [148]. The study reported elevated LCR_i (2.15×10^{-4}) and HQ (1.68) values for benzene, suggesting a potential cancer risk. Kitwattanavong et al. (2013) employed a quantitative observational design to estimate the occupational health risk of petrol station workers [146]. The LCR_i values for benzene (4.13×10^{-5} to $3.57 \times 10^{\wedge-4}$) and ethylbenzene ($2.3 \times 10^{-6}$ to 9.02×10^{-6}) were high, indicating an increased risk of cancer from exposure. Chaiklieng et al. (2019) assessed the health risks of

BTEX exposure among gasoline station workers in Thailand. They reported maximum LCRi (1.5×10^{-4}) and HQ (1.82) values for benzene, which exceeded acceptable levels for fueling operation [145]. Heibati et al. (2017) collected breath samples from tanker loading and gauging workers, drivers, and firefighters in an oil distribution [152] company in Iran and demonstrated elevated LCR_i (13.07×10^{-6} to 56.69×10^{-6}) and HQ (4.87 to 30.46) values for benzene, indicating potential health risks in various work areas. Partovi et al. (2018) analyzed air samples collected from multiple workers' zones: sealing, loading, quality control, and safety operations at a national oil distribution company in Iran [147]. For workers involved in the sealing and loading operations, the LCRi values for Benzene (160×10^{-6} to 170000×10^{-6}) were significantly higher, indicating an increased risk of developing cancer from benzene exposure. Additionally, during quality control, elevated LCRi values for benzene were observed, suggesting a potential health risk for workers involved in these operations. Moreover, the HQ values for toluene and xylene were also elevated in the Quality control operation, further highlighting non-cancer health risks for workers in this area. Regarding workers involved in safety operations, higher HQ values were reported for xylene and toluene, indicating potential non-cancer health risks from exposure to these pollutants. Kumari et al.(2023) analyzed Cancer Risk (CR) and noncancer health risk (HQ) associated with exposure to BTEX compounds for fuel station workers in India [83]. The study finds that the average concentration of BTEX at the fuel station is in the order of toluene > benzene > xylene > ethylbenzene. The 7-month average CR value of benzene exceeds the acceptable range of LCR_i, indicating increased cancer risk for workers. The HQ value for benzene also exceeds the

acceptable value, indicating an increased non-cancer health risk. The HI value for BTEX was also greater than 1, which indicates adverse health effects for workers. Harati et al. (2020) assessed health risks related to exposure to VOCs and hydrogen sulfide (H_2S)in the petrochemical industry in Iran [134]. The study identified benzene as posing the highest risk among the studied chemical substances. The mean cancer risk for workers exposed to benzene was estimated to be higher than the acceptable standard, indicating a potential for increased cancer risk. Non-cancer risk for BTEX was also found to be higher than the acceptable standard. Khoshakhlagh et al. (2023) collected air samples from workers' breathing zones of the oil refinery, specifically those working in the catalytic reforming unit, kerosene transportation area, new transportation area, gasoline post-treatment unit, alkylation unit, wastewater treatment plant, and distillation units [136]. The study found that BTEX concentrations were higher in the summer than in the winter season for all workstations, especially for toluene and ethylbenzene. The mean exposure to benzene for repairmen and site men exceeded the threshold limit value in both seasons. Non-carcinogenic risk values exceeded acceptable levels for several compounds in both seasons, and definite carcinogenic risk was indicated for benzene and ethylbenzene exposure in all workstations in both seasons.

Table 2. 4 Summary of Health Risk Assessment Studies to estimate LCR and HQ in different oil and natural gas operations

Reference	Type of participants	Sampling Scenario	Sampling Duration	No of Samples	[a]Cancer Risk		[b]Hazard Quotient				
					Benzene	EthylBenzene	Benzene	Toluene	EthylBenzene	m,p-Xylene	o-Xylene
Tungsaringkarn (2012)	Workers involved in gasoline station in Thailand	Samples were collected from 6 gasoline station of 24 workers	8 hour	12	DR	—	UAR	—	—	—	—
Kitwattanavong (2013)	Petrol Station workers at six petrol station in Thailand	Two Personal Samples from each workers and one sample from ambient air in petrol stations	8 hour	36	PBR	PR	—	AR	—	AR	
Heibati (2017)	Tank loading workers	Samples were taken from workers equipped with personal samplers from 4 stations in oil distribution company	8 hours	16	*DR		*UAR				
	Tank gauging workers			6	*DR	—	*AR				
	Drivers			5	*PBR	—	*AR				
	Fire-Fighters			5	*PBR	—	*AR				
	Office Workers			18	*PBR	—	* AR				
Partovi (2018)	Security worker	Samples were collected from the breathing zone of workers of Nationa oil distribution company in Iran	8 hour	—	PBR	PR	—	AR	—	UAR	
	Inspection gate worker				PBR	PR	—	AR	—	AR	
	Sealing operator				PBR	PR	—	AR	—	UAR	
	Safety officer				PBR	PBR	—	UAR	—	UAR	
	Quality control officer				PBR	DR	—	UAR	—	UAR	
	Deep handling worker				PBR	PBR	—	AR	—	UAR	
	Loading worker				DR	`DR	—	UAR	—	UAR	
Chaiklieng (2019)	Fueling	Samples were collected from breathing zone of Gasoline station workers	8 hour	137	DR	—	UAR	—	—	—	
	Cashiers			13	DR	—	AR	—	—	—	
Harati (2020)	Petrochemical workers	Samples were collected from the breathing zone of workers	3 hour	120	DR	—	UAR	UAR	—	UAR	
Harbi (2020)	Pump station worker	Breathing Zone of workers	12 hours	—	DR	DR	UAR	—	AR	—	—
	Cashiers				DR	PBR	UAR	—	AR	—	—
	Gasoline station workers				DR	PBR	UAR	—	AR	—	—
Chaiklieng (2021)	Workers at 47 gasoline station in Thailand	Samples were collected from breathing zone of fueling workers	4 hours	47	—	—	UAR	AR	AR	UAR	

Khoshakhlagh (2023)	Oil Refinery Workers (Summer Season)	Samples were collected from breathing zone of oil refinery workers	2 hours	252	DR	DR	UAR	UAR	UAR	UAR
	Oil Refinery Workers (Winter Season)				DR	DR	UAR	AR	UAR	UAR
Alimohammadi (2023)	Gasoline station workers	Samples were collected from the breathing zone of Gasoline station workers	1.5 hours	180	DR	DR	UAR	UAR	UAR	UAR
Kumari (2023)	Workers at Fuel station in Delhi	Fuel station implemented with vapor recovery system	1 hour	—	DR	—	UAR	AR	AR	AR

[a]Lifetime Cancer Risk as per EPA Risk Assessment Guidance for Superfund (RAGS) PART A [b]Hazard Quotient as per EPA Risk Assessment Guidance for Superfund (RAGS) PART F
CANCER RISK > 10^{-4} ==> DEFINITE RISK (DR); $10^{-5} \leq$ CANCER RISK $\leq 10^{-4}$ ==> (PBR) PROBABLE RISK; $10^{-6} \leq$ CANCER RISK $\leq 10^{-5}$ ==> POSSIBLE RISK (PR)
HQ ≤ 1 ==>ACCEPATABLE RISK (AR); HQ >1 ==> UNACCEPTABLE RISK (UAR) *mean risk per 1000 people

Al-Harbi et al. (2020) sampled the breathing zone of workers and reported definite cancer risk and hazard quotient greater than one for benzene[149]. Similarly, Alimohammadi et al. (2023) sampled the breathing zone of workers in a refuelling station in Iran, reported high average LCR_i for benzene (139×10^{-2}), ethylbenzene (27×10^{-2}) and elevated HQ for BTEX (benzene: 173.79, toluene: 14.19, ethylbenzene: 3.61, xylene: 12.87) [135]. Various investigations of health risk assessment encompass both cancer and non-cancer health effects associated with BTEX exposure, revealing pervasive concerns across diverse operational contexts. Personal sampling across various refuelling stations consistently identified heightened LCR_i and HQ values, signifying increased risks of cancer and non-cancer health effects. Loading and refining operations emerge as particularly high-risk scenarios. The detailed hazard assessments, including CR, HI, and specific LCR_i values, provide a nuanced understanding of the gravity of health concerns across different ONG operations. The identified risks, especially during loading and inspection activities, underscore the imperative for comprehensive safety measures and interventions to safeguard workers' well-being in the ONG industry. Additionally, observational studies, such as cohort studies (**Table 2.5**), were also reviewed to analyze potential health effects associated with occupational exposure to benzene or BTEX in the ONG industry. While some studies show a weak association between benzene exposure and leukemia, others highlight potential genotoxicological effects and an increased risk of bladder cancer. Akerstrom et al. (2016) found no significantly elevated risk of multiple myeloma among workers exposed to benzene in oil refineries and harbours [150]. Thetkathuek et al. 2023 highlighted potential genotoxicological effects and an increased risk of

bladder cancer in gas station operators exposed to benzene [151]. Matatiele et al. (2021) also reported potential genotoxicological impacts of exposure to benzene, toluene, and xylene among petroleum refinery workers [152]. Ridderseth et al. (2022) did not find an elevated risk of multiple myeloma among offshore petroleum workers exposed to benzene [153]. Mousavi and Yazdanirad (2023) revealed a positive correlation between benzene and toluene exposure and neurobehavioral symptoms in oil refinery workers [154]. (2022) did not find a significant impact of BTEX exposure on blood and spirometry parameters among oil refinery staff [155]. Elshaer et al. (2022) suggested that chronic BTEX exposure could induce oxidative stress in petroleum refinery workers [156]. (2021) found higher levels of toluene and xylene biomarkers among gasoline station workers, with associated symptoms such as altered mood and headaches [157]. Zhang et al. (2021) reported a significant association between BTEX exposure and lung function decline in petrochemical industry workers [158]. Moridzadeh et al. (2020) found significant levels of BTEX compounds in the urine samples of site workers and staff workers at the gas field [159]. These studies collectively underscore the importance of monitoring and mitigating BTEX exposure among ONG workers to protect their long-term health and safety.

Overall, the results from these observational studies are mixed, with some indicating potential associations between BTEX exposure and specific health outcomes, while others do not show significant correlations. Also, the studies have been conducted at different times, resulting in bimodal findings.

The variability in results underscores the complexity of assessing the health effects of exposure to benzene and BTEX. It emphasizes the need for further research and effective risk management strategies to protect workers' health in the petroleum industry. The variability in risk levels across different locations underscores the significance of site-specific risk assessments. Additionally, various risk assessment models and methodologies make it crucial to adopt standardized protocols to enable better comparison and interpretation of results.

Table 2. 5 Summary of observational studies on health effects of BTEX to workers of ONG industry

Author	Study-Year	Study Type	Type of workers	Exposed	Control	Measured Parameters	Conclusions
Jalilian (2022)	2021	Observational Cross-Sectional	Refinery workers	40 exposed workers	40 not exposed workers	The levels of BTEX exposure in the breathing zone of workers, blood parameters (white blood cells, hemoglobin, platelet, red blood cells, hematocrit), and spirometry parameters (forced vital capacity, forced expiratory volume in 1 second)	Benzene exposure exceeded the allowable limit, there was no statistically significant impact on blood and respiratory parameters in the workers.
Thetkathuek(2023)	2020	Observational Cross-Sectional	Gas Station workers	100	100	The main outcome is the risk of benzene exposure to the nervous system in gas station operators, assessed using the t,t-muconic acid concentration in urine and the presence of neurological symptoms reported by the participants.	The study found that the t,t-muconic acid concentration was higher in employees working at fuel dispensers compared to those working outside fuel dispensers. The majority of participants had low-risk characterization, and there was a statistically significant relationship between t,t-muconic acid concentrations and neurological symptoms.
Ridderseth (2022)	2002-2018	Cross-sectional Study	Offshore petroleum workers	924	___	To characterize benzene exposure among different job groups and examine possible determinants of exposure.	The overall measured benzene exposure increased by 7.6% per year from 2002 to 2018. Mechanics had an annual increase of 8.6%, while laboratory technicians had an annual decrease of 12.6% when including all measurements.No statistically significant time trend was found for process operators.
Elshaer (2021)	2021	Observational Cross-Sectional	Petroleum refining workers	40 exposed workers	40 not exposed workers	This study assess oxidative stress in petroleum workers exposed to BTEX compounds using BTEX biomarkers in urine and serum concentrations of antioxidant trace metals.	Chronic BTEX exposure could potentially induce oxidative stress in petroleum refinery workers via depletion of cellular antioxidant defenses and reduction in the activity of antioxidant enzymes.
Geraldino (2021)	2015-2017	Cross-sectional epidemiological study	Gasoline station workers	275 gasoline station workers	100 office workers	Collection and analysis of urine samples for biomarkers of toluene and xylene exposure (hippuric acid (HA) and methylhippuric acid (MHA)).	Workers exposed to fuels had higher levels of HA and MHA compared to the comparison group. Symptoms like altered mood/depression, cramps, dizziness, headaches, and others were more frequent in exposed workers.

Zhang (2021)	2020	Cross-sectional epidemiological study	Petrochemical Industry worker	635	—	Lung function tests were conducted on the participants, and exposure to BTEXS compounds was assessed based on their work environment.	The study found a significant association between exposure to BTEXS compounds and decline in forced vital capacity percent predicted (FVC% of predicted) and an increased risk of lung ventilation dysfunction (LVD).
Moridzadeh (2020)	2017	Cross-sectional epidemiological study	Gas Field workers	40 site workers	31 staff workers	To assess urinary levels of benzene, toluene, ethylbenzene, and xylenes (BTEX) among workers in the Gas Field	Significant urinary BTEX concentrations differences between the case and control groups,suggest that site workers of Gas Field were exposed to considerable levels of BTEX compounds.
Mousavi (2019)	2018	Observational Cross-Sectional	Refinery workers	78 operational workers	85 administrative staff	To assess the prevalence of neurobehavioral symptoms among operational workers exposed to BTEX compounds in the oil refinery	The frequency of positive neurobehavioral symptoms in the exposure group (operational workers exposed to BTEX compounds) was significantly higher than that in the control group (administrative staff not exposed to BTEX compounds)
Akerstrom (2016)	2011/2013	Observational study	Refinery workers	24	___	The mean exposure levels of benzene and 1,3-butadiene for different occupational groups and evaluate compliance with the Swedish occupational exposure limit (OEL) for benzene and 1,3-butadiene.	The study found that work within the petroleum refinery industry, specifically during the shutdown phase of refinery turnarounds and when handling open product streams containing higher fractions of benzene, posed a risk of high personal benzene exposure compared to normal operations at the refinery.
Matatiele (2021)	2010-2013	Retrospective longitudinal observational study	Refinery workers	29 petroleum refinery workers	___	The outcome results include the levels of exposure to BTX (benzene, toluene, and xylene) in the urine samples of the workers over the four-year monitoring period.	The study reports the variability in exposure levels, and identifies some workers with elevated exposure to certain chemicals.

2.4.3 BTEX detection techniques

This section provides a comprehensive overview and comparative analysis of various analytical methods. It assesses traditional techniques such as GC-MS, PID, and FID, highlighting their accuracy and sensitivity, and introduces emerging technologies, such as MOX and SAW sensors with faster response times (**Table 2.6**). The inclusion of E-Nose techniques is emphasized for their research potential, particularly for real-time measurement and reduced complexity.

Real-time measurement enables immediate, dynamic data acquisition, allowing swift identification of elevated pollutant levels. This feature is crucial for promptly assessing and mitigating health risks in ONG operations, where BTEX emissions can fluctuate rapidly. The ability to monitor BTEX concentrations in real time enhances the effectiveness of safety measures and facilitates timely interventions to protect workers from hazardous exposures. GC-MS has proven to be a powerful and reliable technique for BTEX analysis. The accuracy range of GC-MS for individual compounds is within 1-5% [160], and its Limit of Detection (LOD) falls in the low parts-per-billion to parts-per-trillion range, ensuring high sensitivity for trace-level detection [126-127]. However, the method demonstrates a response time in minutes. Conversely, PID is a rapid technique with response times typically within seconds, making it portable and practical for on-site applications. However, PID may suffer from interference issues, especially when dealing with BTEX isomers, which can affect its selectivity [128-129], [130].

Table 2.6 BTEX detection techniques

Reference	Analysis Technique	Principal	Sampling	Analysis	Percentage Accuracy	Response Time(sec)	Limit of Detection	Advantages	Limitations
Conventional Methodologies									
(Baimatova et al., 2016; Hamid et al., 2023; Orecchio et al., 2017)	GC-MS	Adsorption & GC-MS	Active air sampling	MS	1-5 %	(600-1800)	ppb-ppt	Highly sensitive and specific, widely used for occupational health and environmental monitoring of BTEX	Requires specialized equipment and skilled personnel, time-consuming, can't be used for real-time monitoring
(Coelho Rezende et al., 2019; Liaud et al., 2014; Nasreddine et al., 2016)	PID	Ionization & Detection	Gas sampling	PID	5-10%	(600-1440)	ppm-ppb	Fast response, portable, can detect other VOCs in addition to BTEX	Less sensitive than GC-MS, can suffer from interference and false positives in complex sample matrices
(Liaud et al., 2014; Tunsaringkarn et al., 2012).	FID	Ionization & Detection	Gas sampling	FID	1-5%	(600-1740)	ppm-ppb	High sensitivity to organic compounds, widely available, suitable for a variety of sample types	Destructive method, cannot distinguish between individual BTEX compounds, can't detect at ppb levels
(Liaud et al., 2014; Moufid et al., 2021; Rodríguez-Navas et al., 2012)	TD-GC-MS	Adsorption & GC-MS	Active air sampling	GC-MS	1-5%	(600-2200)	ppb-ppt	Sensitive and specific, capable of trace-level detection, can be used for simultaneous analysis of multiple VOCs	Requires sample pre-concentration, specialized equipment, and skilled personnel, time-consuming, not suitable for real-time monitoring

(Han et al., 2019; Wojnowski et al., 2020)	PTR-MS	Direct Mass spectroscopy	Direct sampling of ambient air	MS analysis	5-10%	(5-60)	ppb-ppt	Real-time monitoring, rapid analysis, no need for sample collection, high sensitivity, and selectivity, suitable for fast detection of trace-level VOCs, and process monitoring in industrial settings.	Limited compound coverage compared to comprehensive GC-MS; requires periodic calibration and standardization; specialized equipment and expertise are necessary for operation and data interpretation.
Unconventional Methodologies									
(Rushi et al., 2014; TGS 822; Unitec SENS-IT; Wang et al., 2019)	MOX Sensors	Electrical resistance change	Air sampling	Sensor array response	10-20%	(3-10)	ppm-ppb	Rapid, non-destructive, portable, cost-effective, suitable for real-time monitoring	Limited selectivity, cross-sensitivity to other VOCs, affected by environmental factors and sensor drift
(Matatagui et al., 2019; Viespe & Miu, 2018)	Surface Acoustic Wave (SAW)	Acoustic Wave Propagation	Air sampling	Frequency Response	5-10%	(60-120)	Low ppb to ppt	Label-free detection, low power consumption, good sensitivity	Relatively expensive sensors, limited to targeted compounds, sensitivity affected by environmental conditions
(Das et al., 2022; Lezzar et al., 2014; Rianjanu et al., 2019)	Quartz Crystal Microbalance (QCM)	Mass Change Measurement	Air sampling	Frequency Response	5-15%	(10-60)	Low ppb-ppt	Highly sensitive, real-time detection, suitable for continuous monitoring	Selectivity limitations, sensitivity to environmental changes, requires regular maintenance
(Camou et al., 2006; Hou et al., 2013; Kari et al., 2021; Silva et al., 2009; St-Gelais et al., 2013)	Optical Sensor	Optoelectronic Components	Air sampling	Optical Response	5-15%	(300-900)	Low ppb to ppt	High sensitivity, potential for remote sensing, suitable for a range of VOCs	Limited to targeted compounds, sensitivity affected by environmental factors, complexity in data analysis
(Lara-Ibeas et al., 2021; Rodríguez-Cuevas et al., 2020; Zampolli et al., 2009)	Poratable Gas chromatography	Chemical Sensors Array	Air sampling	Pattern Recognition	1-5%	(900-1200)	Low ppb to ppt	High selectivity, complementary to GC for compound identification	Requires extensive calibration and data processing, complexity in data analysis, may not be suitable for real-time monitoring

FID, another GC-based technique, offers high sensitivity and a wide linear dynamic range. It can produce reproducible results but lacks selectivity and requires a hydrogen-air flame for the combustion of BTEX compounds [24], [148].TD-GC-MS, a combination of thermal desorption and GC-MS, provides excellent selectivity for BTEX isomers, but it requires specialized equipment and does not offer real-time analysis [129], [131-132]. The PTR-MS instrument offers real-time analysis, high sensitivity, and rapid response time. Still, it has limited selectivity due to potential interference from other compounds and requires calibration with standard compounds [133-134].

Recently, novel analytical techniques have emerged in BTEX detection, offering faster response times and improved sensitivity. Metal oxide sensors (MOX sensors) utilize changes in electrical conductivity when BTEX gases interact with a heated metal oxide surface. While providing quick response times, MOX sensors may suffer from cross-sensitivity to other compounds and require periodic calibration [135-139]. SAW sensors measure changes in surface acoustic waves caused by gas adsorption, enabling real-time detection. Nevertheless, it may face challenges with low selectivity and interference from humidity [140-141]. QCM sensors monitor mass changes on a quartz crystal when exposed to BTEX, demonstrating quick response times. However, they may also suffer from cross-sensitivity to other compounds [142-144]. Optical sensors, including optical waveguides, SPR, IR spectroscopy, and colorimetric sensor arrays, have been explored for BTEX detection. While these methods offer response times of minutes, they may encounter challenges in sensitivity, selectivity, and

quantification [145-149]. Portable GC, a miniaturized version of traditional GC, has also shown promise in BTEX analysis. With response times typically within minutes and accuracy ranging from 1-5% for individual compounds, it is a viable option for on-site quantification [150-152]. The LOD poses a limitation in various E-Nose techniques compared to conventional methods. A comparison of the LODs of multiple E-Nose sensors for BTEX compounds is shown in **Figure 2.3**. In summary, the field of BTEX detection has witnessed significant advancements,

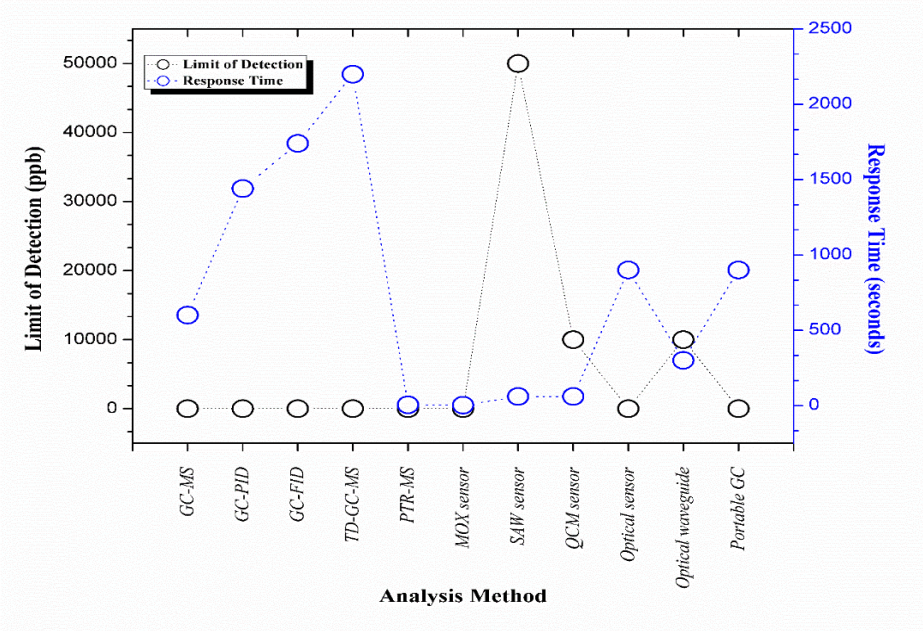

Figure 2.3 Comparison of Limit of Detection (LOD) for different E-Nose sensors used for BTEX detection.

providing a

Variety of techniques to choose from based on specific application requirements. Traditional methods like GC-MS, PID, FID, and TD-GC-MS remain valuable for their accuracy and sensitivity. However, the emergence of novel technologies such as MOX, conducting polymer, SAW, QCM, and optical sensors, as well as

portable GCs, offers faster response times and real-time monitoring capabilities. The optimal choice depends on specific monitoring requirements, cost, and the level of accuracy needed in BTEX monitoring applications. Overall, E-nose techniques have greater research potential than conventional analytical methods for detecting BTEX emissions, particularly in terms of complexity, bulkiness, and real-time measurement.

2.5 Study Limitation

The limitations of the current investigation, listed below, on BTEX emissions in the ONG industry underscore the need for further research in this area:

Geographic Variation: The Majority of studies focus on BTEX emissions and health risks in Asian countries, especially petrol station workers, with limited data from other regions and occupations in the ONG sector. This limits the generalizability of findings to a global context.

Occupational Specificity: While the study population includes workers across all sectors of the oil and gas industry, including upstream, midstream, and downstream operations, the specificity of occupational roles and tasks within these sectors is often poorly documented. This lack of detailed occupational data makes it difficult to assess the specific activities and functions that may contribute to higher BTEX exposure.

Lack of Gender-Specific Analysis: Gender-specific analyses of BTEX exposure and health risks are unavailable because few studies differentiate between male and female workers. This limits the understanding of potential gender-based differences in susceptibility and exposure patterns.

Age Group Representation: Workers in the oil and gas industry span a wide age range, yet studies often lack detailed age-specific data. This lack of age-specific analysis hinders a comprehensive assessment of how different age groups may be affected by BTEX exposure.

Variability in Measurement Techniques: Studies use different methods, leading to inconsistent results across studies. Differences in calibration, sensor types, and operating conditions can impact the accuracy and comparability of BTEX concentration measurements.

2.6 Conclusion

This paper systematically reviews research articles on BTEX emissions and their associated occupational health risks across different ONG operations. The downstream refinery operation zone, with Benzene concentration of 3.5 ± 1.69 ppmv, and the refueling station operation, with Benzene concentration of 1.164 ± 0.408 ppmv, contribute to significant Benzene emissions. A Lifetime Cancer Risk (LCRi) (Benzene) value greater than 10^{-6} was present near the gasoline pump stations (1400×10^{-6}) and loading operation (160×10^{-6}). LCRi (Ethylbenzene) has a significant value (1000×10^{-6}) during a loading operation. In addition, other ONG activities, such as Gas flaring, workforce deployed for inspection operations, and Gasoline station pumps, have Hazard Ratios (HRi) greater than 1. Significant concentrations of benzene, toluene, ethylbenzene, and xylenes (BTEX) are prevalent in oil and natural gas (ONG) operations, particularly in refineries and refueling operations, yet only a limited number of real-time case studies exist, highlighting a critical gap in understanding the immediate health risks workers

face. The scarcity of research articles on real-time health monitoring of workers in ONG industries further exacerbates this issue, hindering the development of proactive health and safety measures. Conventional techniques, while suitable for off-site sampling and for providing detailed data, suffer from poor representation of pollution distribution. On the other hand, onsite analysis using portable techniques in the worker's breathing zone offers a more nuanced understanding of pollutant distribution. To enhance worker safety, there is a pressing need for further research into sensor technologies with lower detection limits and higher sensitivity, which can facilitate real-time monitoring and improve overall management of volatile organic compound exposure in ONG operations.

Chapter 3: Design and Fabrication of QCM Sensor for BTEX Detection

3.1 Abstract

Increased oil and gas industrial activities have led to an abundance of harmful volatile organic compounds such as Benzene, Toluene, Ethylbenzene, and Xylene (BTEX) in the atmosphere. The development of sensitive, low-cost sensors for BTEX detection in both indoor and outdoor environments is crucial for industrial and environmental monitoring. This chapter focuses on the design and fabrication of such sensors, exploring two distinct methodologies for coating a quartz crystal microbalance (QCM) sensor with the sensing layer.

Polyvinyl Acetate (PVAc) Coated QCM Sensor: One approach investigates the optimization of polyvinyl acetate (PVAc) coating on the QCM sensor surface for BTEX detection. Precisely controlled spin-coating speeds varied the thickness of the PVAc film. We characterized the effect of film thickness on the QCM response using multiple experimental approaches, including assessments of sensitivity, repeatability, and reproducibility. Scanning Electron Microscopy (SEM) revealed a rough surface morphology of PVAc, providing abundant active sites for strong interactions with nonpolar BTEX gases**.** The fabricated PVAc-coated QCM sensor demonstrated good sensitivities of 5.14±0.25 Hz/ppm for Benzene, 5.17±0.44 Hz/ppm for Toluene, 5.85±0.31 Hz/ppm for ethylbenzene, and 5±0.31 Hz/ppm for

Xylene at a 1500 rpm spin-coating speed. This method offers the advantage of decreased fabrication complexity.

Tungsten Oxide (WO_3) Coated QCM Sensor: A novel approach explores the feasibility of using Tungsten Oxide (WO_3) coated QCM to detect low concentrations of BTEX compounds under ambient conditions. A WO_3 layer was deposited on the QCM surface using DC magnetron sputtering. The sensor's surface morphology and structure were analysed using Optical Profilometry (OP), Scanning Electron Microscopy (SEM), and X-ray Diffraction (XRD). Adsorption properties were studied through the Langmuir adsorption isotherm, and thermal stability was evaluated by thermogravimetric analysis. The optimized film thickness was determined to be 200.81 ± 0.39 nm for 540 seconds of sputtering. XRD confirmed the amorphous nature of the WO_3, and SEM images revealed a granular microstructure with a diameter of 200 nm. The developed WO_3-coated sensor exhibited high sensitivity, with the highest for toluene (5.69 ± 0.22 Hz/ppm), followed by ethylbenzene (5.3 ± 0.08 Hz/ppm), xylene (5.10 ± 0.31), and benzene (3.36 ± 0.24 Hz/ppm). The limit of detection for BTEX was 1.48 ppm, 0.79 ppm,0.56 ppm, and 0.33 ppm, respectively. Furthermore, the sensor showed faster response times of 30, 32, 30, and 43 seconds for BTEX, along with excellent repeatability (99%) and reproducibility (98%). This fabricated WO_3-coated QCM sensor can effectively detect BTEX vapour at room temperature with high sensitivity and fast response, signifying its potential for occupational health and environmental monitoring systems. Both PVAc- and WO_3-coated QCM sensors demonstrate effective BTEX detection, validating the QCM platform for volatile organic compound sensing. The distinct material properties and fabrication

techniques yield promising results in terms of sensitivity, response time, and reproducibility, establishing viable pathways for occupational health monitoring applications.

3.2 Introduction

Over several decades, many researchers have taken various measures to detect BTEX vapours. These measures include gas chromatography-mass spectrometry [153-154], fluorescence analysis [155-156], semiconductor sensors [157-160], optical [161-162], and so on. Gas chromatography-mass spectrometry equipment is costly and requires professional skills, making it suitable for scientific research but not for real-time analyses [163-164]. Meanwhile, fluorescence analysis also faces similar drawbacks. On the other hand, due to their portability, high sensitivity, and fast response time, semiconductor sensors are widely investigated by researchers for detecting BTEX gases [13-17]. Cao et al. used hierarchical porous Co3O4 structures for xylene detection [196]. Shen et al. improved the Au-ZnO sensor response to BTX using a hierarchical rose-like ZnO architecture [197]. Kang et al. developed a TiO_2-CoPP sensor for enhanced toluene detection[198]. Huihua Li et al. [199] fabricated a mesoporous SnO2-based sensor prepared by a carbon nanotube template. Feihu Zhang et al. [200] presented a selective BTEX sensor based on a SnO2/V2O5 composite, with a detection limit of 500 ppb. Compared to other sensors, semiconductor sensors require high operating temperatures, which limits their applications [201].

The surface-functionalized Quartz Crystal Microbalance (QCM) has shown promising results as gas and humidity sensors [206], electronic noses [207], and

immunosensors [208] owing to its high sensitivity, stability, and especially its low working temperature (0-50°C). The literature shows that polymer-based QCM sensors have been extensively researched for BTEX detection [174-181]. The studied polymers as surface-coated films were pentacene [31], n-octadecylsilane [202], poly(4-vinyl benzylchloride) [32], organosilicate [210], linseed oil-styrene-divinylbenzene copolymer-coated quartz crystal microbalance [26-27], polyvinyl acetate [213], and PDMS [207]. Bearzotti et al. [31] investigated the possibility of using pentacene to detect BTX, exploiting its π-π conjugated structure, which confers affinity for BTX. They reported QCM-coated Pentacene responses to BTX analytes, showing higher sensitivity to benzenes and xylenes than to toluene. Benzene (783, 1566, 2350 ppm), toluene (1563, 3127, 4690 ppm), and p-xylene (465, 930, 1396 ppm) were measured under wet conditions (45% RH at 23 ± 0.5˚C). Wang et al. [202] synthesized a polymerized n-octadecylsilane surface with a micro-nano hierarchical structure on the surface of QCM to detect BTEX in wet conditions. This study reported that the fabricated sensor could detect toluene with different concentrations (100, 200, and 400 ppm). Fan et al. [32] reported that poly(4-vinylbenzyl chloride-co-methyl methacrylate) (P(VBC-co-MMA))-coated QCM sensors were able to detect 1344 ppm of xylene vapour with a LOD of 54 ppm. Sabahy et al. [203] have optimized SiOCH thin film on a QCM sensor as a suitable sensitive material for BTEX detection. The Limit of detection (LOD) was evaluated at 60 ppm for a 100 nm-thick SiOCH layer and 19 ppm for a 300 nm-thick SiOCH layer. Das et al. [26-27] have developed a QCM sensor for BTEX measurement with a coating prepared by copolymerizing styrene, divinyl benzene, and linseed oil at 120 °C, using benzoyl peroxide as the initiator. The sensitivity of

the developed sensor for detecting ethylbenzene, o-xylene, toluene, and benzene was calculated as 1.7, 1.6, 1.3, and 1.1 Hz per ppm, respectively, at 25 ± 2 °C. The response times were 102s, 110s, 94s, and 98s for benzene, toluene, ethylbenzene, and xylene, respectively. Mirmohseni et al.[207] have developed a Polydimethylsiloxane (PDMS)- coated QCM for the detection of organic vapours such as benzene, toluene, ethylbenzene, and xylenes, and reported sensitivities of 4.37 Hz/ppm, 7.72 Hz/ppm, 13.54 Hz/ppm, and 11.40 Hz/ppm for benzene, toluene, ethylbenzene, and xylenes, respectively. Though polymer-coated QCM sensors for detecting BTEX have been studied extensively, few exhibits high sensitivity, while others have good response time.

3.2.1 Quartz Crystal Microbalance sensor

QCM sensors (**Figure 3.1**) are piezoelectric devices that can detect minute changes in the mass absorbed on their surface [182-186]. These sensors consist of AT-cut quartz crystals with metal electrodes oscillating at a resonant frequency. A QCM sensor can operate as a gas sensor and works on the principle of mass loading. When gas molecules interact with the surface of a crystal modified with a suitable sensing layer, they adsorb, thereby changing the crystal's surface mass. This change in mass decreases the crystal's resonant frequency, which can be measured and correlated to the target gas concentration. There is a linear relationship between resonant frequency deviation (Δf) and mass adsorbed on the surface of the QCM sensor, Δm, as expressed in the Sauerbrey **Equation (3.1)**[213]. The negative sign in Equation (1) signifies a decrease in resonance frequency,

$$\Delta m = \frac{A\sqrt{\mu\rho}}{2f_0^2}(-\Delta f) \tag{3.1}$$

Here, f_0^2 is the square of the base resonant frequency in hertz (Hz). Δm is the change in mass on the surface in micrograms (µg). A is the coated surface area in cm^2, ρ_q is the density in g cm^{-3} and μ_q is the shear modulus in $gcm^{-1}s^{-2}$ of the quartz crystal.

Table 3.1 gives the specifications of the QCM sensor used for the experiment**.** Using the Sauerbrey Equation (3.1), approximately 1.249 ng of WO_3 deposition on the active electrode area of the QCM sensor corresponds to a 1 Hz deviation. The advantages of QCM sensors lie in their practicality, room-temperature operation, low power consumption, robust design, and cost-effectiveness.

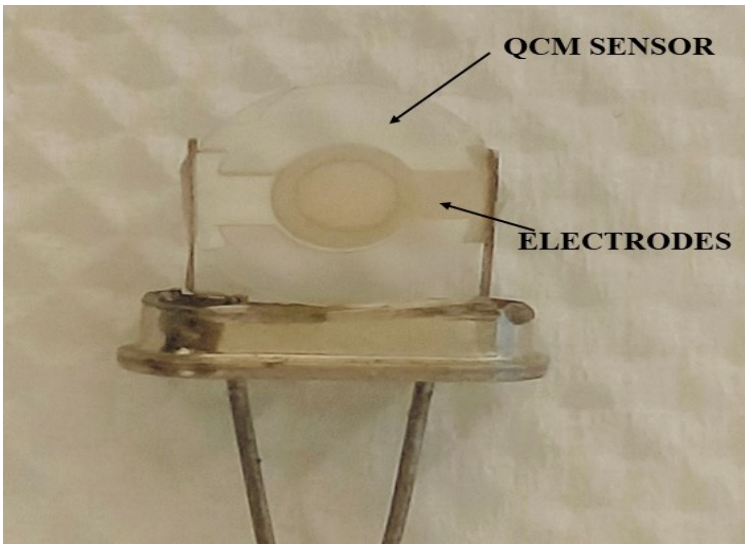

Figure 3.1 Illustration of 10MHz quartz crystal microbalance sensor

Table 3.1 Specifications of Quartz Crystal Microbalance sensor

Dimensions	**Value**
Diameter of Sensing Surface	1.00 cm
Area of Quartz crystal	0.785 cm^2
Diameter of Electrode	0.60 cm
The density of the Quartz crystal (ρ_q)	2.66 g cm^{-3}
Shear Modulus of Quartz Crystal (μ_q)	2.95×10^{11} g cm^{-1} s^{-2}

3.2.2 Polyvinyl Acetate (PVAc)

The selection of Polyvinyl Acetate (PVAc) as the sensing material for Quartz Crystal Microbalance (QCM) functionalization in this study is underpinned by several key characteristics and a critical analysis of existing literature. PVAc is a synthetic polymer widely recognized for its excellent film-forming properties, affordability, and hydrophobic nature. This hydrophobicity arises from the nonpolar vinyl acetate units within its chemical structure, making it particularly well-suited for interactions with nonpolar volatile organic compounds (VOCs) such as Benzene, Toluene, Ethylbenzene, and Xylene (BTEX). In a QCM-based sensor, the principle of operation relies on gravimetric detection of adsorbed analytes; thus, a sensing layer with strong affinity for the target gases is paramount for achieving high sensitivity.

Previous research has explored the use of PVAc in QCM gas sensing, often employing various deposition methodologies. For instance, Triyana et al. (2019)

used an electrospinning method to coat PVAc nanofibers onto a QCM sensor [210]. While electrospinning can produce high-surface-area nanomaterials, which theoretically enhance active sites for gas adsorption, their reported sensitivities were relatively low, specifically below 0.065 Hz/ppm for Xylene, Toluene, and Benzene. This technique, while yielding a nanofibrous structure, often involves intricate setup and precise parameter control, adding to the overall complexity of sensor fabrication. In contrast, Rianjanu et al. (2019) used a spin-coating method to deposit PVAc on QCM sensors, achieving sensitivities of 0.018 Hz/ppm for Benzene, 0.041 Hz/ppm for Toluene, and 0.081 Hz/ppm for Xylene [214]. However, the sensor's response time was high: benzene-225s, toluene-230s, and xylene–260s. Their work demonstrated the viability of spin-coating for PVAc films, providing a direct point of comparison for the present study. More recently, Julian et al. (2020) employed a hybrid approach, using a mixture of polyvinylidene fluoride and polyvinyl acetate (PVDF/PVAc) treated with dimethylformamide (DMF) and subsequently spin-coated onto a QCM sensor [215]. This hybrid film exhibited sensitivities that were significantly higher, exceeding 0.6 Hz/ppm for benzene, toluene, and xylene vapors. While achieving superior performance, the use of a binary polymer blend and the additional solvent treatment step (DMF) inherently introduces greater complexity into the fabrication process, potentially impacting scalability and cost-effectiveness.

Recognizing these challenges and opportunities, the present work focuses on a simplified yet effective fabrication strategy: spin-coating methodology for PVAc functionalization of QCM. The primary rationale for selecting spin-coating is its simplicity, cost-effectiveness, and precise control over film thickness, which directly influences the sensor's sensitivity. While previous studies have employed more

complex techniques or achieved moderate sensitivities via spin coating, this research aims to optimize PVAc film thickness by systematically varying spin-coating parameters. The overarching objective is to achieve higher sensitivity for BTEX detection while significantly reducing the overall complexity of the sensor fabrication process. Importantly, this sensor was also rigorously tested for ethylbenzene detection, demonstrating consistent high sensitivity, further broadening its potential application spectrum.

3.2.3 Tungsten Oxide (WO_3)

Tungsten Oxide (WO_3), as a typical wide-band-gap semiconductor, has attracted much attention for sensor applications due to its good electrochromic[223], photochromic[191-192], and gaschromic [193-194] properties. WO_3 gas sensors have been successfully developed to detect various toxic and hazardous gases, including NO2, H2S, H2, CO, and others [195-199]. Apart from the gases as mentioned earlier, WO_3 has been extensively studied for its unique sensitivity to BTEX compounds [170], [200-201]. Kanda et al. developed a thin-film resistive sensor of WO_3 sputtered onto platinum electrodes [223]. This sensor can detect one ppm of toluene and m-xylene at 693K. Favard et al. have modified a resistive sensor to functionalize gold nanoparticles using the thermal evaporation technique[224]. Au-WO_3 has increased the sensor response and decreased the operating temperature below 593K. The coating thickness was 50 nm, and the detection limit for BTX concentration was 20 ppb. Deng et al. have developed cotton-doped WO_3 (C-WO_3) to detect 100 ppb to 1000 ppb toluene, with response times of 40 seconds for 100 ppb and 10 seconds for 1000 ppb at 593K

[201]. Though WO_3-coated resistive sensors exhibit good response to BTEX, they have certain limitations. Resistive gas sensors often operate at elevated temperatures, with practical implications, such as increased energy consumption [201]. Also, resistive sensors, particularly those operating at higher temperatures, may pose an explosion risk, especially in an industrial environment where flammable gases may be present [225]. However, having both high sensitivity and a faster response time in a single sensor is an essential criterion for any measurement system. To the best of our knowledge, semiconductor-coated QCM sensors, especially for BTEX detection, have not been reported. We have combined the good sensing properties of WO_3 with a QCM sensor to fabricate a highly sensitive, fast-response, stable, and room-temperature-operating sensor for the reliable detection of BTEX.

The novelty of this research lies in integrating WO_3 with a QCM sensor to detect BTEX vapours with good sensitivity, quick response time, and long-term stability in ambient environments. Unlike traditional WO_3-coated resistive sensors, the proposed sensor operates at room temperature. A thin, uniform WO_3 layer was deposited on the QCM sensor surface by DC magnetron sputtering, with thickness directly proportional to the deposition time. WO_3-coated QCM sensors with varying deposition durations were optimized for sensitivity.

Primary characterization techniques, such as Optical Profilometry (OP), Scanning Electron Microscopy (SEM), and X-ray Diffraction (XRD), were employed to analyze the sensor surface morphology and structure. Optimized sensor sensitivity, selectivity, and stability were studied. The effect of humidity on

sensor response was evaluated. The results of the developed WO_3-coated QCM sensor were compared with previously published data for sensitivity, response time, and LOD. The current work using a WO_3-based QCM sensor offers higher sensitivity and lower detection limits for benzene, toluene, ethylbenzene, and xylene. It exhibits good response times at an ambient temperature.

3.3 Methodology

3.3.1 PVAc deposition

3.3.1.1 Material and Methods

N, N-dimethylformamide, Acetone, Xylene, Toluene, and deionized water were purchased from Sigma-Aldrich (Germany). Polyvinyl acetate (PVAc) granules with a molecular weight of 500,000 g/mol were purchased from Research-Lab Fine Chem Industries, Maharashtra, India. All the chemicals used throughout the experiment were of analytical grade and were used as received. Piezoelectric AT-cut quartz crystals with a 10 MHz resonant frequency and an 8mm diameter were obtained from Andhra Electronics, Andhra Pradesh, India. The frequency counter, MetroQ MTQ4040, was used as a reference standard. A teensy microcontroller board was used for frequency monitoring and data logging.

3.3.1.2 Synthesis of PVAc thin films

The QCM sensor was cleaned using acetone and washed with deionized water. The spin-coating method was used to apply PVAc to the QCM surface, as shown in **Figure 3.2**. A solution of PVAc at 0.05 g/mL was prepared by dissolving 0.5 g of PVAc in 10mL of N, N-dimethylformamide (DMF). A homogeneous solution was prepared by mechanical stirring with a magnetic stirrer at 260 rpm until complete

homogeneity was achieved [211]. A 10 µL solution of PVAc was dropped onto the QCM surface using a 1000 µL micropipette. The spin-coating process was performed at different speeds, and the coated crystal was left in a 10 mL desiccator for 24 h to ensure proper adhesion. The sensor response was checked after every coating, and the QCM was spin-coated at 500 rpm (QP500), 1000 rpm (QP1000), and 1500 rpm (QP1500) for 10s, showing good sensitivity to BTEX vapors.

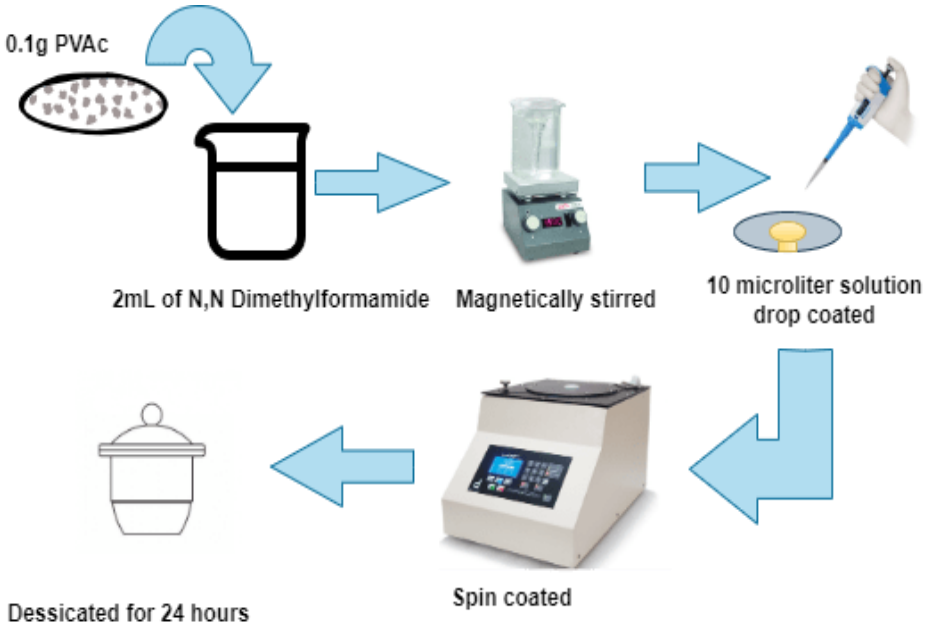

Figure 3.2 Functionalization of QCM sensor with Polyvinyl Acetate

There was no significant frequency drop for the sensor coated at spin coating speeds below 500 rpm due to excessive loading, and an unstable frequency response for the sensor coated at spin coating speeds above 1500 rpm due to non-homogeneous coating.

3.3.2 WO_3 Deposition

3.3.2.1 Material and Methods

Benzene, toluene, xylene, and deionized water were purchased from Sigma Aldrich, Germany. All chemicals used throughout the experiment were of analytical grade (99% purity) and were used as received. Tungsten of 99.99% purity was purchased from Scientific and Analytical Instruments and is used as the target material for WO_3 coating. Piezoelectric AT-cut quartz crystals were acquired from Andhra Electronics, Andhra Pradesh, India.

3.3.2.2 Synthesis of WO_3 thin films

The WO_3 coating on the QCM sensor is deposited by DC-RF magnetron sputtering using a 99.99% pure tungsten target [226]. A model representation of the sputtering process is illustrated in **Figure 3.3**.

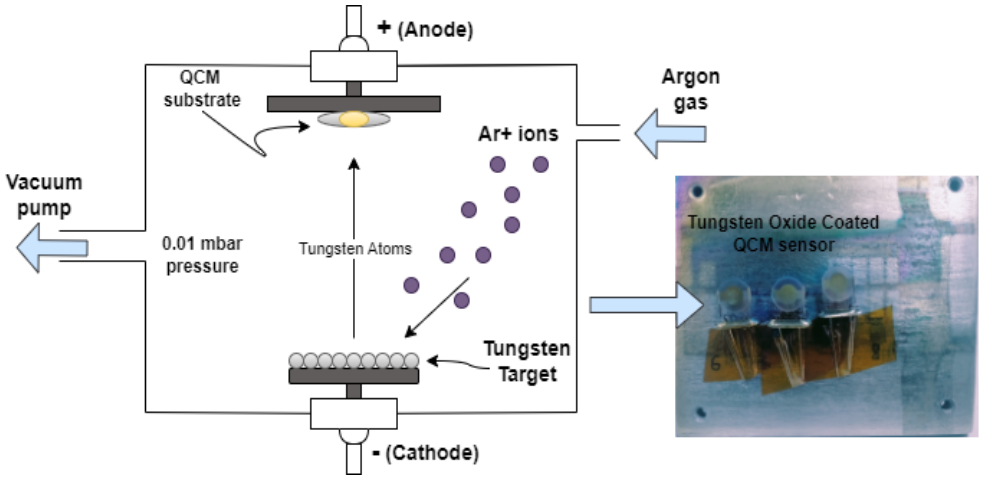

Figure 3.3 Illustration of WO_3 Sputtering on QCM sensor surface.

Table 3.2 The parameters maintained for sputtering on a WO_3 thin layer onto the QCM sensor

Target material	Tungsten (99.99%)
Substrates	Quartz Crystal Microbalance sensor
Base pressure	$2x10^{-6}$ mbar
Target to substrate distance	9 cm
(PaO_2)	5 sccm
Argon flow rate	25 sccm
Working Pressure	$1x10^{-2}$ mbar
DC Magnetron Sputtering	Current=100 mA, Voltage = 520V

The sputtering system includes a vacuum chamber, substrate holder, and gas supply. The sputtering parameters are detailed in **Table 3.2.** A DC power supply is connected to the tungsten target, creating a voltage difference between the target and the chamber walls. Oxygen-argon mixtures form the reactive atmosphere. It generates plasma by accelerating argon ions toward the tungsten target, sputtering tungsten atoms onto the QCM sensor, creating the WO_3 film. Sputtering is performed at 1×10^-2 mbar, with a 9 cm target-to-substrate distance. Film thickness was controlled by adjusting sputtering time (60 to 540 seconds). A 10 MHz AT-cut QCM sensor was used. Before coating, the QCM sensor was adequately washed with ethanol to ensure a clean surface. The cleaned QCM sensor was placed on the substrate holder inside the sputtering chamber. Direct contact between the sensor and holder was avoided using EMI/RFI shielding tape to support the sensor.

3.4 Experimental Setup and Analyte Generation

3.4.1 Electronic Circuit Design

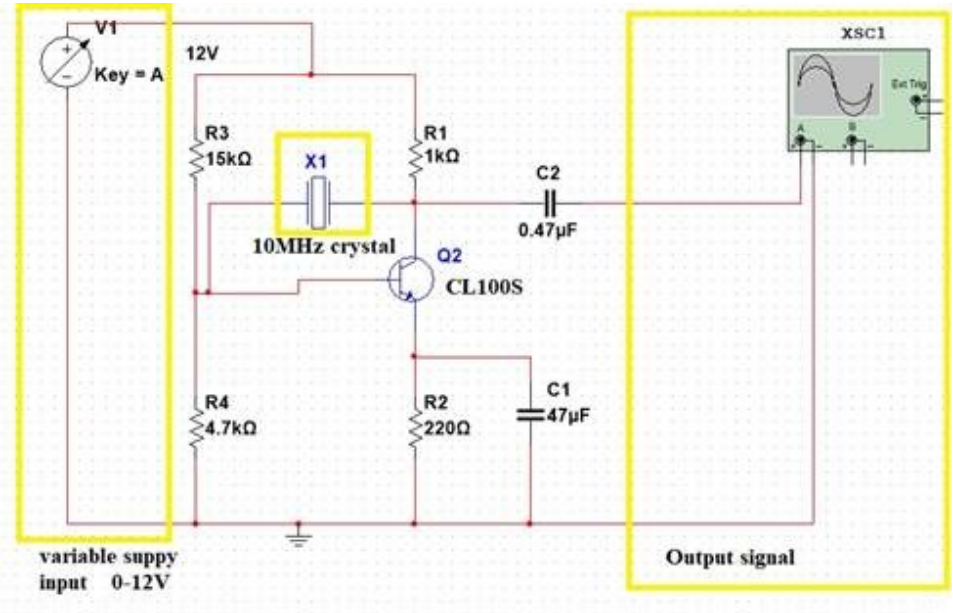

Figure 3.4 Oscillator Circuit Design for 10MHz Crytal

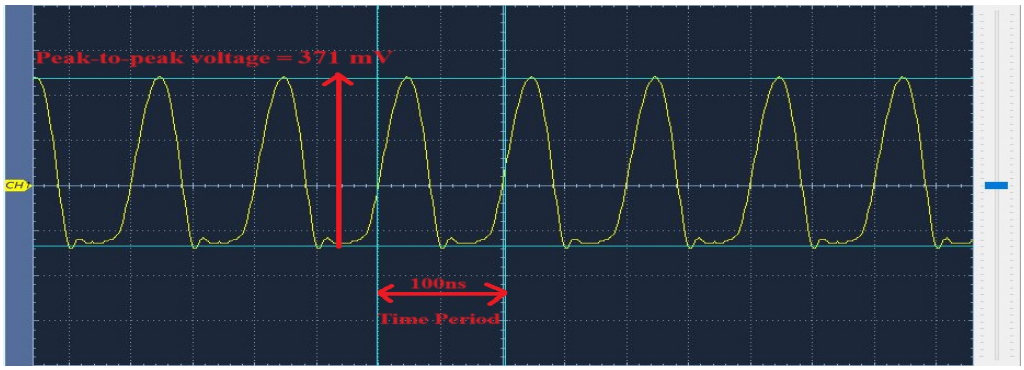

Figure 3.5 Digital storage oscilloscope output of the uncoated QCM sensor signal from the oscillator circuit

The oscillator circuit was designed using resistors (15kΩ,1kΩ,4.7kΩ,220Ω), npn transistor (CL100S/SL100S/ 2N2222), and capacitors(0.47nF,47μF) as depicted in **Figure 3.4** [211]. The oscillator circuit was simulated in Multisim. The oscillator circuit uses voltage-divider biasing, with positive feedback from the base to the collector via a quartz crystal. The peak-to-peak voltage of the generated signal is 300 ± 100 mV, with a period of 100 ns and a duty cycle of 50% (**Figure 3.5**). The teensy microcontroller is programmed to serve as a frequency counter and data-acquisition (DAQ) system. It uses Quad Timers to measure and accumulate input signal frequencies, convert them into Hertz values, and display the results on a TFT screen. It allows for precise frequency measurement with a resolution of 1 mHz and a mean error of 0.037%.

3.4.2 Experimental Setup

The BTEX gas sensing set-up with schematic diagram is shown in **Figure 3.6 (a) & (b)**. The QCM sensor was sealed in a gas-sensing chamber with an air-purging outlet connected to a suction pump. The chamber's internal conditions were monitored using a pressure sensor (MPS-200) and a temperature/humidity sensor (AM1011A). The sensor bed, equipped with a connector for the QCM sensor, was connected to the oscillator circuit. The 10 MHz QCM sensor oscillator circuit employed resistors, NPN transistors, and capacitors, as discussed in our previous section. The crystal required a minimum power of 10 nanowatts. The frequency counter (Teensy microcontroller) was connected to the transistor's collector and measured the oscillation frequency.

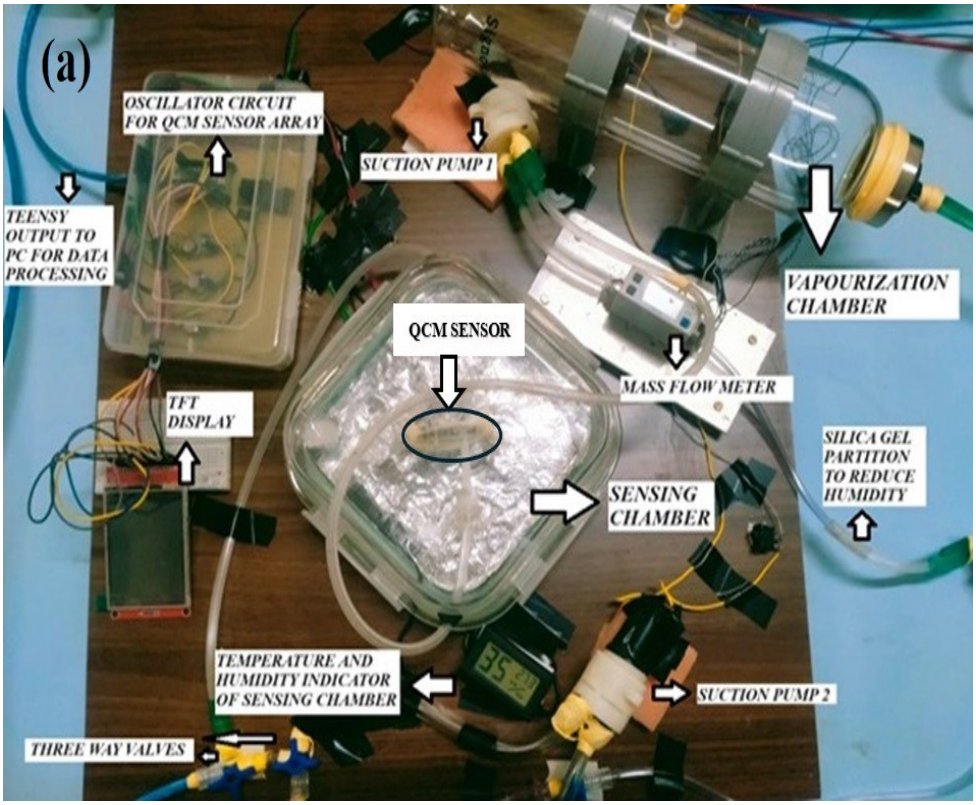

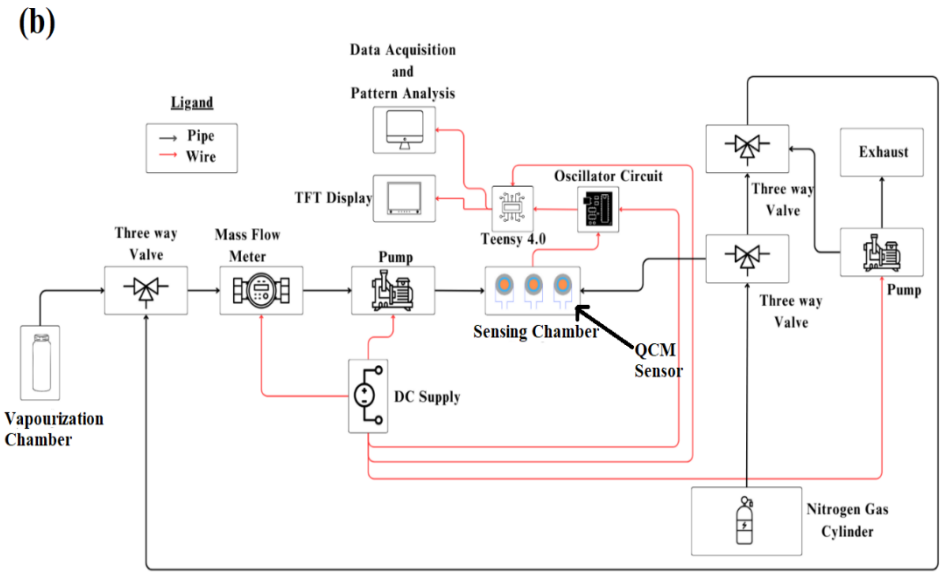

Figure 3.6 (a) Gas Sensing Setup for Detection of BTEX vapors (b) Schematic Illustration of experimental BTEX Sensing Setup

Data acquisition system was also performed using a Teensy microcontroller board. The gas sensing chamber was constructed from glass, which is chemically inert and non-reactive with BTEX vapours, ensuring that the chamber walls do not interact with the gases. Glass is a preferred material in gas sensing applications due to its minimal adsorption properties and its ability to maintain the integrity of volatile organic compounds (VOCs) like benzene, toluene, ethylbenzene and xylene during measurements[227]. Silicone tubing and valves were used in the gas delivery system due to their flexibility, affordability, and moderate chemical resistance. Although silicone has higher permeability than materials like PTFE or stainless steel, it provides adequate resistance to short-term VOC exposure, making it a practical and cost-effective choice for this setup [228]. Silicone's ability to handle flexible routing and its chemical stability at room temperature made it an ideal candidate for this application [229]. Additionally, the base of the chamber was covered with aluminium foil to shield against electromagnetic interference, which could affect the QCM sensor's performance[230]. Aluminium is known for its low adsorption and interaction with gases, especially at ambient temperatures, making it suitable for use in environments where gas purity is critical[231]. Furthermore, Teflon tape was used to seal the QCM sensor's sockets. Teflon (PTFE) is highly resistant to chemical interactions and exhibits excellent non-stick properties, preventing gas adsorption at the sensor connections and ensuring accurate gas concentration measurements [232]. This combination of glass, silicone, aluminium, and Teflon effectively isolates the sensor from external interferences and prevents any unintended interaction with the target gas.

3.4.3 Volatile Test Analyte Preparation

The volatiles were prepared using static headspace sampling. Static headspace sampling isolates and analyses VOCs by equilibrating a sample with a sealed gas phase, followed by extracting and analysing the gas for VOCs. Samples were prepared by placing a known volume of benzene, toluene, ethylbenzene, or xylene in a vaporization chamber to create a saturated ppm concentration, calculated using **Equation (3.2)** [182-184].

$$c = \frac{22 \cdot 4 \rho v_x T}{273 M v} \times 100 \tag{3.2}$$

Where ρ is the density of the volatile in (g mL^{-1}), T is the temperature in K, v_x is the volume of liquid analyte evaporated in µL, M is the volatile molecular weight (g mol^{-1}), v is the volume of the sealed container in L, and c is the concentration of gaseous VOC formed inside the container in ppm. The saturated gaseous VOC sample was taken from the vaporization chamber (900mL). The volume of VOC gases in the vaporization chamber to achieve the required ppm concentration in the sensing chamber was calculated using **Equation (3.3)** [212]. The gas response properties were evaluated by diluting the sample gas with air.

$$c_c v_c = c_i v_i \tag{3.3}$$

Where c_c is the saturated concentration of VOC formed inside the vaporization chamber, v_c is the volume of the vaporization chamber in mL, c_i is the required

concentration inside the sensing chamber in ppm, and v_i is the volume of the sensing chamber in mL.

The QCM sensor was placed inside the sensing chamber at room temperature (27˚C ± 1˚C), atmospheric pressure (760 mm Hg), and controlled relative humidity (50 % ± 5%). The environment inside the chamber was sealed and kept unaltered during the measurement process; hence, the effect of environmental parameters inside the chamber can be considered constant.

Sensor response studies at higher humidity: Vapours of BTEX were generated using the nebulization technique to observe sensor response at higher humidity. The nebulization process evaporates the solution into an aerosol using compressed air or oxygen. These vapours were channelled into a sensing chamber. Two inlets were provided in the chamber: one for the nebulizer inlet (injecting the target vapors) and another for the suction pump (purging). The nebulization rate (NR = 3.33 µL s^{-1}) is the aerosol formation rate specified in the instrument's datasheet. Several factors affect the nebulization rate, including pressure, temperature, and humidity. Higher pressure increases the nebulization rate by forming finer aerosol particles. Increased temperature decreases liquid viscosity, making it easier for the liquid solution to evaporate. Higher Humidity decreases the nebulization rate as aerosol particles grow. The temperature, pressure, and humidity were continuously monitored inside the sensing chamber throughout the experiment. The concentration of vapors in the sensing chamber is calculated using **Equation (3.4)** [212]**.**

$$c = \frac{NR \times NT}{v} \quad (3.4)$$

NT is the nebulization time in seconds, v is the chamber's volume in litres, NR is the nebulization rate in μLs^{-1}, and c is the concentration of the target analyte inside the sensing chamber calculated in ppm. The suction pump will move the target gas molecules from the sensing chamber, which will be air- and nitrogen-purged.

3.5 Results and Discussion

3.5.1 PVAc Sensing Layer characterization and response

3.5.1.1 Thickness Optimization

The thickness of this film (t_c) is controlled by the spin coating speed. The value is theoretically calculated using **Equation (3.5)** [233].

$$t_C = \frac{\Delta m}{\rho_C x A_s} \quad (3.5)$$

Δm = Deposited mass in µg, ρ_c = Coated Compound Density (g/cm³), and As = Surface Area of QCM electrode(cm²). The thickness was experimentally measured using an optical profilometer and reported in **Table 3.3**. As the spin coating speed increases from 500 to 1500 rpm, there is a significant reduction in both the frequency shift (indicating a decrease in mass) and the actual film thickness (tc). This suggests that higher spin coating speeds result in thinner PVAc films, with relatively small standard deviations and error percentages indicating good consistency in the measurements.

Table 3.3 Thickness of PVAc at varied spin coating speed.

Spin Coating speed (rpm)	**500**	**1000**	**1500**
*Frequency Shift (kHz)	219±21.5	62±1.4	10.8±0.21
*Δm (µg)	75±7.4	21±0.6	3.7±0.05
pc(g/cm^3)	1.19	1.19	1.19
As (cm^2)	0.283	0.283	0.283
tc(nm) (Theoretical)	2246	623	109
*tc(nm) (optical profilometer)	2258±446	656±40	115±41
Error %	5.7%	5.3%	5.5%

3.5.1.2 Surface characterization

The surface morphology of PVAc (polyvinyl acetate) is crucial in determining its adsorption properties for gases such as BTEX. BTEX gases are nonpolar and possess various types of electron clouds that can interact with the electron clouds in the polymer chains of PVAc through Van der Waals forces. Hydrogen bonding can occur between functional groups on the PVAc surface and polar moieties present in the BTEX gases. These interactions facilitate the binding of the gas molecules to the material's surface.

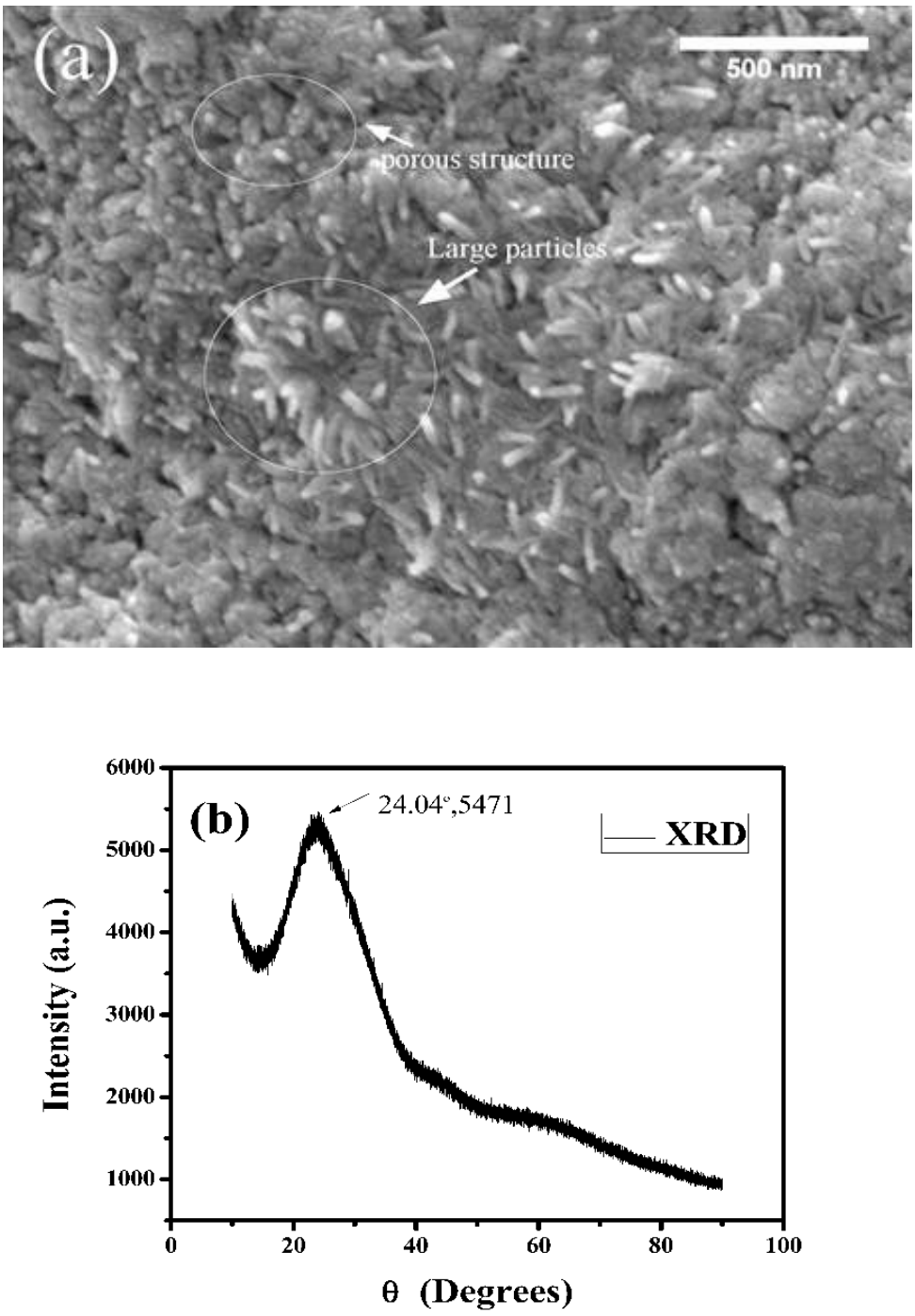

Figure 3.7 (a) SEM images and (b) X-ray diffraction intensity profile of PVAc spin-coated on glass substrate at a spin speed of 1500rpm.

The SEM micrograph of QP1500 (PVAc film spin-coated at 1500rpm) is shown in **Figure 3.7 (a)**. The micrograph reveals a distinctive surface texture comprising densely packed, rod-like nanoparticles that form a highly rough and porous structure. This morphology generates numerous active sites and inter-particle voids, which are fundamental to the film's enhanced adsorption capabilities. ImageJ software is used to analyse particle size and confirms a high level of surface heterogeneity. The original SEM image was calibrated using the 500 nm scale bar. Thresholding was applied to generate a binary image, and the "Analyse Particles" function was used to measure the area and significant axis length (approximated as length) of all distinct particles within a representative field. The resulting raw data were then processed to yield the reported statistical values, including the mean length, mean area, minimum area, and maximum area. It is observed that the mean length of the particle is 71.574 nm, and the mean area is 135.802 nm^2. The minimum size of the particle is 85.734 nm^2, and the maximum size is 222.908 nm^2. It is observed that PVAc material has a rough surface and provides numerous sites for non-covalent interactions, such as Van der Waals forces and hydrogen bonding. The observed particle size and area distribution indicate the available active sites on the surface. The larger particles may have more surface area for adsorption, while smaller particles can contribute to the material's overall porosity, creating additional surface area for gas adsorption. X-ray diffractometer (XRD) analysis of PVAc spin-coated was also performed, as depicted in **Figure 3.7(b)**, and the main peak of the PVAc was obtained at 24.04º compared to 22.70º in the previous study[234]. The label (24.04˚,5471) [Figure. 3.7(b)] denotes the coordinates of the

peak maximum: 24.04˚ is the θ, and 5471 is the measured peak intensity at that θ angle.

The observed shift in the main PVAc peak from 22.70˚ (previous study) to 24.04˚ (current study) is significant. According to Bragg's law (**$n\lambda = 2d\sin(\Theta)$**), this shift to a higher Θ angle corresponds to a decrease in the interplanar spacing (d-spacing) from 0.39 nm to 0.37 nm. This 0.022 nm reduction in d-spacing indicates tighter packing of the PVAc chains, which can be induced by the spin-coating process (e.g., rapid solvent evaporation or surface confinement).

The crystallite size D of the PVAc film, calculated using the Scherrer equation ($D = \frac{K\lambda}{ß\cos(\theta)}$) for the prominent peak at Θ = 24.04, K=0.9 and λ= 0.15, is approximately 0.64nm. This tiny crystallite size strongly supports the observed low degree of crystallinity, estimated at approximately 48%. A crystallite size of 0.64nm indicated that the ordered domains are minimal, suggesting a structure that is predominantly amorphous and highly disordered. A lower degree of crystallinity corresponds to a higher amorphous content, resulting in a significant increase in the boundary area and free volume. This predominantly amorphous structure and the small crystallite size directly provide a higher concentration of readily available adsorption sites for the BTEX molecules, thus correlating positively with the stability of the pore structure and overall adsorption capacity.

3.5.1.4 Sensitivity Analysis

The sensitivity of the fabricated sensor to benzene, toluene, ethylbenzene, and xylene vapours was studied, as shown in **Figure 3.8**. The frequency deviation as a function of concentration was plotted using **Equation (3.6)** [212].

$$Y\ (Hz) = S\left(\frac{Hz}{ppm}\right) X\ (ppm) + const \qquad (3.6)$$

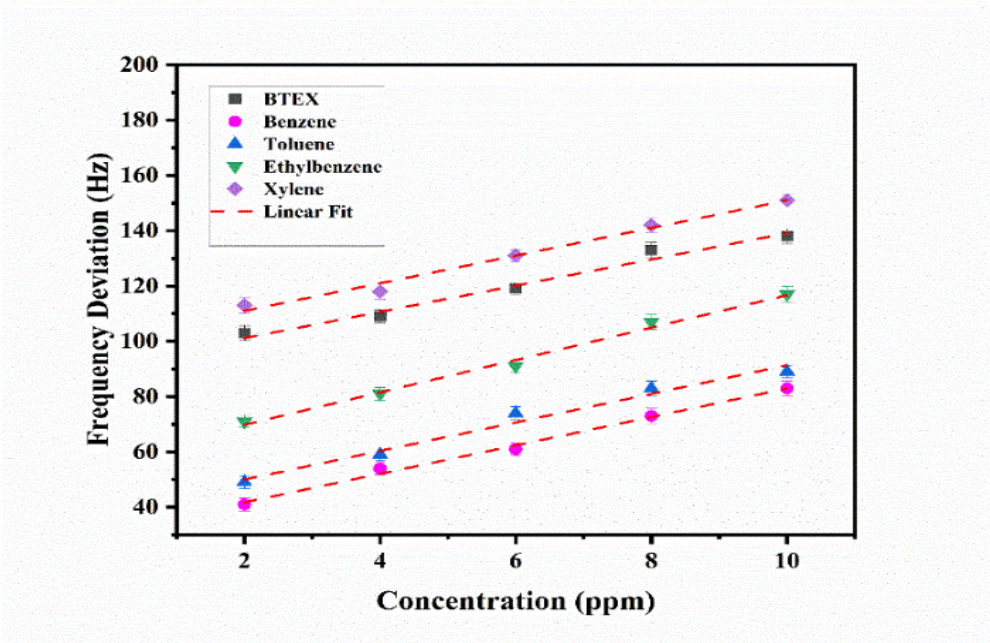

Figure 3.8 Concentration vs. frequency plot of QCM sensor functionalized with Polyvinyl acetate (QP1500) with different concentrations (2-10 ppm) at (27±1) °C, 16% RH, and standard atmospheric pressure.

Here, X is the concentration in ppm, and S is the slope of the linear regression line. The sensor has shown different sensitivities to BTEX vapours at varying PVAc thin-film thicknesses. The sensitivity for Xylene is higher than for Toluene and Benzene, as reported in previous research articles [176], [235]. Also, the QP1500 sensor has shown increased sensitivity values of 5.14 Hz/ppm for benzene, 5.17 Hz/ppm for toluene, 5.85 Hz/ppm for ethylbenzene, and 0.23 Hz/ppm for xylene compared to previous work[176]. The high adjacent R-square values (0.997, 0.996, and 0.999) suggest good linearity in the sensor's response across a wide range of concentrations for these compounds.

The LOD, which is three times the ratio of the noise level at the frequency of interest to the sensor's sensitivity, is evaluated using **Equation (3.7)** [212].

$$LOD = \frac{3 \times s}{m} \tag{3.7}$$

Here, s is the standard deviation of the regression line, and m is the slope.

3.5.1.5 Repeatability and Reproducibility Analysis

The equation for calculating the percentage of reproducibility and reproducibility (R_P, R_D) is given by **Equation (3.8)**, where S is the relative standard deviation.

$$R_P, R_D = (1 - S) \times 100\% \tag{3.8}$$

Figure 3.9 displays the responses of the QP500, QP1000, and QP1500 sensors for three repeated exposures to 10 ppm Benzene, showing similar frequency shifts during exposure and during purging. The response time of the QP1500 sensor is 69 sec for benzene, 73 sec for toluene, 70 sec for ethylbenzene, and 90 sec for xylene.

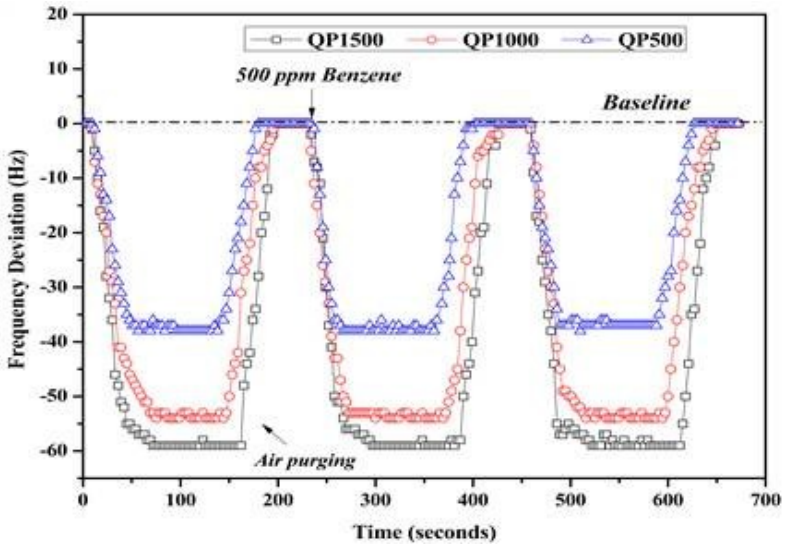

Figure 3.9 PVAc varied thickness coated sensor response to three repeatable exposures of 10 ppm of Benzene.

The average frequency shift for each concentration was calculated, and the average repeatability value obtained was 94.72%, 95%, 93.6%, and 91.32% for QP1500, QP1000, and QP500 sensors, respectively. The sensitivity of the three reproducible sensors, each of QP500, QP1000, and QP1500, was compared for Benzene in **Figure 3.9.** The low coefficient of variance values, such as 4.82% for Benzene, 4.84% for Toluene, 4% for Ethylbenzene, and 2.63% for Xylene, for three reproducible QP1500 sensors highlight the sensor's good precision.

These values indicate minimal variation among repeated measurements, underlining the sensor's consistency and reliability.

3.5.2 WO_3 Sensing Layer characterization and response

3.5.2.1 Thickness Optimization

Depositing WO_3 through DC magnetron sputtering yielded a homogeneous thin layer with a thickness in the nanometer range. The thin-film thickness was optimized to achieve an optimal sensor for detecting BTEX. The investigation was conducted by fabricating nine WO_3-coated QCM sensors with varying deposition durations (60–540 seconds), while keeping all other sensor fabrication steps constant. The deposition time range of 60 to 540 seconds was chosen based on preliminary trials conducted to determine the optimal thickness of the WO_3 thin film for effective sensor performance. Deposition times below 60 seconds resulted in an unstable sensor response due to insufficient material coverage on the QCM surface, leading to poor sensor sensitivity. Beyond 540 seconds, the increased thickness of the WO_3 layer caused excessive loading on the QCM sensor, leading to instability and zero sensor response. Therefore, the range of 60 to 540 seconds

was selected as it provided a balance between achieving adequate material deposition for sensor functionality and avoiding excessive loading that could impair sensor performance. The thickness of the thin film was theoretically calculated using Equation (3.5). The thickness of the prepared thin film was evaluated by measuring step height using the TalySurf CCI optical profilometer. **Figure 3.10 (a).** elucidates the step height of WO_3 coating on the QCM surface for the deposition time of 540 sec, where the X-axis represents the lateral position along the QCM surface in micrometres (µm), and the Y-axis represents the mean elevation due to WO_3 coating in nanometers (nm). The thin-film thickness, i.e., the step height measured using the optical profilometer, was 74 nm. An error of 2.63% was observed between the experimental and theoretical values (Equation (3.5)) for the thickness of the thin film.

The thin-film thickness varied linearly with deposition time, as illustrated in **Figure 3.10(b)**. Nine sensors were exposed to 10 ppm of BTEX, keeping identical experimental conditions. **Figure 3.10(c)** demonstrates that increasing the deposition time (which is directly proportional to the thickness of the WO_3 film) improves the QCM sensor output (frequency deviations) upon exposure to 10 ppm of BTEX. The probable reason is a change in surface morphology to improve binding sites and binding energy, which has been further studied.

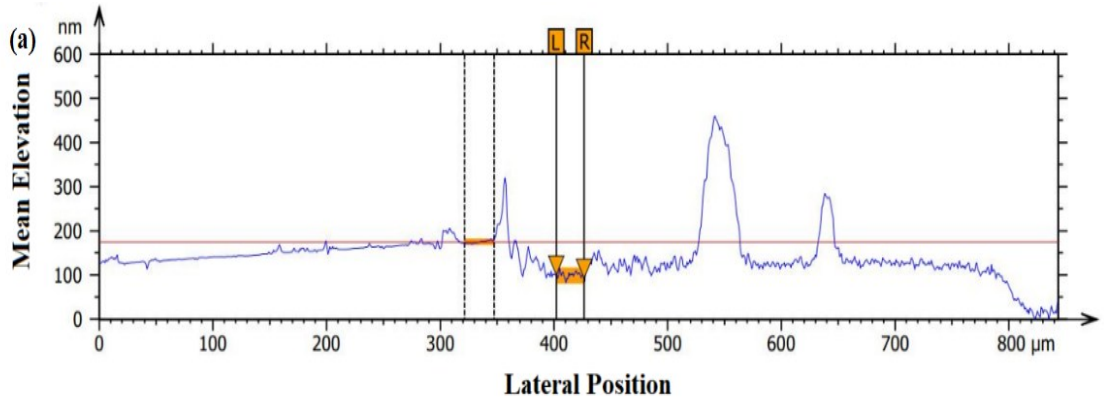
(a)
nm
600
500
400
300
200
100
0
Mean Elevation
L
R
0
100
200
300
400
500
600
700
800 µm
Lateral Position

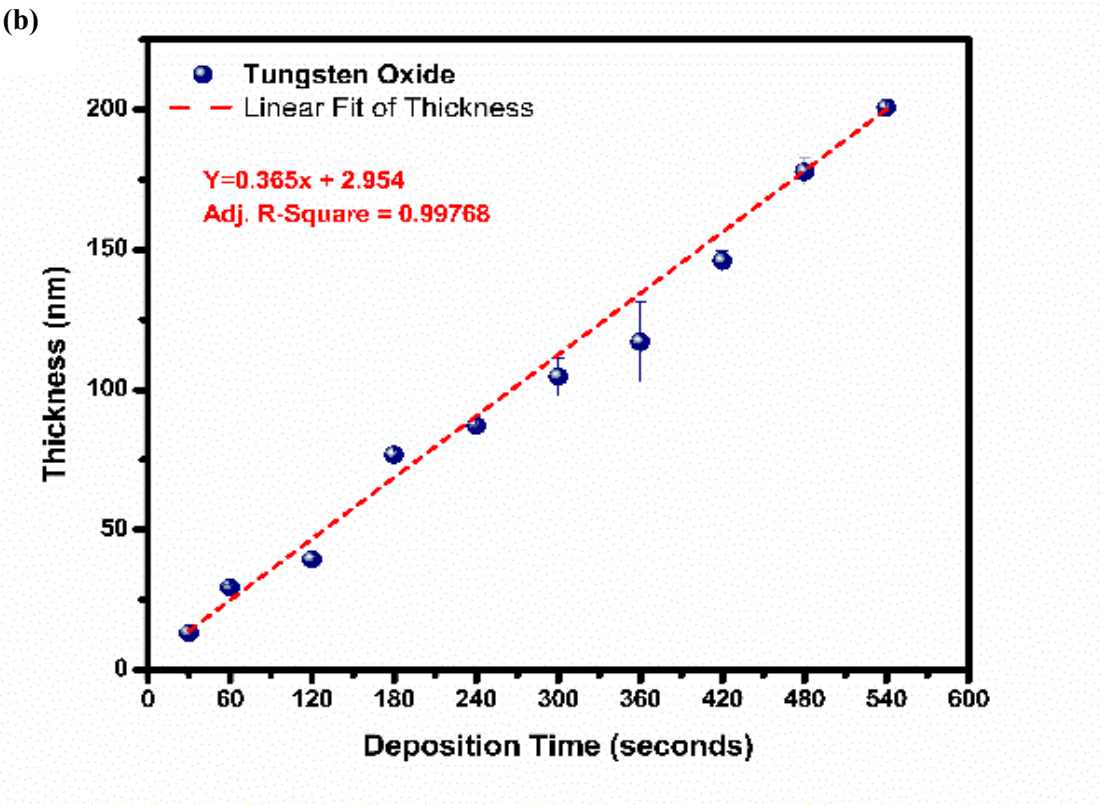
(b)
Tungsten Oxide
Linear Fit of Thickness
Y=0.365x + 2.954
Adj. R-Square = 0.99768
200
150
100
50
0
Thickness (nm)
0
60
120
180
240
300
360
420
480
540
600
Deposition Time (seconds)

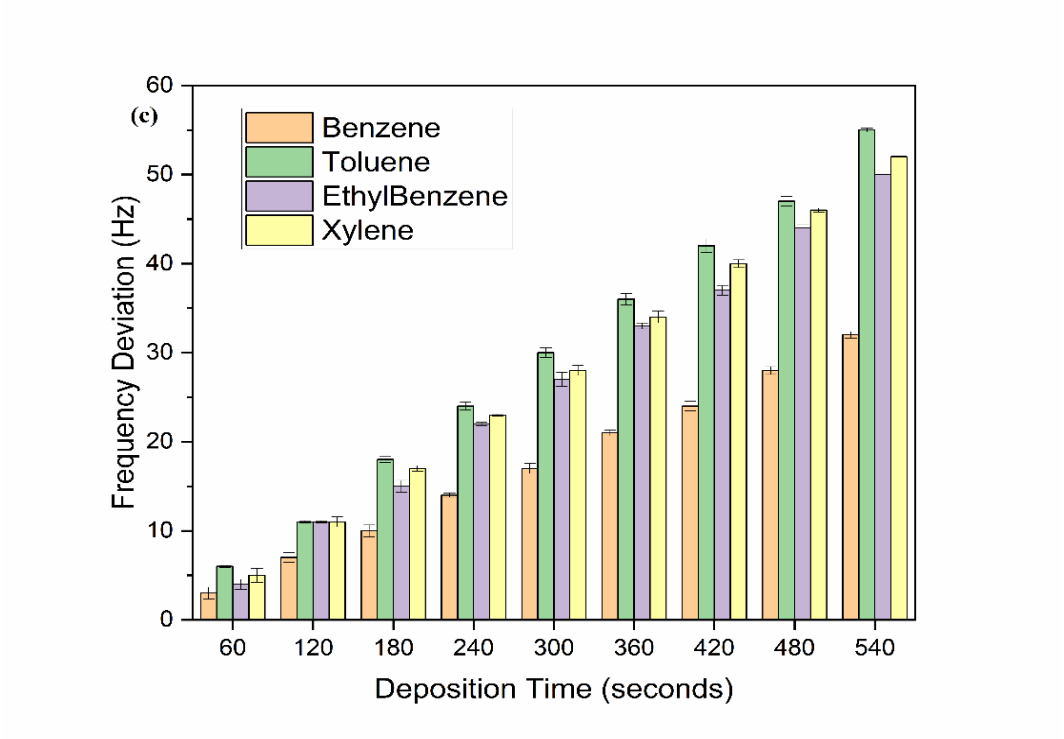

Figure 3.60 (a) The step height of the WO_3 sputtered QCM sensor for a nine-minute deposition time. (b) Variation of thin film thickness with deposition time, (c) Frequency deviation of the sensor for BTEX at different sputtering deposition time.

3.5.2.2 Binding Energy Calculation

Absorption and adsorption are both surface phenomena. Absorption refers to the process by which molecules penetrate and are uniformly distributed within the bulk of material. Adsorption, on the other hand, is the process by which molecules adhere to the surface of a material. At the surface of a QCM electrode, adsorption occurs when molecules adhere, leading to a change in resonant frequency. The surface properties and the sensitizer layer on the electrode surface are essential for controlling adsorption and enhancing the sensor's selectivity and sensitivity. Density Functional Theory (DFT) calculations with the Generalized Gradient Approximation (GGA) exchange-correlation functional method were used to study

the binding energy between a BTEX molecule and a WO_3 substrate. The calculations were carried out using the Vienna ab initio simulation package. The semiempirical DFT-D2 method was applied to correct the van der Waals interactions between the gas molecule and the substrate. The adsorption energy (ΔE_{ad}) was calculated using **Equation (3.9)**[236],

$$\Delta E_{ad} = E_t - (E_s + E_m) + \Delta E_{zp} \quad (3.9)$$

Here, Et, E_s, and E_m account for the total energies of the WO_3 substrate with BTEX molecule, WO_3 substrate, and isolated gas molecule, respectively. E_{zp} represents the zero-point energy difference between the states before and after gas molecule adsorption. A (3×3×1) and a (5×5×1) supercell of WO_3 were modelled with optimized lattice constants a = b = 11.588 Å & a=b=19.313 Å, respectively, for binding energy calculations. The bond length of W-O is 1.931 Å, and the bond length of WO_3 and BTEX molecules is between 1 Å and 6 Å. **Table 3.4** compares simulation results for the BTEX adsorption energy on WO_3 at various crystal densities. Negative ΔE_{ad} values signify favourable, stabilizing adsorption. Each BTEX molecule shows differing adsorption energies in nine and twenty-five crystal structures, with stronger adsorption in the denser structure. ΔE_{ad} absolute values differ notably among BTEX molecules, with xylene and ethylbenzene having the most negative ΔE_{ad}, indicating its highest adsorption affinity among the three. Additionally, the comparison likely shows that the adsorption energies were stronger in the denser crystal structure (5×5×1) than in the less dense structure (3×3×1), indicating that the crystal density of WO_3 can significantly influence the adsorption behaviour of BTEX molecules.

Table 3.4 Comparison of Adsorption Energies (ΔEad in μeV) for BTEX Molecules on WO_3 Substrate in (3×3×1) WO_3 supercell and (5×5×1) WO_3 supercell Configurations.

Compound	(3×3×1) WO_3 supercell			(5×5×1) WO_3 supercell		
	Ead (μeV)	Et (μeV)	Es (μeV)	Ead (μeV)	Et (μeV)	Es (μeV)
Benzene	-457.23	-16856.4	-15865.4	-45611.4	-24452.7	-1208.3
Toluene	-967.58	-16532.7	-15865.4	-48483.7	-27356.4	-1208.3
Ethylbenzene	-3524	-19365	-15865.4	-90702.3	-91208.3	-1208.3
Xylene	-3389.59	-19296.1	-15865.4	-88703.7	-47296.1	-1208.3

3.5.2.3 Structure Analysis

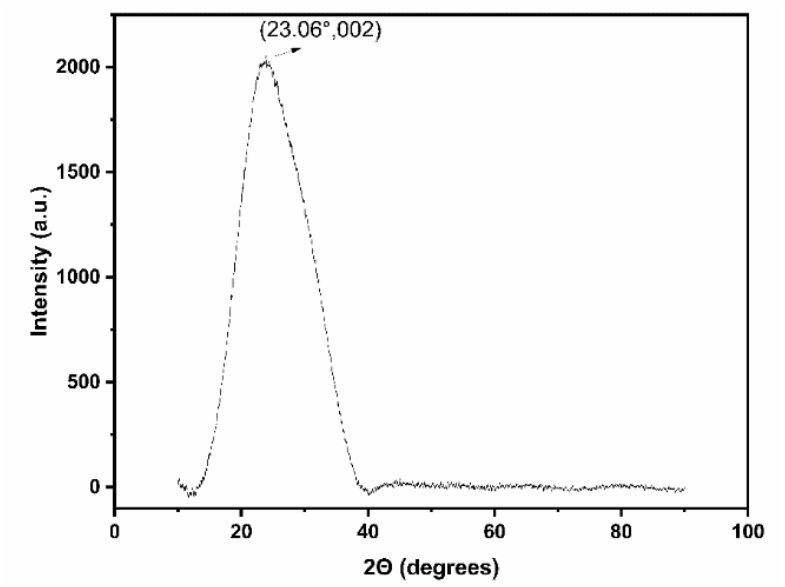

Figure 3.11 XRD pattern of WO_3 deposited (540 seconds) on a quartz crystal substrate.

The XRD pattern of a sputtered WO_3 thin film (540 seconds) deposited on a quartz substrate is shown in **Figure 3.11.** In the XRD analysis, a CuKα source was used with a copper anode. The sample was analyzed over a scan range of 9.997 degrees with a step size of 0.0032 degrees, yielding 24,372 data points. The measurement was conducted in continuous-scan mode, with each step taking approximately 23.97 seconds. The XRD pattern reveals a broadened peak in the range of 2θ values

from 15° to 40° due to the amorphous nature of sputtered WO_3 deposited on the QCM substrate [237], and the peak at 23.027° suggests partial crystallization, corresponding to the (002) plane of WO_3[238].

3.5.2.4 Surface Analysis

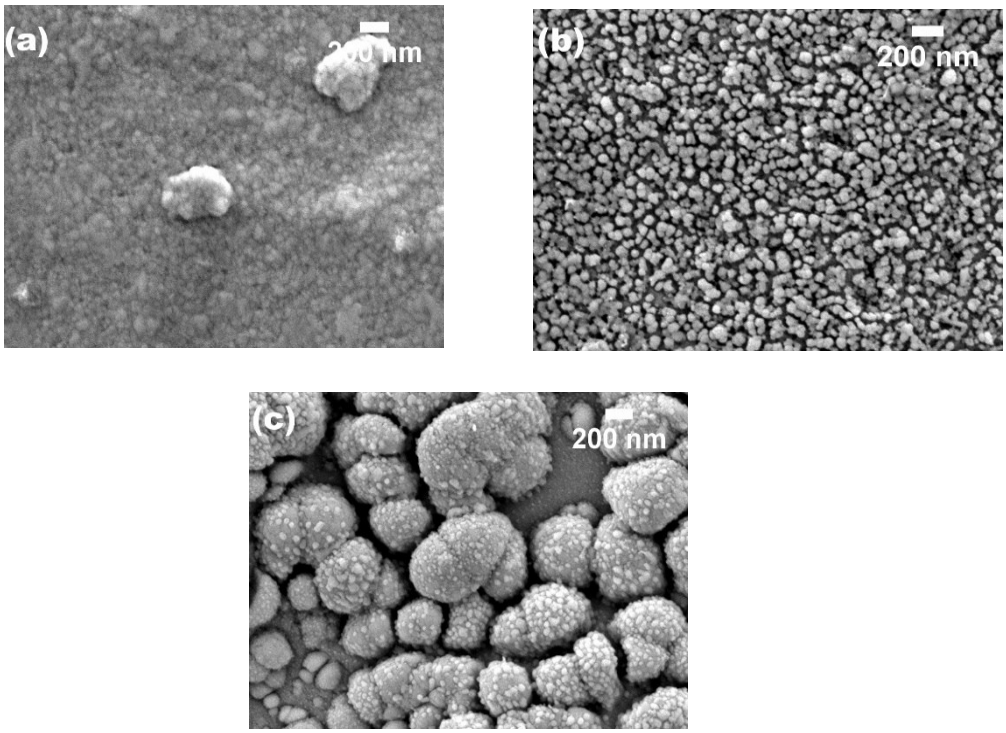

Figure 3.12 FESEM Images of (a) Uncoated QCM electrode, (b) QCM electrode with WO_3 sputtered for 60 seconds, and (c) QCM electrode with WO_3 sputtered for 540 seconds

FESEM analysis **(Figure 3.12)** of uncoated QCM electrodes and QCM electrodes sputtered with WO_3 for 60 seconds and 540 seconds reveals surface differences. Uncoated QCM **(Figure 3.12 (a))** appears flat with minimal variations. The 60-second WO_3 coating displays densely packed particles with a mean length of 55.67 ± 30.16 nm and a mean surface area of 135.75 ± 70 nm^2 **(Figure 3.12 (b))**. For the 540-second deposition (Figure 3.12 (c)), the mean length was 142.94 ± 163.5 nm, and the mean surface area was 337.74 ± 380.03 nm^2. The spheroidal morphology confers increased surface area, optimal particle packing, and enhanced mass transfer, all of which are crucial for efficient adsorption. The 540-second deposition offers a larger surface area with more binding sites. The 540-second deposition was less porous (porosity: 0.14) than the 60-second deposition (porosity: 0.19). The 540-second deposition features a more significant average pore radius (27.15 ± 21.93 nm) than the 60-second deposition (21.24 ± 11.36 nm) **(Figure 3.13 (a) & (b))**.

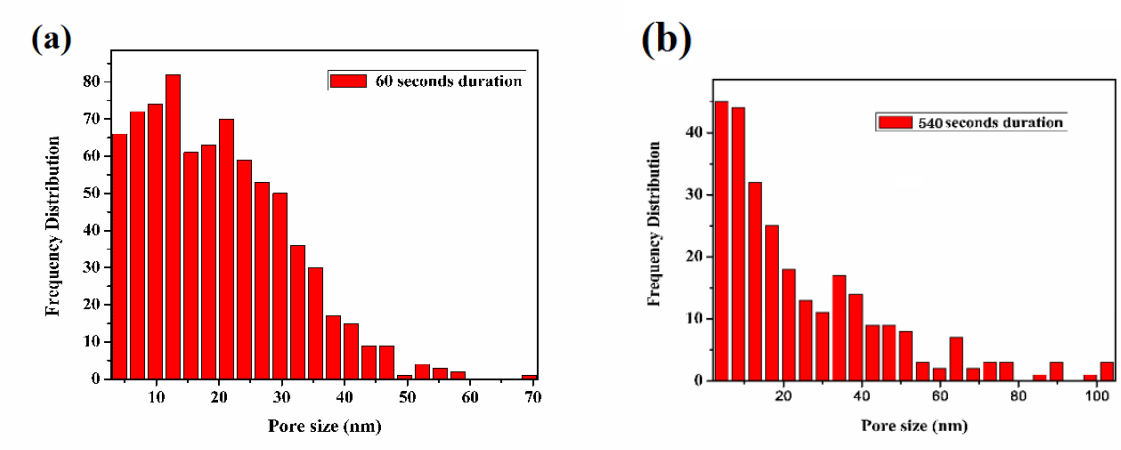

Figure 3.13 Pore size distribution of (a) QCM electrode with WO_3 sputtered for 60 seconds (b) QCM electrode with WO_3 sputtered for 540 seconds.

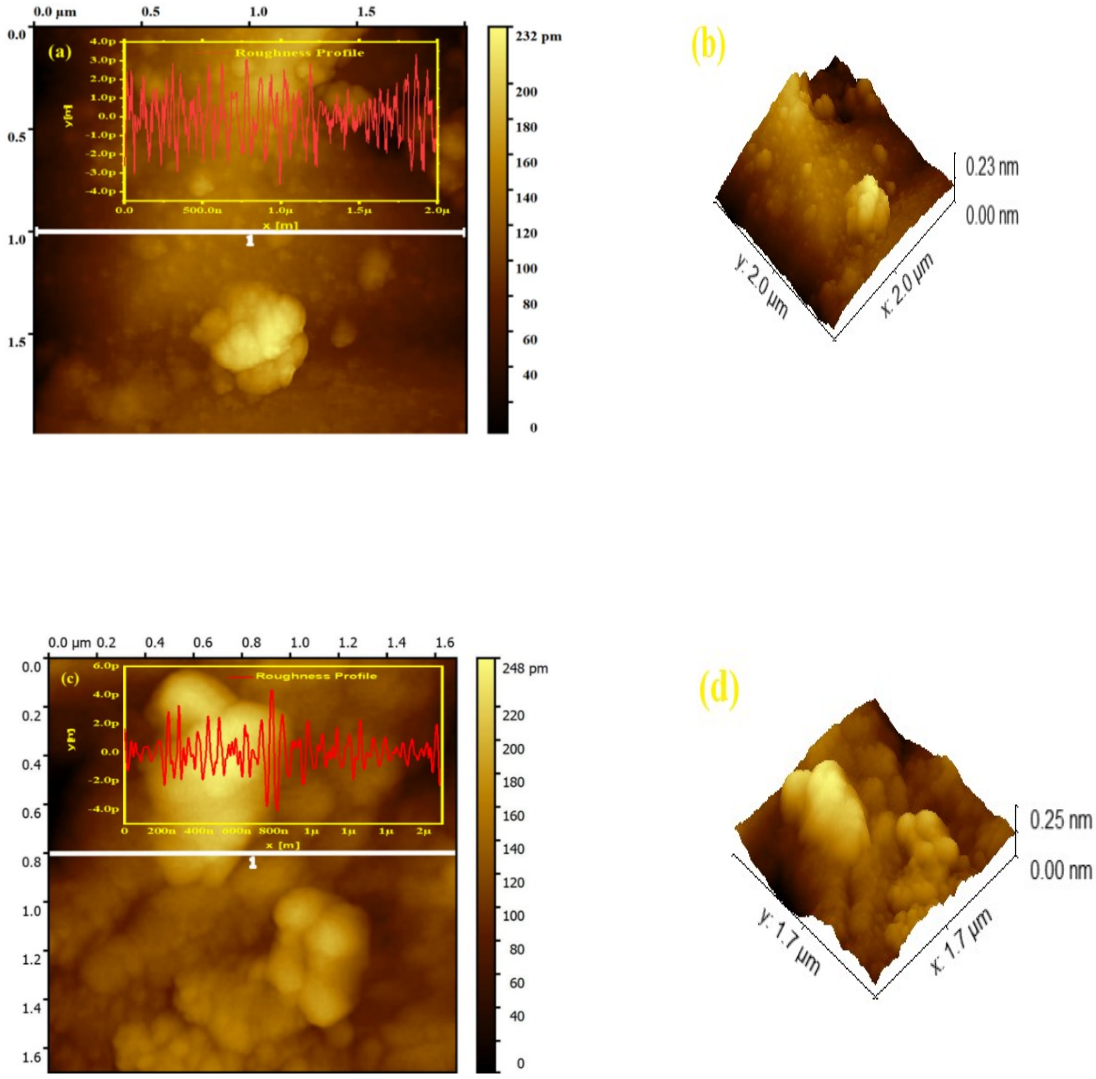

Figure 3.14 (a) 2D surface Profiles (b) 3D surface Profiles of Uncoated QCM Sensor, (c) 2D surface Profiles (d) 3D surface Profiles of WO3-Coated (540 seconds) QCM Sensor

Figure 3.14 (a) and (b) illustrate the 2D and 3D surface profiles of the uncoated QCM sensor. Over the entire surface in **Figure 3.14 (a)**, the average roughness - Ra = (30.89 ± 10.22) nm, and root mean square roughness - Rq = (38.78 ± 10.72)

nm. **Figure 3.14 (c) and (d)** display 2D and 3D surface profiles of the nine-minute WO_3-coated sensor. Over the complete surface in **Figure 3.14 (c)**, Ra = (30.31 ± 12.24) nm, and Rq = (40.7 ± 16.03) nm. The WO_3-coated sensor has a slightly higher Rq, indicating more pronounced height deviations from the mean and a rougher overall surface. This increased roughness is attributed to the deposited WO_3 coating, introducing additional surface features and irregularities.

3.5.2.5 Adsorption – Desorption Isotherm

BTEX vapours adhere to the surface of WO_3 functionalized QCM surface through various interactions, including van der Waals forces, hydrogen bonding, and dipole-dipole interactions[239]. The porous nature of the WO_3 film increases the available surface area for these interactions, enhancing the sensor's sensitivity. Upon exposure to BTEX vapours, the molecules bind to the WO_3 surface, leading to a change in mass detected by the QCM. This mass change results in a frequency shift proportional to the concentration of BTEX in the environment. The fact that the sensor response returns to baseline after purging indicates that the adsorbed molecules can desorb from the surface, demonstrating that the interaction is predominantly physisorption rather than absorption. This reversible adsorption-desorption behaviour is a desirable characteristic for QCM sensors, which is further enhanced by the WO_3 film on the QCM surface. The energy associated with the adsorption process is described by the adsorption isotherm, which relates the amount of gas adsorbed to the gas pressure (or concentration) at a constant temperature.

The Langmuir adsorption isotherm, expressed in Equation (3.10) [250], was used to describe the dynamic change in adsorbed mass (Δm_t) on a QCM sensor over time (t) and the surface's maximum adsorption capacity (m_0).

$$\Delta m_t = m_0(1-e^{-\left(\frac{t}{a}\right)}) \quad (3.10)$$

The m_0 values indicate the maximum amount of each BTEX compound that can be adsorbed onto the WO_3-coated QCM sensor. It is expressed as the mass absorbed per unit mass of adsorbent. Higher m_0 values suggest a greater capacity to adsorb that compound. Time Constant 'a' (seconds) reflects the affinity between the surface and the adsorbate. A higher value indicates a stronger affinity between the WO_3 surface and the BTEX compound.

The parameters derived from fitting the Langmuir isotherm equation to the experimental data (Figure 3.15) for a 150 ppm BTEX exposure on a WO_3-coated QCM sensor are tabulated in **Table 3.5.** This value indicates that at a 150-ppm exposure concentration of benzene, toluene, and xylene, the QCM sensor can adsorb up to 10 ± 0.2 ng, 15 ± 1.73 ng, and 21 ± 0.23 ng, respectively. The greater value suggests slower adsorption and desorption kinetics, meaning the sensor might take longer to reach equilibrium and detect mass changes due to BTEX adsorption. Lower SSR values indicate a better fit of the Langmuir model to the experimental data.

.

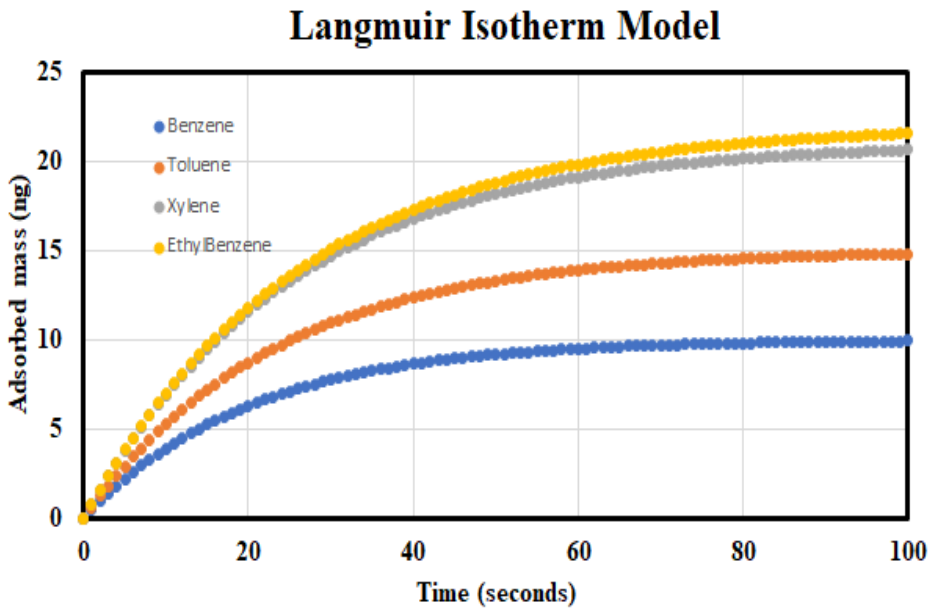

Figure 3.15 Dynamic Adsorption Behavior of BTEX Compounds on WO_3-Coated QCM Sensor.

Table 3.5 Adsorption Parameters and Molecular Properties of BTEX Compounds on WO_3-Coated QCM Sensor.

Parameters	Benzene	Toluene	Ethylbenzene	Xylene
m_0 (ng)	10	15	22	21
a (seconds)	20	23	26	25
SSR	2.17	2.33	3.5	3.33
Molecular weight (g mol^{-1})	78.12	92.15	106.17	106.17
Vapor Pressure (Pa)	12639	3786	950	1173

3.5.2.6 Thermogravimetric Analysis

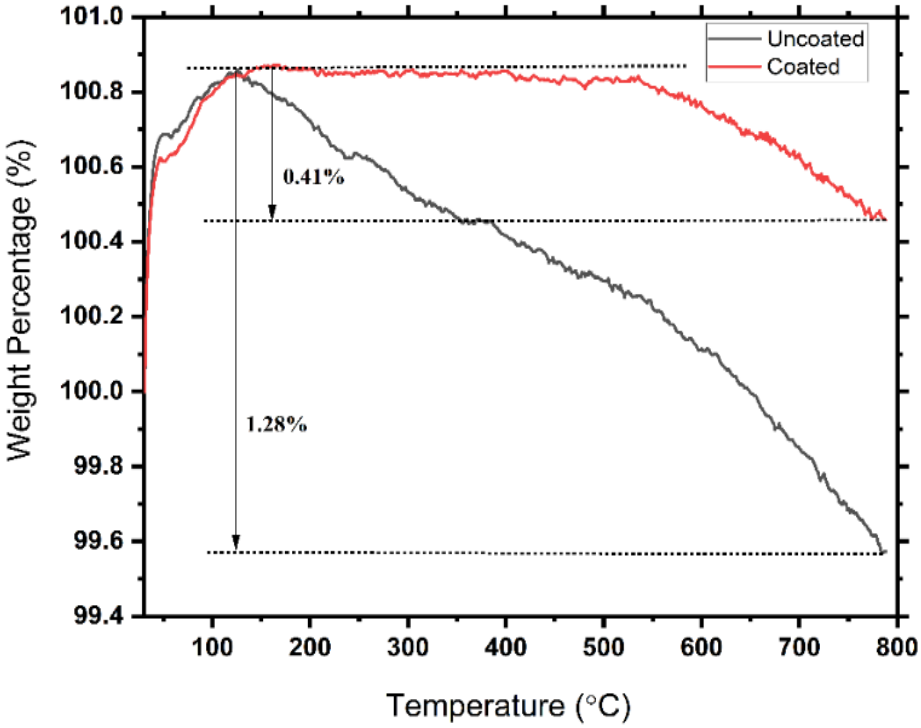

Figure 3.16 TGA thermogram of uncoated and WO_3-Coated QCM sensors.

In **Figure 3.16**, the TGA thermogram of uncoated and WO_3-coated QCM sensors shows an initial weight gain of approximately 0.9% (from Room Temperature to 120˚C). This temporary increase is likely a combination of two factors: 1) the instrumental buoyancy effect, where the decreasing density of the purge gas upon heating causes an apparent increase in weight, and 2) the adsorption of atmospheric moisture onto the hygroscopic surfaces of the QCM and WO_3 film, which is retained during the initial stabilization phase[251-252]. The TGA thermogram (Figure 3.16) shows that the uncoated QCM sensor experiences a decrease in

weight percentage between 100 and 200 °C. The 1.28% weight reduction implies vulnerability to chemical reactions at lower temperatures (100-200°C). In contrast, the WO_3-coated (540 seconds) QCM sensor maintains a stable weight percentage up to around 500-600°C, delaying weight loss and demonstrating enhanced thermal stability compared to the uncoated sensor. The coating protects against early weight loss (100-200°C) and delays potential degradation or chemical reactions up to higher temperatures (500-600°C).

3.5.2.7 Sensitivity Analysis

The sensor's response to BTEX was assessed using a gas-sensing setup employing static headspace sampling. A sealed 1 L glass chamber housed the sensor, with BTEX vapours (2-10 ppm) introduced at a controlled rate of 1 L/min, monitored using a mass flow meter. The chosen flow rate was suitable for maintaining the desired concentration (2-10 ppm), for adsorption kinetics, and for minimizing viscosity and hydrostatic pressure effects on the QCM sensor operating at a high frequency within a 1-litre chamber. The experiment was conducted under constant conditions: ambient temperature (27 ± 1)ºC, Humidity (16 ± 5)%, and standard atmospheric pressure (760 mm Hg) monitored within the chamber. The QCM sensor, coated with a 200 nm-thick (540-second coating) WO_3 layer, demonstrated good sensitivity to BTEX vapours. The frequency change-concentration plot of the WO_3-coated crystal is depicted in **Figure 3.17**, revealing a linear relationship described by **Equation (3.6)**[212]. The sensor's sensitivity values were 3.36±0.24 Hz/ppm, 5.69±0.22 Hz/ppm, 5.3±0.14 Hz/ppm, and 5.10±0.08 Hz/ppm for benzene, toluene, ethylbenzene, and xylene, respectively.

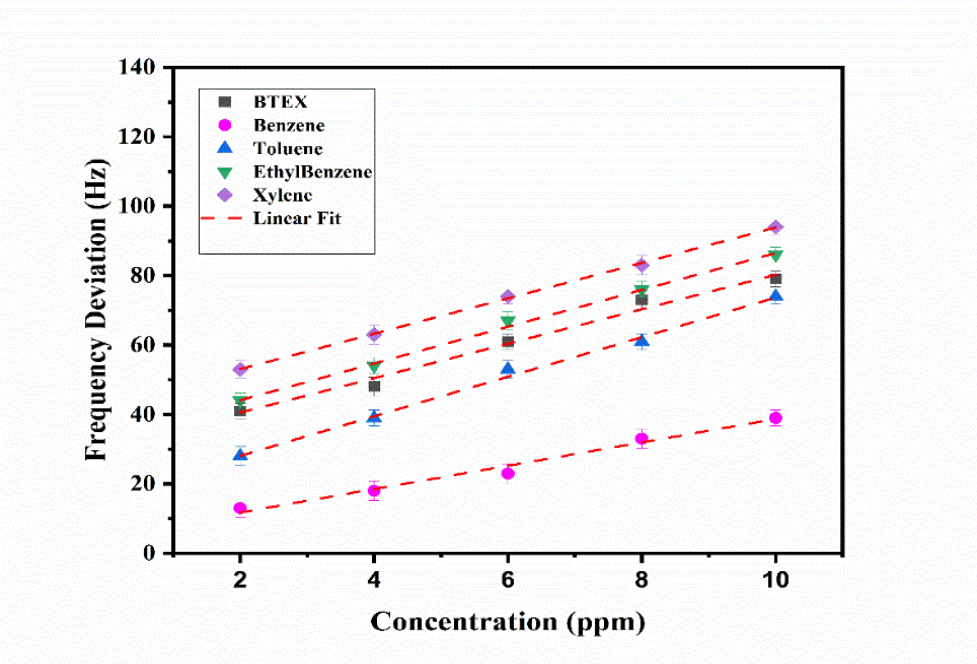

Figure 3.17 Sensitivity plot of WO_3 sputtered sensor after exposure to BTEX with different concentrations (2-10 ppm) at (27±1) °C, 16% RH and standard atmospheric pressure.

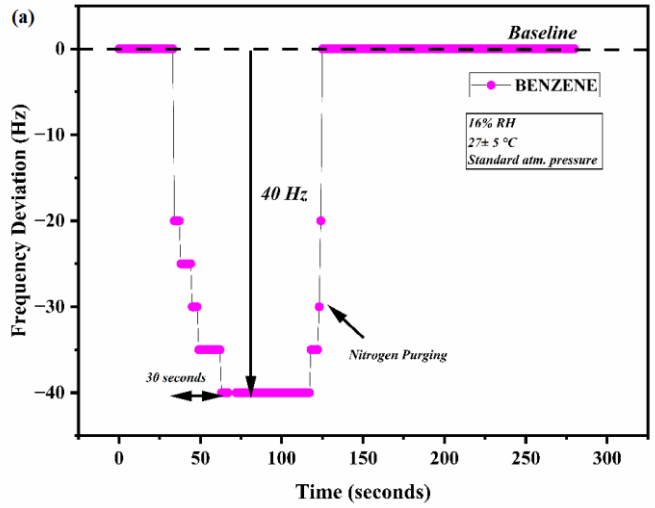

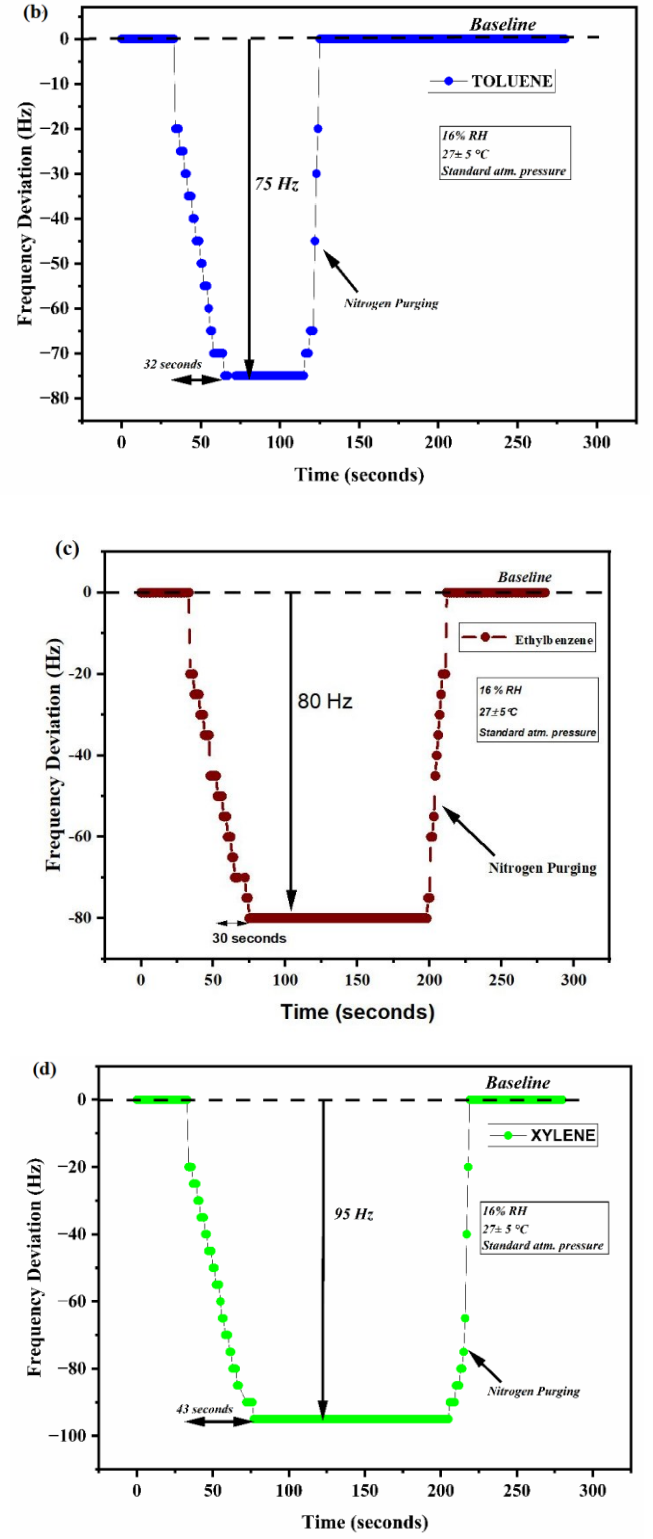

Figure 3.18 Response - Recovery Characteristics of the WO_3-Coated Sensor (540 seconds) for (a) Benzene (b) Toluene (c) Ethylbenzene (d) Xylene at (27±1)°C, 16% RH and standard atmospheric pressure.

The LOD, which is three times the ratio of the noise level at the frequency of interest to the sensor's sensitivity, is evaluated using **Equation (3.7)** [212]. The value of LOD for benzene, toluene, ethylbenzene, and xylene was 1.48 ppm, 0.79 ppm, 0.99 ppm, and 0.33 ppm, respectively. The sensor exhibited frequency drops of 37 ± 1 Hz, 59 ± 1 Hz, 80 ± 1, and 92 ± 1 Hz upon exposure to 8 ppm of benzene, toluene, ethylbenzene, and xylene, respectively **(Figure 3.18 (a) - (d))**. Response time, linked to analyte vapour pressure, is the time needed for the sensor to reach 90% of its steady-state reading. Compounds with lower vapour pressures exhibit delayed QCM responses because fewer vapour-phase molecules are present at a given temperature. Among BTEX, benzene has the lowest vapour pressure and the shortest response time (30 seconds), while toluene and xylene exhibit longer response times (32 and 43 seconds, respectively). After a 10-second response, the sensor was purged with ambient air and nitrogen gas to maintain the same experimental conditions. Benzene recovers in 51 seconds, toluene in 101 seconds, ethylbenzene in 54 seconds, and xylene in 108 seconds during air purging. These differing recovery times are attributed to the compounds' distinct chemical properties. Benzene disperses rapidly from the sensor's surface due to its low molecular weight, resulting in a shorter recovery time. In contrast, greater molecular complexity and weight lead to prolonged desorption and longer recovery times.

3.5.2.9 Repeatability and Reproducibility Analysis

The 540-second WO_3-coated QCM sensor repeatability was assessed by subjecting it to five consecutive exposures to 2-10 ppm of BTEX under consistent experimental conditions. Reproducibility, in contrast, was appraised using measurements from three distinct sensors produced through the same process, all exposed to 2-10 ppm of BTEX. The repeatability (Rp) and reproducibility (Rd) percentages are calculated using **Equation (3.8)**. Repeatability percentages consistently range from 85% to 99%, especially at higher BTEX concentrations, confirming the sensor's consistent responses to repeated exposures at the same concentration. Reproducibility percentages at higher concentrations (95% to 98%) suggest effective performance replication across multiple sensors. Frequency shift measurements exhibit minimal variability, with a margin of error of less than 5% at the 95% confidence level, highlighting stable and reliable sensor performance.

3.5.3 Study of Effect of Humidity

The 540-second WO_3-coated QCM sensor was placed in different humidity conditions in a controlled environment of 27 ± 1°C and standard atmospheric pressure (**Figure 3.19**). There was no significant change in base resonant frequency (9929711 Hz) values at 50%, 55%, and 60% relative humidity (RH), where the frequency deviation for WO_3 was 0 Hz, which could be because the WO_3 coating

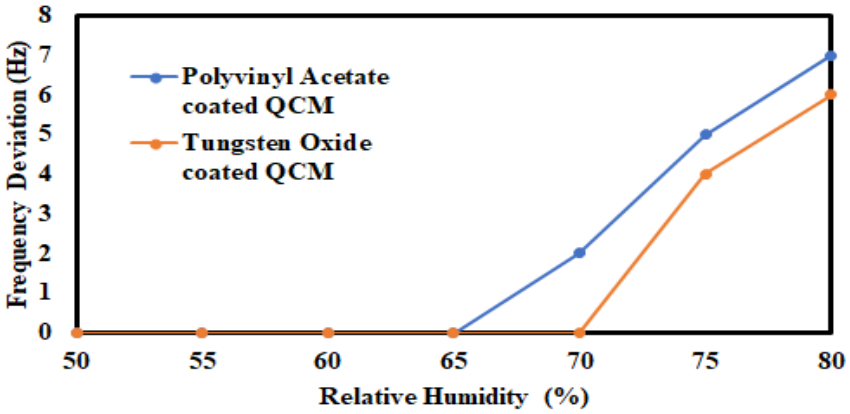

Figure 3.19 WO_3 Coated QCM Sensor (540 seconds sputtered) and PVAc Coated QCM sensor (1500rpm spin coated) frequency deviation at different humidity values.

had not absorbed substantial water molecules at these humidity levels, resulting in minimal mass change and, thus, negligible frequency shift. At 70% RH, the PVAc showed a deviation of 2 Hz. At 75% RH, the frequency deviation of the QCM sensor relative to the base value was 4 Hz for WO_3 and 5 Hz for PVAc. Subsequently, at 80% RH, the frequency deviation changed by a further 2 Hz for WO_3 and 2 Hz for PVAc. This increase in frequency indicates that the WO_3 and PVAc coating has absorbed moisture from the environment. The data demonstrates the frequency deviation for both PVAc and WO_3, showing an increasing trend as humidity rises from 70% to 80% for the WO_3-coated QCM sensor. Humidity values ranging from 50% to 60% represent the optimal operating range for a 540-second WO_3-sputtered QCM sensor and a 1500 rpm PVAc spin-coated QCM sensor.

3.5.4 Stability Analysis

Figure 3.20 depicts the mean frequency deviations for each exposure day, assessed on the 5th, 10th, 15th, 20th, and 30th days following exposure to 10 ppm of BTEX. For the WO_3 sensor, benzene frequency deviations decreased by 2 Hz (from 37 Hz to 35 Hz) over 30 days. Toluene deviations decreased by 3 Hz (from 59 Hz to 56 Hz), ethylbenzene by 3 Hz (from 54 Hz to 51 Hz), and xylene by 1 Hz (from 50 Hz to 49 Hz) over the same period. For the PVAc sensor, benzene deviations decreased by 1 Hz (from 51 Hz to 50 Hz), toluene by 2 Hz (from 53 Hz to 51 Hz), ethylbenzene by 1 Hz (from 59 Hz to 58 Hz), and xylene by 1 Hz (from 49 Hz to 48 Hz) over the 30-day assessment. This consistent decrease in frequency deviation over time indicates a stable sensor response over the specified duration.

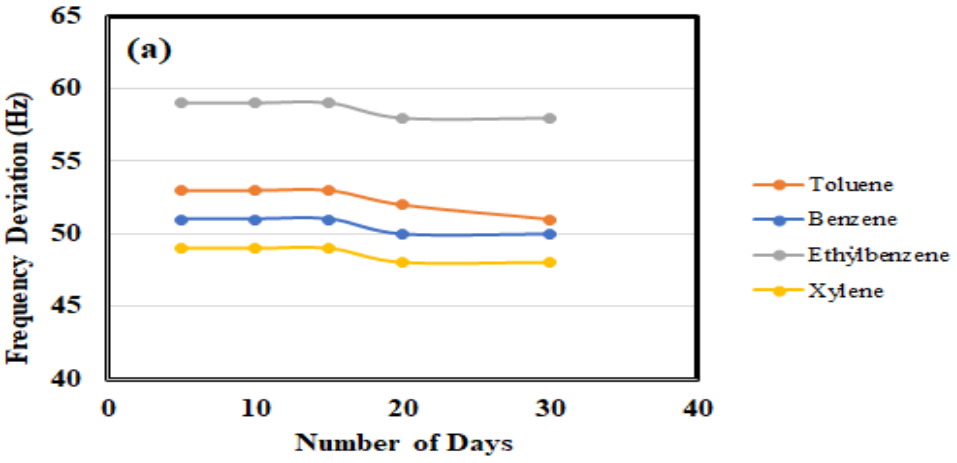

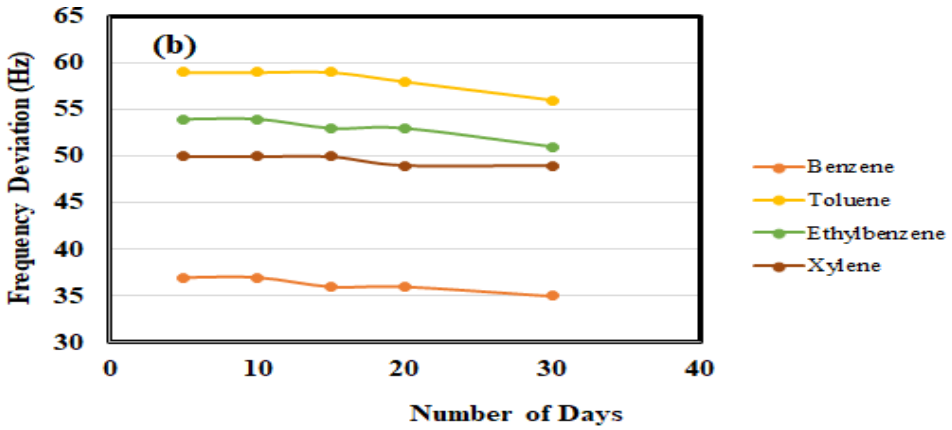

Figure 3.20 Stability Assessment of (a) WO_3 Coated QCM Sensor (540 seconds sputtered) (b) PVAc Coated QCM sensor (1500rpm spin coated)

Table 3.6 presents a comparative analysis of the performance of the PVAc- and WO_3-coated QCM sensor for sensing BTEX. **Table 3.7** compares the performance of the 540-second WO_3-coated QCM sensor with that reported in previous studies. The current work using a WO_3-based Quartz Crystal Microbalance (QCM) sensor offers lower detection limits for benzene, toluene, and xylene. It exhibits good response times at an ambient temperature of 300K, making it a good choice for real-time environment/health monitoring applications. **Table 3.8** represents the sensitivity and response time of the various polymer-coated QCM sensors for BTEX detection. The 540-second WO_3-coated QCM sensor showed higher sensitivity and faster response time than other QCM sensors. We optimized the sensor's performance in the current study and compared it against the reported literature. In the future, these results will be further experimentally validated using standard commercially available sensors.

3.5.5 Parametric Analysis of Fabricated Sensor

Table 3.6 Performance Comparison of PVAc and WO_3 Coatings for QCM Sensors in Detecting BTEX Compounds.

Coating type	Parameters	Benzene	Toluene	Ethyl-benzene	Xylene	BTEX
PVAc	Sensitivity (Hz/ppm)	5.14 ± 0.25	5.17 ± 0.44	5.85 ± 0.31	5 ± 0.31	4.74 ± 0.42
	Intercept	31.52 ± 1.57	39.67 ± 2.84	58.11 ± 1.94	101 ± 2.17	91.68 ± 2.68
	R^2	0.98	0.99	0.99	0.99	0.99
	LOD (ppm)	0.91	1.65	0.99	1.3	1.69
	LOQ (ppm)	3.04	5.5	3.31	4.35	5.66
	Repeatability % ± CI	96	97	97	98	98
	Reproducibility % ± CI	94	95	96	98	98
WO_3	Sensitivity (Hz/ppm)	3.36 ± 0.24	5.69 ± 0.22	5.3 ± 0.14	5.10 ± 0.08	4.96 ± 0.31
	Intercept	5.04 ± 1.66	16.68 ± 1.52	33.48 ± 0.99	42.83 ± 0.57	30.59 ± 2.09
	R^2	0.98	0.99	0.99	0.99	0.98
	LOD (ppm)	1.48	0.79	0.56	0.33	1.26
	LOQ (ppm)	4.93	2.66	1.88	1.12	4.21
	Repeatability % ± CI	98	97	95	98	98
	Reproducibility % ± CI	98	97	96	97	97

Table 3.7 Comparative analysis of optimized WO_3 sputtered QCM sensor against reported works on metal oxide sensors

Thin film Type	**Target Analyte**	**Type of sensor**	**Limit of Detection** (ppm)	**Response Time** (seconds)	**Temperature** K	**Remarks**	**Reference**
Co_3O_4	Benzene, Toluene, Xylene	Resistive	10	1	573-593	Operates at elevated temperature	[196]
Au-ZnO	Benzene, Toluene, Xylene	Resistive	20	5	479	Operates at elevated temperature	[197]
WO_3	Toluene, Xylene	Resistive	1	70 (response + recovery)	693	Operates at elevated temperature	[223]
Au-WO_3	Benzene, Toluene, Xylene	Resistive	20 ppb	_	593	Operates at elevated temperature	[224]
C-WO_3	Toluene	Resistive	1	10	593	Operates at elevated temperature	[201]
h-WO_3	Benzene	Resistive	-	36	593	Operates at elevated temperature	[242]
	Toluene		-	17			
	Xylene		-	23			
WO_3	Benzene	QCM	**1.48**	**30**	300	Operates at room temperature	Current Work
	Toluene		**0.7**	**32**			
	Ethylbenzene		**0.5**	**30**			
	Xylene		**0.3**	**43**			

"-" denotes that the data is not pointed in the literature.

Table 3.8 Comparative analysis of optimized PVAc spin-coated QCM sensor against reported works on polymer-coated QCM sensors.

Coating Material	Target Analyte	Sensitivity (Hz/ppm)	Response Time (s)	Remarks	Reference
Linseed oil, divinyl benzene, styrene	Benzene Toluene Xylene	1.1 1.3 1.6	102 110 98	Low sensitivity and response time	[204]
PVAc	Benzene Toluene Xylene	0.018 0.041 0.081	225 230 260	Low sensitivity and Low response time	[206]
PDMS	Benzene Toluene Xylene	4.37 7.72 11.40	60 74 140	Low response time	[207]
PEMA–DIOA (5%)	Benzene Toluene Xylene	- - -	220 380 -	Low response time	[243]
Polystyrene	Benzene Toluene Xylene	1.33 1.66 1.44	260 470 660	Low sensitivity and response time	[244]
Tetra-tert-butyl copper phthalocyanine	Benzene Toluene Xylene	- 0.12 0.2	- 180 220	Low sensitivity and response time	[245]
PVAc	Benzene Toluene Ethylbenzene Xylene	**5.14** **5.17** **5.85** **5.0**	**69** **73** **70** **90**	High sensitivity and faster response time	Current work

"-" denotes that the data is not pointed in the literature.

3.6 Conclusion

The thickness of PVAc was altered to obtain significant sensitivity values greater than 0.1 Hz/ppm for BTEX. The methodology has reduced fabrication complexity while improving sensitivity. WO_3-coated QCM sensors have been fabricated and characterized for the detection of volatile organic compounds (VOCs): benzene, toluene, ethylbenzene, and xylene. The 540-second optimized WO_3 film thickness was 200.81 ± 0.39 nm. This optimized sensor displayed a remarkable sensitivity for xylene (5.10±0.08 Hz/ppm), followed by toluene (5.69±0.21 Hz/ppm) and benzene (3.36±0.23 Hz/ppm). Response times were less: 30 seconds for benzene and ethylbenzene, 32 seconds for toluene, and 43 seconds for xylene, indicating its ability to detect trace analyte concentrations quickly. High repeatability and reproducibility (>97%) were observed at 10 ppm for all three compounds. Structural analysis revealed an increased surface area of active adsorption sites and enhanced thermal stability compared to an uncoated sensor.

Over 30 days, both sensors maintained consistent performance when exposed to BTEX vapors. In conclusion, this study successfully fabricated and characterized a PVAc and WO_3-coated QCM sensor for efficient BTEX vapour detection at ambient conditions. The sensor displayed high sensitivity, selectivity, and stability, particularly for BTEX vapours. The fabricated QCM sensor, operating at room temperature with a faster response time, may provide a reliable and efficient method for detecting BTEX, with potential widespread applications in occupational health monitoring and safety.

Chapter 4: Development of Breath Analyzer for Real-Time BTEX Detection

4.1 Abstract

This chapter details the development of a portable breath analyser. It enables near real-time detection of BTEX compounds. Benzene is a known human carcinogen, and BTEX compounds pose significant health risks, especially in the oil and gas industry. Traditional GC-MS is highly sensitive but limited to laboratory settings. Portable GC systems often require pre-concentration and suffer from lower efficiency than standard setups. Our system utilizes a Quartz Crystal Microbalance (QCM) sensor array. It features PVAc and WO_3 coatings for enhanced sensitivity. The device is portable, weighing approximately 1 kg, and functions under ambient conditions without requiring a complex preconcentration setup. It can detect BTEX mixtures at levels below 4 ppm in less than 3 minutes. This compact system, with a height of 200mm and an inner diameter of 68mm, is highly portable, unlike bulkier GC-MS systems. It operates on a low-power, robust design, requiring only a 5V,1000mAh rechargeable battery for power. The system's performance was validated against GC-MS. Correlation analysis confirmed a strong linear relationship between sensor responses and GC-MS data. Machine learning models, specifically K-Means and BIRCH, were applied to BTEX classification, demonstrating effective discrimination among compounds. This work presents a robust, portable, and accurate solution for real-time BTEX monitoring.

4.2 Introduction

Benzene is classified as a known human carcinogen[246]. In contrast, toluene, ethylbenzene, and xylene, although not classified as carcinogenic by current regulatory guidelines, are associated with significant health risks[223-226], including neurotoxicity and other toxic effects, particularly in the oil and gas industry[1], [247]. Detecting BTEX emission concentration in these industries is crucial for protecting workers' health, ensuring environmental safety, and complying with regulatory standards. Chromatography-Mass Spectrometry (GC-MS) is considered a gold-standard method for BTEX analysis in air due to its high sensitivity and selectivity [248]. However, its dependence on laboratory settings limits its suitability for real-time monitoring. To overcome this, portable GC systems have been developed, though they typically require pre-concentration and exhibit lower separation efficiency than a standard setup. For instance, Nasreddine et al. developed a miniaturized GC coupled with a Photoionization Detector (GC-PID) optimized for near-real-time ppb-level BTEX detection, offering portability and rapid analysis within 10 min. However, its performance is affected by humidity and temperature, and preconcentration is still needed [249]. Similarly, Rodríguez-Cuevas et al. proposed a portable GC integrated with a novel pre-concentrator detecting benzene down to 0.057 ppb in small-volume air samples. Yet, the system requires longer analysis times (19 min) and controlled lab conditions [250].

Frausto-Vicencio et al. optimized a compact, field-deployable GC-PID system using ambient air as a carrier gas and a Tenax-GR sorbent-based pre-concentrator, achieving sub-ppb sensitivity, though limited by slower response and reliance on preconcentration [102]. You et al. incorporated a Carbon Nanotube (CNT) sponge pre-concentrator with a GC-PID, achieving sub-ppb detection in 5–10 min; however, the CNT pre-concentrator suffers from material degradation over time, and its field performance needs further validation under varying environmental conditions [251]. Yang et al. developed a portable gas chromatograph (protoGC) with a Flame Ionization Detector (FID) for BTEX detection, demonstrated high correlation with lab-based GC and faster analysis (<5 min), but accuracy declines at higher BTEX concentrations [252]. Alternative sensors have also emerged to enhance real-time detection. Thangamani et al. developed a chemiresistive CuO nanoparticle sensor with good sensitivity in the 40–1000 ppm range, although it requires operation at elevated temperatures (160°C) [253]. Khan et al. proposed two deep-UV absorption spectroscopy methods using micro gas chromatography (μGC), one using a compact PEEK cell achieving a 3.5 ppm LOD and another using a hollow-core waveguide achieving a 196 ppb LOD, though both methods are relatively complex and costly [233-234]. Matatagui et al. employed surface acoustic wave (SAW) sensors with ferrite nanoparticle coatings, demonstrating high selectivity at 10–50 ppm, and Das et al. introduced a smartphone-compatible colorimetric sensor (fluorescence-based) using a Meisenheimer complex with a 0.7–9 ppm detection range, though both are still limited in detection range [235-236].

These sensors also exhibit limitations in photostability under prolonged exposure.

Quartz Crystal Microbalance (QCM) sensors are suitable for real-time BTEX detection due to their benefits, such as low power consumption, room-temperature operation, and potential for miniaturization and selective coating [258]. QCM sensors require minimal sample preparation, reduced analysis time, and are inexpensive compared to high-end instruments like GC-MS. Additionally, QCM sensor-array integration enhances sensitivity by using multiple QCM sensors with different coatings that selectively interact with VOCs [259]. For instance, a study on human blood glucose monitoring used a QCM sensor to detect acetone in exhaled breath, employing a zeolite absorbent to enhance sensitivity by pre-concentrating low acetone levels (0.1–10 ppm) before detection [46]. Another study developed a portable gas discrimination instrument that employed a QCM sensor array to detect and quantify multiple gases, including acetone, chloroform, and methanol [260]. Furthermore, a QCM-based electronic nose was developed to identify Chinese liquor flavours utilizing a multi-sensor array combined with a random forest classifier to distinguish subtle differences in VOC profiles. The study emphasized that integrating multiple QCM sensors, each with tailored coatings, allowed precise discrimination of complex VOC mixtures [261]. These studies collectively show that integrating QCM sensor arrays with diverse coatings and pattern recognition algorithms enhances their overall accuracy and reliability. QCM sensor operates on the principle of measuring changes in resonant frequency caused by mass variations on the quartz crystal's surface.

When exposed to gas molecules, the QCM sensor changes its resonant frequency, as expressed by the Sauerbrey Equation (3.1) [277], enabling the detection and quantification of target gas molecules, as discussed in detail in Chapter 3. A QCM sensor array can function as an Electronic Nose (E-Nose) by mimicking the human olfactory system to identify various odours or VOCs [189], [243-244].

Recent advancements in miniaturized gas chromatography systems and sensor technologies have improved the detection of BTEX compounds. However, many of these methods still require preconcentration steps, operate under specific environmental conditions, or involve complex setups. Ongoing research is necessary to overcome these challenges, especially to achieve high sensitivity and selectivity under dynamic field conditions.

In this chapter, we have discussed a portable solution for the real-time detection of BTEX vapors and their mixtures at ambient temperature. An array of three QCM sensors coated with Tungsten oxide (WO_3), Polyvinyl acetate (PVAc), and one uncoated sensor has been used in the system.

The PVAc and WO_3-coated sensors demonstrated good sensitivity and response times to BTEX vapours, as reported in chapter 3 [264]. The system requires a response time of 25 seconds and a total analysis time of 2-3 minutes, which qualifies it as "real-time" detection because it provides timely data that can inform immediate decision-making in industrial applications.

The system's performance has also been validated against GC-MS, demonstrating accurate detection of BTEX mixtures in less than four minutes.

The main contributions of this work are summarized as follows:

- Development of a portable BTEX vapor detection system for near real-time monitoring.
- Integration of PVAc and WO_3-coated QCM sensor array for enhanced BTEX sensitivity: These coatings improve the selective detection of benzene, toluene, ethylbenzene, and xylene.
- Use of PCA and clustering algorithms for BTEX classification: Pattern recognition techniques such as k-Means and BIRCH clustering algorithms to enable accurate, near-real-time classification of BTEX gases.
- Demonstration of the system's performance through breath sample analysis: The developed device was validated with respect to GC-MS by analysing the breath of petrol station workers.

4.3 Methodology

This section outlines the design and implementation aspects of the BTEX measurement system, which is structured into three main components: (A) BTEX sampling and detection system, (B) Data acquisition system, and (C) Data processing system. **Figure 4.1.** presents a block diagram of the overall system architecture.

4.3.1 Breath Analyzer Design

4.3.1.1 Breath Sampling and Detection System

The BTEX sampling and detection system **(Figure 4.1)** includes a BTEX sampling unit, a sensing unit, and a nitrogen and dry air purging unit. The measurement process typically comprises three phases: 1) BTEX vapor sampling, 2) BTEX sensing, and 3) Purging. Before running an experiment, a protocol was prepared outlining activities such as the experiment's start time, measurement count, purging durations, measurement phases, and delay times.

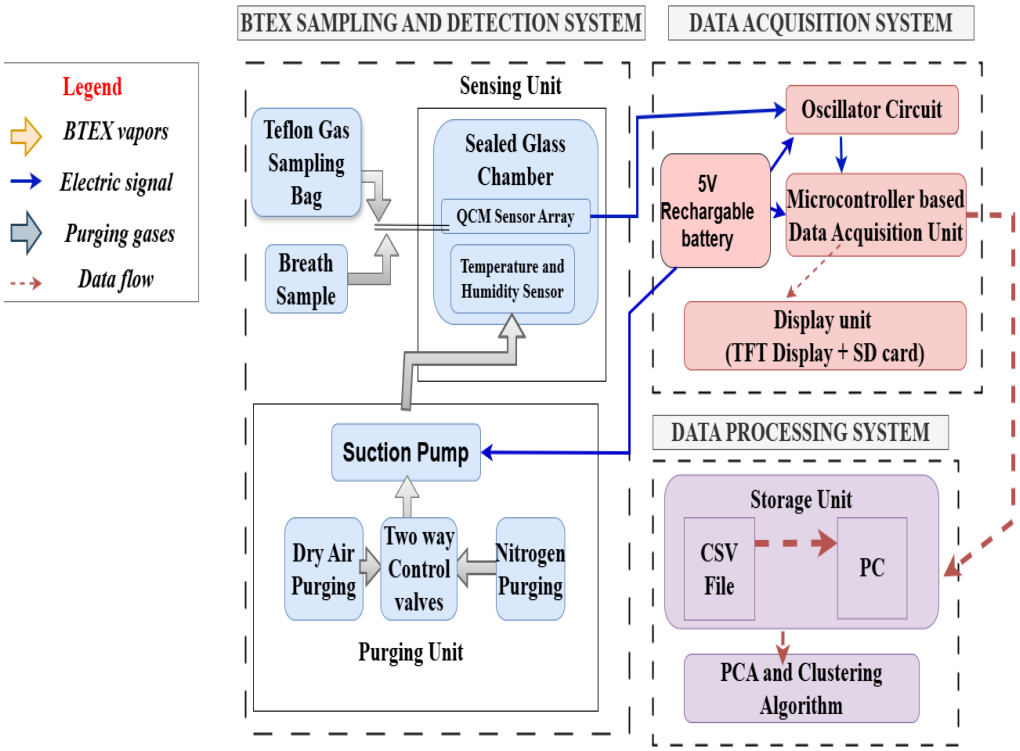

Figure 4.1 Block diagram representation of a Breath analyzer.

BTEX vaporization unit: BTEX vapors were generated in a 1 L glass vaporization chamber (Borosil, India) using a static headspace sampling technique [263]. Static headspace sampling is an analytical technique used to measure volatile compounds in a sample by allowing the sample to equilibrate at ambient temperature in a sealed container and then extracting a portion of the gas phase (headspace) above the sample for analysis. This method relies on the compounds' natural volatility to partition between the sample and the headspace. The sampling process starts by injecting 1-10 µl of BTEX samples (using a Hamilton 700 Series Microliter syringe with a 10 µl capacity) into the vaporization chamber to form a headspace of these volatile compounds. The concentration "C" of the BTEX vapors was calculated using **Equations (3.2)&(3.3)[281] of Chapter** 3. The volatiles vapourized were injected into the gas sampling bag (Aluminium Multi-layer Foil Composite Film Gas Sampling Bag with Side-opening Stopcock Dual-valve Silicone Septum Syringe Port 1/4" 6.35m) through a two-way control valve, suction pump (Adafruit Industries LLC, 4700), and mass flow controller (AFM0725). A suction pump circulates BTEX volatiles through a sampling bag at a constant rate of 0.5 L/min, which is further directed to the sensing unit using an inlet pipe. For breath sample analysis, these samples were directly injected into the sensing unit, and frequency changes were measured using a Teensy 4.0 microcontroller board (PJRC, USA) running ARM Cortex-M7 at 600 MHz.

Sensing unit: A sealed, cylindrical Teflon chamber with a 0.5 L capacity, designed for BTEX vapor analysis. The chamber has a height of 13.8 cm, an inner diameter of 6.8 cm, and features two 5 mm openings on opposite sides for controlled input and purging. Within the chamber, three detachable QCM sensors (Piezoelectric AT-cut quartz crystals with a 10 MHz resonant frequency and an 8mm diameter) were placed, enabling flexibility for different analytical configurations. The QCM sensors include one coated with PVAc, another coated with WO_3, and an uncoated sensor serving as a reference baseline. Temperature and humidity within the chamber are continuously monitored using a Digital Thermometer-Hygrometer. This device measures temperature from -50°C to +70°C (accuracy: ±1°C) and relative humidity from 10% to 99% RH (accuracy: ±5% RH). All the measurements were performed in ambient conditions.

Purging unit: Before exposing the sensors to the target volatile compounds, the sensor chamber was purged with dry air and nitrogen using a suction pump and a control valve. A silica gel partition at the inlet of the sensor chamber facilitates dry air purging to remove humidity and maintain the experimental conditions at STD. Nitrogen purging is performed on both the sensing chamber to create an inert environment before the BTEX sampling experiment. Nitrogen and dry air purging were employed to reset the sensor response to the baseline.

4.3.1.2 Data Acquisition System

The data acquisition system includes an oscillator circuit that converts the physical response of the QCM sensor into an electronic signal, reflected as a variation in resonance frequency [265]. The signal produced has a peak-to-peak voltage ranging from 300 ± 100 mV and a time period of 100 ns. This frequency variation is then counted using a microcontroller-based frequency counter, and the results are displayed on a TFT screen and plotted via a graphical user interface. The oscillator circuit uses a 10 MHz QCM sensor as the resonant element. The CL100S transistor operates in a common-emitter configuration to create the necessary feedback loop for oscillation. The schematic diagram of the circuit designed for the QCM sensor array is illustrated in **Figure 4.2(a)**. The Teensy 4.0 microcontroller counts the frequency of signals generated by three oscillator circuits. The Teensy 4.0, featuring an ARM Cortex-M7 processor running at 600 MHz, provides robust computational power and numerous input/output options. It uses its quad-timer modules to measure frequency changes accurately. The frequency-counting mechanism employs timer interrupts to define precise gate intervals and accumulates counts over 100 intervals to improve stability. It allows for precise frequency measurement with a resolution of 1 mHz and a mean error of 0.03717%. The mean error percentage is the average difference between measured and actual frequency values across multiple measurements, indicating the system's high accuracy and reliability. Base frequencies of oscillations were established during

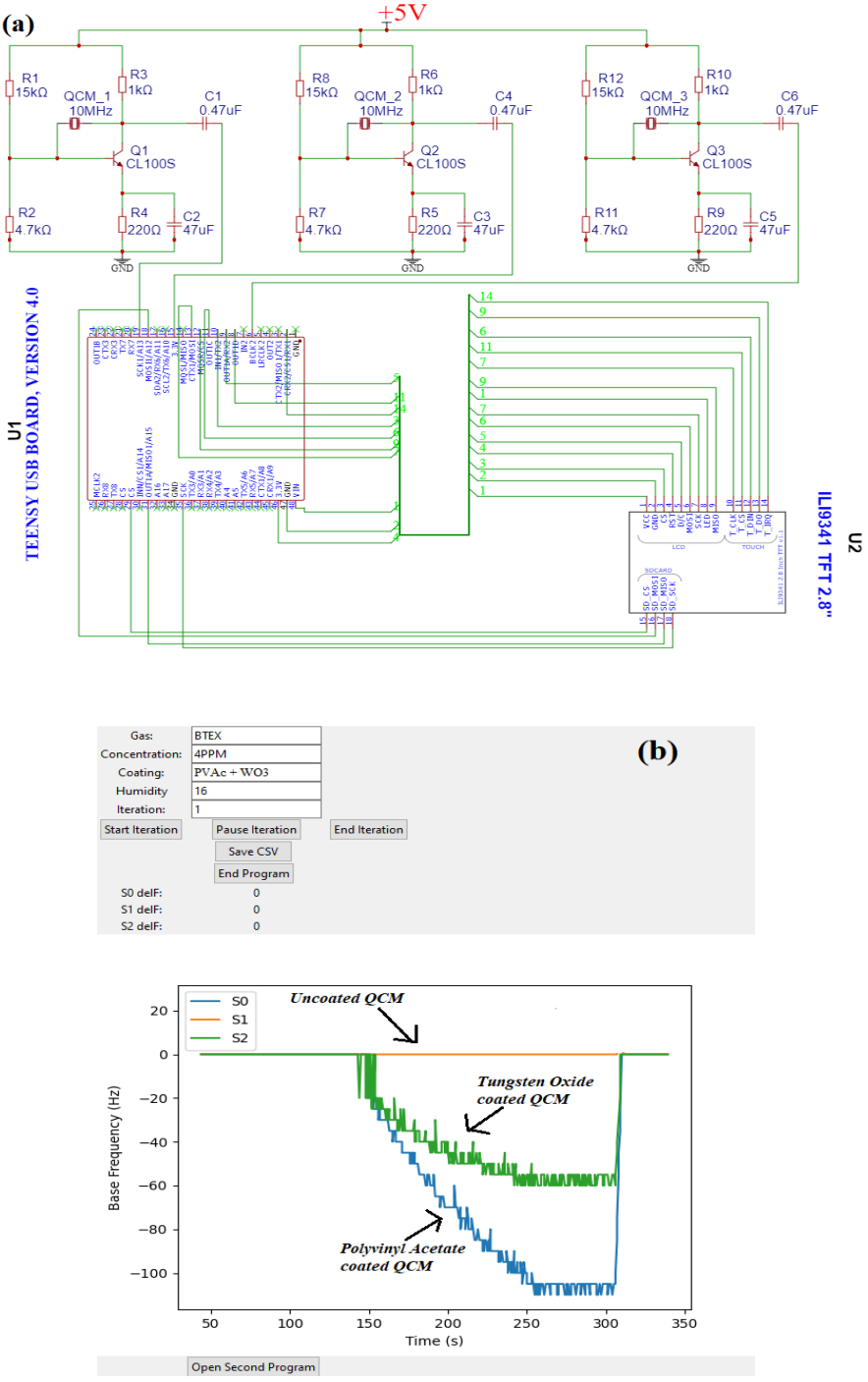

Figure 4. 2 (a) Schematic diagram of an electronic circuit for a 10 MHz QCM sensor array (b) Graphical user interface for the acquisition of QCM sensor array data (QCM sensor coated with PVAc (S0), uncoated QCM sensor (S1) and QCM sensor coated with WO_3 (S2)).

initial runs, and subsequent frequency deviations were calculated and displayed on an ILI9341 TFT screen for monitoring sensor outputs. The data, including base frequency, frequency deviation, and elapsed time, were displayed on the TFT screen to monitor the E-Nose Sensor array output. Additionally, a Python-based GUI program was developed using the Tkinter library to facilitate the recording and visualization of data from the QCM sensors as shown in **Figure 4.2(b).** A negative frequency shift represents a decrease in resonance frequency due to mass loading on the sensor surface when analytes bind to it. Although the frequency values themselves are positive, the shift is conventionally plotted as negative to indicate a reduction in frequency, with larger negative values correlating with greater mass. A Python program interfaces with a Teensy 4.0 via a serial connection to capture and process data in real time. The program periodically reads data from the serial port, processes it, and updates both the plot and the displayed values.

Key Contributions of the Data Acquisition System are indicated below:

1) Stable Oscillator Circuit: A carefully designed oscillator circuit, with optimized resistor and capacitor placements, enhances stability in oscillations at the 10 MHz QCM sensor's resonant frequency, providing consistent and reliable frequency readings.

2) Adaptability for Multi-Sensor Arrays: Currently, the system is designed to handle input from three sensors, each connected to a separate I/O pin. However, the system can be expanded to accommodate a larger sensor array, which is crucial for multi-gas detection and E-nose applications.

3) User-Controlled Data Recording: The system's GUI includes features for controlling recording sessions, streamlining experiment management and data retrieval.

4) Real-Time Data Visualization and Storage: Through a Python-based GUI, data is visualized in real-time, plotted dynamically using Matplotlib, and stored in a CSV format with specific metadata to facilitate reproducibility and subsequent analysis.

Integration with Data Analysis Tools: The system provides a framework for integrating secondary analysis programs, enabling automated clustering that extends the functionality of the primary acquisition system.

This setup includes a novel data-acquisition system for QCM-based sensors, delivering precision, modularity, and efficient software integration, essential for BTEX detection in real-world applications. The novelty of our DAQ circuit lies in its custom-designed architecture, which integrates low-power analog front-end processing with a precise digital-to-analog conversion mechanism to create an optimized platform for E-Nose data capture. The DAQ circuit is designed to be compact and modular, which facilitates real-time BTEX detection.

4.3.1.3 Data Processing System

The data processing system of the BTEX measurement setup has a software module for real-time data acquisition from the QCM sensors, followed by comprehensive data analysis utilizing PCA and clustering algorithms.

The system employs a Teensy 4.0 microcontroller to log the base frequencies and frequency shifts from the QCM sensors. QCM sensor data is read from the serial port, parsed, and stored in lists. Once data is collected, it is saved to CSV files for further analysis. The data acquisition system initializes the serial connection and periodically updates plots to provide real-time visualization of sensor responses. Post-acquisition, PCA is employed for dimensionality reduction, transforming the sensor data into principal components to highlight the dataset's variance. Clustering analysis using the BIRCH (Balanced Iterative Reducing and Clustering using Hierarchies) and K-Means algorithms further categorizes the data into distinct clusters for pattern recognition and BTEX classification.

4.3.2 GC-MS Calibration

The BTEX sensing setup was validated using gas chromatography-mass spectrometry (GC-MS) to detect BTEX compounds. The methodology for sample preparation involved preparing specific concentration solutions of BTEX by diluting the solution with methanol (**Figure 4.3**). A 10 µL glass syringe was used to inject different concentrations of BTEX solutions into a 1-liter gas-vaporization chamber, where they were vaporized for 5 min. The vapours were then transferred via a suction pump to a 1-L gas sampling bag and subsequently to 20-mL glass vials with silicone septa at a flow rate of 1 L/min. Before transferring the vapour to the 20 mL vials, the vials were evacuated using a vacuum pump for 3 min, resulting in a weight loss of 1 ± 0.8 mg due to the removal of residual air. Upon transferring the vapor, a weight increase of 2 ± 0.2 mg was observed.

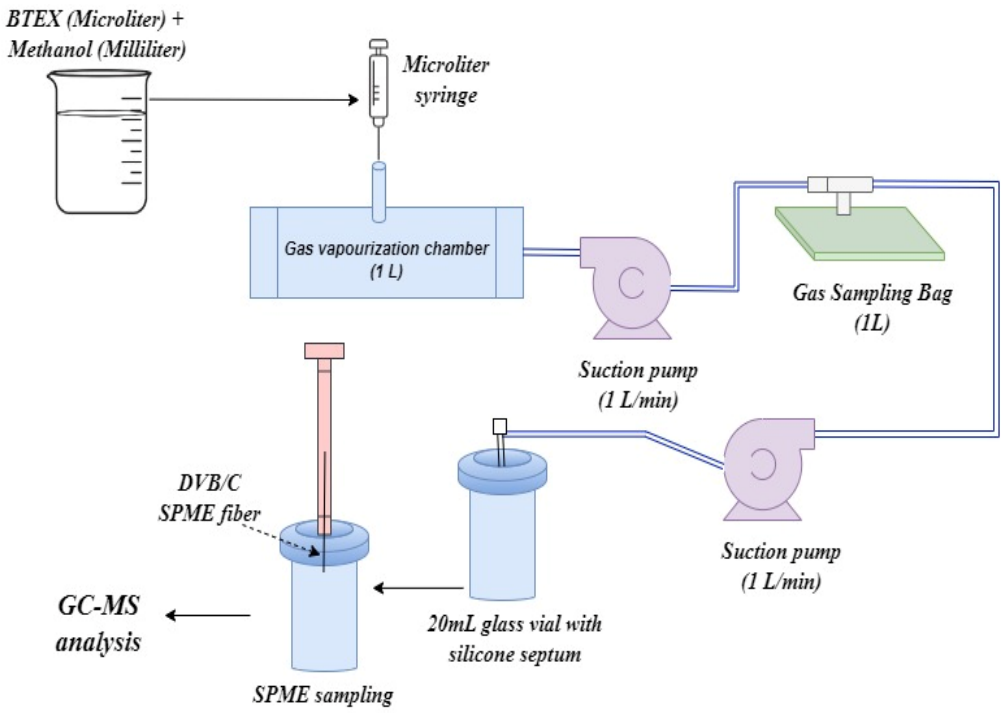

Figure 4.3 Experimental setup sample formation for GC-MS Analysis.

The vials were sealed using Teflon tape, and GC-MS analysis was conducted within six hours of sample preparation. The calibration curve in GC-MS is a fundamental tool for quantitatively determining the concentration of specific compounds in a sample based on their chromatographic peak areas. Three sets of BTEX samples, each with concentrations ranging from 2 to 10 ppm, were used to construct the GC-MS calibration curve. The calibration curve for GC-MS analysis of BTEX compounds is presented in **Table 4.1**, with a correlation coefficient (R^2) greater than 0.99, indicating high analytical accuracy and reproducibility. The GC-MS calibration curve is used to detect and quantify unknown concentration BTEX compounds accurately.

GC-MS analysis of BTEX compounds was conducted using a solid-phase microextraction (SPME) technique with a divinylbenzene/carboxen on polydimethylsiloxane (DVB/C-PDMS) fiber, with a 80 µm coating thickness. The SPME fiber was selected for its efficiency in adsorbing BTEX from air samples, offering a rapid, solvent-free method for sample preparation. During the SPME process, the fiber was exposed to the headspace of the sample vial at a penetration depth of 40 mm with a speed of 20 mm/s.

Table 4.1 GC-MS Calibration data for Benzene, Toluene, Ethyl-Benzene, and Xylene

Compound	Retention Time	Calibration curve	LOD	LOQ	RSD
Benzene	2.0743±0.28475	y = 832272x + 37205	3.06	10.2	0.545
Toluene	3.6677±0.71495	y = 1073804x + 84217	2.4	8	0.960
EthylBenzene	5.4568±0.89075	y = 88246063x + 8588471	1.01	3.36	0.622
p-Xylene	5.5514±0.9494	y = 80570751x + 6425103	2.21	7.37	0.359

To enhance the adsorption of BTEX compounds, the sample was incubated at 60°C for 5 min with continuous agitation at 250 rpm, enabling the VOCs to equilibrate between the gas phase and the fibre coating. The fibre was then inserted into the gas chromatograph (GC) injector for thermal desorption at 280°C for 2 min, ensuring complete transfer of analytes to the GC column.

The GC-MS system, set to splitless injection mode, used helium as the carrier gas at 1.2 mL/min for the front inlet and 0.45 mL/min for the back inlet to optimize the separation of BTEX compounds. The analysis employed two capillary columns: HP-5MS UI and HP-5MS Inert, each with dimensions of 30 m × 250 µm × 0.25 µm. The temperature program was designed to provide efficient separation, starting at 50°C (held for 2 min), ramping at 10°C/min to 130°C (held for 1 min), followed by 4°C/min to 210°C (held for 1 min), and a final increase to 250°C at 10°C/min, held for 4 min. This configuration enabled precise separation and identification of individual BTEX components. The mass spectrometer was configured to operate with a transfer line temperature of 290°C, ensuring optimal transmission of analytes from the GC to the mass detector.

4.4 Results and Discussion

4.4.1 Parametric Analysis of the Developed Breath Analyzer

Research papers have proposed different techniques for real-time detection of BTEX compounds, as tabulated in **Table 4.2.** The developed BTEX detection system weighs approximately 1 kg, making it portable and functioning under ambient conditions without requiring a complex preconcentration setup. It can detect BTEX mixtures at levels below 4 ppm in less than 3 min. This compact system, with a height of 200mm and an inner diameter of 68mm, is highly portable, unlike bulkier GC-MS systems. It operates on a low-power, robust design, requiring only 5V 1000mAh for power.

Additionally, our system, shown in **Figure 4.6(a)**, was validated through a pilot study involving breath samples from petrol station workers as discussed in Chapter 5. The portable device consists of a Teflon sensing chamber, a data acquisition unit, and a purging unit. The QCM sensor response plot (**Figure 4.6(b)**) demonstrated that the breath of petrol station workers exhibited higher and more prolonged frequency shifts due to the presence of BTEX compounds compared to the breath samples of controls.

Table 4.2 Summary of Portable devices developed for real-time detection of BTEX

Sensor Type	**Detection Limit**	**Total Analysis Time**	**Operating Temperature**	**Portability (weight)**	**Reference**
Miniaturized GC-PID	< 3ppb	10 min	60°C - 80°C	4 Kg	[249]
Novel preconcentrator with portable GC	0.06 ppb	19 min	330°C	5 Kg	[250]
Compact GC-PID	1 ppb	15 min	60°C	15 Kg	[102]
PID combined with a Carbon Nanotube Sponge Preconcentrator	0.1-0.2 ppb	10 min	—	5Kg	[251]
Portable Gas Chromatograph with Flame Ionization Detector (GC/FID)	1.12 ppm	5 min	24°C	—	[252]
Chemoresistive	240 ppm	8 min	160°C	—	[253]
Deep UV absorbance	196 ppb	15 min	60°C	—	[254]
Deep UV absorbance	196 ppb	3 - 17 min	80°C	—	[255]
Surface Acoustic Wave (SAW) Sensors	10-50 ppm	2-3 min	25°C	—	[257]
Fluorescent sensor based on a Meisenheimer complex	1.4 ppm	10 min	80°C	—	[256]
Present Work	**< 4ppm**	**3 min**	**27°C**	**~ 0.8 Kg**	—

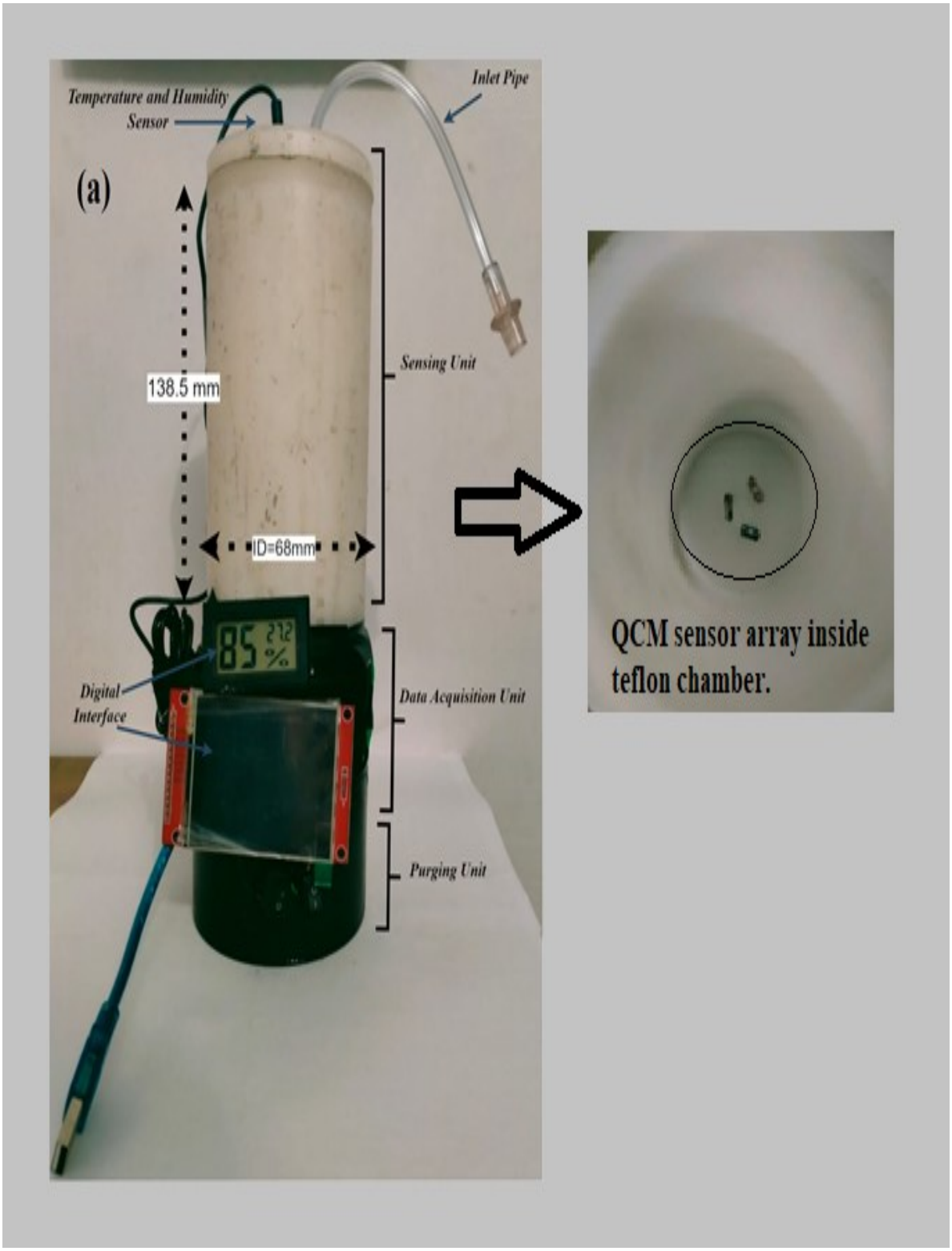
Temperature and Humidity Sensor
Inlet Pipe
(a)
138.5 mm
Sensing Unit
ID=68mm
Digital Interface
Data Acquisition Unit
Purging Unit
QCM sensor array inside teflon chamber.

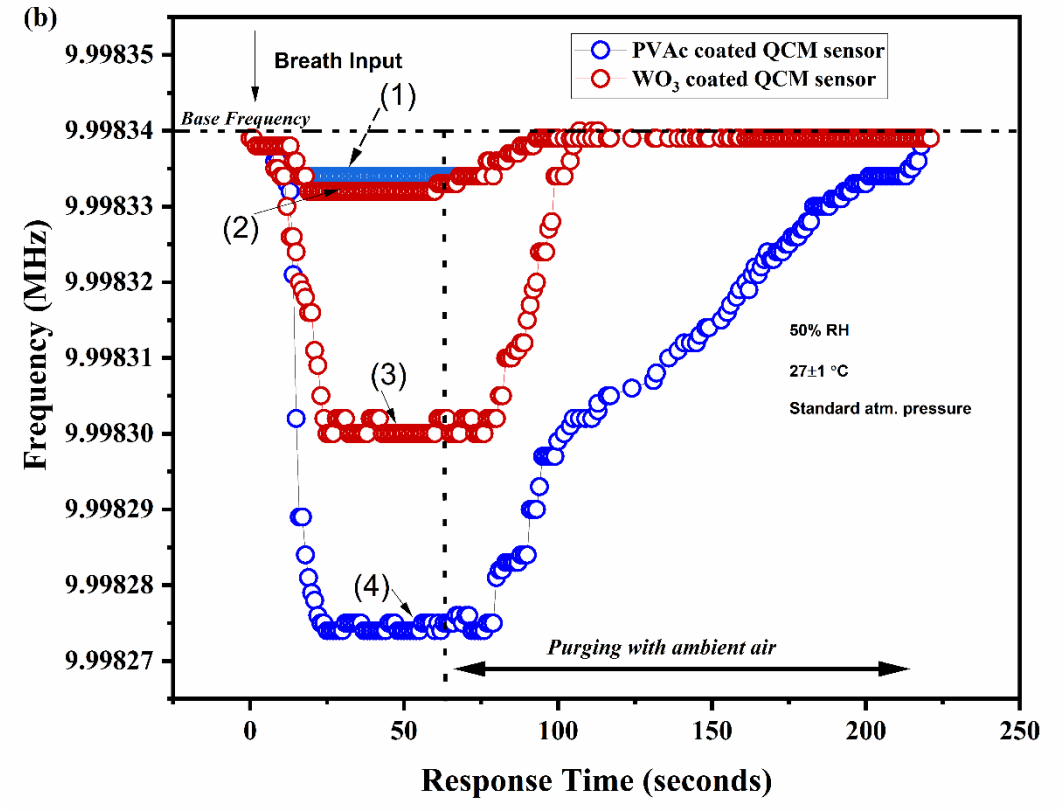

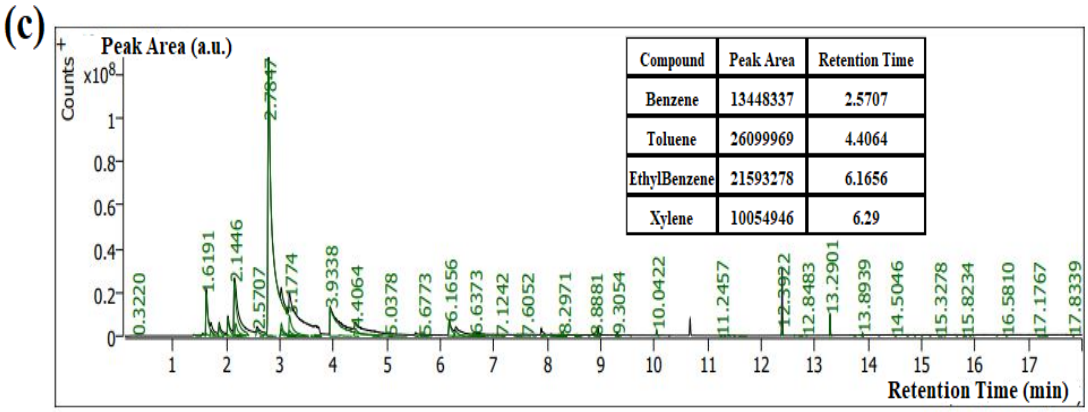

Compound	Peak Area	Retention Time
Benzene	13448337	2.5707
Toluene	26099969	4.4064
EthylBenzene	21593278	6.1656
Xylene	10054946	6.29

Figure 4.4 (a) Image of the portable BTEX detection system using a QCM-based electronic nose, (b) Response curve of PVAc and WO_3 coated QCM sensor when exposed to the normal breath sample (1 & 2) and breath sample of petrol station worker (3 & 4) (c) GC-MS chromatogram confirming BTEX compound.

Frequency dips at 5 Hz and 7 Hz were observed for PVAc and WO_3-coated QCM sensors in the control breath sample. Meanwhile, PVAc- and WO_3-coated QCM sensors showed frequency dips of 65 Hz and 40 Hz, respectively, for breath samples from petrol station workers. Additionally, GC-MS analysis was conducted on the same breath sample of petrol station workers to confirm the presence of BTEX, as shown in **Figure 4.4(c)**. A detailed discussion on breath sampling of petrol station workers is presented in Chapter 5.

4.4.2 Correlation Analysis

Correlation analysis quantifies the strength and direction of a linear relationship between two or more variables[266]. Pearson correlation coefficient ('r'), which ranges from -1 to +1, indicates whether the QCM sensor response accurately mirrors the actual concentration measured by GC-MS. The primary objective of performing this correlation analysis was to validate the performance of the developed PVAc and WO_3-coated QCM sensors for the real-time detection of BTEX compounds. A strong correlation indicates that the QCM sensor's response can be directly translated into concentration, thereby eliminating the need for complex and time-consuming GC-MS analysis in routine monitoring applications. The correlation coefficients illustrated in **Figure 4.5** are close to +1, indicating a positive linear relationship between the QCM sensor responses (frequency dips) and the actual BTEX concentrations measured by GC-MS. This high degree of correlation

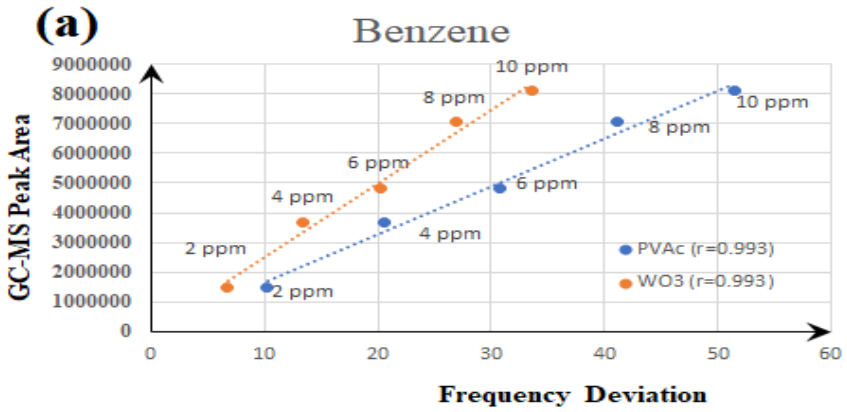
(a)
Benzene
GC-MS Peak Area
9000000
8000000
7000000
6000000
5000000
4000000
3000000
2000000
1000000
0
0
10
20
30
40
50
60
Frequency Deviation
2 ppm
4 ppm
6 ppm
8 ppm
10 ppm
2 ppm
4 ppm
6 ppm
8 ppm
10 ppm
PVAc (r=0.993)
WO3 (r=0.993)

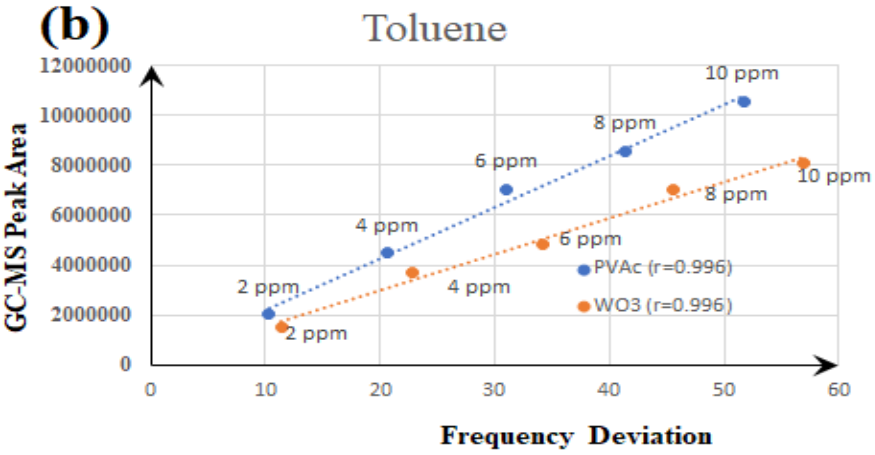
(b)
Toluene
GC-MS Peak Area
12000000
10000000
8000000
6000000
4000000
2000000
0
0
10
20
30
40
50
60
Frequency Deviation
2 ppm
4 ppm
6 ppm
8 ppm
10 ppm
2 ppm
4 ppm
6 ppm
8 ppm
10 ppm
PVAc (r=0.996)
WO3 (r=0.996)

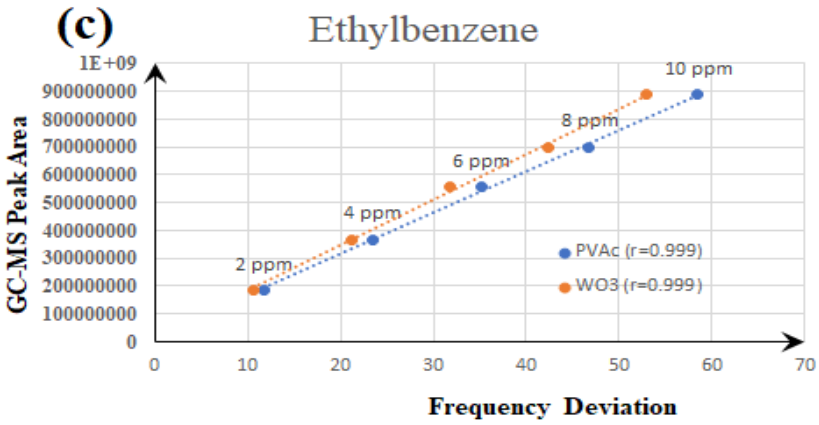
(c)
Ethylbenzene
GC-MS Peak Area
1E+09
900000000
800000000
700000000
600000000
500000000
400000000
300000000
200000000
100000000
0
0
10
20
30
40
50
60
70
Frequency Deviation
2 ppm
4 ppm
6 ppm
8 ppm
10 ppm
PVAc (r=0.999)
WO3 (r=0.999)

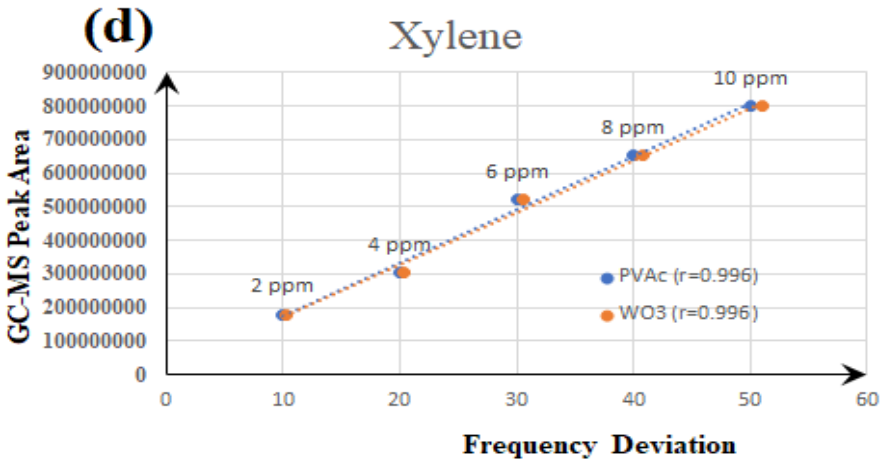

Figure 4.5 Correlation Analysis of QCM sensor frequency deviation versus GC-MS peak area of (a) Benzene (b) Toluene (c) Ethylbenzene (d) Xylene

Signifies that as the concentration of each BTEX compound increases, the frequency shift recorded by both the PVAc and WO_3-coated QCM sensors also increases proportionally and consistently. They confirm that the QCM sensors provide accurate and reliable measurements directly comparable to those obtained with a sophisticated analytical technique, such as GC-MS.

4.4.3 Machine learning models for BTEX Classification

The developed E-Nose system performs data analysis using Principal Component Analysis (PCA), followed by a clustering algorithm to analyse and classify sensor response data from CSV files. The dataset used in this study comprises frequency deviation data from three sensors exposed to five different vapors: Benzene, Toluene, Xylene, Ethylbenzene, and a quinary mixture (Vapors of BTEX in equal proportion) of these compounds.

These exposures were conducted at different concentrations of 2-10 ppm. Five data samples were collected at five stages, resulting in a total dataset of 25 (5 samplings × 5 stages) × 3 (sensors) samples for each vapour. Initially, data preprocessing involved handling missing values through mean imputation, ensuring no data gaps that could affect subsequent analyses. The dataset, containing various sensor readings excluding gas names, was standardized using the StandardScaler to achieve a mean of zero and a standard deviation of one. PCA was applied to capture the maximum variance in the dataset while minimizing information loss. PCA reduces the dimensionality of complex sensor data by transforming it into a set of uncorrelated principal components, enabling easier visualization and interpretation. Clustering algorithms are then applied in the principal component space to group sensor responses by similarity, effectively distinguishing between different VOC exposures. The clustering analysis for BTEX classification is implemented using real-time data on an embedded processing platform. A subroutine in the developed GUI system provides the option to open a secondary program to perform PCA and clustering of real-time acquired data.

Five Clustering algorithms [249-254], the k-Means algorithm, the Agglomerative Hierarchical Clustering (AHC) algorithm, the Gaussian Mixture Models (GMM) algorithm, the Fuzzy C Means, and Balanced Iterative Reducing and Clustering using Hierarchies (BIRCH), were used to group data points into clusters based on similarity. Each cluster is labelled by the majority gas name among the data points in that cluster.

Figure 4.6 presents a flowchart outlining the steps for executing the Python program for PCA and clustering analysis. In this analysis, different clustering algorithms were applied to a dataset comprising frequency deviation data from three sensors exposed to Benzene, Toluene, Xylene, Ethylbenzene, and a BTEX mixture in equal proportions. K-Means and BIRCH achieve strong results, with Silhouette scores of 0.53 and 0.51, respectively **(Table 4.3)**. These Silhouette scores, approaching 1, indicate well-separated clusters, suggesting adequate distinction between similar compounds such as toluene and xylene with minimal overlap.

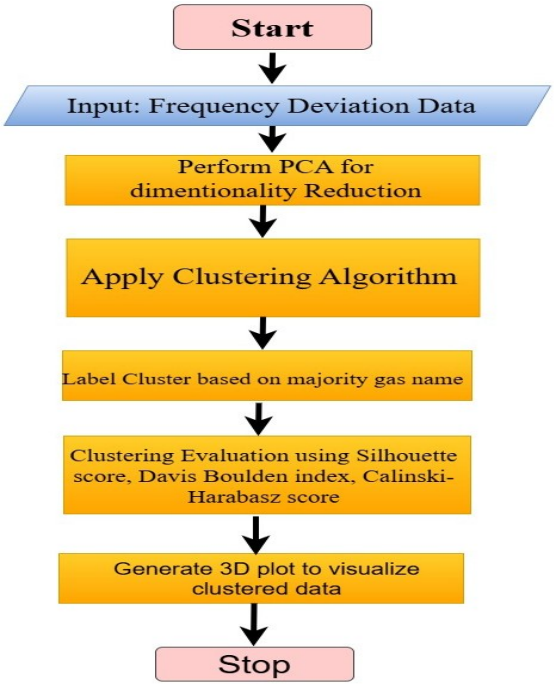

Figure 4.6 Flowchart illustrating the execution flow PCA and clustering analysis.

Table 4.3 Performance Metrics of Various Clustering Algorithms applied to the QCM sensor array dataset.

Clustering Algorithm	**Silhouette score**	**Davis boulden index**	**Calinski-Harabasz score**
k-Means	0.53	0.93	7952
Agglomerative Hierarchical Clustering	0.48	0.98	7671
Gaussian Mixture Models	0.42	1.36	6589
Fuzzy C Means	0.39	1.01	9385
BIRCH	0.51	0.78	10902

The choice of k-Means and BIRCH over GMM and Fuzzy C-Means was based on their superior performance, as evidenced by higher Silhouette scores, lower Davies-Bouldin index values, and better Calinski-Harabasz scores, indicating more compact, well-separated clusters. Furthermore, k-Means and BIRCH provided faster convergence and lower computational complexity, which are advantageous for real-time embedded system applications. A 3D plot is generated to visualize the clustered data, with different markers and cluster names to distinguish the clusters, as shown in **Figure 4.7.** We configured the BIRCH algorithm with a threshold of 0.1 and a predefined number of clusters of 5. The algorithm iteratively reduced the data and constructed a clustering feature tree, effectively organizing the data points into cohesive clusters. The k-means and BIRCH clustering have given good results among the algorithms tested for identifying vapours in the dataset.

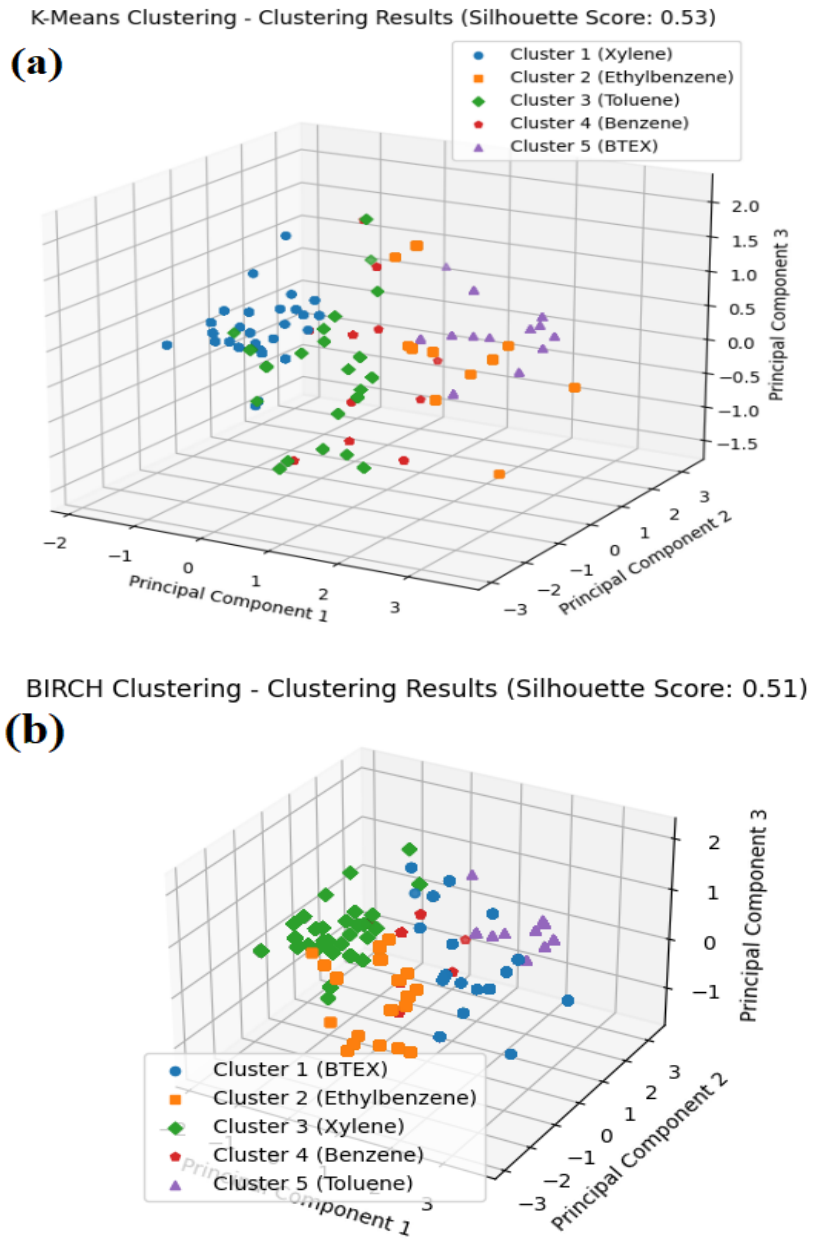

Figure 4.7 Clustering Results of QCM sensor-based e-nose system (a) k-Means (b) BIRCH.

4.5 Conclusion

This chapter successfully detailed the development of a portable breath analyser. It is designed for near real-time detection of BTEX vapours and mixtures. The system integrates an array of three QCM sensors. These include one coated with PVAc, another with WO_3, and an uncoated reference sensor. These coated sensors showed good sensitivity and rapid response times to BTEX vapours. The device achieves a response time of 25 seconds and a total analysis time of 2-3 minutes. This qualifies it for real-time industrial applications. The system is compact, weighing approximately 0.8 kg, and operates at ambient temperature. Its low-power, robust design requires minimal power (5V 1000mAh). Validation against GC-MS confirmed accurate detection of BTEX mixtures. Correlation analysis demonstrated a strong positive linear relationship between QCM sensor frequency shifts and GC-MS concentrations. This confirms that the QCM sensors provide accurate, reliable calibration measurements. Furthermore, Principal Component Analysis (PCA) and clustering algorithms (k-Means and BIRCH) were effectively used for BTEX classification. These algorithms showed good Silhouette scores, indicating well-separated clusters and practical distinction between similar compounds. The overall system provides a precise, modular, and portable solution for real-time BTEX exposure monitoring in industrial environments.

Chapter 5: Real-Time Testing and Validation of the Breath Analyzer

5.1 Abstract

This chapter evaluates the occupational exposure of petrol station workers in Bengaluru, India, to benzene, toluene, ethylbenzene, and xylene (BTEX) using exhaled breath analysis as a non-invasive biomonitoring approach. The methodology directly reflects internal dose, enhancing exposure assessment accuracy compared to ambient air monitoring. Breath samples of 20 workers at eight petrol stations were analyzed using a breath analyzer fabricated from a QCM sensor and calibrated with gas chromatography-mass spectrometry (GC-MS) results. Benzene concentrations ranged from 1.82 ppm to 66.81 ppm, with a mean of 20.89 ± 25.1 ppm, while toluene concentrations ranged from 3.84 ppm to 64.63 ppm, with a mean of 20.91 ± 26.68 ppm. Ethylbenzene and xylene concentrations were lower, with means of 3.75 ± 3.86 ppm and 3.53 ± 3.57 ppm, respectively. A health risk assessment using USEPA guidelines revealed that hazard quotients (HQ) for benzene exceeded the safety threshold in approximately 75% of workers, suggesting significant non-carcinogenic risks. Excess lifetime cancer risk (ELCR) for benzene was elevated, exceeding the acceptable threshold of 1×10^{-6} in all workers, with values ranging from 2.59×10^{-4} to 9.51×10^{-3}. The novelty of this study lies in employing breath analysis to assess BTEX exposure and evaluate internal exposure among petrol station workers in India. Furthermore, this pilot study used

a one-sample t-test to statistically assess whether the mean BTEX concentrations in breath samples were significantly higher than established reference values, revealing a significant occupational exposure to Benzene. Sensor validation via Bland-Altman analysis demonstrated that a multi-sensor array combining WO_3 and PVAc coatings can provide accurate and precise BTEX detection, with WO_3 excelling for Benzene and Toluene, and PVAc for Ethylbenzene and Xylene, laying the groundwork for real-time, on-site monitoring systems.

5.2 Introduction

The occupational environment of petrol station workers poses significant health risks due to continuous exposure to volatile organic compounds (VOCs), including benzene, toluene, ethylbenzene, and xylene (BTEX). These compounds, prevalent in petroleum vapours, are released during refuelling operations, fuel storage, and accidental spillage. Benzene, a known Group 1 carcinogen, is associated with haematological disorders, including leukaemia, while toluene, ethylbenzene, and xylene are linked to neurotoxic and respiratory effects [273]. India, with its growing urbanization and vehicular density, faces heightened concerns about BTEX emissions and their occupational and environmental impacts. Cities in India have emerged as hotspots for VOC exposure due to the dense clustering of fuel stations [256-258]. Understanding the exposure levels and corresponding health risks in such environments is critical for safeguarding worker health.

Some studies have addressed this by utilizing personal area monitoring techniques to assess BTEX exposure. This involves collecting air samples from the immediate work environment, which can provide insights into workers' exposure levels during work hours. In Delhi, Kumari et al. measured VOC levels at fuel stations using personal-area air samples collected with low-flow sampling pumps and analyzed by gas chromatography with flame ionization detection, reporting high concentrations—especially benzene (217 µg/m³)—despite vapor recovery systems [275]. Risk assessments showed both cancer and non-cancer risks exceeded safety thresholds.

In Chennai, Jayaraj et al. monitored BTEX and particulate matter, noting peak TVOC levels during refueling that far exceeded EPA standards [276]. These studies underscore the need for stricter air quality regulations to protect fuel station workers. Similarly, several studies across Asia have also reported significant health risks from BTEX exposure at fuel stations, with benzene identified as the most hazardous compound. In Bangkok, Tunsaringkarn et al. measured BTEX levels at gasoline stations and nearby roads, finding slightly higher concentrations at stations[277]. Benzene exposure was linked to fatigue and cancer risks exceeding acceptable limits.

In Kuwait, Al-Harbi et al. measured benzene levels exceeding NIOSH standards, with workers reporting symptoms such as headaches, fatigue, and throat irritation [149]. The study advocated for improved ventilation, vapor recovery systems, and better hygiene practices.

Chaiklieng et al. conducted a risk assessment in Thailand and identified high-risk zones near fuel dispensers, recommending control measures, including vapor recovery installation and ignition source management [278]. Giao et al. in Vietnam evaluated BTEX and other toxic gases, identifying elevated cancer and non-cancer risks and emphasizing the need for comprehensive protective strategies[279]. Allahabady et al. measured BTEX levels at 13 fuel stations in Mashhad, Iran, and found that benzene concentrations exceeded national standards by 5.5 times in high-traffic areas [280]. The study recommended improving fuel quality, minimizing evaporation, and implementing engineering controls such as vapor recovery systems. Alimohammadi et al. in Karaj, Iran, conducted health and carcinogenic risk assessments at gasoline fuel stations and found that benzene and ethylbenzene concentrations during work shifts significantly exceeded acceptable limits [281]. They proposed measures such as limiting exposure duration, upgrading PPE, and enhancing exposure monitoring through regular risk assessments.

In the studies mentioned above, air samples surrounding the petrol station worker were collected is analyzed. The current research discussed in the paper takes a different approach by analyzing breath samples from petrol station workers. The presence of BTEX in the breath of petrol station workers serves as a crucial biomarker for assessing occupational exposure and associated health risks. To our knowledge, significantly little work lies in this area, hence in the current study, we have collected the breath sample of a petrol station worker and analyzed it for

The possible health-related risk. The breath samples were collected from 20 petrol station workers in Bengaluru, India, using a breath analyzer fabricated using a QCM sensor and Teflon gas sampling bags for GC-MS analysis. The breath analyzer response was compared with the GC-MS results for calibration. Furthermore, this study contributes to the limited body of research on Bengaluru, addressing gaps in occupational health assessments in high-density urban areas of India.

Previous research on BTEX measurement in breath has primarily relied on advanced analytical techniques and specialized sampling methods to capture and concentrate volatile compounds in exhaled air (Table 5.1). The most common approaches involve gas chromatography (GC) coupled with mass spectrometry (MS) or flame ionization detection (FID).

Table 5.1 Comparison of Breath VOC Sampling and Analysis Methods Used in BTEX Exposure Studies.[47], [282]

Methodology	**Sampling Method**	**Analytical Technique**	**Limitations**
Tedlar Bags/Gas Sampling Bags	Exhale directly into inert Tedlar bags.	GC-MS or GC-FID after sample transfer.	Can suffer from sample stability issues over time due to the permeability of the bag material for some VOCs; potential for adsorption onto the bag walls; requires laboratory analysis, not suitable for real-time.
Sorbent Tubes	Tubes packed with adsorbent materials (e.g., Tenax, Carboxen, Carbopack) trap VOCs from exhaled breath.	Thermal desorption followed by GC-MS or GC-FID.	Requires specialized thermal desorbers; potential for breakthrough at high concentrations or long sampling times; moisture interference can be an issue; not suitable for real-time.
Online Breath Analyzers (e.g., PTR-MS, SIFT-MS)	Direct introduction of exhaled breath into the instrument.	Proton Transfer Reaction-Mass Spectrometry (PTR-MS) or Selected Ion Flow Tube-Mass Spectrometry (SIFT-MS).	High initial cost and complexity of instrumentation; not always truly portable; may require frequent calibration; some compounds might have isobaric interferences.
Gas Chromatography-Mass Spectrometry (GC-MS)	Post-sampling, samples are introduced into a GC system for separation, followed by MS for identification and quantification.	Gold standard for identification and quantification based on mass spectra.	Time-consuming for sample preparation and analysis; requires highly trained personnel; expensive equipment; not suitable for real-time, on-site monitoring.
Gas Chromatography-Flame Ionization Detection (GC-FID)	Post-sampling, samples are introduced into a GC system for separation, followed by FID for quantification.	Highly sensitive for many organic compounds but does not provide structural confirmation.	Lacks the definitive compound identification of MS; less sensitive for some compounds compared to MS; not suitable for real-time, on-site monitoring.

5.3 Methodology

5.3.1 Study Design

We conducted a study to assess the presence of BTEX in the breath of petrol station workers in Bengaluru, India, during May 2024. Bengaluru, with a tropical savanna climate, experiences warm summers with average temperatures ranging from 25°C to 35°C, moderate humidity, and occasional breezes. The study included 20 workers from eight petrol stations, with three samples collected from each of Stations 2, 3, 6, 7, and 8, and one sample from each of Stations 4 and 5 **(Figure 5.1)**. Additionally, 3 samples from aviation fuel workers at Station 1 were included in the study.

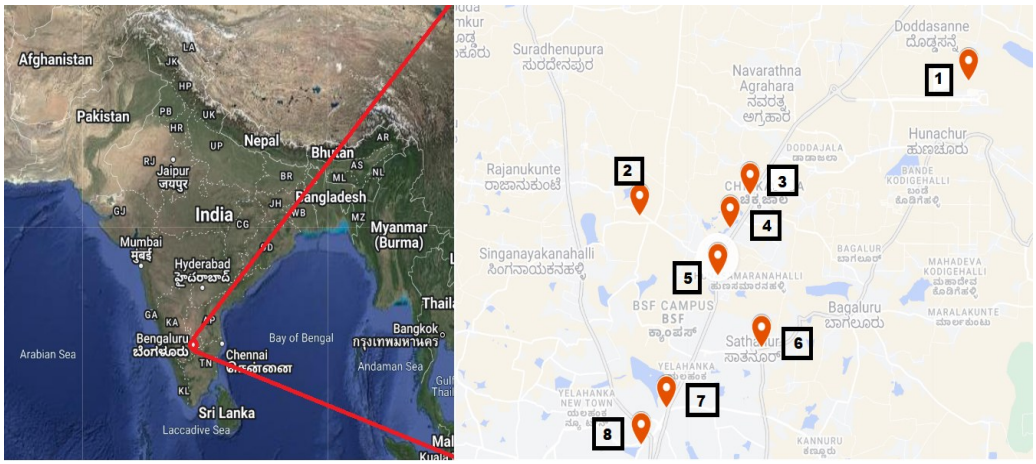

Figure 5.1 Satellite image showing the location of petrol stations where breath sampling was performed.

Personal and environmental factors, such as temperature, humidity, and wind velocity, were recorded during sample collection. Workers' demographics, including age, marital status, smoking and alcohol habits, fasting period, exposure

duration and work schedule were documented in a consent form. Breath samples were collected during workers' routine activities, ensuring the study reflects real-world occupational exposure. The collected breath samples were analysed using a breath analyser, and the responses were recorded. The samples were also collected in gas sampling bags and analysed within 24 hours using GC-MS to characterize BTEX.

5.3.2 Sampling and Analysis

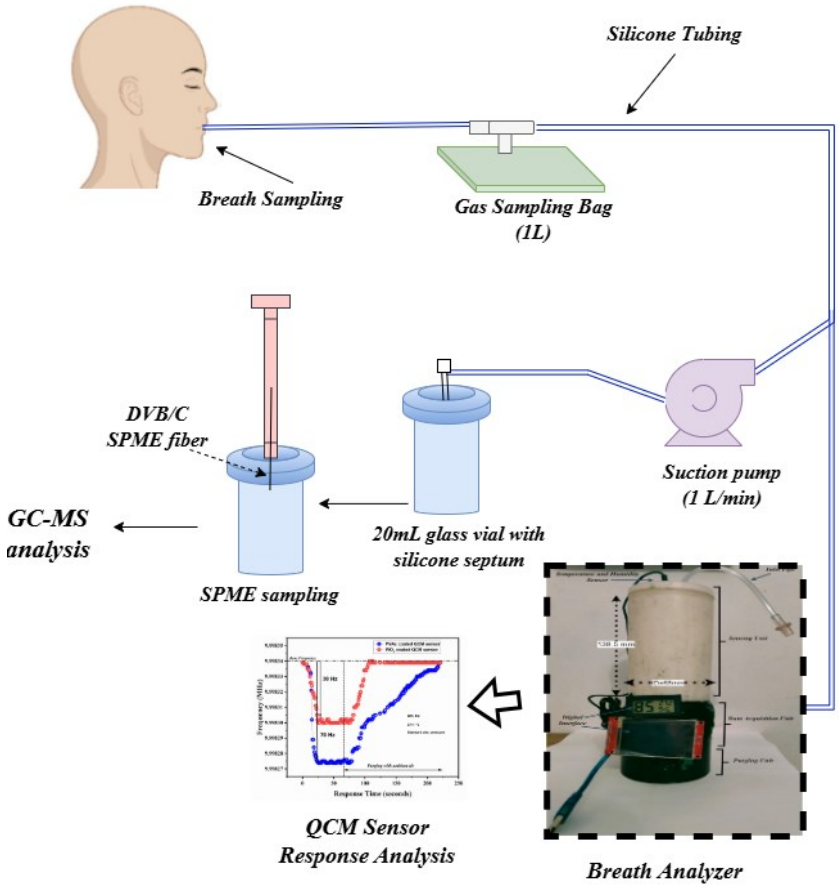

Figure 5.2 Illustration of methodology for breath sampling using a QCM-based breath analyzer and GC-MS.

The block diagram representation of sampling and analysis methodology is shown in **Figure 5.2.** Breath samples from petrol station workers were collected using a one-litre Teflon gas sampling bag made of an aluminium multi-layer foil composite with a side-opening stopcock, a dual-valve silicone septum, and a syringe port. Workers were instructed to take a deep breath and exhale the initial 3 seconds into the opening of the two-way valve to remove dead-space air. In contrast, the remaining breath was collected in the sampling bag through silicone tubing. Fifty per cent of the collected breath samples were introduced to the developed breath analyser, and the remaining were transferred into 20 mL glass vials sealed with silicone septa using a suction pump at a controlled flow rate of 1 L/min to ensure minimal contamination and loss of BTEX vapours. The breath analyser produces real-time frequency deviation and acquires sensor response for further analysis. Solid-phase microextraction (SPME) was employed to extract BTEX compounds from the headspace of the glass vials using a divinylbenzene/carboxen (DVB/C) fibre with an 80 µm coating. The fibre was conditioned at 250 °C before use to remove any residual contaminants. The vial was agitated at 250 rpm and incubated at 60 °C for 5 minutes to allow the breath sample to equilibrate in the headspace, ensuring efficient adsorption of BTEX onto the fiber. The adsorbed analytes were thermally desorbed into the injection port of a gas chromatography-tandem mass spectrometry (GC-MS/MS) system operated in splitless mode. The GC-MS/MS utilized an HP-5MS UI capillary column (30 m × 250 µm × 0.25 µm) for separation. The oven temperature was programmed from 50 °C (2-minute hold) to 250 °C at variable

ramp rates, with a total runtime of 40 minutes. Helium was used as the carrier gas at a constant flow rate of 1.2 mL/min. The mass spectrometer operated in electron ionization (EI) mode with a transfer line temperature of 290 °C, ensuring sensitive and accurate quantification of BTEX compounds.

5.3.3 Statistical Analysis

We conducted the study to investigate the presence of BTEX in the breath of petrol station workers. The objective behind conducting a pilot study with 20 breath samples was to (1) test the feasibility of a larger study, (2) refine methodologies, (3) gather preliminary data, and (4) perform real-time analysis on the developed system. While a larger sample size would offer greater statistical power for definitive conclusions, 20 samples provide a sufficient basis for observing initial trends and estimating population parameters. Furthermore, logistical constraints were encountered during the collection of biological samples in occupational settings.

We have postulated two hypotheses for this study to analyse the study's outcomes.

- **Primary Hypothesis:** We hypothesized that the mean concentrations of individual BTEX compounds (Benzene, Toluene, Ethylbenzene, Xylene) in the exhaled breath of petrol station workers is higher than established occupational exposure limits.
- **Validation Hypothesis:** Another hypothesis was that the BTEX concentrations measured by the developed QCM sensor would show a strong agreement and

Correlation with those obtained from the gold standard (GC-MS) analysis. This hypothesis underpinned the validation process, asserting that the QCM sensor provides reliable measurements comparable to a high-precision laboratory method. The first hypothesis was examined using a one-sample t-test, and the second using the Bland-Altman analysis.

5.4 Results and Discussion

5.4.1 Sensor Implementation and Validation

To ensure the reliability of the QCM sensor measurements, calibration was first performed using GC-MS, which served as the reference analytical method for quantifying BTEX concentrations in breath samples[283]. Calibration curves were established for both PVAc and WO_3-coated QCM sensors, translating frequency shifts (Δf) into corresponding concentrations (ppm) using linear regression equations as discussed in chapters 3 and 4. To evaluate the agreement between the QCM sensors and GC-MS measurements, Bland-Altman analysis was employed [284], [285]. The results of the study are presented in Figures 5.3 and 5.4**.** This method was chosen for its ability to assess both the bias (mean difference) and the limits of agreement (LoA) between two quantitative measurement techniques, making it a

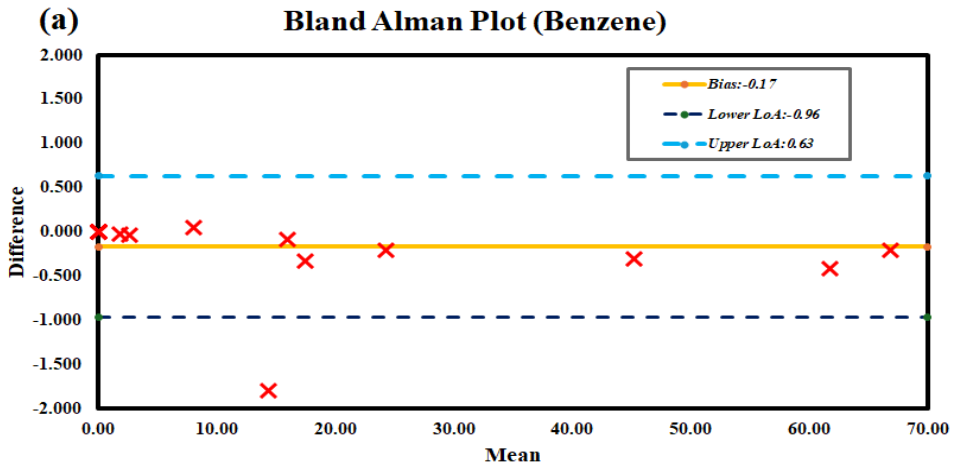
(a)
Bland Alman Plot (Benzene)
Bias:-0.17
Lower LoA:-0.96
Upper LoA:0.63
Difference
Mean
2.000
1.500
1.000
0.500
0.000
-0.500
-1.000
-1.500
-2.000
0.00
10.00
20.00
30.00
40.00
50.00
60.00
70.00

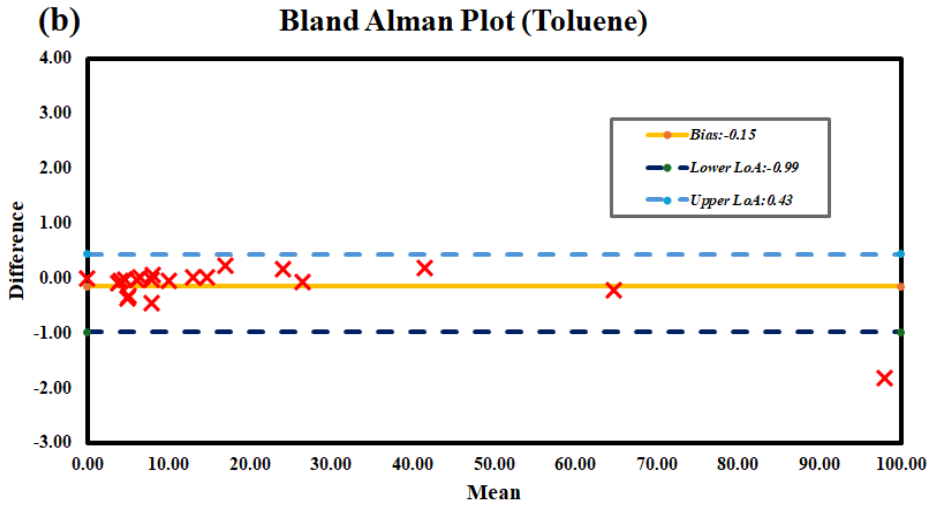
(b)
Bland Alman Plot (Toluene)
Bias:-0.15
Lower LoA:-0.99
Upper LoA:0.43
Difference
Mean
4.00
3.00
2.00
1.00
0.00
-1.00
-2.00
-3.00
0.00
10.00
20.00
30.00
40.00
50.00
60.00
70.00
80.00
90.00
100.00

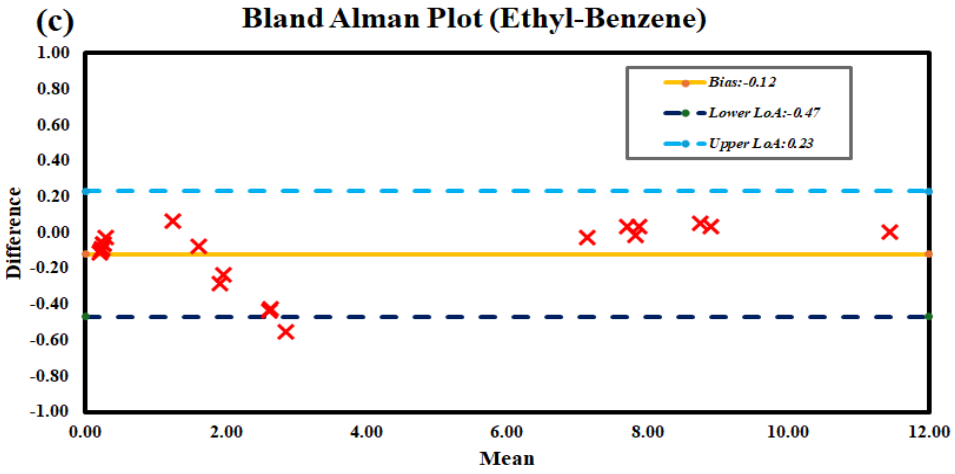
(c)
Bland Alman Plot (Ethyl-Benzene)
Bias:-0.12
Lower LoA:-0.47
Upper LoA:0.23
Difference
Mean
1.00
0.80
0.60
0.40
0.20
0.00
-0.20
-0.40
-0.60
-0.80
-1.00
0.00
2.00
4.00
6.00
8.00
10.00
12.00

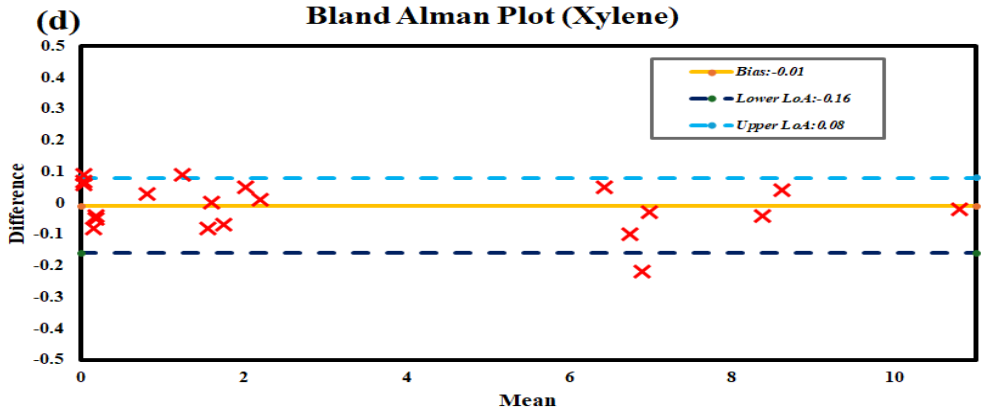

Figure 5.3 Bland Altman Analysis graph of PVAc coated QCM sensor for (a) Benzene (b) Toluene (c) Ethylbenzene and (d) Xylene.

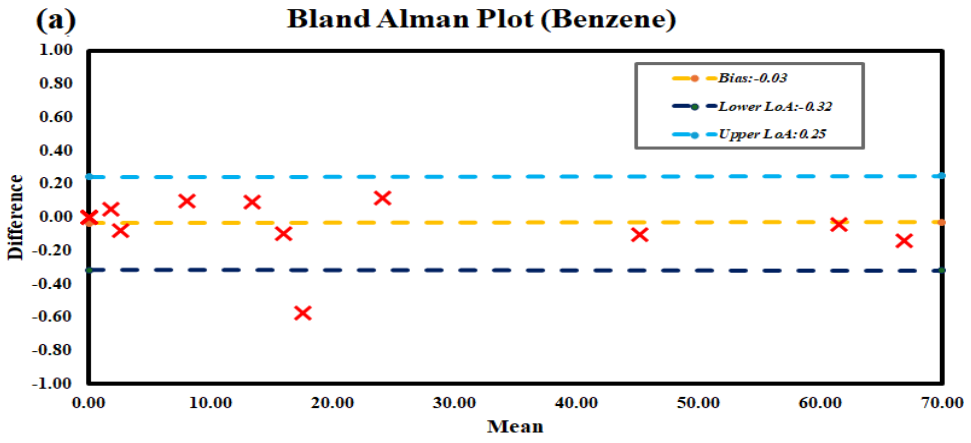

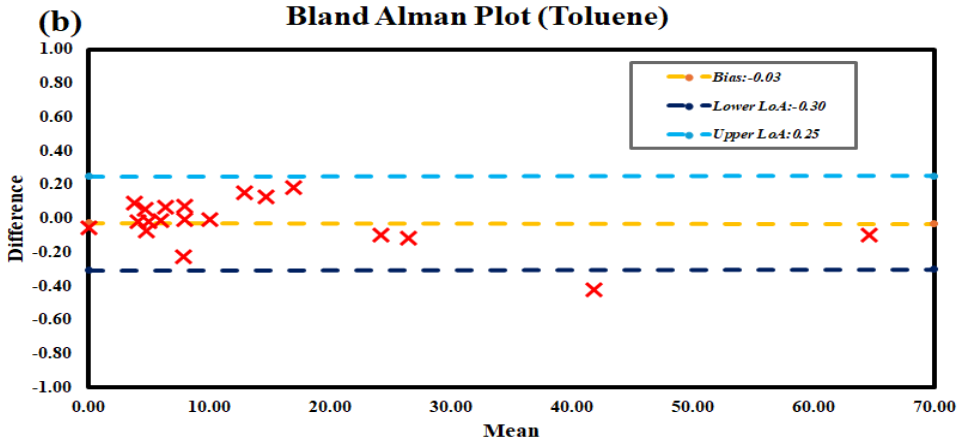

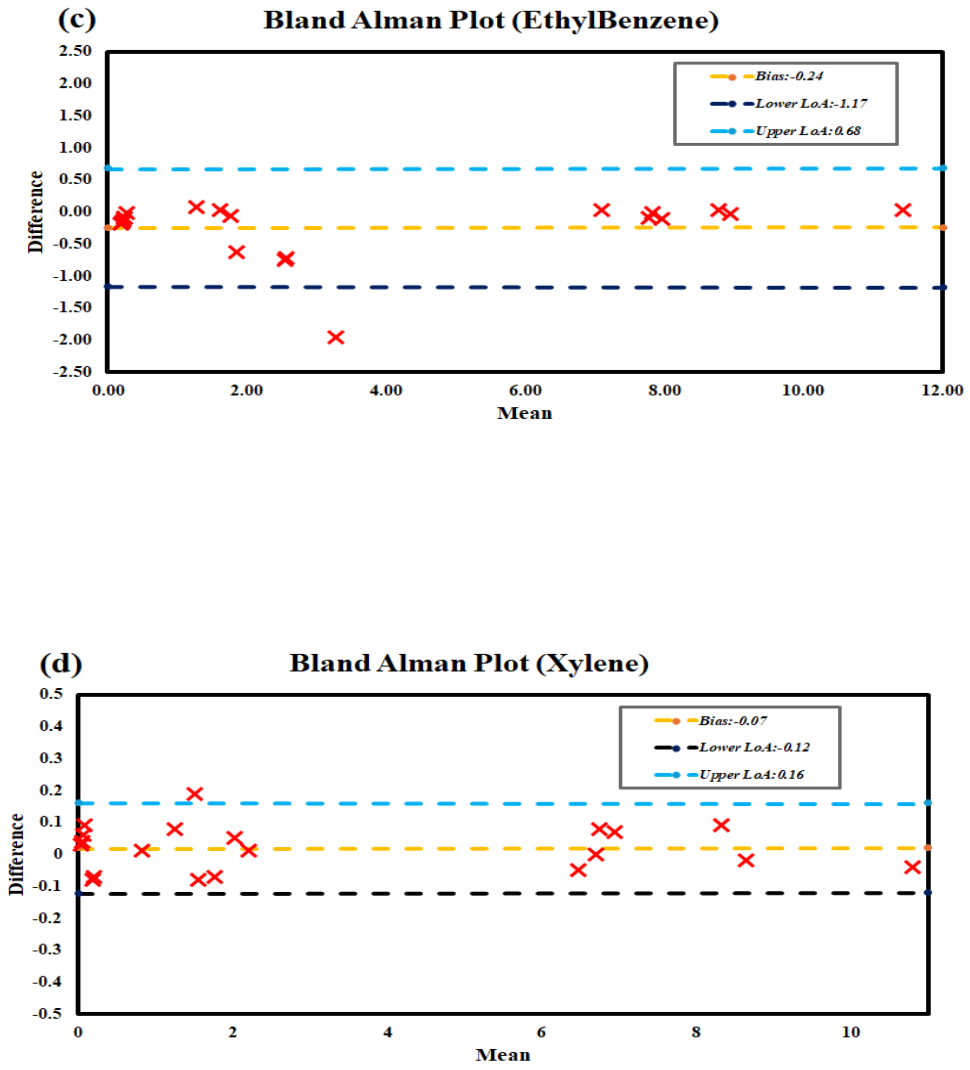

Figure 5.4 Bland Altman Analysis graph of WO_3-coated QCM sensor for (a) Benzene, (b) Toluene, (c) Ethylbenzene, and (d) Xylene.

Suitable tool to judge the accuracy and precision of the sensor system. Unlike correlation coefficients, which only assess the strength of a relationship, Bland-Altman analysis provides insight into the magnitude of disagreement and its consistency across the measurement range. A comparative study of the Bland-Altman results for PVAc and WO_3 coatings reveals distinct differences in their agreement with GC-MS measurements across BTEX.

For **Benzene**, the PVAc coating shows an Upper LoA of 0.63 and a Lower LoA of -0.96, with a consistent bias of -0.17 across both x-values (0 and 70). This indicates a slight tendency for the PVAC sensor to underestimate benzene concentrations compared to GC-MS. In contrast, the WO_3 coating for benzene exhibits tighter limits of agreement (Upper LoA: 0.25, Lower LoA: -0.32) and a smaller bias of -0.03. The standard deviation (SD) of 0.14 for WO_3 further suggests better precision and less spread in the differences. This indicates that the WO_3 coating provides a more accurate and precise agreement for benzene measurements than PVAc.

Regarding **Toluene**, the PVAc coating presents an Upper LoA of 0.43 and a Lower LoA of -0.99, with a bias of -0.15. Similar to benzene, this suggests a slight underestimation by the PVAC sensor. For the WO_3 coating, the limits of agreement for toluene are tighter (Upper LoA: 0.25, Lower LoA: -0.30) and the bias is also -0.03, again indicating a closer deal with GC-MS. The SD of 0.14 for WO_3 reinforces its superior precision for toluene.

For **Ethylbenzene**, the PVAc coating shows an Upper LoA of 0.23 and a Lower LoA of -0.47, with a bias of -0.12. The WO_3 coating, however, displays wider limits of agreement (Upper LoA: 0.68, Lower LoA: -1.17) and a larger bias of -0.24, coupled with a higher SD of 0.47. This suggests that for ethylbenzene, the PVAc coating shows better agreement with GC-MS in terms of both precision and accuracy than the WO_3 coating, which tends to underestimate and exhibits greater measurement variability.

Finally, for **Xylene**, the PVAc coating has an Upper LoA of 0.08 and a Lower LoA of -0.16, with a minimal bias of -0.01. This indicates excellent agreement with GC-MS for xylene. The WO_3 coating also shows good agreement, with an Upper LoA of 0.16 and a Lower LoA of -0.12, and a slight positive bias of 0.02, with an SD of 0.07. While both coatings perform well for xylene, the PVAc coating appears to offer slightly better accuracy (closer to zero bias) and slightly tighter limits of agreement.

Bland-Altman analysis provides critical insights into the performance of PVAc- and WO_3-coated sensors relative to the established GC-MS method for BTEX detection. For benzene and toluene, the WO_3 coating consistently demonstrates superior agreement with GC-MS, characterized by significantly tighter Limits of Agreement (LoA) and markedly smaller biases. This translates to a more precise and accurate measurement capability. Conversely, the PVAc coating proves to be the more effective choice for ethylbenzene, exhibiting a narrower LoA and a smaller negative bias, indicating better precision and less systematic underestimation compared to WO_3. The exceptional performance of the PVAc coating for Xylene, evidenced by its remarkably tight LoA and a nearly negligible bias, highlights its strong potential for highly accurate and precise detection of this compound. The consistent bias values across different concentrations for each coating and BTEX imply a systematic, rather than random, discrepancy between the sensor and GC-MS measurements.

Furthermore, the standard deviation (SD) values for the WO_3 coating, especially for Benzene and Toluene, provide a quantitative measure of the spread in differences, reinforcing the precision demonstrated by the tighter LoA and smaller biases.

While GC-MS remains the gold standard for its unparalleled accuracy and broad applicability, the detailed agreement quantified by the Bland-Altman method enables us to assess the utility of QCM-coated sensors precisely. This analysis provides empirical evidence for the deployment of these cost-effective, portable sensor technologies in specific scenarios where their level of agreement with GC-MS is deemed acceptable. For instance, in applications requiring rapid, on-site, or continuous monitoring of BTEX. The disparate strengths of the PVAc and WO_3 coatings across the BTEX compounds also advocate for the use of an array of sensors, integrating both coating types. Such a multi-sensor array design leverages the optimized performance of each coating for its respective target analytes. By combining WO_3-coated sensors for enhanced Benzene and Toluene detection with PVAc-coated sensors for superior ethylbenzene and xylene measurements, a comprehensive and robust BTEX detection system is realized. This approach mitigates the individual limitations of each coating, providing a more accurate and reliable overall BTEX monitoring solution than relying on a single coating type.

5.4.2 Data Analysis

The GC-MS analysis of 20 breath samples from petrol station workers revealed significant variations in BTEX concentrations as tabulated in **Table 5.2.** The GC-MS peak areas and calibration curves are discussed in the table in Chapter 4**.** A GC-MS peak area vs concentration plot for sample no. 2 is shown in Figure 5.5. Benzene, a known carcinogen, ranged from 1.82 ppm to 66.81 ppm, with a mean of 20.89 ppm, in breath samples from 20 petrol station workers.

However, in several samples, no benzene was detected, suggesting variability in exposure due to individual work conditions, tasks, or environmental factors at the petrol stations. Similarly, toluene levels ranged from 3.84 ppm to 97.08 ppm, with a mean of 20.91 ppm. Ethylbenzene and p-xylene showed lower concentrations, with means of 3.75 ppm and 3.53 ppm, respectively.

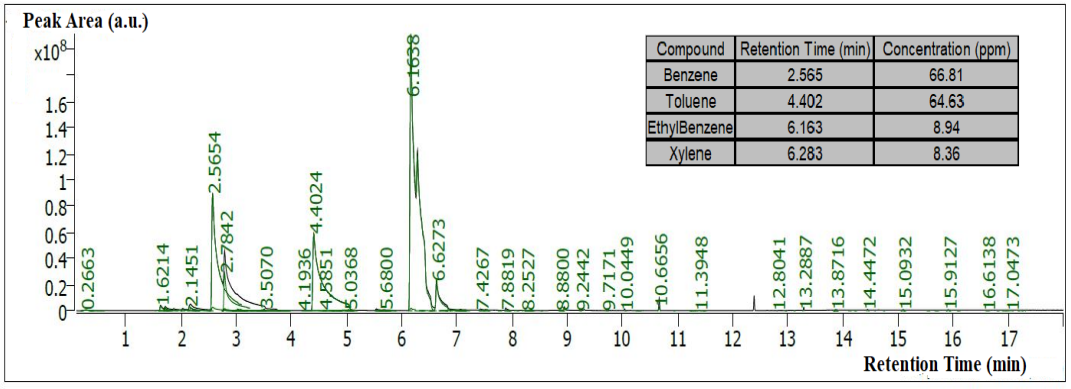

Figure 5.5 GC-MS peak area vs concentration plot of sample no 2

Table 5.2 Concentrations of BTEX Compounds in Breath Samples of Petrol Station Workers.

Breath Sample No.	**Benzene (ppm)**	**Toluene (ppm)**	**Ethylbenzene (ppm)**	**Xylene (ppm)**
1	24.21	26.48	0.27	0.15
2	66.81	64.63	8.94	8.36
3	15.96	24.21	0.15	0.06
4	61.55	7.74	8.8	8.64
5	13.47	17.11	0.19	0.12
6	8.12	14.77	0.2	0.16
7	17.27	41.64	11.44	10.78
8	2.59	4.68	0.12	0.09
9	45.12	97.08	7.11	6.45
10	1.82	3.84	0.1	0.07
11	0	4.08	1.54	1.52
12	0	6.02	2.18	2.21
13	0	8.04	2.3	1.73
14	0	7.96	1.73	1.29
15	0	4.73	1.63	1.6
16	0	4.96	2.21	2.05
17	0	0	1.31	0.83
18	0	13.04	7.91	6.97
19	0	6.45	7.81	6.7
20	0	10.07	7.74	6.78
Mean	20.89	20.91	3.75	3.53
Median	4.04	7.85	1.68	1.67
Standard Deviation	25.10	26.68	3.86	3.57
Min	0	0	0.1	0.06
Max	66.81	97.08	11.44	10.78

The wide standard deviations, particularly for benzene (20.89 ppm) and toluene (20.91 ppm), highlight the variability in exposure levels among workers. The median concentrations for all compounds are relatively low (ranging from 1.68 ppm

to 7.85 ppm), suggesting that most samples had lower exposure levels. In contrast, exposure to the carcinogen Benzene exceeds the 1ppm reference threshold.

The mean exposure levels for Toluene, Ethylbenzene, and Xylene remain low relative to their respective 100 ppm - 200 ppm occupational limits. However, the presence of these compounds in workers' breath still indicates occupational exposure, as ethylbenzene and xylene have potential adverse effects with prolonged or cumulative exposure.

The health risk assessment evaluates both non-carcinogenic and carcinogenic risks associated with exposure to BTEX, as discussed in Chapter 2. Non-carcinogenic risks are quantified using the Hazard Quotient (HQ), while carcinogenic risks are assessed using the Excess Lifetime Cancer Risk (ELCR).

To evaluate HQ and ELCR, the exposure dose (D) is calculated (Equation (5.1)), which quantifies the daily intake of a compound via inhalation based on environmental concentrations and physiological parameters.

$$D = \frac{Concentration \times Intake\ rate \times Exposure\ duration \times Exposure\ frequency}{Body\ weight \times Average\ Time} \quad (5.1)$$

Here, C = Inhaled concentration in µg/m^3, Intake Rate = volume of air inhaled daily is assumed to be 20 m^3/day, Exposure Duration = Workers are exposed continuously for 8 hours/day, Exposure Frequency =Exposure occurs 365 days/year, Body Weight =Average body weight is 62 kg, Averaging Time: 70 years × 365 days/year = 25,550 days.

The HQ is used to assess non-carcinogenic risks, which are evaluated using **Equation (5.2)**. If HQ > 1, there may be a potential non-carcinogenic risk.

$$HQ = \frac{D}{RfD} \tag{5.2}$$

Where RfD is the reference dose, which is 0.004 mg/kg/day for Benzene,0.08 mg/kg/day for Toluene, and 0.1 mg/kg/day for Ethylbenzene. 0.2 mg/kg/day for Xylene. The ELCR evaluates the carcinogenic risk of benzene using **Equation (5.3)**.

$$ELCR = D \times SF \tag{5.3}$$

Where SF is the slope factor and its value is 0.029 $(mg/kg/day)^{-1}$. An ELCR greater than 1×10^{-6} indicates a potential carcinogenic risk. The HQ and ELCR value of each sample is tabulated in **Table 5.3.**

The health risk assessment highlights significant variability in both non-carcinogenic and carcinogenic risks across the analysed BTEX compounds. The non-carcinogenic risk, assessed by the HQ, shows that Benzene and Toluene are the primary contributors to risk. In 10 samples, HQ values were well above the safety threshold of 1, reaching a maximum of 81.975. Similarly, Toluene's HQ exceeded 1 in 7 samples, with a peak of 7.025. The combined risk, represented by the Hazard Index (HI) (sum of all HQ), was greater than 1 in 13 out of 20 samples, peaking at 87.528 (Sample 2). HI value above 1 suggests that workers, particularly

those corresponding to Samples 1-10, 18, 19, and 20, are likely exposed to concentrations that could cause adverse non-carcinogenic health effects.

The ELCR for benzene reached a maximum of 9.51×10^{-3}, indicating a significant carcinogenic risk in some samples and exceeding the acceptable threshold of 1×10^{-6}. This shows a very high probability of excess cancer cases occurring in the exposed worker population over a lifetime.

Table 5.3 Health Risk Assessment result of 20 samples of petrol station workers.

Sample No.	Benzene (HQ)	Toluene (HQ)	Ethylbenzene (HQ)	Xylene (HQ)	Hazard Index (HI)	Benzene (ELCR)
1	29.706	1.916	0.018	0.005	31.645	3.45×10−3
2	81.975	4.677	0.596	0.279	87.528	9.51×10−3
3	19.583	1.752	0.01	0.002	21.347	2.27×10−3
4	75.521	0.56	0.587	0.288	76.957	8.76×10−3
5	16.528	1.238	0.013	0.004	17.782	1.92×10−3
6	9.963	1.069	0.013	0.005	11.051	1.16×10−3
7	21.19	3.013	0.763	0.36	25.326	2.46×10−3
8	3.178	0.339	0.008	0.003	3.528	3.69×10−4
9	55.362	7.025	0.474	0.215	63.077	6.42×10−3
10	2.233	0.278	0.007	0.002	2.52	2.59×10−4
11	0	0.295	0.103	0.051	0.449	0.00×10+00
12	0	0.436	0.145	0.074	0.655	0.00×10+00
13	0	0.582	0.153	0.058	0.793	0.00×10+00
14	0	0.576	0.115	0.043	0.734	0.00×10+00
15	0	0.342	0.109	0.053	0.504	0.00×10+00
16	0	0.359	0.147	0.068	0.575	0.00×10+00
17	0	0	0.087	0.028	0.115	0.00×10+00
18	0	0.944	0.528	0.232	1.704	0.00×10+00
19	0	0.467	0.521	0.223	1.211	0.00×10+00
20	0	0.729	0.516	0.226	1.471	0.00×10+00

We have performed a one-sample t-test to determine if the mean breath BTEX concentrations in petrol station workers are significantly elevated compared to established reference values. The results of the statistical test are tabulated in **Table 5.4**

Table 5.4 BTEX Concentrations in Breath Samples of Petrol Station Workers (n=20) and Statistical Significance Against Reference Values

Compound	Concentration Range (ppm)	Mean ± SD (ppm)	Reference Value (μ0, ppm)	t-statistic	P-value (one-tailed)
Benzene	0.00–66.81	20.89±25.10	1	3.544	0.00108
Toluene	0.00–97.08	20.91±26.68	200	-30.019	1
Ethylbenzene	0.10–11.44	3.75±3.86	100	-111.514	1
Xylene	0.06–10.78	3.53±3.57	100	-120.848	1

The t-test assessed whether the mean worker exposure level for each compound is statistically greater than its occupational limit (μ0). A p-value < 0.05 indicates a statistically significant exceedance.

Benzene: With a mean concentration of 20.89 ppm against a reference of 1 ppm, the t-statistic of 3.544 is highly positive. The resulting p-value of < 0.001 is substantially lower than 0.05. This indicates strong statistical evidence to reject the null hypothesis, concluding that the mean Benzene concentration in the breath of petrol station workers is higher than the one ppm reference value.

Toluene: The sample mean of 20.91ppm is lower than the 200-ppm reference, resulting in a negative t-statistic of -30.019. The p-value of 0.995 (which is much greater than 0.05) indicates that there is no statistical evidence to reject the null

hypothesis. This suggests that the mean Toluene concentration in the workers' breath is not significantly higher than the 200-ppm reference; in fact, the sample mean is considerably lower.

Ethylbenzene: The sample mean of 3.75 ppm is considerably lower than the 100-ppm reference, yielding a large negative t-statistic of -111.514. The p-value of 1.000 (greater than 0.05) leads to no rejection of the null hypothesis. This signifies that the mean Ethylbenzene concentration is not statistically significantly higher than the 100-ppm reference.

Xylene: Similarly, the sample mean of 3.53 ppm is significantly below the 100-ppm reference, resulting in a large negative t-statistic of -83.149. The p-value of 1.000 (greater than 0.05) indicates no statistical evidence to reject the null hypothesis. This suggests that the mean Xylene concentration is not significantly higher than the 100-ppm reference.

A one-sample t-test of these 20 breath samples indicates occupational exposure to Benzene above its reference limit, providing preliminary evidence of a health concern within this group. In contrast, for Toluene, Ethylbenzene, and Xylene, the measured mean concentrations in the breath samples are not statistically higher than their respective reference values.

5.4.3 Study Limitation

While this pilot study provides valuable preliminary insights into BTEX exposure among petrol station workers in Bengaluru, certain limitations warrant acknowledgement and consideration for future research.

- **Sample Size:** The study was conducted as a pilot with a small sample size of 20 participants. While sufficient for initial feasibility testing and trend observation, this limits the generalizability of the findings to the broader population of petrol station workers in Bengaluru or India.
- **Cross-sectional Design:** The study employed a cross-sectional design, collecting breath samples at a single point in time. This approach provides a snapshot of BTEX exposure. Still, it does not account for temporal variations that daily work routines, seasonal changes, specific refuelling activities, or the implementation of vapor recovery systems could influence.
- **Limited Environmental Factor Analysis:** While various personal and environmental factors, such as temperature, humidity, and wind velocity, were recorded during sample collection, a detailed statistical analysis of their specific influence could not be established due to a lack of generalizability.
- **Potential for Sample Stability Issues:** GC-MS sampling and calibration methodology involved collecting breath samples in 1 L Teflon gas sampling bags for subsequent GC-MS analysis. Although analysis was performed within 24 hours, gas sampling bags can suffer from sample stability issues over time due to the permeability of the bag material.
- **Reliance on Self-Reported Data:** Demographic and occupational data, including smoking and alcohol habits, fasting period, and exposure duration, were documented via a consent form. Reliance on self-reported information can introduce recall bias or social desirability bias, potentially affecting the accuracy of these personal and lifestyle factors.

- **Absence of Direct Control Group:** The study focused exclusively on petrol station workers and did not include a direct control group of individuals not occupationally exposed to BTEX.

Building upon the valuable insights and foundational data gathered in this pilot study, several avenues for future research emerge, promising to advance further our understanding of BTEX exposure and the utility of breath analysis in occupational health monitoring.

- **Expanded Sample Size and Diversity:** A critical next step involves conducting a larger-scale study with a significantly increased sample size, encompassing a wider range of petrol stations across different geographical regions and operational characteristics within India.
- **Longitudinal Studies:** Implementing longitudinal sampling designs, involving repeated breath sample collection from the same workers over extended periods (e.g., across different shifts, seasons, or years), would provide invaluable data on long-term exposure trends, temporal variability, and the cumulative impact of BTEX exposure on workers' health.
- **Biomarker Integration:** While breath analysis provides a direct measure of internal dose, integrating it with other biological markers (e.g., urinary metabolites, blood samples for adducts) would offer a more comprehensive

multi-matrix biomonitoring approach, providing converging evidence of exposure and potential health effects.

- **Development of Predictive Models:** Leveraging the validated sensor technology, future work could focus on developing predictive models that correlate real-time sensor readings with potential health risks, enabling proactive alerts and personalized intervention strategies for workers with elevated exposure.
- **Intervention Studies:** Based on the identified risks, future research could design and implement intervention studies to evaluate the effectiveness of various control measures (e.g., improved ventilation, vapor recovery systems, enhanced personal protective equipment, changes in work practices) in reducing BTEX exposure and associated health risks among petrol station workers.
- **Global Health Implications:** Expanding similar studies to petrol station workers in other developing countries facing similar environmental and occupational challenges would contribute significantly to the global understanding of BTEX exposure.

5.5 Conclusion

This present study highlights significant occupational health risks faced by petrol station workers in Bengaluru, India, due to elevated exposure to BTEX compounds. Breath analysis using GC-MS revealed mean benzene concentrations of 20.89 ± 25.10 ppm, far exceeding safe exposure limits, with approximately 75% of workers

exhibiting hazard quotients (HQ) above 1, indicating substantial non-carcinogenic risks.

Excess lifetime cancer risk (ELCR) for benzene ranged from 2.59×10^{-4} to 9.51×10^{-3}, exceeding the acceptable threshold of 1×10^{-6} in all workers, underscoring a pronounced carcinogenic risk. Although lower, mean concentrations of toluene, ethylbenzene, and xylene contributed to cumulative health risks. Our study employed statistical analyses to identify exposure variability. The statistical significance of elevated Benzene levels, confirmed by a one-sample t-test, even with 20 breath samples, provides robust preliminary evidence of its critical impact on this occupational group. The Bland-Altman analysis further validates the use of PVAc and WO_3-coated QCM sensors, demonstrating their specific strengths for different BTEX compounds. Such a system offers a cost-effective and portable alternative for continuous exposure assessment, complementing traditional GC-MS methods. These findings lay a strong foundation for future, larger-scale studies and the implementation of advanced sensor-based solutions for proactive occupational health surveillance.

Chapter 6: Conclusions and Future Scope

6.1 Summary of Key Findings

This research addressed the critical need for a portable, real-time BTEX breath analyser, particularly for occupational health monitoring. The study demonstrates the optimization of QCM sensors functionalized with PVAc and WO_3 for the detection of BTEX compounds.

6.1.1 Sensor Design and Performance

A Quartz Crystal Microbalance (QCM)-based sensor system was developed for detecting BTEX compounds at low concentrations.

- Two sensing materials—**Polyvinyl Acetate (PVAc)** and **Tungsten Oxide (WO_3)**—were coated onto QCM electrodes. Both materials were optimized for thickness and characterized using surface morphology analysis techniques (e.g., SEM, AFM), confirming structural features favourable for strong interactions with nonpolar BTEX molecules.
- The **PVAc-coated QCM sensor** exhibited the following sensitivities and LOD:
    - Benzene: 5.14 Hz/ppm, 0.91 ppm (LOD)
    - Toluene: 5.17 Hz/ppm, 1.65 ppm (LOD)
    - Ethylbenzene: 5.85 Hz/ppm, 0.99 ppm (LOD)
    - Xylene: 5.00 Hz/ppm, 1.3 ppm (LOD)

- The **WO_3-coated QCM sensor** demonstrated the following sensitivities and LOD:
    - Benzene: 3.36 Hz/ppm, 1.48 ppm (LOD)
    - Toluene: 5.69 Hz/ppm, 0.79 ppm (LOD)
    - Ethylbenzene: 5.30 Hz/ppm, 0.56 ppm (LOD)
    - Xylene: 5.10 Hz/ppm, 0.33 ppm (LOD)
- WO_3 coatings provided **rapid response times** (30–43 seconds) and demonstrated **excellent sensor performance**, with repeatability and reproducibility values of 99% and 98%, respectively.

6.1.2 Portable Breath Analyzer Development

- The optimized sensors were integrated into a **portable breath analyzer** designed for real-time monitoring of BTEX in exhaled breath.
- Key specifications of the developed system include:
    - Weight: approximately 1 kg
    - Dimensions: 200 mm in height, 68 mm inner diameter
    - Power requirement: 5V, 1000 mAh rechargeable battery
- The device operates efficiently under ambient conditions and can detect BTEX mixtures below 4 ppm within 3 minutes.
- Its compact, low-power design presents a **practical alternative to conventional GC-MS** and other portable GC devices, which often require complex and bulky preconcentration modules.

6.1.3 Validation Against GC-MS

- Sensor calibration and validation were performed against **Gas Chromatography-Mass Spectrometry (GC-MS)**, the gold standard in VOC detection **(Table 6.1 and Table 6.2)**.
- **Correlation analysis** between QCM sensor responses and GC-MS data for all BTEX compounds yielded high correlation coefficients (R^2 = 0.993 to 0.999), indicating strong agreement and quantitative reliability.
- **Bland-Altman analysis** further confirmed the accuracy and precision of the multi-sensor array:
    - WO_3 performed best for benzene and toluene.
    - PVAc performed best for ethylbenzene and xylene.

6.1.4 Real-World Exposure Assessment

- A **pilot study** involving breath samples from petrol station workers was conducted to assess occupational exposure. Measured benzene concentrations ranged from **1.82 ppm to 66.81 ppm**, highlighting significant variability in exposure.
- Health risk assessments based on **USEPA guidelines** revealed:
    - **Hazard Quotient (HQ)** values for benzene exceeded the threshold value in **75% of the workers**.
    - **Excess Lifetime Cancer Risk (ELCR)** was found to be **elevated in all workers**.

Table 6.1 Comparison of the PVAc-coated QCM sensor results with the GC-MS results for breath samples.

Compound	**Benzene**			**Toluene**			**Ethylbenzene**			**Xylene**		
Breath Sample No.	GC-MS conc. (ppm)	Δf (Hz)	Sensor conc. (ppm)	GC-MS conc. (ppm)	Δf (Hz)	Sensor conc. (ppm)	GC-MS conc. (ppm)	Δf (Hz)	Sensor conc. (ppm)	GC-MS conc. (ppm)	Δf (Hz)	Sensor conc. (ppm)
1	24.21	157	24	26.48	177	26.56	0.27	60	0.32	0.15	102	0.2
2	66.81	376	67	64.63	375	64.86	8.94	110	8.87	8.36	143	8.4
3	15.96	114	16	24.21	164	24.05	0.15	60	0.32	0.06	101	0
4	61.55	350	62	7.74	82	8.19	8.8	109	8.70	8.64	144	8.6
5	13.47	110	15	17.11	127	16.89	0.19	60	0.32	0.12	102	0.2
6	8.12	73	8	14.77	116	14.76	0.2	60	0.32	0.16	102	0.2
7	17.27	122	18	41.64	254	41.46	11.44	125	11.43	10.78	155	10.8
8	2.59	45	3	4.68	64	4.71	0.12	60	0.32	0.09	101	0
9	45.12	265	45	97.08	551	98.90	7.11	100	7.16	6.45	133	6.4
10	1.82	41	2	3.84	60	3.93	0.1	60	0.32	0.07	101	0
11	0	10	0	4.08	61	4.13	1.54	68	1.69	1.52	109	1.6
12	0	10	0	6.02	71	6.06	2.18	76	3.06	2.21	112	2.2
13	0	10	0	8.04	81	7.99	2.3	78	3.40	1.73	110	1.8
14	0	10	0	7.96	81	7.99	1.73	71	2.20	1.29	107	1.2
15	0	10	0	4.73	66	5.09	1.63	71	2.20	1.6	109	1.6
16	0	10	0	4.96	67	5.29	2.21	76	3.06	2.05	111	2
17	0	10	0	0	5	0.00	1.31	65	1.18	0.83	105	0.8
18	0	10	0	13.04	107	13.02	7.91	104	7.84	6.97	136	7
19	0	10	0	6.45	73	6.45	7.81	104	7.84	6.7	135	6.8
20	0	10	0	10.07	92	10.12	7.74	103	7.67	6.78	136	7

Table 6.2 Comparison of the WO_3-coated QCM sensor results with the GC-MS results for breath samples.

Compound	**Benzene**			**Toluene**			**Ethylbenzene**			**Xylene**		
Breath Sample No.	GC-MS conc. (ppm)	Δf (Hz)	Sensor conc. (ppm)	GC-MS conc. (ppm)	Δf (Hz)	Sensor conc. (ppm)	GC-MS conc. (ppm)	Δf (Hz)	Sensor conc. (ppm)	GC-MS conc. (ppm)	Δf (Hz)	Sensor conc. (ppm)
1	24.21	86	24.10	26.48	168	26.59	0.27	35	0.29	0.15	44	0.23
2	66.81	230	66.95	64.63	385	64.73	8.94	81	8.97	8.36	85	8.27
3	15.96	59	16.06	24.21	155	24.31	0.15	35	0.29	0.06	43	0.03
4	61.55	212	61.60	7.74	62	7.96	8.8	80	8.78	8.64	87	8.66
5	13.47	50	13.38	17.11	113	16.93	0.19	35	0.29	0.12	43	0.03
6	8.12	32	8.02	14.77	100	14.64	0.2	35	0.29	0.16	44	0.23
7	17.27	65	17.85	41.64	256	42.06	11.44	94	11.42	10.78	98	10.82
8	2.59	14	2.67	4.68	43	4.63	0.12	35	0.29	0.09	43	0.03
9	45.12	157	45.23	97.08	570	97.24	7.11	71	7.08	6.45	76	6.5
10	1.82	11	1.77	3.84	38	3.75	0.1	35	0.29	0.07	43	0.03
11	0	5	0.00	4.08	40	4.10	1.54	45	2.17	1.52	51	1.6
12	0	5	0.00	6.02	51	6.03	2.18	49	2.93	2.21	54	2.2
13	0	5	0.00	8.04	62	7.96	2.3	56	4.25	1.73	52	1.8
14	0	5	0.00	7.96	62	7.96	1.73	43	1.80	1.29	49	1.21
15	0	5	0.00	4.73	44	4.80	1.63	42	1.61	1.6	50	1.41
16	0	5	0.00	4.96	45	4.98	2.21	49	2.93	2.05	53	2
17	0	5	0.00	0	17	0.06	1.31	40	1.23	0.83	47	0.82
18	0	5	0.00	13.04	90	12.89	7.91	76	8.02	6.97	78	6.9
19	0	5	0.00	6.45	53	6.38	7.81	75	7.83	6.7	77	6.7
20	0	5	0.00	10.07	74	10.07	7.74	75	7.83	6.78	77	6.7

6.1.5 Machine Learning-Based BTEX Classification

- **Unsupervised learning algorithms**, namely K-Means and BIRCH clustering, were applied to QCM sensor data for pattern recognition and compound classification.
- These models effectively distinguished between individual BTEX compounds based on sensor response patterns.
- The results demonstrate the potential for integrating **intelligent data analytics** into the portable sensor system, enhancing its utility for selective and semi-quantitative field analysis.

6.2 Contribution of the Research to Occupational Health

The research contributes to occupational health by providing a novel, practical, and highly effective tool for real-time monitoring of BTEX exposure.

- **Enhanced Exposure Assessment:** Traditional methods, often relying on ambient air monitoring, may not accurately reflect the internal dose of BTEX in workers. By focusing on exhaled breath analysis, this study directly assesses internal exposure, offering a more precise and relevant measure of occupational risk. This non-invasive biomonitoring approach is a key novelty of this work.
- **Proactive Risk Management:** The ability to detect BTEX in near real-time (less than 3 minutes) allows for immediate identification of exposure events. This enables prompt corrective actions, such as ventilation improvements

or personal protective equipment (PPE) adjustments, thereby reducing chronic exposure and its associated health risks, including cancer and neurotoxicity.

- **Empowering Workers and Employers:** The portability and ease of use of the developed system empower both workers and employers. Workers can be more aware of their exposure levels, fostering safer work practices. Employers gain a cost-effective, efficient way to comply with occupational safety regulations and ensure a healthier work environment, particularly in industries such as oil and gas, where BTEX exposure is prevalent. The pilot study results, showing high BTEX concentrations in petrol station workers' breath and elevated health risks, underscore the critical need for such real-time monitoring devices.

6.3 Advantages and Limitations of the Study

The key advantages stem from the present system's design, performance, and application in occupational health are outlined as below:

- **Portability and Real-Time Monitoring:**
  - The developed system is **compact** (approx. 1 kg) and consumes **low-power** (5V, 1000 mAh rechargeable battery).
  - It offers a **practical alternative** to bulky, complex conventional methods like GC-MS.

- It provides **real-time** detection of BTEX mixtures (below 4 ppm) **within 3 minutes**, enabling **proactive risk management** and immediate corrective actions.

- **Enhanced Exposure Assessment (Biomonitoring):**
  - By focusing on **exhaled breath analysis**, the device performs **non-invasive biomonitoring**, which directly assesses the **internal dose** of BTEX in workers.
  - This provides a **more precise and relevant measure of occupational risk** compared to traditional ambient air monitoring.
- **Sensor Performance and Validation:**
  - The dual sensing materials (**PVAc and WO_3**) were optimized, yielding good sensitivity and LOD.
  - Validation against the gold standard, **GC-MS**, showed **high quantitative reliability**, with strong correlation coefficients (R^2= 0.993 to $0.999).

There are several inherent limitations or areas for improvement:

- **Need for Further Miniaturization and Power Optimization:**
  - While already compact, the research suggests that **further miniaturization** of the sensing chamber and electronic components, along with **continued optimization of power consumption**, is needed to extend battery life for longer-duration monitoring.

- **Limited Durability Data:**
    - The study calls for **extensive long-term field testing** under varying environmental conditions (extreme temperatures, humidity fluctuations) to fully assess the **robustness and field durability** of the device, implying that this long-term data is not yet available.
- **Need for Connectivity and Automation:**
    - The system currently lacks features for advanced utility, such as **wireless connectivity** for real-time data clouding/remote monitoring and **automated, on-site calibration and self-diagnosis**, which are crucial for reducing maintenance and ensuring consistent accuracy in industrial settings.
- **Pilot Study Scope:**
    - The real-world application was a **pilot study** with a limited cohort (petrol station workers). A need for **clinical validation across larger cohorts in diverse geographic and occupational settings is recommended to yield** more statistically significant and generalizable health risk data.

6.4 Future Scope

6.4.1 Future Improvements in Sensor Design and System Integration

While the developed system represents a significant leap forward, several areas can be targeted for future improvements:

- **Enhanced Selectivity:** Although the current sensor array showed good classification with machine learning, further research into novel sensing materials or hybrid coatings could improve the individual selectivity of sensors towards specific BTEX compounds or other common interfering VOCs. This could involve exploring nanomaterials with tailored adsorption properties.
- **Miniaturization and Power Optimization:** Although already compact, further miniaturization of the sensing chamber and electronic components could enhance portability even further. Continued power consumption optimization would extend battery life, making the device suitable for longer-duration monitoring without frequent recharging.
- **Robustness and Field Durability:** While designed for robustness, extensive long-term field testing under varying environmental conditions (e.g., extreme temperatures, humidity fluctuations beyond the current study) would provide valuable data for further improvements in material selection and system packaging to ensure sustained performance and durability.

- **Wireless Connectivity and Data Clouding:** Integrating advanced wireless communication modules (e.g., Bluetooth Low Energy, Wi-Fi) could enable real-time data transmission to mobile devices or cloud platforms. This would facilitate remote monitoring, data logging, and immediate alerts, thereby enhancing the device's utility in various industrial settings.
- **Automated Calibration and Self-Diagnosis:** Developing features for automated, on-site calibration or self-diagnosis of sensors could reduce maintenance requirements and ensure consistent accuracy over time.

6.4.2 Potential Applications in Other Industries

The portable QCM-based BTEX detection system holds immense potential for applications beyond the oil and gas industry:

- **Environmental Monitoring:** The device can be deployed for real-time monitoring of ambient air quality in urban areas, near industrial zones, or even residential communities located close to potential BTEX emission sources. This would aid in identifying pollution hotspots and assessing public health risks.
- **Indoor Air Quality (IAQ) Assessment:** BTEX compounds can originate from various indoor sources such as building materials, paints, glues, and consumer products. The portable system could be used by homeowners, building managers, and environmental consultants to assess IAQ and identify sources of contamination.

- **Automotive Industry:** Monitoring BTEX levels inside vehicle cabins or in repair shops could be valuable for assessing exposure risks for drivers and mechanics.
- **Forensic and Emergency Response:** In scenarios involving chemical spills or hazardous material incidents, the rapid and portable detection capability could aid first responders in assessing immediate dangers and defining safe perimeters.

6.4.3 Recommendations for Future Research

Based on the findings and current limitations, the following recommendations are proposed for future research:

- **Expanded Analyte Spectrum:** Investigate the development of QCM sensors or sensor arrays with enhanced selectivity and sensitivity for a broader range of VOCs beyond BTEX, relevant to various industrial and environmental contexts.
- **Advanced Machine Learning Integration:** Explore more sophisticated machine learning algorithms for real-time data processing and pattern recognition. This methodology will include deep learning models for enhanced classification accuracy, even with complex mixtures of VOCs, and the development of predictive models for long-term exposure trends.

- **Long-Term Stability Studies:** Conduct comprehensive long-term stability tests of the sensors and the integrated system under diverse environmental conditions (e.g., varying humidity, temperature cycles, and the presence of other common interferents) to understand their lifespans and performance degradation characteristics fully.
- **Clinical Validation with Larger Cohorts:** Expand the pilot study to include larger cohorts of exposed and control individuals across different geographic locations and occupational settings. This would provide more statistically significant data for health risk assessments and further validate the breath analysis approach for biomonitoring.

List of Publications

[1] A. Das, P. R. Muduli and R. Manjunatha, "QCM-Based Electronic Nose for Near-Real-Time BTEX Detection," in *IEEE Transactions on Instrumentation and Measurement*, vol. 74, pp. 1-8, 2025.

[2] A. Das, R. Manjunatha, K. N. Kumar, D. De, and R. Bandyopadhyay, "Fabrication of surface functionalized QCM sensor for BTX detection at ambient conditions," Talanta, vol. 283, p. 127081, 2025.

[3] A. Das, B. S. Giri, and R. Manjunatha, "Systematic review on benzene, toluene, ethylbenzene, and xylene (BTEX) emissions; health impact assessment; and detection techniques in oil and natural gas operations," Environ. Sci. Pollut. Res., vol. 32, no. 1, pp. 1–22, Dec. 2024.

[4] A. Das and R. Manjunatha, "Optimization of QCM sensor for BTX detection," in 2023 IEEE 9th International Conference on Smart Instrumentation, Measurement and Applications (ICSIMA), IEEE, pp. 225–229, 2023.

[5] A. Das, B. Lal, and R. Manjunatha, "Advances in gravimetric electronic nose for biomarkers detection," Ser. Biomech., vol. 36, no. 2, 2022.

[6] A. Das and R. Manjunatha, "Modeling of Graphene Oxide Coated QCM Sensor for E-Nose Application," in Recent Trends in Materials, vol. 18, K. Geetha, F. M. Gonzalez-Longatt, and H.-M. Wee, Eds., in Springer Proceedings in Materials, vol. 18., pp. 179–188, 2022.

References

[1] H. Rajabi, M. H. Mosleh, P. Mandal, A. Lea-Langton, and M. Sedighi, "Emissions of volatile organic compounds from crude oil processing–Global emission inventory and environmental release," Sci. Total Environ., vol. 727, p. 138654, 2020.

[2] "Case Studies, Oil Industry Safety Directorate." Available: https://www.oisd.gov.in/en-in/CaseStudies

[3] Lachenmayer, Emily, I-Ting Ku, Arsineh Hecobian, Katherine B. Benedict, Yong Zhou, Brent Buck, and Jeffrey L. Collett. "Source apportionment of airborne volatile organic compounds near unconventional oil and gas development," *Environ. Res. Commun.*, vol. 6, no. 10 pp.101013, 2024.

[4] VanEtten, Kati J. "Source Apportionment And Emission Rates Of Volatile Organic Compounds In The Bakken Shale Oil And Natural Gas Region," PhD diss., Appalachian State University, 2017.

[5] Mangotra, Anju, and Shailesh Kumar Singh, "Volatile organic compounds: A threat to the environment and health hazards to Living Organisms - A Review.," *J. Biotechnol.*, Jan. 2024, doi: 10.1016/j.jbiotec.2023.12.013.

[6] D. A. Garcia-Gonzales, S. B. C. Shonkoff, J. Hays, and M. Jerrett, "Hazardous Air Pollutants Associated with Upstream Oil and Natural Gas Development: A Critical Synthesis of Current Peer-Reviewed Literature," *Annu. Rev. Public Health*, vol. 40, no. 1, pp. 283–304, Apr. 2019, doi: 10.1146/annurev-publhealth-040218-043715.

[7] Bencsik, Dániel, Tanush Wadhawan, Ferenc Házi, and Tamás Karches."Plant-Wide Models for Optimizing the Operation and Maintenance of BTEX-Contaminated Wastewater Treatment and Reuse," *Environments*, Apr. 2024, doi: 10.3390/environments11050088.

[8] S. Malakar and P. D. Saha, "Estimation of VOC emission in petroleum refinery ETP and comparative analysis with measured VOC emission rate," *The IJES*, vol. 4, no. 10, pp. 20–29, 2015.

[9] Y. Attaqwa, M. Mahachandra, and H. Prastawa, "Analysis of benzene exposure considering workers characteristic in the oil and gas industry," in *IOP Conference Series: Materials Science and Engineering*, IOP Publishing, p. 012059.2020,

[10] V. A. Benignus, "Health effects of toluene: a review.," *Neurotoxicology*, vol. 2, no. 3, pp. 567–588, 1981.

[11] Afrasiabi, Sedighe, Marzieh Fattahi Darghlou, Younes Mohammadi, and Mostafa Leili."Effects of short and long-term exposure to benzene, toluene, ethylbenzene, and xylenes (BTEX) in indoor environment air on human health: A systematic review and meta-analysis," *J. Air Pollut. Health*, Jan. 2025, doi: 10.18502/japh.v9i4.17653.

[12] F. Gamberale, G. Annwall, and M. Hultengren, "Exposure to xylene and ethylbenzene: III. Effects on central nervous functions," *Scand. J. Work. Environ. Health*, pp. 204–211, 1978.

[13] C. Holder *et al.*, "Evaluating potential human health risks from modeled inhalation exposures to volatile organic compounds emitted from oil and gas operations," *J. Air Waste Manag. Assoc.*, vol. 69, no. 12, pp. 1503–1524, Dec. 2019, doi: 10.1080/10962247.2019.1680459.

[14] Md. A. Bari and W. B. Kindzierski, "Ambient volatile organic compounds (VOCs) in communities of the Athabasca oil sands region: Sources and screening health risk assessment," *Environ. Pollut.*, vol. 235, pp. 602–614, Apr. 2018, doi: 10.1016/j.envpol.2017.12.065.

[15] T. S. McMullin, A. M. Bamber, D. Bon, D. I. Vigil, and M. Van Dyke, "Exposures and Health Risks from Volatile Organic Compounds in Communities Located near Oil and Gas Exploration and Production Activities in Colorado (U.S.A.)," *Int. J. Environ. Res. Public. Health*, vol. 15, no. 7, p. 1500, Jul. 2018, doi: 10.3390/ijerph15071500.

[16] M. Sadeghi-Yarandi, F. Golbabaei, and A. Karimi, "Evaluation of pulmonary function and respiratory symptoms among workers exposed to 1,3-Butadiene in a petrochemical industry in Iran," *Arch. Environ. Occup. Health*, vol. 75, no. 8, pp. 483–490, Nov. 2020, doi: 10.1080/19338244.2020.1749018.

[17] B. Harati, S. J. Shahtaheri, H. A. Yousefi, A. Harati, A. Askari, and N. Abdolmohamadi, "Cancer Risk Assessment for Workers Exposed to Pollution Source, a Petrochemical Company, Iran," *Iran. J. Public Health*, Jul. 2020, doi: 10.18502/ijph.v49i7.3587.

[18] Z. Zhang *et al.*, "Emission and health risk assessment of volatile organic compounds in various processes of a petroleum refinery in the Pearl River Delta, China," *Environ. Pollut.*, vol. 238, pp. 452–461, Jul. 2018, doi: 10.1016/j.envpol.2018.03.054.

[19] E. Webb *et al.*, "Neurodevelopmental and neurological effects of chemicals associated with unconventional oil and natural gas operations and their potential effects on infants and children," *Rev. Environ. Health*, vol. 33, no. 1, pp. 3–29, Mar. 2018, doi: 10.1515/reveh-2017-0008.

[20] B. Durant, N. Abualfaraj, M. S. Olson, and P. L. Gurian, "Assessing dermal exposure risk to workers from flowback water during shale gas hydraulic fracturing activity," *J. Nat. Gas Sci. Eng.*, vol. 34, pp. 969–978, Aug. 2016, doi: 10.1016/j.jngse.2016.07.051.

[21] He, Yan Su, Hong Qiu, Wen Qiao Wang, and Kin Fai Ho "Exposure to monocyclic aromatic hydrocarbons - BTEX is associated with cardiovascular disease, dyslipidemia and leukocytosis in national US population," *Environ. Health Perspect.*, Sep. 2023, doi: 10.1289/isee.2023.ep-144.

[22] Crosby, Benjamin T., Adam Ridzuan-Allen, and John P. O'Neill "(Volatile organic compound analysis for the diagnosis of pancreatic cancer," *ResearchGate*, doi: 10.21037/apc-20-39.

[23] T. Majchrzak, W. Wojnowski, M. Lubinska-Szczygeł, A. Różańska, J. Namieśnik, and T. Dymerski, "PTR-MS and GC-MS as complementary techniques for analysis of volatiles: A tutorial review," *Anal. Chim. Acta*, vol. 1035, pp. 1–13, 2018.

[24] C. Liaud, N. T. Nguyen, R. Nasreddine, and S. Le Calvé, "Experimental performances study of a transportable GC-PID and two thermo-desorption based methods coupled to FID and MS detection to assess BTEX exposure

at sub-ppb level in air," *Talanta*, vol. 127, pp. 33–42, Sep. 2014, doi: 10.1016/j.talanta.2014.04.001.

[25] Constantinou, Marios."Nanowire Field-Effect Transistors for Gas Sensor Applications," University of Surrey (United Kingdom),2017.

[26] S. Yang, J. Wickliffe, G. Kibelka, E. B. Overton, C. T. Lungu, and J. Oh, "Laboratory evaluation of a prototype portable gas chromatograph (GC) with a flame ionization detector (FID) for toluene, ethylbenzene, and xylenes (TEX) analysis," *J. Anal. Sci. Technol.*, vol. 14, no. 1, p. 36, Aug. 2023, doi: 10.1186/s40543-023-00404-2.

[27] Burel, Antoine." Discrimination in the solid state during crystallization: application to Phenanthrene ultrapurification," PhD diss., Normandie Universiete,2017

[28] C. Rodríguez-Navas, R. Forteza, and V. Cerdà, "Use of thermal desorption–gas chromatography–mass spectrometry (TD–GC–MS) on identification of odorant emission focus by volatile organic compounds characterisation," *Chemosphere*, vol. 89, no. 11, pp. 1426–1436, Nov. 2012, doi: 10.1016/j.chemosphere.2012.06.013.

[29] Stewart, Trenton K., Ines E. Carotti, Yasser M. Qureshi, and James A. Covington. "Trends in Chemical Sensors for Non-Invasive Breath Analysis," TrAC, Trends in Analytical Chemistry, p.117792, 2024 doi: 10.1016/j.trac.2024.117792.

[30] O. C. Lezzar, A. Bellel, M. Boutamine, S. Sahli, Y. Segui, and P. Raynaud, "Thin Film Coated QCM-Sensors and Pattern Recognition Methods for Discrimination of VOCs," *Int. J. Smart Sens. Intell. Syst.*, vol. 7, no. 5, pp. 1–6, Jan. 2014, doi: 10.21307/ijssis-2019-015.

[31] A. Bearzotti, A. Macagnano, P. Papa, I. Venditti, and E. Zampetti, "A study of a QCM sensor based on pentacene for the detection of BTX vapors in air," *Sens. Actuators B Chem.*, vol. 240, pp. 1160–1164, 2017.

[32] X. Fan and B. Du, "Selective detection of trace p-xylene by polymer-coated QCM sensors," *Sens. Actuators B Chem.*, vol. 166, pp. 753–760, 2012.

[33] N. Alanazi, M. Almutairi, and A. N. Alodhayb, "A Review of Quartz Crystal Microbalance for Chemical and Biological Sensing Applications," *Sens. Imaging*, vol. 24, no. 1, p. 10, Mar. 2023, doi: 10.1007/s11220-023-00413-w.

[34] Kou, Lu, David Zhang, Jane You, and Yingbin Jiang. "Breath Analysis for Detecting Diseases on Respiratory, Metabolic and Digestive System," *J. Biomed. Sci. Eng.*, vol. 12, no. 1, pp. 40–52, Jan. 2019.

[35] Phillips, Michael, Nasser Altorki, John HM Austin, R. B. Cameron, R. N. Cataneo, J. Greenberg, R. Kloss et al"Karunagaran, Monika, Pratibha Ramani, S. Gheena, R. Abilasha, and R. Hannah. "Volatile Organic Compounds in Human Breath," *Indian J. Dent. Res.*, vol. 33, pp. 100–104, Jan. 2022.

[36] Phillips, Michael, Nasser Altorki, John HM Austin, R. B. Cameron, R. N. Cataneo, J. Greenberg, R. Kloss et al "Prediction of lung cancer using volatile biomarkers in breath."Journal of Clinical Oncology vol.23, no.16, pp: 9510,2005.

[37] A. K. Greenberg and M. S. Lee, “Biomarkers for lung cancer: clinical uses,” *Curr. Opin. Pulm. Med.*, vol. 13, no. 4, pp. 249–255, 2007.

[38] F. C. De Abreu, J. L. R. Da Silva Júnior, and M. F. Rabahi, “The Fraction Exhaled Nitric Oxide as a Biomarker of Asthma Control,” *Biomark. Insights*, vol. 14, p. 1177271919826550, Jan. 2019, doi: 10.1177/1177271919826550.

[39] A. Menzies-Gow, A. H. Mansur, and C. E. Brightling, “Clinical utility of fractional exhaled nitric oxide in severe asthma management,” *Eur. Respir. J.*, vol. 55, no. 3, 2020.

[40] T. H. Risby and S. F. Solga, “Current status of clinical breath analysis,” *Appl. Phys. B*, vol. 85, no. 2, pp. 421–426, Nov. 2006, doi: 10.1007/s00340-006-2280-4.

[41] A. Rydosz, “Sensors for enhanced detection of acetone as a potential tool for noninvasive diabetes monitoring,” *Sensors*, vol. 18, no. 7, p. 2298, 2018.

[42] M. Phillips, M. Sabas, and J. Greenberg, “Increased pentane and carbon disulfide in the breath of patients with schizophrenia.,” *J. Clin. Pathol.*, vol. 46, no. 9, pp. 861–864, 1993.

[43] B. M. Ross, S. Shah, and M. Peet, “Increased breath ethane and pentane concentrations in currently unmedicated patients with schizophrenia,” *Open J. Psychiatry*, vol. 1, no. 1, pp. 1–7, 2011.

[44] N. Porozova, E. Danilova, I. Senshinov, A. Tsakalof, and A. Nosyrev, “Experiences and perspectives of GC-MS application for the search of low molecular weight discriminants of schizophrenia,” *Molecules*, vol. 28, no. 1, p. 324, 2022.

[45] Y. Li, X. Wei, Y. Zhou, J. Wang, and R. You, “Research progress of electronic nose technology in exhaled breath disease analysis,” *Microsyst. Nanoeng.*, vol. 9, no. 1, p. 129, Oct. 2023, doi: 10.1038/s41378-023-00594-0.

[46] H. M. Saraoglu and M. Kocan, “Determination of Blood Glucose Level-Based Breath Analysis by a Quartz Crystal Microbalance Sensor Array,” *IEEE Sens. J.*, vol. 10, no. 1, pp. 104–109, Jan. 2010, doi: 10.1109/JSEN.2009.2035769.

[47] O. Lawal, W. M. Ahmed, T. M. E. Nijsen, R. Goodacre, and S. J. Fowler, “Exhaled breath analysis: a review of ‘breath-taking’ methods for off-line analysis,” *Metabolomics*, vol. 13, no. 10, Oct. 2017, doi: 10.1007/s11306-017-1241-8.

[48] A. Bajtarevic *et al.*, “Noninvasive detection of lung cancer by analysis of exhaled breath,” *BMC Cancer*, vol. 9, no. 1, p. 348, Dec. 2009, doi: 10.1186/1471-2407-9-348.

[49] C. Benson, C. Dimopoulos, C. Argyropoulos, C. Varianou Mikellidou, and G. Boustras, “Assessing the common occupational health hazards and their health risks among oil and gas workers,” *Saf. Sci.*, vol. 140, p. 105284, Aug. 2021, doi: 10.1016/j.ssci.2021.105284.

[50] S. Liu, E. N. K. Nkrumah, L. S. Akoto, E. Gyabeng, and E. Nkrumah, “The state of occupational health and safety management frameworks (OHSMF) and occupational injuries and accidents in the Ghanaian oil and gas industry: Assessing the mediating role of safety knowledge,” *BioMed Res. Int.*, vol. 2020, 2020.

[51] R. Z. Witter, L. Tenney, S. Clark, and L. S. Newman, "Occupational exposures in the oil and gas extraction industry: State of the science and research recommendations," *Am. J. Ind. Med.*, vol. 57, no. 7, pp. 847–856, 2014.

[52] M. F. Milazzo, G. Ancione, and R. Lisi, "Emissions of volatile organic compounds during the ship-loading of petroleum products: Dispersion modelling and environmental concerns," *J. Environ. Manage.*, vol. 204, pp. 637–650, Dec. 2017, doi: 10.1016/j.jenvman.2017.09.045.

[53] H. Rajabi, M. Hadi Mosleh, P. Mandal, A. Lea-Langton, and M. Sedighi, "Emissions of volatile organic compounds from crude oil processing – Global emission inventory and environmental release," *Sci. Total Environ.*, vol. 727, p. 138654, Jul. 2020, doi: 10.1016/j.scitotenv.2020.138654.

[54] P. S. Rao, M. F. Ansari, A. G. Gavane, V. I. Pandit, P. Nema, and S. Devotta, "Seasonal variation of toxic benzene emissions in petroleum refinery," *Environ. Monit. Assess.*, vol. 128, pp. 323–328, 2007.

[55] M. Aksoy, K. Dinçol, Ş. Erdem, and G. Dinçol, "Acute leukemia due to chronic exposure to benzene," *Am. J. Med.*, vol. 52, no. 2, pp. 160–166, 1972.

[56] P. Decoufle, W. A. Blattner, and A. Blair, "Mortality among chemical workers exposed to benzene and other agents," *Environ. Res.*, vol. 30, no. 1, pp. 16–25, 1983.

[57] P. Infante, J. Wagoner, R. Rinsky, and R. Young, "Leukaemia in benzene workers," *The Lancet*, vol. 310, no. 8028, pp. 76–78, 1977.

[58] D. Loomis *et al.*, "Carcinogenicity of benzene," *Lancet Oncol.*, vol. 18, no. 12, pp. 1574–1575, Dec. 2017, doi: 10.1016/S1470-2045(17)30832-X.

[59] M. A. Mehlman, "Dangerous and cancer-causing properties of products and chemicals in the oil refining and petrochemical industry: VIII. Health effects of motor fuels: carcinogenicity of gasoline—scientific update," *Environ. Res.*, vol. 59, no. 1, pp. 238–249, 1992.

[60] "Ethylbenzene (IARC Summary & Evaluation, Volume 77, 2000)." Accessed: Mar. 31, 2024. [Online]. Available: https://www.inchem.org/documents/iarc/vol77/77-05.html

[61] J. Taylor, *Toxicological profile for ethylbenzene*. US Department of Health & Human Services, Public Health Service, Agency for …, 2010 [Online].

[62] C. dinuoscio, "XYLENE (ALL ISOMERS)," ACGIH. Accessed: Mar. 31, 2024. [Online]. Available: https://www.acgih.org/xylene-all-isomers/

[63] M. Fay, J. Risher, and J. D. Wilson, "Toxicological profile for xylene," 2007, [Online].Available: https://stacks.cdc.gov/view/cdc/6958

[64] F. Gamberale, G. Annwall, and M. Hultengren, "Exposure to xylene and ethylbenzene: III. Effects on central nervous functions," *Scand. J. Work. Environ. Health*, pp. 204–211, 1978.

[65] S. T. Rajan and N. Malathi, "Health hazards of xylene: a literature review," *J. Clin. Diagn. Res. JCDR*, vol. 8, no. 2, p. 271, 2014.

[66] N. Barros *et al.*, "Environmental and biological monitoring of benzene, toluene, ethylbenzene and xylene (BTEX) exposure in residents living near gas stations," *J. Toxicol. Environ. Health A*, vol. 82, no. 9, pp. 550–563, May 2019, doi: 10.1080/15287394.2019.1634380.

[67] P. Amir-Heidari, H. Farahani, and M. Ebrahemzadih, "Risk assessment of oil and gas well drilling activities in Iran – a case study: human factors," *Int. J. Occup. Saf. Ergon.*, vol. 21, no. 3, pp. 276–283, Jul. 2015, doi: 10.1080/10803548.2015.1085162.

[68] D. A. Garcia-Gonzales, S. B. C. Shonkoff, J. Hays, and M. Jerrett, "Hazardous Air Pollutants Associated with Upstream Oil and Natural Gas Development: A Critical Synthesis of Current Peer-Reviewed Literature," *Annu. Rev. Public Health*, vol. 40, no. 1, pp. 283–304, Apr. 2019, doi: 10.1146/annurev-publhealth-040218-043715.

[69] R. Z. Witter, L. Tenney, S. Clark, and L. S. Newman, "Occupational exposures in the oil and gas extraction industry: State of the science and research recommendations," *Am. J. Ind. Med.*, vol. 57, no. 7, pp. 847–856, Jul. 2014, doi: 10.1002/ajim.22316.

[70] L. I. Silva, T. A. Rocha-Santos, and A. C. Duarte, "Remote optical fibre microsensor for monitoring BTEX in confined industrial atmospheres," *Talanta*, vol. 78, no. 2, pp. 548–552, 2009.

[71] T. Srebotnjak and M. Rotkin-Ellman, "Fracking fumes: Air pollution from hydraulic fracturing threatens public health and communities," *NRDC Issue Brief*, vol. 14, 2014,

[72] A. S. Akinyemi, *Green Completion as a mitigation for BTEX exposure in Gas flaring: Nigeria case study (Exposure assessment and Cost model)*. West Virginia University, 2020.

[73] J. N. Egwurugwu and A. Nwafor, "Prolonged exposure to oil and gas flares ups the risks for hypertension," *Am. J. Health Res.*, vol. 1, no. 3, pp. 65–72, 2013.

[74] C. O. Ehumadu and B. O. Ndekwu, "Soil Pollution Assessment of a Gas Flare Site in the Niger Delta Region," *Gas*, vol. 1, p. 2, 2021.

[75] F. Leusch and M. Bartkow, *A short primer on Benzene, Toluene, Ethylbenzene and Zylenes (BTEX) in the Environment and in Hydraulic Fracturing Fluids*. Griffith University, 2010.

[76] N. M. A. Al-Rawhani, V. Alekhin, and L. Poluyan, "Risk assessment of storage tanks in the oil and gas industry," *E3S Web Conf.*, vol. 474, p. 01059, 2024, doi: 10.1051/e3sconf/202447401059.

[77] M. Kamel and K. Al Shehhi, "VOC Recovery System for Crude Oil Tanker Loading," in *Abu Dhabi International Petroleum Exhibition and Conference*, SPE, 2022, p. D041S119R002. Accessed: Mar. 31, 2024. [Online]. Available: https://onepetro.org/SPEADIP/proceedings-abstract/22ADIP/4-22ADIP/513477

[78] M. F. Milazzo, G. Ancione, and R. Lisi, "Emissions of volatile organic compounds during the ship-loading of petroleum products: Dispersion modelling and environmental concerns," *J. Environ. Manage.*, vol. 204, pp. 637–650, 2017.

[79] V. Pshenin, N. Zaripova, and K. Zaynetdinov, "Modeling of the crude oil (or petroleum products) vapor displacement during rail tanks loading," *Pet. Sci. Technol.*, vol. 37, no. 24, pp. 2435–2440, Dec. 2019, doi: 10.1080/10916466.2019.1655442.

[80] M. Al-Jebouri, *A study on respiratory infections among oil refineries workers of Iraq*. 2012.

[81] M. A. Mehlman, "Dangerous and cancer-causing properties of products and chemicals in the oil refining and petrochemical industry," *Environ. Res.*, vol. 59, no. 1, pp. 238–249, Oct. 1992, doi: 10.1016/S0013-9351(05)80243-9.

[82] Z. Abdulhussein, Z. T. Al-sharify, and M. Alzuraiji, *Flow of crude oil in pipes and its environmental impact. A review*. 2023. doi: 10.1063/5.0150151.

[83] P. Kumari, G. Garg, D. Soni, and S. Aggarwal, "Measurement of benzene and other volatile organic compounds: implications for its inhalation health risk associated with the workers at a fuel station in Delhi," *Asian J. Atmospheric Environ.*, vol. 17, Jul. 2023, doi: 10.1007/s44273-023-00007-8.

[84] R. L. Morgan, P. Whaley, K. A. Thayer, and H. J. Schünemann, "Identifying the PECO: A framework for formulating good questions to explore the association of environmental and other exposures with health outcomes," *Environ. Int.*, vol. 121, pp. 1027–1031, Dec. 2018, doi: 10.1016/j.envint.2018.07.015.

[85] N. R. Haddaway, M. J. Page, C. C. Pritchard, and L. A. McGuinness, "PRISMA2020: An R package and Shiny app for producing PRISMA 2020-compliant flow diagrams, with interactivity for optimised digital transparency and Open Synthesis," *Campbell Syst. Rev.*, vol. 18, no. 2, p. e1230, 2022.

[86] A. A. Rooney, A. L. Boyles, M. S. Wolfe, J. R. Bucher, and K. A. Thayer, "Systematic Review and Evidence Integration for Literature-Based Environmental Health Science Assessments," *Environ. Health Perspect.*, vol. 122, no. 7, pp. 711–718, Jul. 2014, doi: 10.1289/ehp.1307972.

[87] OSHA, "Permissible Exposure Limits - Annotated Tables | Occupational Safety and Health Administration." [Online]. Available: https://www.osha.gov/annotated-pels

[88] ACGIH, "TLV/BEI Guidelines," ACGIH. [Online]. Available: https://www.acgih.org/science/tlv-bei-guidelines/

[89] NIOSH, "Pocket Guide to Chemical Hazards Introduction | NIOSH | CDC." [Online]. Available: https://www.cdc.gov/niosh/npg/pgintrod.html

[90] A. L. Rich and H. T. Orimoloye, "Elevated Atmospheric Levels of Benzene and Benzene-Related Compounds from Unconventional Shale Extraction and Processing: Human Health Concern for Residential Communities," *Environ. Health Insights*, vol. 10, p. EHI.S33314, Jan. 2016, doi: 10.4137/EHI.S33314.

[91] O. US EPA, "Risk Assessment Guidance for Superfund (RAGS): Part A." Accessed: Jul. 29, 2023. [Online]. Available: https://www.epa.gov/risk/risk-assessment-guidance-superfund-rags-part

[92] I. Molaei, S. M. Khezri, M. S. Sekhavatjou, A. Karbassi, and A. Hosseni Alhashemi, "Health risk assessment of heavy metals, BTEX and polycyclic aromatic hydrocarbons (PAHs) in the workplace in a secondary oil re-refining factory," *J. Adv. Environ. Health Res.*, vol. 8, no. 2, pp. 79–94, 2020.

[93] EPA, "Risk Assessment Guidance for Superfund Volume I: Human Health Evaluation Manual (Part F, Supplemental Guidance for Inhalation Risk

Assessment).” 2009. [Online]. Available: https://semspub.epa.gov/work/HQ/140530.pdf

[94] M. Al-Harbi, I. Alhajri, A. AlAwadhi, and J. K. Whalen, “Health symptoms associated with occupational exposure of gasoline station workers to BTEX compounds,” *Atmos. Environ.*, vol. 241, p. 117847, 2020.

[95] R. Tong, Y. Yang, G. Shao, Y. Zhang, S. Dou, and W. Jiang, “Emission sources and probabilistic health risk of volatile organic compounds emitted from production areas in a petrochemical refinery in Hainan, China,” *Hum. Ecol. Risk Assess. Int. J.*, vol. 26, no. 5, pp. 1407–1427, May 2020, doi: 10.1080/10807039.2019.1579049.

[96] Y. S. Huang and C. C. Hsieh, “VOC characteristics and sources at nine photochemical assessment monitoring stations in western Taiwan,” *Atmos. Environ.*, vol. 240, p. 117741, Nov. 2020, doi: 10.1016/j.atmosenv.2020.117741.

[97] I. Molaei, S. M. Khezri, M. S. Sekhavatjou, A. Karbassi, and A. Hosseni Alhashemi, “Health risk assessment of heavy metals, BTEX and polycyclic aromatic hydrocarbons (PAHs) in the workplace in a secondary oil re-refining factory,” *J. Adv. Environ. Health Res.*, vol. 8, no. 2, Apr. 2020, doi: 10.22102/jaehr.2020.212994.1153.

[98] R. Tong, Y. Yang, G. Shao, Y. Zhang, S. Dou, and W. Jiang, “Emission sources and probabilistic health risk of volatile organic compounds emitted from production areas in a petrochemical refinery in Hainan, China,” *Hum. Ecol. Risk Assess. Int. J.*, vol. 26, no. 5, pp. 1407–1427, May 2020, doi: 10.1080/10807039.2019.1579049.

[99] E. Partovi, M. Fathi, M. J. Assari, R. Esmaeili, A. Pourmohamadi, and R. Rahimpour, “Risk assessment of occupational exposure to BTEX in the National Oil Distribution Company in Iran.,” 2016.

[100] E. Yahyaei, B. Majlesi, Y. Pourbakhshi, S. Ghiyasi, M. J. Rastani, and M. Heidari, “Occupational exposure and risk assessment of formaldehyde in the pathology departments of hospitals,” *Asian Pac. J. Cancer Prev. APJCP*, vol. 21, no. 5, p. 1303, 2020.

[101] M. Kitwattanavong, T. Prueksasit, D. Morknoy, T. Tunsaringkarn, and W. Siriwong, “Health Risk Assessment of Petrol Station Workers in the Inner City of Bangkok, Thailand, to the Exposure to BTEX and Carbonyl Compounds by Inhalation,” *Hum. Ecol. Risk Assess. Int. J.*, vol. 19, no. 6, pp. 1424–1439, Nov. 2013, doi: 10.1080/10807039.2012.685814.

[102] I. Frausto-Vicencio, A. Moreno, H. Goldsmith, Y.-K. Hsu, and F. M. Hopkins, “Characterizing the performance of a compact btex gc-pid for near-real time analysis and field deployment,” *Sensors*, vol. 21, no. 6, p. 2095, 2021.

[103] C. L. Faiola, M. H. Erickson, V. L. Fricaud, B. T. Jobson, and T. M. VanReken, “Quantification of biogenic volatile organic compounds with a flame ionization detector using the effective carbon number concept,” *Atmospheric Meas. Tech.*, vol. 5, no. 8, pp. 1911–1923, 2012.

[104] L. F. da Silva *et al.*, “BTEX gas sensor based on hematite microrhombuses,” *Sens. Actuators B Chem.*, vol. 326, p. 128817, 2021.

[105] T. Sarkar and S. Srinives, "Electrochemically functionalized single-walled carbon nanotubes for ultrasensitive detection of BTEX vapors," *Microelectron. Eng.*, vol. 247, p. 111584, 2021.
[106] S. Stepina, A. Berzina, G. Sakale, and M. Knite, "BTEX detection with composites of ethylenevinyl acetate and nanostructured carbon," *Beilstein J. Nanotechnol.*, vol. 8, no. 1, pp. 982–988, 2017.
[107] D. Matatagui, F. A. Bahos, I. Gràcia, and M. del C. Horrillo, "Portable low-cost electronic nose based on surface acoustic wave sensors for the detection of BTX vapors in air," *Sensors*, vol. 19, no. 24, p. 5406, 2019.
[108] A. Iyer, V. Mitevska, J. Samuelson, S. Campbell, and V. R. Bhethanabotla, "Polymer–plasticizer coatings for BTEX detection using quartz crystal microbalance," *Sensors*, vol. 21, no. 16, p. 5667, 2021.
[109] R. St-Gelais *et al.*, "Gas sensing using polymer-functionalized deformable Fabry–Perot interferometers," *Sens. Actuators B Chem.*, vol. 182, pp. 45–52, 2013.
[110] M. El Kazzy *et al.*, "An overview of artificial olfaction systems with a focus on surface plasmon resonance for the analysis of volatile organic compounds," *Biosensors*, vol. 11, no. 8, p. 244, 2021.
[111] D. Kou, W. Ma, S. Zhang, R. Li, and Y. Zhang, "BTEX Vapor Detection with a Flexible MOF and Functional Polymer by Means of a Composite Photonic Crystal," *ACS Appl. Mater. Interfaces*, vol. 12, no. 10, pp. 11955–11964, Mar. 2020, doi: 10.1021/acsami.9b22033.
[112] S. Khan, D. Newport, and S. Le Calvé, "A sensitive and portable deep-UV absorbance detector with a microliter gas cell compatible with micro GC," *Chemosensors*, vol. 9, no. 4, p. 63, 2021.
[113] R. Nasreddine, V. Person, C. A. Serra, and S. Le Calvé, "Development of a novel portable miniaturized GC for near real-time low level detection of BTEX," *Sens. Actuators B Chem.*, vol. 224, pp. 159–169, 2016.
[114] Y.-C. Hsieh and D.-J. Yao, "Intelligent gas-sensing systems and their applications," *J. Micromechanics Microengineering*, vol. 28, no. 9, p. 093001, Jun. 2018, doi: 10.1088/1361-6439/aac849.
[115] S. Y. Park, Y. Kim, T. Kim, T. H. Eom, S. Y. Kim, and H. W. Jang, "Chemoresistive materials for electronic nose: Progress, perspectives, and challenges," *InfoMat*, vol. 1, no. 3, pp. 289–316, Sep. 2019, doi: 10.1002/inf2.12029.
[116] S. Fanget *et al.*, "Gas sensors based on gravimetric detection—A review," *Sens. Actuators B Chem.*, vol. 160, no. 1, pp. 804–821, Dec. 2011, doi: 10.1016/j.snb.2011.08.066.
[117] R. Bogue, "Detecting gases with light: A review of optical gas sensor technologies," *Sens. Rev.*, vol. 35, no. 2, pp. 133–140, 2015.
[118] L. M. McKenzie, R. Z. Witter, L. S. Newman, and J. L. Adgate, "Human health risk assessment of air emissions from development of unconventional natural gas resources," *Sci. Total Environ.*, vol. 424, pp. 79–87, May 2012, doi: 10.1016/j.scitotenv.2012.02.018.
[119] J. B. Gilman, B. M. Lerner, W. C. Kuster, and J. A. De Gouw, "Source Signature of Volatile Organic Compounds from Oil and Natural Gas

Operations in Northeastern Colorado," *Environ. Sci. Technol.*, vol. 47, no. 3, pp. 1297–1305, Feb. 2013, doi: 10.1021/es304119a.

[120] T. Colborn, K. Schultz, L. Herrick, and C. Kwiatkowski, "An Exploratory Study of Air Quality Near Natural Gas Operations," *Hum. Ecol. Risk Assess. Int. J.*, vol. 20, no. 1, pp. 86–105, Jan. 2014, doi: 10.1080/10807039.2012.749447.

[121] N. Ramírez, A. Cuadras, E. Rovira, F. Borrull, and R. M. Marcé, "Chronic risk assessment of exposure to volatile organic compounds in the atmosphere near the largest Mediterranean industrial site," *Environ. Int.*, vol. 39, no. 1, pp. 200–209, Feb. 2012, doi: 10.1016/j.envint.2011.11.002.

[122] N. Ramírez, A. Cuadras, E. Rovira, F. Borrull, and R. M. Marcé, "Chronic risk assessment of exposure to volatile organic compounds in the atmosphere near the largest Mediterranean industrial site," *Environ. Int.*, vol. 39, no. 1, pp. 200–209, 2012.

[123] R. Moolla, C. J. Curtis, and J. Knight, "Assessment of occupational exposure to BTEX compounds at a bus diesel-refueling bay: A case study in Johannesburg, South Africa," *Sci. Total Environ.*, vol. 537, pp. 51–57, 2015.

[124] R. Moolla, C. J. Curtis, and J. Knight, "Assessment of occupational exposure to BTEX compounds at a bus diesel-refueling bay: A case study in Johannesburg, South Africa," *Sci. Total Environ.*, vol. 537, pp. 51–57, 2015.

[125] M. A. Mirrezaei and A. A. Orkomi, "Gas flares contribution in total health risk assessment of BTEX in Asalouyeh, Iran," *Process Saf. Environ. Prot.*, vol. 137, pp. 223–237, May 2020, doi: 10.1016/j.psep.2020.02.034.

[126] M. A. Mirrezaei and A. A. Orkomi, "Gas flares contribution in total health risk assessment of BTEX in Asalouyeh, Iran," *Process Saf. Environ. Prot.*, vol. 137, pp. 223–237, 2020.

[127] T. Chen *et al.*, "Volatile organic compounds and ozone air pollution in an oil production region in northern China," *Atmospheric Chem. Phys.*, vol. 20, no. 11, pp. 7069–7086, Jun. 2020, doi: 10.5194/acp-20-7069-2020.

[128] H. Zheng *et al.*, "Monitoring of volatile organic compounds (VOCs) from an oil and gas station in northwest China for 1 year," *Atmospheric Chem. Phys.*, vol. 18, no. 7, pp. 4567–4595, Apr. 2018, doi: 10.5194/acp-18-4567-2018.

[129] S. Jalilian, S. Sabzalipour, M. Mohammadi Rouzbahani, E. Rajabzadeh Ghatrami, and L. Ibrahimy Ghavamabadi, "Health Risk Assessment of Occupational Exposure of Refinery Unit Site Workers to BTEX in an Oil Refinery Company," *J. Health Sci. Surveill. Syst.*, vol. 10, no. 1, Jan. 2022, doi: 10.30476/jhsss.2021.90475.1193.

[130] S. Chaiklieng, P. Suggaravetsiri, and H. Autrup, "Risk assessment on benzene exposure among gasoline station workers," *Int. J. Environ. Res. Public. Health*, vol. 16, no. 14, p. 2545, 2019.

[131] S. Chaiklieng, "Risk assessment of workers' exposure to BTEX and hazardous area classification at gasoline stations," *PloS One*, vol. 16, no. 4, p. e0249913, 2021.

[132] B. Heibati *et al.*, "BTEX exposure assessment and quantitative risk assessment among petroleum product distributors," *Ecotoxicol. Environ. Saf.*, vol. 144, pp. 445–449, 2017.

[133] Z. Yousefi, A. Allahabady, R. A. Mohammadpour, and Z. Sharif, "Measurement of BTEX (benzene, toluene, ethylbenzene and xylene) concentration at gas," Mar. 2022, doi: 10.34172/EHEM.2022.04.

[134] B. Harati, S. J. Shahtaheri, H. A. Yousefi, A. Harati, A. Askari, and N. Abdolmohamadi, "Cancer risk assessment for workers exposed to pollution source, a petrochemical company, Iran," *Iran. J. Public Health*, vol. 49, no. 7, p. 1330, 2020.

[135] M. Alimohammadi, A. Behbahaninia, M. Farahani, and S. Motahari, "Carcinogenic and Health Risk Assessment of Respiratory Exposure to BTEX Compounds in Gasoline Refueling Stations in Karaj–Iran," *Pollution*, vol. 9, no. 2, pp. 726–744, 2023.

[136] A. H. Khoshakhlagh, S. Yazdanirad, M. Mousavi, A. Gruszecka-Kosowska, M. Shahriyari, and H. Rajabi-Vardanjani, "Summer and winter variations of BTEX concentrations in an oil refinery complex and health risk assessment based on Monte-Carlo simulations," *Sci. Rep.*, vol. 13, no. 1, p. 10670, 2023.

[137] A. J. McMichael, "Carcinogenicity of benzene, toluene and xylene: epidemiological and experimental evidence," *IARC Sci. Publ.*, no. 85, pp. 3–18, 1988.

[138] S. Ziaei Seginsara and L. Khazini, "Experimental study of emitted volatile organic pollutants from wastewater treatment ponds in oil refineries," *J. Water Wastewater Ab Va Fazilab Persian*, vol. 33, no. 2, pp. 49–61, 2022.

[139] F. E. Nyieku, F. T. Kabutey, S. K. Kyei, H. M. Essandoh, F. A. Armah, and E. Awuah, "Oilfield produced water and constructed wetlands technology: a comprehensive review," *Water Reuse*, vol. 14, no. 4, pp. 481–509, 2024.

[140] M. Nasiri, I. Jafari, and B. Parniankhoy, "Oil and Gas Produced Water Management: A Review of Treatment Technologies, Challenges, and Opportunities," *Chem. Eng. Commun.*, vol. 204, no. 8, pp. 990–1005, Aug. 2017, doi: 10.1080/00986445.2017.1330747.

[141] F. Nath, M. O. S. Chowdhury, and M. M. Rhaman, "Navigating produced water sustainability in the oil and gas sector: A Critical review of reuse challenges, treatment technologies, and prospects ahead," *Water*, vol. 15, no. 23, p. 4088, 2023.

[142] H. Al-Mebayedh, A. Niu, and C. Lin, "Petroleum hydrocarbon composition of oily sludge and contaminated soils in a decommissioned oilfield waste pit under desert conditions," *Appl. Sci.*, vol. 12, no. 3, p. 1355, 2022.

[143] V. L. Penuelas and D. D. Lo, "Burn pit exposure in military personnel and the potential resulting lung and neurological pathologies," *Front. Environ. Health*, vol. 3, p. 1364812, 2024.

[144] S. R. Woskie, A. Bello, C. Rennix, L. Jiang, A. N. Trivedi, and D. A. Savitz, "Burn pit exposure assessment to support a cohort study of US veterans of the wars in Iraq and Afghanistan," *J. Occup. Environ. Med.*, vol. 65, no. 6, pp. 449–457, 2023.

[145] S. Chaiklieng, "Risk assessment of workers' exposure to BTEX and hazardous area classification at gasoline stations," *PLOS ONE*, vol. 16, no. 4, p. e0249913, Apr. 2021, doi: 10.1371/journal.pone.0249913.

[146] M. Kitwattanavong, T. Prueksasit, D. Morknoy, T. Tunsaringkarn, and W. Siriwong, "Health Risk Assessment of Petrol Station Workers in the Inner

City of Bangkok, Thailand, to the Exposure to BTEX and Carbonyl Compounds by Inhalation," *Hum. Ecol. Risk Assess. Int. J.*, vol. 19, no. 6, pp. 1424–1439, Nov. 2013, doi: 10.1080/10807039.2012.685814.

[147] E. Partovi, M. Fathi, M. J. Assari, R. Esmaeili, A. Pourmohamadi, and R. Rahimpour, "Risk assessment of occupational exposure to BTEX in the National Oil Distribution Company in Iran," *Chronic Dis. J.*, vol. 4, no. 2, Feb. 2018, doi: 10.22122/cdj.v4i2.223.

[148] T. Tunsaringkarn *et al.*, "Cancer risk analysis of benzene, formaldehyde and acetaldehyde on gasoline station workers," *J. Environ. Eng. Ecol. Sci.*, vol. 1, no. 1, p. 1, 2012, doi: 10.7243/2050-1323-1-1.

[149] M. Al-Harbi, I. Alhajri, A. AlAwadhi, and J. K. Whalen, "Health symptoms associated with occupational exposure of gasoline station workers to BTEX compounds," *Atmos. Environ.*, vol. 241, p. 117847, 2020.

[150] M. Akerstrom, P. Almerud, E. Andersson, B. Strandberg, and G. Sällsten, "Personal exposure to benzene and 1,3-butadiene during petroleum refinery turnarounds and work in the oil harbour," *Int. Arch. Occup. Environ. Health*, vol. 89, Nov. 2016, doi: 10.1007/s00420-016-1163-1.

[151] A. Thetkathuek, C. Polyong, and W. Jaidee, "Benzene health risk assessment for neurological disorders of gas station employees in Rayong Province, Thailand," *Rocz. Panstw. Zakl. Hig.*, vol. 74, pp. 231–241, Jun. 2023, doi: 10.32394/rpzh.2023.0262.

[152] P. Matatiele, B. Dabula, and B. Kgarebe, *An assessment of exposure to benzene, toluene and xylene in a group of South African petroleum refinery workers.* 2021. doi: 10.21203/rs.3.rs-968320/v1.

[153] H. Ridderseth *et al.*, "Occupational Benzene Exposure in the Norwegian Offshore Petroleum Industry, 2002-2018," *Ann. Work Expo. Health*, vol. 66, May 2022, doi: 10.1093/annweh/wxac022.

[154] S. Mousavi and S. Yazdanirad, "A Survey of Neurobehavioral Symptoms among Operational Workers Exposed to Mixture of an Organic Solvent (BTEX): a case study in an oil refinery," *Pak. J. Med. Health Sci.*, vol. 13, pp. 577–581, Jun. 2019.

[155] S. Jalilian, S. Alipour, M. Roozbahani, E. Ghatrami, and L. Ghavamabadi, "Assessing the effect of BTEX on blood and spirometry parameters staff in a petroleum refinery," *Front. Public Health*, vol. 10, Nov. 2022, doi: 10.3389/fpubh.2022.1037413.

[156] N. Elshaer, B. Daoud, N. Foda, H. Mannaa, and E. Hussain, "Evaluation of Oxidative Stress among Petroleum Workers Exposed to Benzene, Toluene, Ethylbenzene, and Xylene in Alexandria, Egypt," *Evaluation*, vol. 45, no. 07, 2022.

[157] B. R. Geraldino *et al.*, "Evaluation of exposure to toluene and xylene in gasoline station workers," *Adv. Prev. Med.*, vol. 2021, 2021,

[158] Y. Zhang *et al.*, "The Dose-Effect and Risk Assessment on Lung Function Decline of Long-Term Co-Exposure to BTEXS in Petrochemical Workers in Southern China", [preprint]

[159] M. Moridzadeh, S. Dehghani, A. Rafiee, M. S. Hassanvand, M. Dehghani, and M. Hoseini, "Assessing BTEX exposure among workers of the second largest natural gas reserve in the world: a biomonitoring approach," *Environ.*

Sci. Pollut. Res., vol. 27, no. 35, pp. 44519–44527, Dec. 2020, doi: 10.1007/s11356-020-10379-x.

[160] S. Orecchio, M. Fiore, S. Barreca, and G. Vara, "Volatile profiles of emissions from different activities analyzed using canister samplers and gas chromatography-mass spectrometry (GC/MS) analysis: A case study," *Int. J. Environ. Res. Public. Health*, vol. 14, no. 2, p. 195, 2017.

[161] N. Baimatova, B. Kenessov, J. A. Koziel, L. Carlsen, M. Bektassov, and O. P. Demyanenko, "Simple and accurate quantification of BTEX in ambient air by SPME and GC–MS," *Talanta*, vol. 154, pp. 46–52, 2016.

[162] H. H. A. Hamid, M. S. M. Nadzir, K. E. Lee, A. Ayatillah, M. T. Latif, and M. Othman, "Indoor level of BTEX and health risk assessment at science laboratories in a university," in *IOP Conference Series: Earth and Environmental Science*, IOP Publishing, 2023, p. 012086.

[163] G. Coelho Rezende, S. Le Calvé, J. J. Brandner, and D. Newport, "Micro photoionization detectors," *Sens. Actuators B Chem.*, vol. 287, pp. 86–94, May 2019, doi: 10.1016/j.snb.2019.01.072.

[164] R. Nasreddine, V. Person, C. A. Serra, and S. Le Calvé, "Development of a novel portable miniaturized GC for near real-time low level detection of BTEX," *Sens. Actuators B Chem.*, vol. 224, pp. 159–169, Mar. 2016, doi: 10.1016/j.snb.2015.09.077.

[165] M. Moufid, B. Bouchikhi, C. Tiebe, M. Bartholmai, and N. El Bari, "Assessment of outdoor odor emissions from polluted sites using simultaneous thermal desorption-gas chromatography-mass spectrometry (TD-GC-MS), electronic nose in conjunction with advanced multivariate statistical approaches," *Atmos. Environ.*, vol. 256, p. 118449, Jul. 2021, doi: 10.1016/j.atmosenv.2021.118449.

[166] C. Han *et al.*, "Pollution profiles of volatile organic compounds from different urban functional areas in Guangzhou China based on GC/MS and PTR-TOF-MS: Atmospheric environmental implications," *Atmos. Environ.*, vol. 214, p. 116843, Oct. 2019, doi: 10.1016/j.atmosenv.2019.116843.

[167] W. Wojnowski, K. Kalinowska, J. Gębicki, and B. Zabiega\la, "Monitoring the BTEX volatiles during 3D printing with acrylonitrile butadiene styrene (ABS) using electronic nose and proton transfer reaction mass spectrometry," *Sensors*, vol. 20, no. 19, p. 5531, 2020.

[168] A. Favard, T. Contaret, K. Aguir, A. Dumas, and M. Bendahan, "Highly sensitive WO3 thin films integrated on microsensor platforms for ppb BTEX detection in a gas mixture with high rate of humidity," in *2017 IEEE SENSORS*, Glasgow: IEEE, Oct. 2017, pp. 1–3. doi: 10.1109/ICSENS.2017.8234314.

[169] A. D. Rushi, K. P. Datta, P. S. Ghosh, A. Mulchandani, and M. D. Shirsat, "Selective Discrimination among Benzene, Toluene, and Xylene: Probing Metalloporphyrin-Functionalized Single-Walled Carbon Nanotube-Based Field Effect Transistors," *J. Phys. Chem. C*, vol. 118, no. 41, pp. 24034–24041, Oct. 2014, doi: 10.1021/jp504657c.

[170] TGS 822, "TGS 822 - for the detection of Organic Solvent Vapors." [Online]. Available: https://datasheetspdf.com/pdf-file/789388/Figaro/TGS822/1

[171] Unitec SENS-IT, "Sens-It Thick Film Solid State Sensors for Environmental Air Quality Monitoring, UNITEC s.r.l., VIA A. VOLTA, 25/B, 35030 VEGGIANO (PD)—ITALY." [Online]. Available: http://www.unitec-srl.com/site/wpcontent/uploads/2015/04/SENS-IT-Datasheet.pdf

[172] Y. Wang *et al.*, "Fast recognition of trace volatile compounds with a nanoporous dyes-based colorimetric sensor array," *Talanta*, vol. 192, pp. 407–417, Jan. 2019, doi: 10.1016/j.talanta.2018.09.028.

[173] D. Matatagui, F. A. Bahos, I. Gràcia, and M. del C. Horrillo, "Portable low-cost electronic nose based on surface acoustic wave sensors for the detection of BTX vapors in air," *Sensors*, vol. 19, no. 24, p. 5406, 2019.

[174] C. Viespe and D. Miu, "Characteristics of Surface Acoustic Wave Sensors with Nanoparticles Embedded in Polymer Sensitive Layers for VOC Detection," *Sensors*, vol. 18, no. 7, p. 2401, Jul. 2018, doi: 10.3390/s18072401.

[175] A. Das, B. Lal, and R. Manjunatha, "Advances in Gravimetric Electronic Nose for Biomarkers Detection," *Ser. Biomech.*, vol. 36, no. 2, Jun. 2022, doi: 10.7546/SB.36.2022.02.13.

[176] Rianjanu, Hasanah, Nugroho, Kusumaatmaja, Roto, and Triyana, "Polyvinyl Acetate Film-Based Quartz Crystal Microbalance for the Detection of Benzene, Toluene, and Xylene Vapors in Air," *Chemosensors*, vol. 7, no. 2, p. 20, Apr. 2019, doi: 10.3390/chemosensors7020020.

[177] S. Camou, T. Horiuchi, and T. Haga, "Ppb Level Benzene Gas Detection by Portable BTX Sensor Based on Integrated Hollow Fiber Detection Cell," in *2006 5th IEEE Conference on Sensors*, Daegu: IEEE, Oct. 2006, pp. 235–238. doi: 10.1109/ICSENS.2007.355765.

[178] C. Hou *et al.*, "Discrimination of Lung Cancer Related Volatile Organic Compounds with a Colorimetric Sensor Array," *Anal. Lett.*, vol. 46, no. 13, pp. 2048–2059, Sep. 2013, doi: 10.1080/00032719.2013.782550.

[179] N. Kari *et al.*, "Sensing behavior of metal-free porphyrin and Zinc phthalocyanine thin film towards Xylene-Styrene and HCl vapors in planar optical waveguide," *Nanomaterials*, vol. 11, no. 7, p. 1634, 2021.

[180] L. Silva, T. Rocha-Santos, and A. Duarte, "Remote optical fibre microsensor for monitoring BTEX in confined industrial atmospheres," *Talanta*, vol. 78, pp. 548–52, May 2009, doi: 10.1016/j.talanta.2008.12.011.

[181] R. St-Gelais *et al.*, "Gas sensing using polymer-functionalized deformable Fabry–Perot interferometers," *Sens. Actuators B Chem.*, vol. 182, pp. 45–52, 2013.

[182] I. Lara-Ibeas, A. R. Cuevas, and S. Le Calvé, "Recent developments and trends in miniaturized gas preconcentrators for portable gas chromatography systems: A review," *Sens. Actuators B Chem.*, vol. 346, p. 130449, 2021.

[183] A. Rodríguez-Cuevas, I. Lara-Ibeas, A. Leprince, M. Wolf, and S. Le Calvé, "Easy-to-manufacture micro gas preconcentrator integrated in a portable GC for enhanced trace detection of BTEX," *Sens. Actuators B Chem.*, vol. 324, p. 128690, 2020.

[184] S. Zampolli *et al.*, "Real-time monitoring of sub-ppb concentrations of aromatic volatiles with a MEMS-enabled miniaturized gas-chromatograph," *Sens. Actuators B Chem.*, vol. 141, no. 1, pp. 322–328, 2009.

[185] A. Bahrami, H. Mahjub, M. Sadeghian, and F. Golbabaei, "Determination of benzene, toluene and xylene (BTX) concentrations in air using HPLC developed method compared to gas chromatography," 2011.

[186] D. J. DiScenza, L. E. Intravaia, A. Healy, S. B. Dubrawski, and M. Levine, "Fluorescence-Based Detection of Benzene, Toluene, Ethylbenzene, Xylene, and Cumene (BTEXC) Compounds in Fuel-Contaminated Snow Environments," *Chemosensors*, vol. 7, no. 1, p. 5, 2019.

[187] C. Xia, S. Zhang, D. Sun, B. Jiang, W. Wang, and X. Xin, "Coassembly of Mixed Weakley-Type Polyoxometalates to Novel Nanoflowers with Tunable Fluorescence for the Detection of Toluene," *Langmuir*, vol. 34, no. 22, pp. 6367–6375, Jun. 2018, doi: 10.1021/acs.langmuir.8b00283.

[188] E. Subramanian, P. Santhanamari, and C. Murugan, "Sensor Functionality of Conducting Polyaniline-Metal Oxide (TiO2/SnO2) Hybrid Materials Films toward Benzene and Toluene Vapors at Room Temperature," *J. Electron. Mater.*, vol. 47, no. 8, pp. 4764–4771, Aug. 2018, doi: 10.1007/s11664-018-6338-y.

[189] P. B. Shinde and U. D. Shiurkar, "MEMS for detection of environmental pollutants: A review pertains to sensors over a couple of decades in 21st century," *Mater. Today Proc.*, vol. 44, pp. 615–624, 2021.

[190] H. Li *et al.*, "Mesoporous SnO2 sensor prepared by carbon nanotubes as template and its sensing properties to indoor air pollutants," *Procedia Eng.*, vol. 7, pp. 172–178, 2010.

[191] F. Zhang, X. Wang, J. Dong, N. Qin, and J. Xu, "Selective BTEX sensor based on a SnO2/V2O5 composite," *Sens. Actuators B Chem.*, vol. 186, pp. 126–131, 2013.

[192] C. R. Young *et al.*, "Infrared Hollow Waveguide Sensors for Simultaneous Gas Phase Detection of Benzene, Toluene, and Xylenes in Field Environments," *Anal. Chem.*, vol. 83, no. 16, pp. 6141–6147, Aug. 2011, doi: 10.1021/ac1031034.

[193] M. Girschikofsky, M. Rosenberger, S. Belle, M. Brutschy, S. R. Waldvogel, and R. Hellmann, "Optical planar Bragg grating sensor for real-time detection of benzene, toluene and xylene in solvent vapour," *Sens. Actuators B Chem.*, vol. 171, pp. 338–342, 2012.

[194] A. Atif *et al.*, "Volatile organic compounds: classification, sampling, extraction, analysis and health impacts," *Pharm Chem J*, vol. 4, pp. 52–65, 2017.

[195] S. Orecchio, M. Fiore, S. Barreca, and G. Vara, "Volatile profiles of emissions from different activities analyzed using canister samplers and gas chromatography-mass spectrometry (GC/MS) analysis: A case study," *Int. J. Environ. Res. Public. Health*, vol. 14, no. 2, p. 195, 2017.

[196] J. Cao, S. Wang, J. Li, Y. Xing, X. Zhao, and D. Li, "Porous nanosheets assembled Co3O4 hierarchical architectures for enhanced BTX (Benzene, Toluene and Xylene) gas detection," *Sens. Actuators B Chem.*, vol. 315, p. 128120, 2020.

[197] Z. Shen, X. Zhang, X. Ma, R. Mi, Y. Chen, and S. Ruan, "The significant improvement for BTX (benzene, toluene and xylene) sensing performance

based on Au-decorated hierarchical ZnO porous rose-like architectures," *Sens. Actuators B Chem.*, vol. 262, pp. 86–94, 2018.

[198] Y. Kang, K. Kim, B. Cho, Y. Kwak, and J. Kim, "Highly Sensitive Detection of Benzene, Toluene, and Xylene Based on CoPP-Functionalized TiO 2 Nanoparticles with Low Power Consumption," *ACS Sens.*, vol. 5, no. 3, pp. 754–763, Mar. 2020, doi: 10.1021/acssensors.9b02310.

[199] H. Li *et al.*, "Mesoporous SnO2 sensor prepared by carbon nanotubes as template and its sensing properties to indoor air pollutants," *Procedia Eng.*, vol. 7, pp. 172–178, 2010.

[200] F. Zhang, X. Wang, J. Dong, N. Qin, and J. Xu, "Selective BTEX sensor based on a SnO2/V2O5 composite," *Sens. Actuators B Chem.*, vol. 186, pp. 126–131, 2013.

[201] L. Deng, X. Ding, D. Zeng, S. Zhang, and C. Xie, "High sensitivity and selectivity of C-Doped ${\backslashrm WO} _ {3} $ Gas sensors toward toluene and xylene," *IEEE Sens. J.*, vol. 12, no. 6, pp. 2209–2214, 2011.

[202] L. Wang *et al.*, "Superhydrophobic Polymerized *n* -Octadecylsilane Surface for BTEX Sensing and Stable Toluene/Water Selective Detection Based on QCM Sensor," *ACS Omega*, vol. 3, no. 2, pp. 2437–2443, Feb. 2018, doi: 10.1021/acsomega.8b00061.

[203] J. El Sabahy, J. Berthier, F. Ricoul, and V. Jousseaume, "Toward optimized SiOCH films for BTEX detection: Impact of chemical composition on toluene adsorption," *Sens. Actuators B Chem.*, vol. 258, pp. 628–636, 2018.

[204] R. Das, R. Bandyopadhyay, and P. Pramanik, "Efficient detection of volatile aromatic hydrocarbon using linseed oil–styrene–divinylbenzene copolymer coated quartz crystal microbalance," *RSC Adv.*, vol. 5, no. 73, pp. 59533–59540, 2015.

[205] R. Das, S. Biswas, R. Bandyopadhyay, and P. Pramanik, "Polymerized linseed oil coated quartz crystal microbalance for the detection of volatile organic vapours," *Sens. Actuators B Chem.*, vol. 185, pp. 293–300, 2013.

[206] A. Rianjanu, S. A. Hasanah, D. B. Nugroho, A. Kusumaatmaja, R. Roto, and K. Triyana, "Polyvinyl acetate film-based quartz crystal microbalance for the detection of benzene, toluene, and xylene vapors in air," *Chemosensors*, vol. 7, no. 2, p. 20, 2019.

[207] A. Mirmohseni and V. Hassanzadeh, "Application of polymer-coated quartz crystal microbalance (QCM) as a sensor for BTEX compounds vapors," *J. Appl. Polym. Sci.*, vol. 79, pp. 1062–1066, Feb. 2001, doi: 10.1002/1097-4628(20010207)79:6<1062::AID-APP90>3.0.CO;2-V.

[208] X. Wang, F. Cui, J. Lin, B. Ding, J. Yu, and S. S. Al-Deyab, "Functionalized nanoporous TiO2 fibers on quartz crystal microbalance platform for formaldehyde sensor," *Sens. Actuators B Chem.*, vol. 171–172, pp. 658–665, Aug. 2012, doi: 10.1016/j.snb.2012.05.050.

[209] W. Huang *et al.*, "Highly sensitive formaldehyde sensors based on polyvinylamine modified polyacrylonitrile nanofibers," *RSC Adv.*, vol. 3, no. 45, pp. 22994–23000, 2013.

[210] K. Triyana *et al.*, "A highly sensitive safrole sensor based on polyvinyl acetate (PVAc) nanofiber-coated QCM," *Sci. Rep.*, vol. 9, no. 1, p. 15407, 2019.

[211] A. Das and R. Manjunatha, "Optimization of QCM sensor for BTX detection," in *2023 IEEE 9th International Conference on Smart Instrumentation, Measurement and Applications (ICSIMA)*, Oct. 2023, pp. 225–229. doi: 10.1109/ICSIMA59853.2023.10373452.

[212] N. Debabhuti *et al.*, "Development of QCM sensor to detect α-terpinyl acetate in cardamom," *Sens. Actuators Phys.*, vol. 319, p. 112521, Mar. 2021, doi: 10.1016/j.sna.2020.112521.

[213] G. Sauerbrey, "Verwendung von Schwingquarzen zur Wägung dünner Schichten und zur Mikrowägung," *Z. Für Phys.*, vol. 155, no. 2, pp. 206–222, Apr. 1959, doi: 10.1007/BF01337937.

[214] A. Rianjanu, S. A. Hasanah, D. B. Nugroho, A. Kusumaatmaja, R. Roto, and K. Triyana, "Polyvinyl Acetate Film-Based Quartz Crystal Microbalance for the Detection of Benzene, Toluene, and Xylene Vapors in Air," *Chemosensors*, vol. 7, no. 2, p. 20, Apr. 2019, doi: 10.3390/chemosensors7020020.

[215] T. Julian, S. N. Hidayat, A. Rianjanu, A. B. Dharmawan, H. S. Wasisto, and K. Triyana, "Intelligent Mobile Electronic Nose System Comprising a Hybrid Polymer-Functionalized Quartz Crystal Microbalance Sensor Array," *ACS Omega*, vol. 5, no. 45, pp. 29492–29503, Nov. 2020, doi: 10.1021/acsomega.0c04433.

[216] M. Ranjbar, N. T. Garavand, and S. M. Mahdavi, "Electroless plating of palladium on WO3 films for gasochromic applications," *Sol. Energy Mater. Sol. Cells*, vol. 94, no. 2, pp. 201–206, 2010.

[217] D. Li, G. Wu, G. Gao, J. Shen, and F. Huang, "Ultrafast Coloring-Bleaching Performance of Nanoporous WO $_3$ –SiO $_2$ Gasochromic Films Doped with Pd Catalyst," *ACS Appl. Mater. Interfaces*, vol. 3, no. 12, pp. 4573–4579, Dec. 2011, doi: 10.1021/am200781e.

[218] C. S. Prajapati and N. Bhat, "ppb level detection of NO2 using a WO3 thin film-based sensor: material optimization, device fabrication and packaging," *RSC Adv.*, vol. 8, no. 12, pp. 6590–6599, Feb. 2018, doi: 10.1039/C7RA13659E.

[219] M. He, L. Xie, X. Zhao, X. Hu, S. Li, and Z.-G. Zhu, "Highly sensitive and selective H2S gas sensors based on flower-like WO3/CuO composites operating at low/room temperature," *J. Alloys Compd.*, vol. 788, pp. 36–43, 2019.

[220] R. Godbole, S. Ameen, U. T. Nakate, M. S. Akhtar, and H.-S. Shin, "Low temperature HFCVD synthesis of tungsten oxide thin film for high response hydrogen gas sensor application," *Mater. Lett.*, vol. 254, pp. 398–401, 2019.

[221] M. Ahsan, T. Tesfamichael, M. Ionescu, J. Bell, and N. Motta, "Low temperature CO sensitive nanostructured WO3 thin films doped with Fe," *Sens. Actuators B Chem.*, vol. 162, no. 1, pp. 14–21, 2012.

[222] Y. Xu *et al.*, "Highly sensitive and selective detection of acetone based on platinum sensitized porous tungsten oxide nanospheres," *Sens. Actuators B Chem.*, vol. 307, p. 127616, 2020.

[223] K. Kanda and T. Maekawa, "Development of a WO3 thick-film-based sensor for the detection of VOC," *Sens. Actuators B Chem.*, vol. 108, no. 1, pp. 97–101, Jul. 2005, doi: 10.1016/j.snb.2005.01.038.

[224] A. Favard, T. Contaret, K. Aguir, A. Dumas, and M. Bendahan, "Highly sensitive WO 3 thin films integrated on microsensor platforms for ppb BTEX detection in a gas mixture with high rate of humidity," in *2017 IEEE SENSORS*, IEEE, 2017, pp. 1–3. Accessed: Oct. 04, 2024. [Online]. Available: https://ieeexplore.ieee.org/abstract/document/8234314/

[225] L. Zhu and W. Zeng, "Room-temperature gas sensing of ZnO-based gas sensor: A review," *Sens. Actuators Phys.*, vol. 267, pp. 242–261, 2017.

[226] A. Das, R. Manjunatha, K. N. Kumar, D. De, and R. Bandyopadhyay, "Fabrication of surface functionalized QCM sensor for BTX detection at ambient conditions," *Talanta*, vol. 283, p. 127081, 2025.

[227] A. D. Wilson and M. Baietto, "Applications and advances in electronic-nose technologies," *sensors*, vol. 9, no. 7, pp. 5099–5148, 2009.

[228] F. Fauzi, A. Rianjanu, I. Santoso, and K. Triyana, "Gas and humidity sensing with quartz crystal microbalance (QCM) coated with graphene-based materials–A mini review," *Sens. Actuators Phys.*, vol. 330, p. 112837, 2021.

[229] T. Kim and D. Kwak, "Flexible VOC sensors using conductive polymers and porous membranes for application to textiles," *Fibers Polym.*, vol. 13, no. 4, pp. 471–474, Apr. 2012, doi: 10.1007/s12221-012-0471-7.

[230] R. J. Ch, B. Shivamurthy, and S. B. Gowda, "Flexible linear low-density polyethylene laminated aluminum and nickel foil composite tapes for electromagnetic interference shielding," *Eng. Sci.*, vol. 21, no. 5, p. 777, 2022.

[231] S. Seethapathy, T. Górecki, and X. Li, "Passive sampling in environmental analysis," *J. Chromatogr. A*, vol. 1184, no. 1, pp. 234–253, Mar. 2008, doi: 10.1016/j.chroma.2007.07.070.

[232] J. G. Drobny, *Technology of fluoropolymers*. CRC Press, 2008.

[233] K. Triyana *et al.*, "A highly sensitive safrole sensor based on polyvinyl acetate (PVAc) nanofiber-coated QCM," *Sci. Rep.*, vol. 9, no. 1, p. 15407, Oct. 2019, doi: 10.1038/s41598-019-51851-0.

[234] M. Rahman, *Nanomaterials*. BoD–Books on Demand, 2011.

[235] T. Julian, S. N. Hidayat, A. Rianjanu, A. B. Dharmawan, H. S. Wasisto, and K. Triyana, "Intelligent Mobile Electronic Nose System Comprising a Hybrid Polymer-Functionalized Quartz Crystal Microbalance Sensor Array," *ACS Omega*, vol. 5, no. 45, pp. 29492–29503, Nov. 2020, doi: 10.1021/acsomega.0c04433.

[236] L. Yang, W. Xiao, J. Wang, X. Li, and L. Wang, "Adsorption and sensing properties of formaldehyde on chemically modified graphene surfaces," *Crystals*, vol. 12, no. 4, p. 553, 2022.

[237] B. Yang, P. Miao, and J. Cui, "Characteristics of amorphous WO3 thin films as anode materials for lithium-ion batteries," *J. Mater. Sci. Mater. Electron.*, vol. 31, no. 14, pp. 11071–11076, Jul. 2020, doi: 10.1007/s10854-020-03656-5.

[238] C. V. Ramana, A. K. Battu, P. Dubey, and G. A. Lopez, "Phase-Control-Enabled Enhancement in Hydrophilicity and Mechanical Toughness in Nanocrystalline Tungsten Oxide Films for Energy-Related Applications," *ACS Appl. Nano Mater.*, vol. 3, no. 4, pp. 3264–3274, Apr. 2020, doi: 10.1021/acsanm.9b02576.

[239] S. Hashemipour, M. R. Yaftian, H. Kalhor, and M. Ghanbari, "A study on the discrimination of xylene isomers vapors by quartz crystal microbalance sensors," *J. Iran. Chem. Soc.*, vol. 18, no. 4, pp. 751–763, Apr. 2021, doi: 10.1007/s13738-020-02064-0.

[240] N. Saadatkhah *et al.*, "Experimental methods in chemical engineering: Thermogravimetric analysis—TGA," *Can. J. Chem. Eng.*, vol. 98, no. 1, pp. 34–43, Jan. 2020, doi: 10.1002/cjce.23673.

[241] W. Xu, S. Li, N. Whitely, and W.-P. Pan, "Fundamentals of TGA and SDT," 2005, Accessed: Nov. 13, 2025. [Online]. Available: https://ruc.udc.es/bitstreams/cd8757e5-03fd-4bfe-931b-42201737996a/download

[242] D. Zhang *et al.*, "Highly sensitive BTEX sensors based on hexagonal WO3 nanosheets," *Sens. Actuators B Chem.*, vol. 293, pp. 23–30, 2019.

[243] A. Iyer, V. Mitevska, J. Samuelson, S. Campbell, and V. R. Bhethanabotla, "Polymer–plasticizer coatings for BTEX detection using quartz crystal microbalance," *Sensors*, vol. 21, no. 16, p. 5667, 2021.

[244] A. Mirmohseni and K. Rostamizadeh, "Quartz crystal nanobalance in conjunction with principal component analysis for identification of volatile organic compounds," *Sensors*, vol. 6, no. 4, pp. 324–334, 2006.

[245] A. Kumar *et al.*, "Tetra-tert-butyl copper phthalocyanine-based QCM sensor for toluene detection in air at room temperature," *Sens. Actuators B Chem.*, vol. 210, pp. 398–407, 2015.

[246] NIOSH "Benzene: Systemic Agent | NIOSH | CDC." .

[247] A. Das, B. S. Giri, and R. Manjunatha, "Systematic review on benzene, toluene, ethylbenzene, and xylene (BTEX) emissions; health impact assessment; and detection techniques in oil and natural gas operations," *Environ. Sci. Pollut. Res.*, vol. 32, no. 1, pp. 1–22, Dec. 2024, doi: 10.1007/s11356-024-35698-1.

[248] N. Baimatova, B. Kenessov, J. A. Koziel, L. Carlsen, M. Bektassov, and O. P. Demyanenko, "Simple and accurate quantification of BTEX in ambient air by SPME and GC–MS," *Talanta*, vol. 154, pp. 46–52, 2016.

[249] R. Nasreddine, V. Person, C. A. Serra, and S. Le Calvé, "Development of a novel portable miniaturized GC for near real-time low level detection of BTEX," *Sens. Actuators B Chem.*, vol. 224, pp. 159–169, 2016.

[250] A. Rodríguez-Cuevas, I. Lara-Ibeas, A. Leprince, M. Wolf, and S. Le Calvé, "Easy-to-manufacture micro gas preconcentrator integrated in a portable GC for enhanced trace detection of BTEX," *Sens. Actuators B Chem.*, vol. 324, p. 128690, 2020.

[251] D.-W. You, Y.-S. Seon, Y. Jang, J. Bang, J.-S. Oh, and K.-W. Jung, "A portable gas chromatograph for real-time monitoring of aromatic volatile organic compounds in air samples," *J. Chromatogr. A*, vol. 1625, p. 461267, 2020.

[252] S. Yang, J. Wickliffe, G. Kibelka, E. B. Overton, C. T. Lungu, and J. Oh, "Laboratory evaluation of a prototype portable gas chromatograph (GC) with a flame ionization detector (FID) for toluene, ethylbenzene, and xylenes (TEX) analysis," *J. Anal. Sci. Technol.*, vol. 14, no. 1, p. 36, Aug. 2023, doi: 10.1186/s40543-023-00404-2.

[253] J. G. Thangamani and S. K. Pasha, "Hydrothermal synthesis of copper (II) oxide-nanoparticles with highly enhanced BTEX gas sensing performance using chemiresistive sensor," *Chemosphere*, vol. 277, p. 130237, 2021.
[254] S. Khan, D. Newport, and S. Le Calvé, "Low-volume PEEK gas cell for BTEX detection using portable deep-UV absorption spectrophotometry," *Spectrochim. Acta. A. Mol. Biomol. Spectrosc.*, vol. 243, p. 118727, 2020.
[255] S. Khan, D. Newport, and S. Le Calvé, "A sensitive and portable deep-UV absorbance detector with a microliter gas cell compatible with micro GC," *Chemosensors*, vol. 9, no. 4, p. 63, 2021.
[256] T. Das and M. Mohar, "Development of a smartphone-based real time cost-effective VOC sensor," *Heliyon*, vol. 6, no. 10, 2020, Accessed: Sep. 09, 2024. [Online]. Available: https://www.cell.com/heliyon/fulltext/S2405-8440(20)32010-7
[257] D. Matatagui, F. A. Bahos, I. Gràcia, and M. del C. Horrillo, "Portable low-cost electronic nose based on surface acoustic wave sensors for the detection of BTX vapors in air," *Sensors*, vol. 19, no. 24, p. 5406, 2019.
[258] N. Debabhuti *et al.*, "A study of vegetable oil modified QCM sensor to detect β-pinene in Indian cardamom," *Talanta*, vol. 236, p. 122837, 2022.
[259] Q. Li, Y. Gu, and J. Jia, "Classification of multiple Chinese liquors by means of a QCM-based e-nose and MDS-SVM classifier," *Sensors*, vol. 17, no. 2, p. 272, 2017.
[260] A. Ozmen and E. Dogan, "Design of a Portable E-Nose Instrument for Gas Classifications," *IEEE Trans. Instrum. Meas.*, vol. 58, no. 10, pp. 3609–3618, Oct. 2009, doi: 10.1109/TIM.2009.2018695.
[261] Q. Li, Y. Gu, and N.-F. Wang, "Application of random forest classifier by means of a QCM-based e-nose in the identification of Chinese liquor flavors," *IEEE Sens. J.*, vol. 17, no. 6, pp. 1788–1794, 2017.
[262] S. Okur *et al.*, "Identification of mint scents using a QCM based e-nose," *Chemosensors*, vol. 9, no. 2, p. 31, 2021.
[263] N. Debabhuti *et al.*, "Discrimination of the maturity stages of Indian mango using QCM based electronic nose," in *2019 IEEE International Symposium on Olfaction and Electronic Nose (ISOEN)*, IEEE, 2019, pp. 1–2. Accessed: Dec. 05, 2024. [Online]. Available: https://ieeexplore.ieee.org/abstract/document/8823154/
[264] A. Das, P. R. Muduli, and R. Manjunatha, "QCM-Based Electronic Nose for Near Real-time BTEX Detection," *IEEE Trans. Instrum. Meas.*, pp. 1–1, 2025, doi: 10.1109/TIM.2025.3578708.
[265] A. Das and R. Manjunatha, "Optimization of QCM sensor for BTX detection," in *2023 IEEE 9th International Conference on Smart Instrumentation, Measurement and Applications (ICSIMA)*, IEEE, 2023, pp. 225–229. Accessed: Dec. 05, 2024. [Online]. Available: https://ieeexplore.ieee.org/abstract/document/10373452/
[266] R. Weber, "Correlation Analysis," in *The International Encyclopedia of Communication*, John Wiley & Sons, Ltd, 2008. doi: 10.1002/9781405186407.wbiecc148.
[267] K. P. Sinaga and M.-S. Yang, "Unsupervised K-means clustering algorithm," *IEEE Access*, vol. 8, pp. 80716–80727, 2020.

[268] T. Li, A. Rezaeipanah, and E. M. T. El Din, "An ensemble agglomerative hierarchical clustering algorithm based on clusters clustering technique and the novel similarity measurement," *J. King Saud Univ.-Comput. Inf. Sci.*, vol. 34, no. 6, pp. 3828–3842, 2022.

[269] S. Wierzchoń and M. Kłopotek, *Modern Algorithms of Cluster Analysis*, vol. 34. in Studies in Big Data, vol. 34. Cham: Springer International Publishing, 2018. doi: 10.1007/978-3-319-69308-8.

[270] E. Patel and D. S. Kushwaha, "Clustering cloud workloads: K-means vs gaussian mixture model," *Procedia Comput. Sci.*, vol. 171, pp. 158–167, 2020.

[271] M. S. Alam *et al.*, "Automatic human brain tumor detection in MRI image using template-based K means and improved fuzzy C means clustering algorithm," *Big Data Cogn. Comput.*, vol. 3, no. 2, p. 27, 2019.

[272] F. Ramadhani, M. Zarlis, and S. Suwilo, "Improve BIRCH algorithm for big data clustering," in *IOP conference series: materials science and engineering*, IOP Publishing, 2020, p. 012090. Accessed: Jun. 19, 2025. [Online]. Available: https://iopscience.iop.org/article/10.1088/1757-899X/725/1/012090/meta

[273] C. J. Davidson, J. H. Hannigan, and S. E. Bowen, "Effects of inhaled combined Benzene, Toluene, Ethylbenzene, and Xylenes (BTEX): Toward an environmental exposure model," *Environ. Toxicol. Pharmacol.*, vol. 81, p. 103518, 2021.

[274] N. Kumar *et al.*, "Volatile Organic Compounds (VOCs) in Ambient Air - A Case Study at the Vicinity of Fuel Filling Stations in New Delhi, India," presented at the 18th Asia Pacific Automotive Engineering Conference, SAE International, Mar. 2015. doi: 10.4271/2015-01-0055.

[275] P. Kumari, G. Garg, D. Soni, and S. G. Aggarwal, "Measurement of benzene and other volatile organic compounds: implications for its inhalation health risk associated with the workers at a fuel station in Delhi," *Asian J. Atmospheric Environ.*, vol. 17, no. 1, p. 7, Jul. 2023, doi: 10.1007/s44273-023-00007-8.

[276] S. Jayaraj and S. M. Shiva Nagendra, "Health risk assessment of workers' exposure to BTEX and PM during refueling in an urban fuel station," *Environ. Monit. Assess.*, vol. 195, no. 12, p. 1507, Dec. 2023, doi: 10.1007/s10661-023-12130-8.

[277] T. Tunsaringkarn, W. Siriwong, A. Rungsiyothin, and S. Nopparatbundit, "Occupational exposure of gasoline station workers to BTEX compounds in Bangkok, Thailand," 2012, Accessed: Nov. 20, 2024. [Online]. Available: https://www.sid.ir/EN/VEWSSID/J_pdf/139220120303.pdf

[278] S. Chaiklieng, "Risk assessment of workers' exposure to BTEX and hazardous area classification at gasoline stations," *PLoS One*, vol. 16, no. 4, p. e0249913, 2021.

[279] N. T. Giao, P. K. Anh, and H. T. H. Nhien, "Health risk assessment for the exposure of workers to BTEX at the gasoline stations," *J. Appl. Sci. Environ. Manag.*, vol. 25, no. 1, pp. 71–77, 2021.

[280] A. Allahabady, Z. Yousefi, R. A. Mohammadpour Tahamtan, and Z. Payandeh Sharif, "Measurement of BTEX (benzene, toluene, ethylbenzene

and xylene) concentration at gas stations," *Environ. Health Eng. Manag. J.*, vol. 9, no. 1, pp. 23–31, 2022.

[281] M. Alimohammadi, A. Behbahaninia, M. Farahani, and S. Motahari, "Carcinogenic and Health Risk Assessment of Respiratory Exposure to BTEX Compounds in Gasoline Refueling Stations in Karaj–Iran," *Pollution*, vol. 9, no. 2, pp. 726–744, 2023.

[282] M. Xu, Z. Tang, Y. Duan, and Y. Liu, "GC-Based Techniques for Breath Analysis: Current Status, Challenges, and Prospects," *Crit. Rev. Anal. Chem.*, vol. 46, no. 4, pp. 291–304, Jul. 2016, doi: 10.1080/10408347.2015.1055550.

[283] H. Shu, Y. Chen, and Z. Huang, "Titanium dioxide nanotube fiber using in headspace solid-phase microextraction with GC–MS for BTEX detection," *J. Chin. Chem. Soc.*, vol. 70, no. 11, pp. 2005–2015, Nov. 2023, doi: 10.1002/jccs.202300276.

[284] B. M. Cesana and P. Antonelli, "Bland and Altman agreement method: to plot differences against means or differences against standard? An endless tale?," *Clin. Chem. Lab. Med. CCLM*, vol. 62, no. 2, pp. 262–269, Jan. 2024, doi: 10.1515/cclm-2023-0306.

[285] O. Gerke, "Reporting standards for a Bland–Altman agreement analysis: A review of methodological reviews," *Diagnostics*, vol. 10, no. 5, p. 334, 2020.

APPENDIX-A

A. 1 Risk of bias summary: review authors' judgements about each risk of bias item for each included study,"+", "-", and "?" indicate low, high, and unclear risk of bias (b) Risk of bias graph: review authors' judgments about each risk of bias item presented as percentages across all included studies.

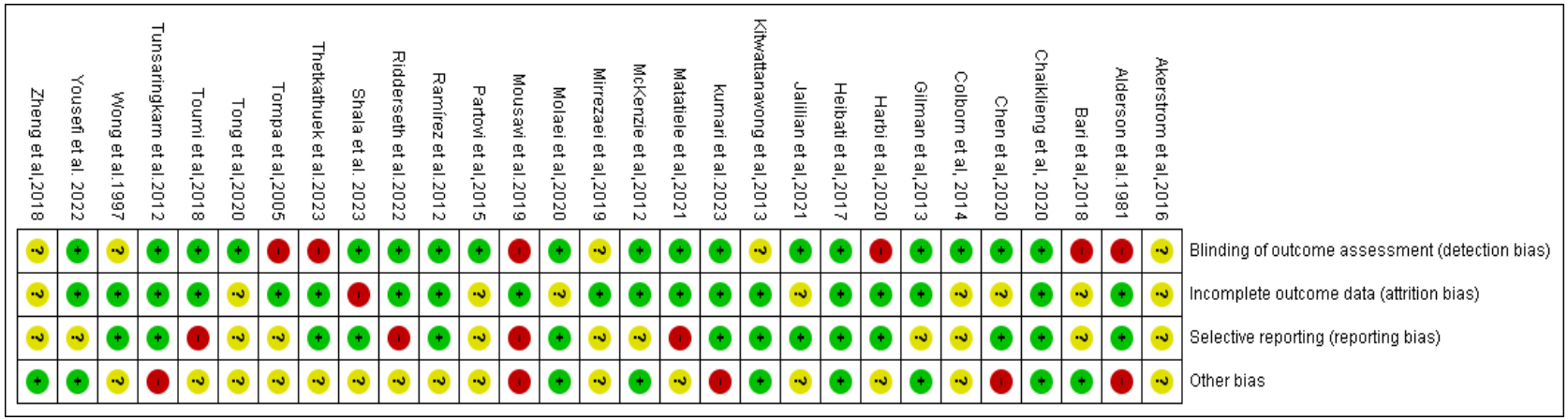

(a)

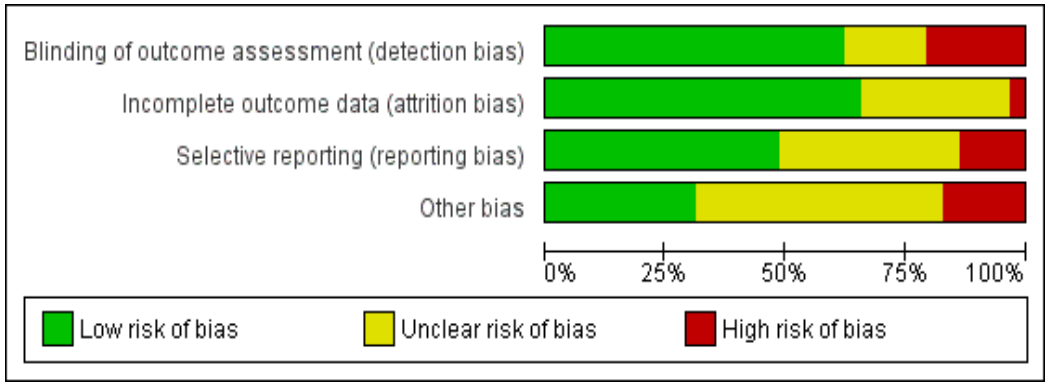

(b)

A.2: Conversion formula in unit conversion

In the included studies, the detection of BTEX compounds was reported using various metrics, including parts per million (ppm) and other units such as milligrams per cubic meter (mg/m³) or parts per billion (ppb). To convert milligrams per cubic meter (mg/m³) to ppm, the following formula can be used:

$$concentration\ in\ ppm\ = (\frac{\frac{\text{Concentration in } mg}{m^3}}{Molecular\ weight\ of\ the\ compound}) \times 24.45$$

Concentration in mg/m^3 is the concentration of the compound in milligram per cubic meter.

Molecular weight of the compound is the molecular weight of the specific BTEX compound being measured.

The molecular weights of the BTEX compounds are as follows:

Benzene (C_6H_6): 78.11 g/mol

Toluene (C_7H_8): 92.14 g/mol

Ethylbenzene (C_8H_{10}): 106.17 g/mol

Xylene (C_8H_{10}): 106.17 g/mol

Using this formula, concentrations reported in units other than PPM can be converted to PPM for consistent analysis and comparison.